UNIVERSITY OF THESSALY

DEPARTMENT OF MECHANICAL ENGINEERING


Thesis


# Catalytic Hydrogenation of Carbon Dioxide


BY

## Konstantinos Peppas


**A thesis submitted in partial fulfilment of the**

**requirements for the**


DIPLOMA OF MECHANICAL ENGINEERING


2014

# Acknowledgments

This thesis was completed in the Alternative Energy Conversion Systems Laboratory of the Mechanical engineering Department, University of Thessaly, under the guidance of Prof. Panagiotis Tsiakaras who I would like to gratefully thank for his useful advises on scientific level and more, as well as for giving me the chance to work and cooperate on a laboratory level.

I would also like to thank the members of the tripartite committee Prof. Nikos Andritsos and Prof. Herrikos Stapountzis for the study of this work as well as Dr.Stratigoula Mitri, the main researcher of the program, for her support and guidance that made this thesis possible.

I am especially grateful to the other laboratory members and friends Dr. Angeliki Brouzgou, Dr. Antonios Seretis and Fotini Tzorbatzoglou for their advises and help. I also want to thank Sisi Kontou for reading this thesis and correcting my English.

Finally, I would like to thank my parents for their unconditional support during my time at the University. Without their support and faith in me, I would not be the man I am today.

K. Peppas

# Abstract

The modern world is highly dependent on fossil fuels and petroleum to cover its demand for energy. However, this constant increasing demand and the simultaneous need to protect environment and prevent the climate change, make the development of alternative means of producing hydrocarbon fuels from other energy sources greatly important. In the present thesis, the carbon dioxide hydrogenation for hydrocarbon production was studied with the aid of solid-state hydrogen reactor cells.

The first important part of the study is the thermodynamic analysis of a number of possible $CO_2$ hydrogenation reactions in order to achieve a theoretical prediction of the expected values of the products' composition. The analysis was performed at a pressure of 1 atm with the method of equilibrium constant. Afterwards, one of the reactions was selected in order to me further studied woth the method of the Gibbs free energy minimization. The results regarding the molar fractions derived by the two methods, show high similarity, which comes in accordance with the theory.

The second part of the thesis includes the protocol design of the experimental $CO_2$ hydrogenation and the experiments with the results. The proton conductor used was $BaCe_{0.5}Zr_{0.3}Y_{0.08}Yb_{0.08}Cu_{0.04}O_3-\delta$ in a form of pellet. The working electrodes-catalysts examined where Co, Cu, Fe in a form of nano-powder mixed with mineral oil and deposited on the surface of the electrolyte. The hydrogenation of $CO_2$ was examined in a single chamber reactor. For the support of the better contact of the ionic conductor / metal catalyst mixture inside the reactor, special bases made of inert material mica were constructed. This system of pellet, mica and electrodes-electrolyte was inserted into a quartz tube and gold wires were guided on the outside of the reactor in suitable sockets for receiving the experimental measurements. Furthermore, in order to prevent possible reduction of the electrolyte, the potential between the working and the counter electrode was tested so that it would never exceed 2 V.

The working electrode covered the one side of the pellet, whereas the counter and the reference electrodes covered the other side in a ratio 2/1. The input gas mixture was either $H_2/He$ or $H_2/CO_2$. The values of the conducted current were higher in the first case which attributed to the presence of pure hydrogen.

In the case of Cu, four different experiments were made. Au was used in the first one for the construction of counter and reference electrode, and only working was made by Cu. In the case of Co and Fe, the two sides of the pellet were made exclusively by the same catalytic material. Polarization studies gave good results. In the case of $H_2/CO_2$ mixture, small amount of products were identified (basically CO ~500ppm).

# Contents

## List of Figures

iv

# List of Tables

# CHAPTER I

## Catalytic Hydrogenation of Carbon Dioxide:

## Utilizing CO$_2$

As a major greenhouse gas, carbon dioxide with increased concentration in the atmosphere is being considered responsible for the global warming and climate changes. Therefore, the reduction of CO$_2$ concentration becomes the global focus. Hydrogenation of CO$_2$ is a feasible process, which leads to the conversion of CO$_2$ to fuels and chemicals offing opportunities to mitigate the increasing CO$_2$ buildup.

# 1 Catalytic Hydrogenation of Carbon Dioxide

Human life and the ecological environment have been affected by global warming and climate changes, due to the increasing emissions of carbon dioxide ($CO_2$). In order to minimize $CO_2$ concentration in the atmosphere various strategies have been implemented such as separation, storage, and utilization of $CO_2$. Hydrogenation reaction is an important representative among chemical conversions of $CO_2$, as it offers challenging opportunities for sustainable development in energy and the environment. The hydrogenation of $CO_2$ not only reduces the increasing $CO_2$ buildup but also could permit the production of fuels and useful chemicals [1].

## 1.1 General Introduction

Carbon dioxide concentration has been varied world-widely over the Earth's long history and for its estimation various proxy measurements have been used. Among them, the most accepted method is the measurement of air bubbles (fluid or gas inclusions) trapped in the Antarctic or Greenland ice sheets. The results indicate that, in pre-industrial period (1832), Antarctic ice core $CO_2$ levels were approximately 284 ppmv.

Man-made emissions of carbon dioxide are derived from the burning of fossil fuels for heating, power generation and transport, as well as some industrial processes. Those emissions support the greenhouse effect, a process by which thermal radiation from a planetary surface is absorbed by atmospheric greenhouse gases, and is re-radiated in all directions. Since part of this re-radiation is back towards the surface and the lower atmosphere, it results in an elevation of the average surface temperature above what it would be in the absence of those extra gases. Carbon dioxide is believed to have played an important effect in regulating Earth's temperature (Figure 1-1),
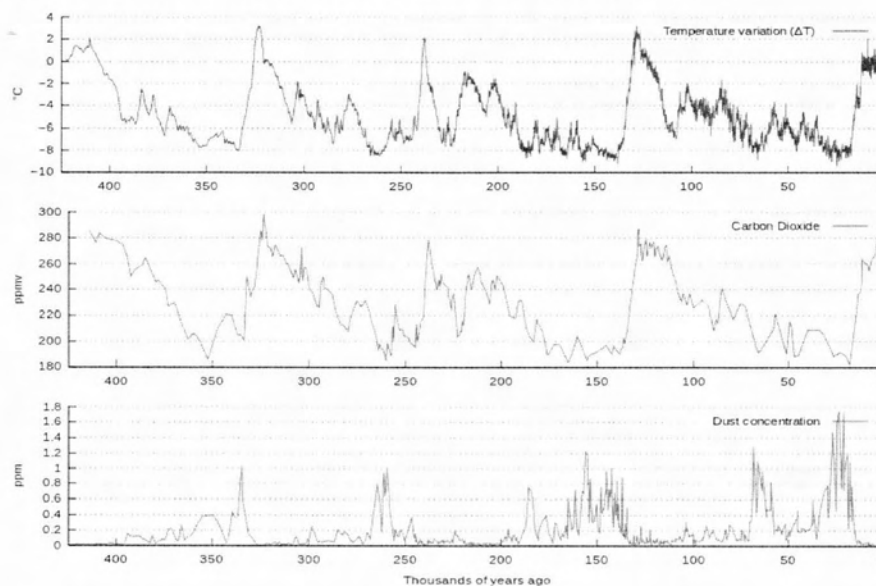


**Figure 1-1 Graph of $CO_2$ (green), reconstructed temperature (blue) and dust (red) from the Vostok ice core for the past 420,000 years [2].**

2

In the period 1751 to 1900, about 12 gigatonnes of carbon were released as carbon dioxide to the atmosphere from burning of fossil fuels, whereas from 1901 to 2008 the figure was about 334 gigatonnes. This lead to an increase in $CO_2$ levels to 395 ppm today.
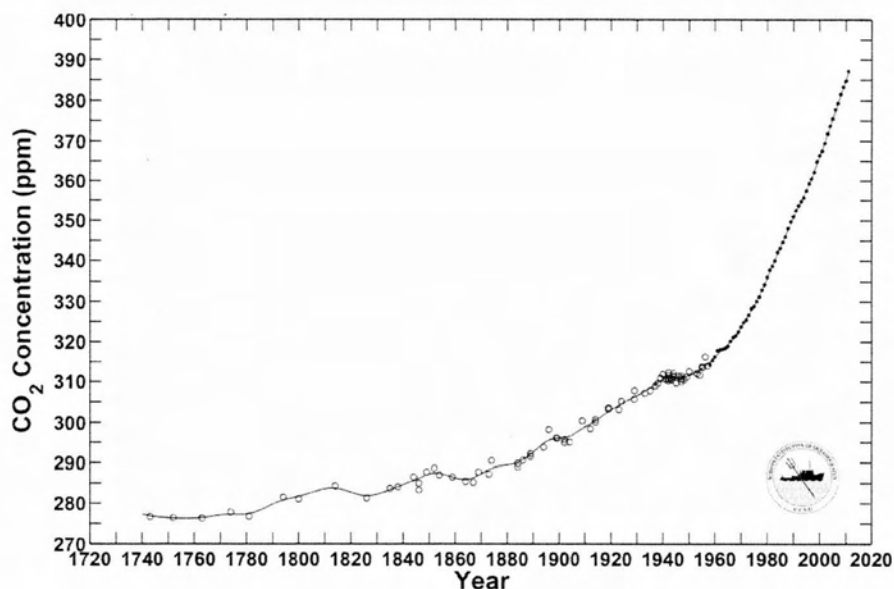


**Figure 1-2 Merged ice-core record of the time trend of the concentration of $CO_2$, in ppm, in air extracted from an Antarctic ice core combined with the trend based on direct atmospheric measurements [3].**

According to the previously mentioned facts, the increase in $CO_2$ emissions arguably contributes to the increase in global temperatures and climate changes due to the "greenhouse effect". Hence, there has been increasing pressure for countries and scientists to curb $CO_2$ emissions and develop efficient $CO_2$ capture and utilization systems [4, 5].

Reducing $CO_2$ emissions is an extensive and long-term task. In principle, there are three possible strategies with this regard—reduction of the amount of $CO_2$ produced, storage of $CO_2$, and usage of $CO_2$ [6, 7]. The first strategy requires energy efficient improvements and switching from fossil fuels toward less carbon intensive energy sources such as hydrogen and renewable energy[6]. Storage of $CO_2$, involving the development of new technologies for capture and sequestration of $CO_2$, is a relatively well established process [6, 8, 9].

As an economical, safe, and renewable carbon source, $CO_2$ turns out to be an attractive $C_1$ building block for making organic chemicals, materials, and carbohydrates (e.g., foods) [10].The utilization of $CO_2$ as a feedstock for producing chemicals not only contributes to alleviating global climate changes caused by the increasing $CO_2$ emissions, but also provides a grand challenge in exploring new concepts and opportunities for catalytic and industrial development[11].

However, $CO_2$ is not used extensively as a source of carbon in current laboratory and industrial practices. Indeed, the use of $CO_2$ as chemical feedstock is limited to a few industrial processes—synthesis of urea and its derivatives, salicylic acid, and carbonates. This is primarily due to the thermodynamic stability of $CO_2$ and thus high energy substances or electroreductive processes are typically required to transform $CO_2$ into other chemicals[12-14].

Hydrogen is a high energy material and can be used for $CO_2$ transformation as the reagent. The main products of $CO_2$ hydrogenation can fall into two categories—fuels and chemicals (Figure 1-3). Indeed, the needs for fuels are ever-increasing with growing energy consumption. However, the resources of fossil fuels are being diminished and fuel prices have undergone strong fluctuation in recent years. Therefore, it would be highly desirable to develop alternative fuels from non-fossil fuel sources and processes. The products of $CO_2$ hydrogenation such as methanol, dimethyl ether (DME), and hydrocarbons, are excellent fuels in internal combustion engines, and also are easy for storage and transportation. Furthermore, methanol and formic acid are raw materials and intermediates for many chemical industries. However, we must recall potential issues associated with hydrogen such as production, storage, and transportation. Hydrogen sources for the chemical recycling of $CO_2$ could be generated either by using still-existing significant sources of fossil fuels (mainly natural gas) or from splitting water (by electrolysis or other cleavage) [15].
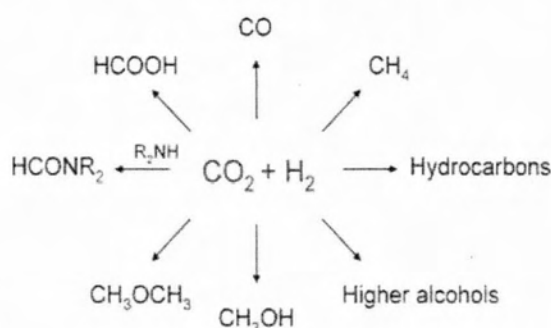


**Figure 1-3 Products for $CO_2$ hydrogenation.**

Hydrogenation of $CO_2$ has been more intensively investigated recently, due to fundamental and practical significance in the context of catalysis, surface science, biology, nano science and nanotechnology, and environmental science. Both homogeneous and heterogeneous catalysts have been used to hydrogenate $CO_2$.[11, 16, 17]

Homogeneous catalysts show satisfactory activity and selectivity, but the recovery and regeneration are problematic. Alternatively, heterogeneous catalysts are preferable in terms of stability, separation, handling, and reuse, as well as reactor design, which reflects in lower costs for large-scale productions[7, 12, 13, 16].

To combine the desirable reactivity of homogeneous catalysts with the recyclability of heterogeneous catalysts, significant progress has been made in this direction, including the

4

immobilization of homogeneous catalysts, exploitation of novel heterogeneous catalysts, and the use of green solvents such as ionic liquids (ILs) and supercritical $CO_2$ (sc $CO_2$) [18]

There have been several excellent reviews regarding $CO_2$ conversions as well as catalytic hydrogenation of $CO_2$ [4, 7, 10, 12, 16]. However, these reviews primarily focus on general aspects of $CO_2$ applications and homogenously catalyzed hydrogenation of $CO_2$.

Advances have been made in the past decade, especially on hydrogenation of $CO_2$ via heterogeneous catalysts. Current understanding of catalytic reactivity, and reaction mechanism over various types of catalysts, will be presented bellow.

## 1.2    State-of the Art

### 1.2.1    Synthesis of carbon monoxide via reverse water gas shift (RWGS) reaction

Catalytic conversion of $CO_2$ to CO via RWGS reaction has been generally deemed as one of the most promising processes for $CO_2$ conversions [19].

$$CO_2 + H_2 \leftrightarrow CO + H_2O, \quad \Delta H_{298K} = 41.2 \text{ kJ mol}^{-1}$$
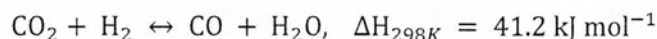
Indeed, the RWGS reaction occurs in many processes, wherever $CO_2$ and $H_2$ are present in a reaction mixture. Due to the importance of this reaction from both fundamental and practical points of view, the design and characterization of RWGS catalysts have attracted considerable attention.

As RWGS is a reversible reaction, catalysts active in the water gas shift (WGS) reaction are often active in the reverse reaction [18]. Copper-based catalysts, the most popularly studied catalytic systems for the WGS reaction, have also been applied to the RWGS reaction. Liu et al. have developed a series of bimetallic Cu–Ni/g-$Al_2O_3$ catalysts for $CO_2$ hydrogenation [20]. The ratio of Cu/Ni has a significant effect on conversion and selectivity. . Cu favors CO formation, while Ni is active for CH4 production. Cu/ZnO and Cu–Zn/ $Al_2O_3$ catalysts used for methanol synthesis and WGS reaction have also been tested for the RWGS reaction[21]. The most active catalyst for the reaction is Cu rich (Cu/Zn > 3) with alumina as a support. A linear relationship between the activity of the catalyst and the surface area of metallic Cu was obtained [21]. Additionally, Chen et al. have reported that Cu/$SiO_2$ with a potassium promoter offers better catalytic activity (12.8% of $CO_2$ conversion at 600 °C) than that without promoter (5.3% of $CO_2$ conversion at 600 °C) [22].

The created new active sites located at the interface between copper and potassium favor the formation of formate (HCOO) species, which is the key intermediate for CO production. The major role of $K_2O$ is to provide active sites for decomposition of formates, in addition to acting as a promoter for $CO_2$ adsorption.

RWGS reaction is an endothermic reaction, and thus high temperature would facilitate the formation of CO. However, copper-based catalyst is not suitable at high temperature because of its

5

poor thermal stability (e.g., sintering of copper nanoparticles) unless modified by adding a thermal stabilizer. For example, upon the addition of a small amount of iron, catalytic activity and stability of $Cu/SiO_2$ at high temperature can be effectively improved [23]. Large copper surface area is provided by Cu–Fe catalysts, even if the catalysts are pretreated at high temperature. At 600 °C and atmospheric pressure, the Cu–Fe catalysts exhibit high and stable catalytic activity up for 120h. In contrast, 10 wt% $Cu/SiO_2$ without Fe additives deactivates rapidly, due to the decreased surface area of copper and oxidation of copper at high temperature [24]. The new active species around the interface between Cu and Fe particles were proposed to account for the enhanced catalytic activity. At high temperature, the sintering of Cu is effectively prevented by the formation of small particles of iron species around Cu particles [24]. Chen et al. have developed a $Cu/SiO_2$ catalyst by atomic layer epitaxy (ALE), which has favorable thermal stability to resist the sintering of Cu particles under high temperature condition [25]. Due to the formation of small Cu particles, the ALE–$Cu/SiO_2$ catalysts could strongly bind CO and provide high catalytic activity for the RWGS reaction.

Cerium-based catalysts are also active in both WGS and RWGS reactions [26]. $Ni/CeO_2$ (2wt%Ni) showed excellent catalytic performance in terms of activity, selectivity, and stability for the RWGS reaction [27]. CO yield is ~35% at 600 °C for a continuous period of 9 h. Oxygen vacancies formed in the lattice of ceria and highly dispersed Ni are key active components for the reaction, and bulk Ni favors the formation of methane. However, deactivation of ceria- supported catalysts is a crucial issue we need to consider. It has been reported that a very small coverage of deposited carbon on the ceria support leads to strong deactivation of the catalyst, indicating that the fraction of the support involved in the reaction is small, probably located next to the supported metal [28].

Supported noble metal catalysts (e.g., Pt, Ru, and Rh) typically have high ability toward $H_2$ dissociation, and thus they have been used as efficient catalysts for $CO_2$ hydrogenation. Bando et al. performed $CO_2$ hydrogenation over Li-promoted Rh ion-exchanged zeolites (Li/RhY) [29]. Main product transforms from methane to CO with increased amount of Li. When an atomic ratio of Li/Rh is higher than 10, the main product becomes CO (87% of selectivity) and formation of methane is greatly suppressed (8.4% of selectivity). The presence of Li atoms on the surface creates new active sites that enhance $CO_2$ adsorption and stabilization of adsorbed CO species [29].

Moreover, the type of metal precursor employed in the catalyst preparation affects catalytic reactivity. Arakawa et al. prepared silica-supported Rh catalysts ($Rh/SiO_2$) from acetate, chloride, and nitrate precursors via impregnation for $CO_2$ hydrogenation [30]. The main product was CO over the catalysts prepared from acetate and nitrate, whereas the amount of $CH_4$ was relatively high using the catalyst synthesized from the chloride precursor. Detailed X-ray photo electron

spectroscopy (XPS) measurements elucidated the effect of metal precursor on the $CO_2$ hydrogenation reactivity. It was found that the ratio of hydroxyl species to Rh atoms on $SiO_2$ surface determined reactivity (high ratio favors the formation of CO). The ratio based on different metal precursors follows the order: chloride < nitrate < acetate.

### 1.2.1.1  Reactor aspects

It has been generally recognized that the fluidized beds can be utilized efficiently for multiphase reactions such as the catalytic hydrogenation of $CO_2$, because it can achieve higher mass and heat transfer rates in comparison with any other contacting mode [31]. For instance, a fluidized bed reactor was used to investigate the characteristics of the RWGS reaction with Fe/Cu/K/Al catalyst; $CO_2$ conversion in the fluidized bed reactor (46.8%) was higher than that in the fixed bed reactor (32.3%) [32]. Electrochemical promotion of the RWGS reaction has been studied in the solid oxide fuel cell (SOFC). For $Cu/SrZr_{0.9}Y_{0.1}O_3$ a, higher reaction rates were observed when hydrogen was electrochemically supplied as $H^+$ than as molecular hydrogen [33]. In case of Pt/YSZ (yttrium-stabilized zirconia), the rate-determining step of the RWGS reaction is the formation of surface-bound carbon and its interaction with adsorbed hydrogen [34]. The observation is due to the combination of direct electrocatalysis (electrode composition of $CO_2$, electro-oxidation of $H_2$) and electrochemical promotion. For Pd/YSZ, CO formation is improved by up to 6 times upon employing either negative or positive overpotentials [35]. SOFC displays great stability and durability in the RWGS reaction, and can be considered as one of the alternative routes for the production of renewable energy.

### 1.2.1.2  Reaction mechanisms

Considerable work has been recently conducted with a variety of advanced characterization tools to unravel mechanism of the RWGS reaction. The mechanism of the reaction has been primarily discussed over Cu-based catalysts, which is, however, still controversial. Two major reaction mechanisms—redox and formate decomposition—have been proposed. The redox mechanism for the RWGS reaction can be simply modeled by the following scheme:

$$CO2 + 2Cu^0 \rightarrow Cu_2O + CO$$

$$H_2 + Cu_2O \rightarrow 2Cu^0 + H_2O$$
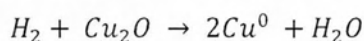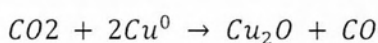
$Cu^0$ atoms are apparently active to dissociate $CO_2$, while the reduction of oxidized Cu catalyst has to be faster than the oxidation process [36]. Hydrogen is proposed to be a reducing reagent without

direct participation in the formation of intermediates in the RWGS reaction. The other model, which is based on the formate decomposition suggests that CO, is created from the decomposition of formate intermediate, derived from the association of hydrogen with $CO_2$ [22].

Chen et al. examined desorption energies of $CO_2$, active sites, and reaction mechanism of the RWGS reaction on Cu nanoparticles [37]. The Cu nanoparticles strongly bind $CO_2$ molecules, as evidenced by two main peaks with maxima at 353 K ($\alpha$ peak) and 525 K (b peak) in $CO_2$-TPD (temperature-programmed desorption of $CO_2$) spectra. $\beta$-Type $CO_2$ is substantiated as the major species for the RWGS reaction. Since an infrared band at 2007 $cm^{-1}$ was observed and assigned to CO adsorbed on low-index copper facets, the authors proposed that reaction pathways mainly include the formation of the formate species [38].

Different mechanisms have also been proposed for the reaction over Pd- and Pt-based catalysts. In a study using $Pd/Al_2O_3$ catalysts and supercritical mixture of $CO_2$ and $H_2$, infrared spectra indicated the formation of surface species such as carbonate, formate, and CO [39]. However, only carbonate and formate were observed on a bare alumina support. This contrast deduces that Pd facilitates the dissociative adsorption of $H_2$ and the formation of formates and CO.

A reaction model involving three kinds of mechanism is proposed in Figure 1-4. Both of the formates and Pt-bound carbonyls species were observed, but neither of them was the main reaction intermediate, although the formation of CO from formates was likely to occur to a limited extent. The RWGS reaction proceeds mainly via surface carbonate intermediates, including reaction between the surface carbonates and oxygen vacancies or the diffusion of the vacancies in the ceria [40].

Theoretical investigations using model systems can also shed some light on the nature of molecular interactions. Qin et al. investigated the mechanism of the RWGS reaction on a Ni surface using density functional theory (DFT) calculations and predicted that the C–O bond cleavage of $CO_2$ occurred before the dissociation of the $H_2$ [41].

The $H_2$ moiety could promote the charge transfer in the Ni insertion process and facilitate the dissociation of coordinated $CO_2$ molecule by reducing the energy barrier. The rate-determining step for the reaction is the migration of hydrogen atom from Ni center to oxygen atom with the formation of water.
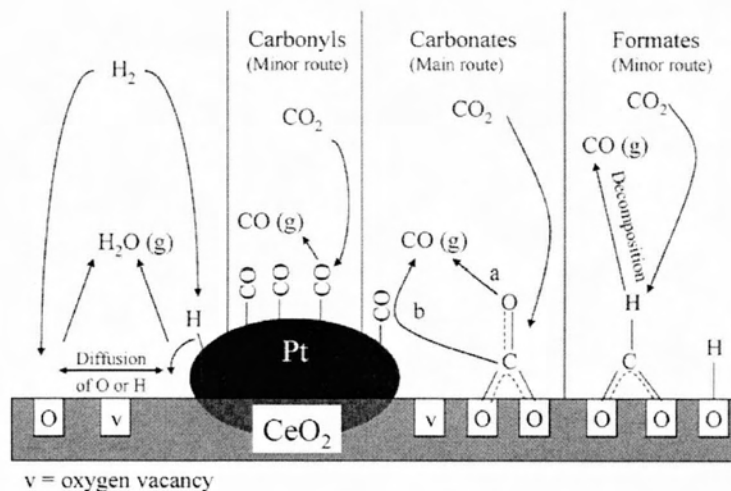
**Figure 1-4 Model for the reaction mechanism of the RWGS reaction over Pt/CeO2[42].**

Liu et al. reported the modeling of the reaction mechanism for the RWGS reaction with first-row transition metal catalysts L' M (L' = $C_3N_2H_5^-$ ; M = Sc, Ti, V, Cr, Mn, Fe, Co, Ni, Cu, Zn). The first step of catalytic reaction is the coordination of a $CO_2$ molecule (L'M($CO_2$)). The second step is the scission of L'M($CO_2$) to produce L'M(CO) and L'M(O) by adding L'M, which is followed by hydrogenation of the oxo complex L'M(O) to generate L'M($H_2O$). The last step involves dissociation of $H_2O$ and CO. Reaction enthalpies for all the steps are depicted in Figure 1-5. For catalytic cycle of the RWGS reaction, the key discriminating steps are the coordination and reduction of $CO_2$. Early metals show a thermodynamic favor in these steps; however, late metals are more feasible for the hydrogenation of oxo complex [43].
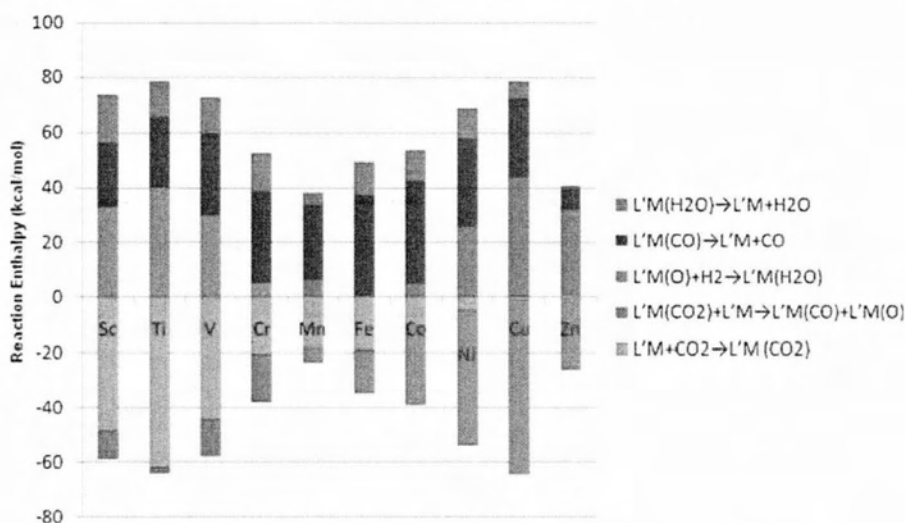


**Figure 1-5 Reaction enthalpies (kcal mol1 ) for each metal based enthalpies calculations [44].**

### 1.2.2  Synthesis of hydrocarbons

Production of hydrocarbons from $CO_2$ hydrogenation is essentially a modification of the Fischer–Tropsch (FT) synthesis, where $CO_2$ is used instead of CO. Catalyst component for $CO_2$ hydrogenation is analogous to that for FT synthesis but is amended to maximize the production of hydrocarbons. A number of studies have been carried out on this subject, which can be divided into two categories—methanol-mediated and non-methanol-mediated reactions [45]. In the methanol-mediated approach, $CO_2$ and $H_2$ react over Cu–Zn-based catalysts to produce methanol, which is subsequently transformed into other hydrocarbons such as gasoline [46]. In spite of considerable efforts made in the development of composite catalysts, this approach usually yields light alkanes as major products owing to the further catalytic hydrogenation of the alkenes [47]. In the case of non-methanol-mediated process, $CO_2$ hydrogenation proceeds via two steps—RWGS reaction and FT synthesis.

Cobalt catalysts are widely used in FT synthesis, owing to the high performance-to-cost ratio. Upon switching feeding gas from syngas to the gas mixture of $CO_2$ and $H_2$, cobalt performs as a methanation catalyst rather than acting as an FT catalyst [48]. Mixed Fe/Co catalysts have also exhibited low selectivity to the desired hydrocarbons [49]. Akin et al. observed that products of $CO_2$ hydrogenation contain ~70 mol% methane over $Co/Al_2O_3$ catalyst [50]. They proposed that the conversion of CO and $CO_2$ occurs via different reaction pathways: the former involving mainly species of C–H and O–H produced from hydrogenation, the latter involving surface-bound intermediates of H–C–O and O–H [50]. In order to better clarify the difference in product distributions of CO and $CO_2$ hydrogenation, Figure 1-6 shows typical Anderson-Schulz-Flory (ASF) diagrams in terms of selectivity of total hydrocarbons in CO and $CO_2$ hydrogenation [51]
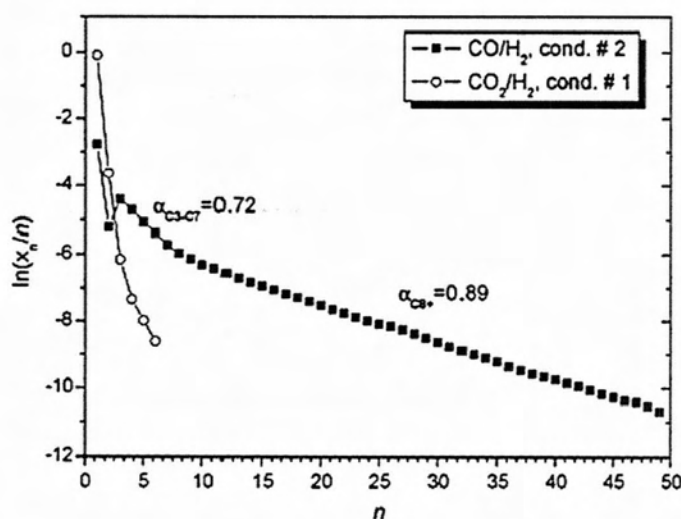


Figure 1-6 ASF plots in terms of hydrocarbons selectivity during CO and $CO_2$ hydrogenation.

10

It is obvious that hydrogenation of $CO_2$ does not lead to a typical ASF distribution, different from what takes place for CO hydrogenation. During $CO_2$ hydrogenation a low C/H ratio is obtained due to the slow $CO_2$ adsorption rate on the surface. This favors the hydrogenation of surface-adsorbed intermediates, leading to formation of methane and a decrease in chain growth.

Iron oxides have been used as FT catalysts for many years, which are also active in both WGS and RWGS reactions [52]. Iron-based catalysts are attractive for the synthesis of hydrocarbons due to the highly olefinic nature of the obtained products [53]. $CO_2$ hydrogenation over an iron catalyst proceeds via a two-step process, with initial reduction of $CO_2$ to CO via the RWGS reaction followed by the conversion of CO to hydrocarbons via a FT reaction.

$$CO2 + H2 \rightarrow CO + H2O, \qquad \Delta_R H_{573K} = 38 \ kJ \ mol^{-1}$$

$$CO + 2H2 \rightarrow -CH2- + H2O, \qquad \Delta_R H_{573K} = -166 \ kJ \ mol^{-1}$$
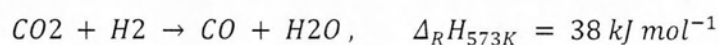
In order to increase the yield of the desired hydrocarbons products, promoters are often added to catalysts to tailor and optimize product distribution. Potassium is a favorable promoter and has significant influence on catalytic performance. Addition of potassium not only leads to a significant shift in olefin production (4-fold) but also an increase in $CO_2$ conversion [54]. In addition to be present in the oxide form, potassium could also form an alanate phase (KAlH4), which has recently attracted much attention for its ability of reversible hydrogen storage at high temperature. Potassium acts as an electronic promoter to the iron, as well as suppresses the hydrogenation of the products as a reversible $H_2$ reservoir. For example, K/Mn/Fe-based catalyst displays a high chain growth [54].

Ceria is highly active in the WGS reaction at low temperature, and thus is of immense interest in applications such as fuel cells. Ceria added to an iron catalyst has little effect on the conversion of $CO_2$ to hydrocarbons, but shortens the time of stationary-state operation conditions. Although low loading of ceria to a Fe–Mn/Al2O3 catalyst leads to a marginal improvement in $CO_2$ conversion and product selectivity, a decrease in reactivity was observed when the doping amount is increased to 10 wt%. Ceria particles are formed over iron nanoparticles causing the blocking of the chain-growth sites. Other additives including Zr, Zn, Mg, Ru, and La have also been investigated but promoting effect is nearly negligible.

Iron-based catalysts dispersed on different supports have also been examined extensively and the product distributions are greatly dependent on supporting materials. The support tends to act purely as a stabilizer to avoid sintering of active particles during the reaction. Generally, alumina

11

performs best, since it could prevent sintering as a result of the strong metal-support interaction, followed by silica and titania [46].

### 1.2.3 Methanation of carbon dioxide

Catalytic hydrogenation of $CO_2$ to methane, also called the Sabatier reaction, is an important catalytic process.

$$CO_2 + 4H_2 \leftrightarrow CH_4 + 2H_2O, \quad \Delta H_{298K} = -252.9 \text{ kJ mol}^{-1}$$
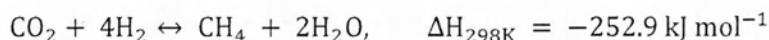
The methanation of $CO_2$ has a range of applications including the production of syngas and the formation of compressed natural gas. Research is being conducted by the National Aeronautics and Space Administration on the application of this reaction in manned space colonization on Mars [55]. It is possible to convert the Martian $CO_2$ atmosphere into methane and water for fuel and astronaut life-support systems [56].

The methanation of $CO_2$ is thermodynamically favorable ($\Delta G_{298\,K} = 130.8$ kJ mol$^{-1}$); however, the reduction of the fully oxidized carbon to methane is an eight-electron process with significant kinetic limitations, which thus requires a catalyst to achieve acceptable rates and selectivities [57]. Extensive studies have been conducted on metal-based catalytic systems on the hydrogenation of $CO_2$ to methane.

#### 1.2.3.1 Metal-based heterogeneous catalysts

Hydrogenation of $CO_2$ toward methane has been investigated using a number of catalytic systems based on VIIIB metals (e.g., Ru and Rh) supported on various oxides (e.g., $SiO_2$, $TiO_2$, $Al_2O_3$, $ZrO_2$, and $CeO_2$). Supported nickel catalysts remain the most widely studied materials. Supports with high surface area, usually oxides, have been applied extensively for the preparation of metal catalysts. The nature of support plays a crucial role in the interaction between nickel and support, and thus determines catalytic performances toward activity and selectivity for $CO_2$ methanation [58].

RANEY ® nickel, which is well known as an active catalyst for hydrogenation, appears to have high reactivity in the methanation reaction [59]. The notable catalytic performance is attributed to its unique thermal and structural stability as well as a large BET surface area. Main products were observed to be CH4 and CO over Ni–Al alloys [60].

An increase in Ni content leads to higher selectivity to methane (100%), since Ni (compared to Al) readily dissociates CO. Moreover, a series of mono- and bi-metallic Ni-based catalysts supported on alumina were examined via a computational screening study [61]. The conversion of $CO_2$ to methane is significantly increased over Ni–Fe alloy compared to the pure nickel or iron catalyst, and the best catalyst has a Ni/Fe ratio higher than 1.

One of major problems of Ni-based catalysts is the deactivation at low temperature due to the interaction of the metal particles with CO and formation of mobile nickel subcarbonyls [62]. Instead, noble metal (e.g. Ru, Pd, and Pt) is stable at operating conditions and more active for $CO_2$ methanation than nickel [63].

Kowalczyk et al. studied the effect of the support on catalytic properties of Ru nanoparticles in $CO_2$ hydrogenation [64]. They found that TOFs of Ru-based catalysts were dependent on the Ru dispersion and the type of supports. For high metal dispersion, the following order of (turnover frequency) TOFs $(10^3 s^{-1})$ for the reaction was obtained: $Ru/Al_2O_3(16.5)$> $Ru/MgAl2O4(8.8)$ > $Ru/MgO$ (7.9) > $Ru/C$ (2.5) [64].

The catalytic activity of ruthenium nanoparticles is strongly affected by the metal-support interaction. In the case of Ru/C systems, the carbon moiety partially covers the metal surface and reduces the number of active sites (i.e., site blocking effect) [64]. Under steady-state conditions, reaction rate of a highly loaded $15wt\%Ru/Al_2O_3$ is about 10 times higher than that of Ni-based catalysts. Highly dispersed Ru nanoparticles were also synthesized on TiO2 prepared by a barrel sputtering method [65]. Remarkably, a 100% yield was achieved over this catalyst at 433 K, which was significantly higher compared to that prepared by conventional wet impregnation.

The prepared Ru/TiO2 sample can catalyze the methanation reaction at low temperature (300 K) with a reaction rate of 0.04 µmol $min^{-1}$ $g^{-1}$. Furthermore, the addition of yttrium to Ru-based catalysts not only increases the active surface area and the dispersion of ruthenium but also benefits catalytic activity and anti-poisoning capacity of the catalysts [66].

Ru/g-Al2O3 was also used as a probe catalyst to determine kinetic parameters for $CO_2$ methanation [67]. Apparent activation energy reaches a minimum (82.6 kJ $mol^{-1}$) at a ruthenium dispersion of 50%. Reaction order with respect to hydrogen decreases with the increase of H/Ru ratio, which could be attributed to a change in adsorption heat of hydrogen and an increased number of low-coordination sites.

Park et al. have investigated bifunctional Pd–Mg/SiO2 for $CO_2$ methanation motivated by the property of Pd to dissociate molecular hydrogen [57]. At 723 K, the Pd–Mg/SiO2 catalyst shows a high selectivity (>95%) to $CH_4$ with 59% of $CO_2$ conversion, whereas Pd supported on silica reduces $CO_2$ primarily to CO whereas Mg/SiO2 alone is inactive. A bifunctional mechanism was proposed that Pd provides disassociated hydrogen to Mg carbonates to form methane, and upon the desorption of the methane, the carbonate is reformed by gas phase $CO_2$ .
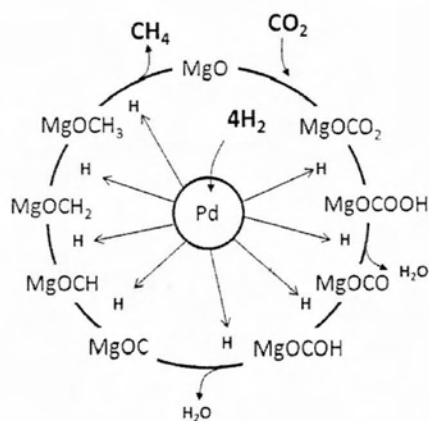
**Figure 1-7 Potential bifunctional model for Pd–Mg/SiO2 [68].**

Recently, platinum supported on titania nanotubes (Pt/Tnt) with high surface area (187 $m^2 g^{-1}$) has been prepared [69]. The catalyst contains scrolled multi-walled titania-nanotubes uniformly dispersed with Pt nanoparticles in the mixed-valence states. $CO_2$-TPD results indicated that a large amount of $CO_2$ adsorbed on the Pt/Tnt is ascribed to the combined effect of the tubular structure with high surface area and Pt nanoparticles with the mixed-valence. In situ FTIR demonstrated that $CH_4$ was the unique product during the reaction and Pt/Tnt catalyst showed high activity for $CO_2$ methanation at low temperature (450 K).

### 1.2.3.2 Reaction mechanism

Although the methanation of $CO_2$ is a comparatively simple reaction, its reaction mechanism appears to be difficult to establish. There are different opinions on the nature of the intermediate and the methane formation process. Reaction mechanisms proposed for $CO_2$ methanation fall into two main categories. The first one involves the conversion of $CO_2$ to CO prior to methanation, and the subsequent reaction follows the same mechanism as CO methanation [70]. The other one involves the direct hydrogenation of $CO_2$ to methane without forming CO as intermediate [52]. We note that, even for CO methanation, there is still no consensus on the kinetics and mechanism. It has been proposed that the rate-determining step is either the formation of the CHxO intermediate and its hydrogenation or the formation of surface carbon in CO dissociation and its interaction with hydrogen [70].

Steady-state transient measurements have been employed in kinetic investigations on a Ru/TiO2 catalyst to identify reaction intermediates [71]. CO is a key intermediate and its hydrogenation leads to the formation of methane. Formates, also as intermediates for the formation of CO, are bound more strongly on the support in equilibrium with the active formate species on the interface between metal and support. A reaction mechanism (Figure 1-8) is proposed including the formation of the formate through a carbonate species.

14
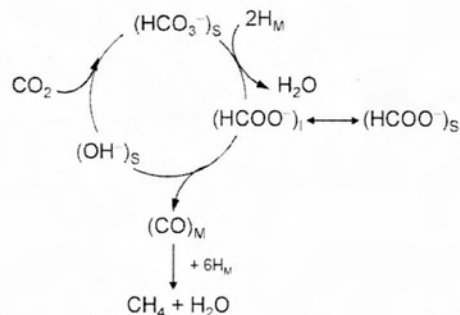
S: the support; M: the metal; I: the metal-support interface.

**Figure 1-8 Proposed reaction mechanism for $CO_2$ methanation,[72].**

Choe et al. investigated the $CO_2$ methanation on a Ni(111) surface in a detailed manner [73]. The elementary reaction steps are listed below.

$$CO_{2,ads} \rightarrow CO_{ads} + O_{ads}$$

$$CO_{ads} \rightarrow C_{ads} + O_{ads}$$

$$2CO_{ads} \rightarrow C_{ads} + CO_{2,gas}$$

$$C_{ads} + H_{ads} \rightarrow CH_{ads}$$

$$CH_{ads} + H_{ads} \rightarrow CH_{2,ads}$$

$$CH_{2,ads} + 2H_{ads} \rightarrow CH_{4,gas}$$
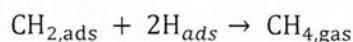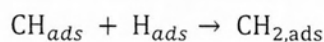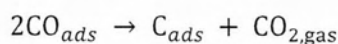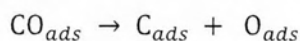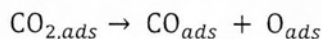
These elementary steps consist of two mechanisms—carbon formation and carbon methanation. For the first mechanism, the activation energies were calculated to be 1.27 eV for $CO_2$ dissociation, 2.97 eV for the CO dissociation, and 1.93 eV for the 2CO dissociation. For the carbon methanation mechanism, following activation energies were reported: 0.72 eV for methyl dyne, 0.52 eV for methylene, and 0.50 eV for methane [73]. Thus, CO dissociation is the rate-determining step.

## 1.2.4 Synthesis of methanol

Methanol is a common solvent, an alternative fuel, and a starting material in chemical industry. As an alternative feedstock, $CO_2$ has replaced CO and is considered as an effective way for $CO_2$ utilization in the methanol production [12].

$$CO_2 + 3H_2 \leftrightarrow CH_3OH + H_2O, \quad \Delta H_{298K} = -49.5 \text{ kJ mol}^{-1}$$
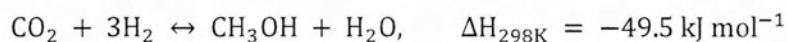
From the thermodynamic point of view, a decrease in reaction temperature or an increase in reaction pressure could favor the synthesis of methanol [12]. Furthermore, other by-products are formed during the hydrogenation of $CO_2$, such as CO, hydrocarbons, and higher alcohols [74]. Therefore, a highly selective catalyst is in need to avoid the formation of undesired by-products for methanol synthesis. Typically, catalysts used in $CO_2$ hydrogenation are those for methanol

15

synthesis from CO hydrogenation. A number of investigations have addressed the effects of active components, supports, promoters, preparation methods, and surface morphology on reactivity.

### 1.2.4.1 Reactivity and structure of heterogeneous catalysts

Although many kinds of metal-based catalysts have been examined for the synthesis of methanol, Cu remains the main active catalyst component, together with different modifiers (Zn, Zr, Ce, Al, Si, V, Ti, Ga, B, Cr, etc.) [75]. An appropriate support not only affects the formation and stabilization of the active phase of the catalyst but also is capable of tuning the interactions between the major component and promoter. In addition, basicity and/or acidity characteristics of the catalyst are also determined by the selected support [76].

### 1.2.4.2 Theoretical studies

Owing to great complexity of methanol synthesis from $CO_2$ hydrogenation, atomic level understanding regarding the reaction mechanism has been a long-standing challenge. Up to now, the key issues in the field, such as how and where $CO_2$ is activated over the surface of the catalysts, remain elusive [76]. The synthesis of methanol is generally regarded as occurring at interfaces of Cu and oxides. In other words, $CO_2$ can adsorb on bare oxides and $H_2$ can dissociate on Cu species [77]. However, the nature of the active Cu phase at interface is still in dispute. Koeppel et al. found that active copper species is present predominantly as $Cu^0$ over $Cu/ZrO2$ based on X-ray diffraction (XRD) measurements [78]. In contrast, $Cu^+$ was proposed to be the active component for a $Cu/ZnO/SiO2$ catalyst employing static low-energy ion scatter experiments [79]. However, it has also been suggested that Cu metal and low valence of Cu ($Cu^{\delta+}$ and $Cu^+$) may all affect the catalytic activity of Cu-based oxide catalysts. Resolution of the electronic and geometrical structures of the active site is the first step towards the rational design of catalyst with high activity and selectivity [80].

### 1.3 Aim of thesis

According to the state of the art, there are many pathways of $CO_2$ utilization; however there are not techniques that can be used in order to massively convert $CO_2$ in useful chemicals and fuels.

In this thesis, we're interested in the use of catalysts that can actually give useful products (methanol, carbon monoxide, methane etc.) through $CO_2$ hydrogenation process. Electrolyte is of major importance that is why an extended analysis about it happens in chapter 2. In chapter 3, the thermodynamic analysis of carbon dioxide hydrogenation is made, for the main products that are expected to be recorded. Finally, experimental data of the catalytic systems used, will be exported and analyzed.

# *CHAPTER II*

## Solid State Materials and Solid Electrolytes

In this chapter, a general introduction on the properties and the characteristics of molecular structures is presented, as well as solids classification according to their crystal structure. Electrolytes are distinguished among those solid structures and several important facts of them are listed. Finally, the thermodynamic and kinetic analysis of the electrochemical reduction reaction is presented. This analysis is essential in order to understand the behaviour of those materials.

## 2    Solid Materials and Solid Electrolytes

### 2.1    Properties and Characteristics of molecular structures

When atoms come together to form a compound, their atom orbital energies mix to form molecular orbital energies. As more atoms begin to mix and more molecular orbitals are formed, it is expected that many of these energy levels will start to be very close to, or even completely degenerate, in energy. These energy levels are then said to form *bands* of energy.

### 2.1.1    Band Theory

Band theory is the basis of the modern theory of solids. It has made it possible to understand the nature of and explain the most important properties of metals, semiconductors, and dielectrics. Solids are made of an infinite number of atoms so it is a common misconception to consider each atom individually. Thus the structure of a solid is considered as a whole. This provides the basis for the description of metals and other types of solids to account for their unique chemical and physical properties. To fully understand the properties, it is essential to start with molecular orbital theory. In the basic theory, it was assumed that if atoms were brought together, they would form bonding, non-bonding and antibonding orbitals of different energies. These molecular orbitals are described by wave functions. The most important point to come out of the theory is that for N atomic orbitals in a molecule, N molecular orbitals must be the outcome.
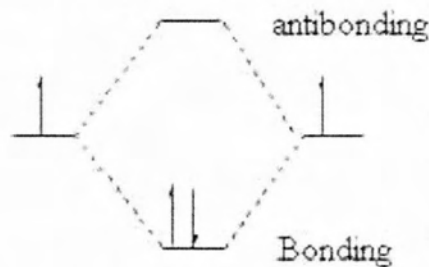


**Figure 2-1 For a molecule with two atomic orbitals the result must be that two molecular orbitals will be formed from these atomic orbitals: one bonding and one antibonding, separated by certain energy.**



18
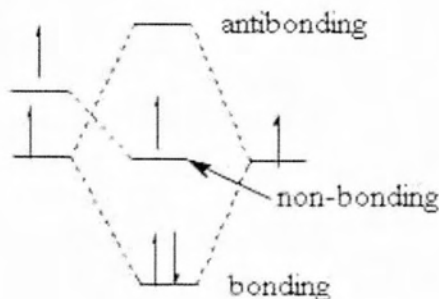
**Figure 2-2 For a molecule with three atoms, assuming 1 atomic orbital for each, then the result must be that 3 molecular orbitals will be formed: one bonding, one non-bonding and one anti-bonding.**
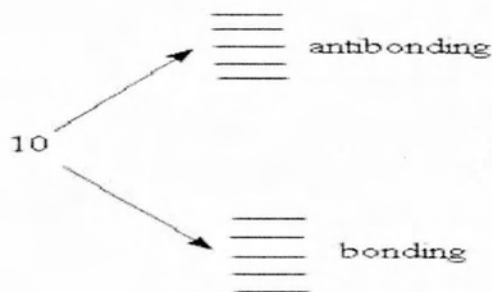


**Figure 2-3 For a molecule with 10 atoms, 10 molecular orbitals will be produced( 5 bonding, 5 anti-bonding).**

Regarding with the separation between each set of orbitals, as the number of molecular orbitals increases, the energy difference between the lowest bonding and the highest antibonding increases, while the space between each individual orbital decreases. As the number of the molecular orbitals increases, the spacing between the lowest bonding and highest antibonding orbital will reach a maximum. This will form an infinite number of molecular orbitals so close together they blur into one another forming a band.
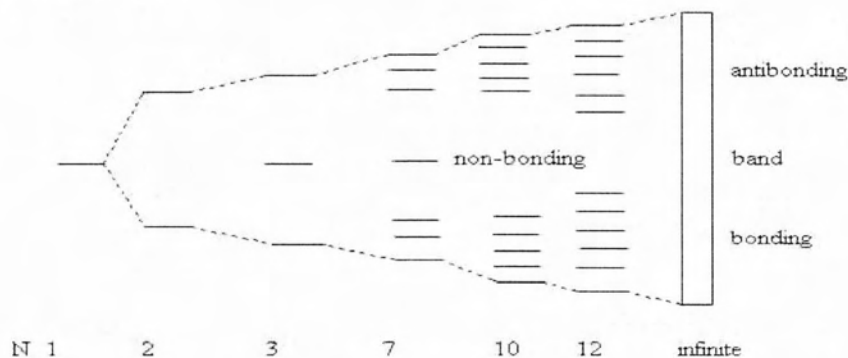


**Figure 2-4 As the number of molecular orbitals increases, they bonding and antibonding orbitals get closer together filling in the middle.**

A crystal is a solid consisting of a regular and repetitive arrangement of atoms or molecules (strictly speaking, ions) in space. If the positions of the atoms in the crystal are represented by points, called lattice points, we get a crystal lattice. The distance between the atoms in a crystal is fixed and is termed the 'lattice constant' of the crystal. If we consider that a solid may contain approximately $10^{23}$ atoms per $cm^{3}$, we can understand how these levels form a nearly continuous band that is.[81]

19
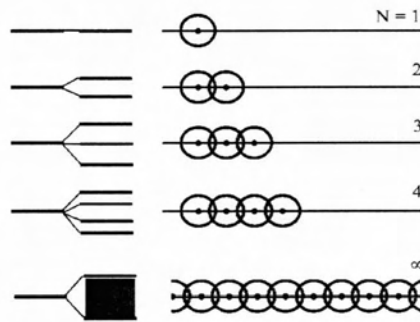
**Figure 2-5 As the crystal contains a large number of atoms the spacing between the discrete levels in a band is so small that the band can be treated as continuous.**

In conclusion:

- As there are many atomic levels, bands are formed in a crystal.
- For a monatomic solid (1 atom per base) that contains N identical atoms, in each band there are N spaces of energy. Taking account of the spin, each band can then accommodate 2N electrons.
- If the solid is not monatomic but made of NR identical structural units (composed from a base of more atoms) that are repeated in periodic form in each band, there are NR spaces of energy. Each band can accommodate 2 NR electrons. The presence of more joined a structure atoms helps to form more bands.
- The bands are separated by gaps of energy
- At the same interatomic distance the deeper levels have their atomic wave function more localized than the outer levels. Thus their overlap is minor.
- 
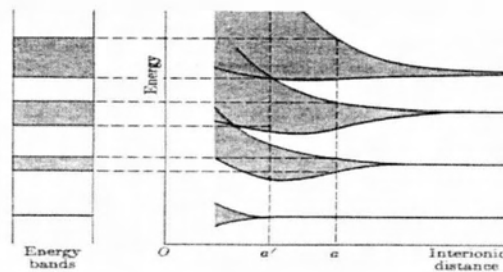


**Figure 2-6 At the same interatomic distance, wave function is more localized for deeper levels.**

- When the interatomic distance decreases under a certain limit the bands (resulting from atomic orbitals) begin to overlap. In this case, a description considering a single atomic orbital is no longer adequate

Since the inner electrons remain practically anchored to their ions, bands arising from the valence electrons are the ones that determine the physical properties of solids. On the basis of the band structure, crystals can be classified into metals, insulators, and semiconductors.

## 2.1.2 Classification of crystals

On the basis of the band structure, crystals can be classified into metals, insulators, and semi-conductors.

    – Metal

A crystalline solid is called a metal if the uppermost energy band is partly filled or the uppermost filled band and the next unoccupied band overlap in energy. Here, the electrons in the uppermost band find neighboring vacant states to move in, and thus behave as free particles. In the presence of an applied electric field, these electrons gain energy from the field and produce an electric current, so that a metal is a good conductor of electricity. The partly filled band is called the conduction band. The electrons in the conduction band are known as free electrons or conduction electrons.

    – Insulator

In some crystalline solids, the forbidden energy gap between the uppermost filled band, called the valence band, and the lowermost empty band, called the conduction band, is very large. In such solids, at ordinary temperatures only a few electrons can acquire enough thermal energy to move from the valence band into the conduction band. Such solids are known as insulators. Since only a few free electrons are available in the conduction band, an insulator is a bad conductor of electricity. Diamond having a forbidden gap of 6 eV is a good example of an insulator.

    – Semiconductor

A material for which the width of the forbidden energy gap between the valence and the conduction band is relatively small (~ 1 eV) is referred to as a semiconductor. Germanium and silicon having forbidden gaps of 0.78 and 1.2 eV, respectively, at 0 K are typical semiconductors. As the forbidden gap is not very wide, some of the valence electrons acquire enough thermal energy to go into the conduction band. These electrons then become free and can move about under the action of an applied electric field. The absence of an electron in the valence band is referred to as a hole. The holes also serve as carriers of electricity. The electrical conductivity of a semiconductor is less than that of a metal but greater than that of an insulator.
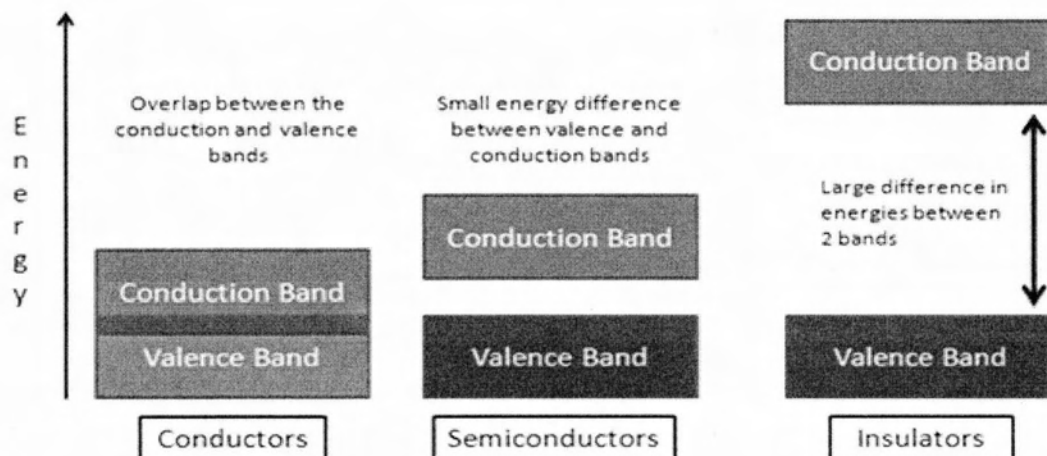


**Figure 2-7 Energy band structure of, insulators, conductors and semiconductors.**

21

## 2.2 Electrolytes

Electrolytes are substances that ionize when dissolved in suitable ionizing solvents such as water. They behave as conductors of electricity because they can transmit electric current through positively and negatively charged ions (as opposed to electrons in metals). For this reason they are classified as ionic conductors or conductors.

Electrolyte solutions are normally formed when a salt is placed into a solvent such as water and the individual components dissociate due to the thermodynamic interactions between solvent and solute molecules, in a process called solvation. For example, when table salt (sodium chloride), NaCl, is placed in water, the salt (a solid) dissolves into its component ions, according to the dissociation reaction:

$$NaCl(s) \rightarrow Na + (aq) + Cl - (aq)$$
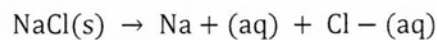
The most common electrolytes are salt, acids and basis solution such as: $Na+$, $K^+$, $Ca^{2+}$, $Mg^{2+}$, $Cl^-$, $PO_4^{3-}$ and $HCO3^-$. Some gases such as hydrogen chloride (HCl), under condition of high temperature or low pressure can also function as electrolytes. However there are some solid electrolytes that are crystalline solids. Different names are given to these materials such as:

- Solid Electrolytes
- Fast Ion Conductors
- Superionic Conductors

Some of the properties of the electrolytes are:

- ionic conductivity: is the movement of anion from one site to another through defects in the crystal lattice of a solid or aqueous solution
- colligative properties
- the PH of the solution is increased

The list of the available electrolytes has expanded with representative materials of significantly different nature and proprieties such as: liquid solutions, solid mixed oxides, polymer membranes etc. Thus for every technical application a significantly large list of candidate electrolytes exist. Electrolytic conductors are used in electronic devices where the chemical reaction at a metal/electrolyte interface yields useful effects.

- In batteries, two materials with different electron affinities are used as electrodes; electrons flow from one electrode to the other outside of the battery, while inside the battery the circuit is closed by the electrolyte's ions. Here, the electrode reactions convert chemical energy to electrical energy. [82]
- In some fuel cells, a solid electrolyte or proton conductor connects the plates electrically while keeping the hydrogen and oxygen fuel gases separated.

22

- In electroplating tanks, the electrolyte simultaneously deposits metal onto the object to be plated, and electrically connects that object in the circuit.

- In operation-hours gauges, two thin columns of mercury are separated by a small electrolyte-filled gap, and, as charge is passed through the device, the metal dissolves on one side and plates out on the other, causing the visible gap to slowly move along.

- In electrolytic capacitors the chemical effect is used to produce an extremely thin 'dielectric' or insulating coating, while the electrolyte layer behaves as one capacitor plate.

- In some hygrometers the humidity of air is sensed by measuring the conductivity of a nearly dry electrolyte.

- Hot, softened glass is an electrolytic conductor, and some glass manufacturers keep the glass molten by passing a large current through it.

Also currently used electrolytes cover range of application in the temperature range of 80-1500°C and are classified according to their natural state as follow:

- in liquid solutions for applications in low temperature fuel cells,

- in solid polymer membranes for application in low temperature, and

- in solid electrolytes for application in almost every kind of fuel cells application depends on the case

We will be looking at materials which behave as solid electrolytes, their properties and applications.

### 2.2.1  Solid electrolytes

Solid electrolytes are an unusual group of solid-state materials which have high ionic conductivity with negligible electronic conductivity. The criteria used for the successful development of a solid electrolyte are:

1) high ionic conductivity ($> 10^{-3}$ S cm$^{-1}$) which is equivalent with the requirement for minimum energy losses in the cell due to ohmic phenomena,

2) numbers of ionic transfer close to unity, i.e.

$$ t_i = (\sigma_i / \sigma_{total}) \approx 1 $$

Where $\sigma_{total} = (\sigma_e + \Sigma_i \sigma_i)$ is the sum of the conductivities of the specific ion being transferred,

3) chemical and mechanical integrity under operation

4) low cost

5) long life performance

6) Electronic conductivity near zero in order to avoid short-circuits.

Solid electrolytes exhibit higher conductivities than semiconductors ($10^{-5}$-$10^{-8}$ S cm$^{-1}$) but, obviously, lower than metals ($10^{-1}$-$10^{5}$ S cm$^{-1}$). For most of them, the dependence of their ionic conductivity on temperature can be expressed adequately through the semi-empirical equation,

$$\sigma=(\sigma_o/T)\exp(-E/K_bT)$$

where $\sigma_o$ is a function of a) the ionic valence, b) the concentration of mobile ions, c) the attempt frequency and d) the distance of ionic transition. $K_b$ and T stand for Boltzmann's constant and temperature, while the activation energy, E, usually varies between 0.5 and 2eV [83].
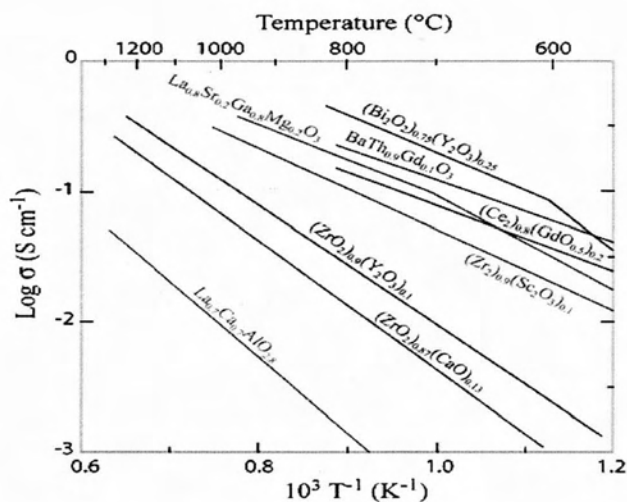


**Figure 2-8 Successful development of a solid electrolyte requires high ionic conductivity (>10$^{-3}$S cm$^{-1}$).**

### 2.2.2 Historical Background

Starting in 1800, Davy carried out many investigations into the electrolysis of water and aqueous solutions. After doing many experiments, David observed that dried solid alkali compounds were non-conductors, but became electrically conducting through just a little moisture.

Faraday, in his continuous investigation, introduced the basic terminology of electrochemistry and with the aid of many results concerning the concept "electrolyte" in 1834 he came to classification of substance into first and second types of conductors. Faraday encountered problems with the classification of silver sulfide, $Ag_2S$, which exhibited conductivities comparable to metal in the high temperature, but in contrast to metal, lost its conductivity upon cooling down. At the end in 1839 he also discovered that $PbF_2$ and $Ag_2S$ are good conductors of electricity. These solids are the first ever discovered solid electrolyte.

In 1884 Warburg demonstrated $Na^+$ conduction in glass and in 1888 he and Tegetmeier carried out the first measurements of transference number. Towards the end of 19th century the term "solid electrolyte" was in use, and many facts were known about the behavior of these materials. A technological interest in solid ion conductors first arose in connection with the development of electric lighting devices.

24

Early carbon filament lamps manufactured since about 1880 could not compete with the existing gas incandescent light. In 1897, Nernst suggested in a patent that second-class conductors in the form of a thin rod could be made electrically conducting by means of an auxiliary heating appliance and then kept glowing by the passage of an electric current.

At first Nernst mentioned only ``lime, magnesia, and those sort of substances" as appropriate conductors. Later investigations stimulated by experiences with gas mantles led to his observation ``that the conductivity of pure oxides rises very slowly with temperature and remains relatively low, whereas mixtures possess an enormously much greater conductivity, a result in complete agreement with the known behavior of liquid electrolytes". He pointed out that, for example, the conductivity of pure water and pure common salt is low but that of an aqueous salt solution is high.

In a short time many of the mixed oxides which exhibit high conductivity at elevated temperatures, including the particularly favorable composition 85% zirconia and 15% yttria, the so-called Nernst mass, were identified. Therefore Nernst invented the "Nernst glower" that is an oxide ion conductor. It follows that Nernst lamps were the first commercial produced solid electrolytes gas cells.

In 1914 Tubandt and Lorenz discovered the high $Ag^+$ conductivity in AgI at 150°C. After 1960, there was rapidly increasing number application; in fact in 1966 Kummer and Webber developed Na/S battery using $Na^+$ conductor (sodium beta conductor $\beta$-$Al_2O_3$).

In 1973 and 1978 Wright introduced the first polymers electrolyte. By 1970 the results of investigations on electrical properties and possibilities of the application of solid oxide electrolytes were already so numerous as to make them very difficult to survey. A comprehensive review by Etsell and Flengas includes 674 references. Thus, within a relatively short time, the basis was established on which the broad technologically orientated development of solid oxide fuel cells proceeds today.[84]

### 2.2.3 Ionic conductivity

Ionic conduction (denoted by $\lambda$-lambda) is the movement of an ion from one site to another through defects in the crystal lattice of a solid or aqueous solution. Ionic conduction is one mechanism of current[85]. In solids, ions typically occupy fixed positions in the crystal lattice and do not move. However, ionic conduction can occur, especially as the temperature increases.

The factors that influence the conductivity in the solid state are the concentration of charge carriers, temperature of the crystal, the availability of vacant-accessible sites which is controlled by the density of defects in the crystal and the ease with which an ion can jump to another site etc. The last of the above discussed factors, namely, the ease with which an ion can jump to a neighbouring site is controlled by the activation energy. The 'activation energy' is a phenomenological quantity. It

25

may be said to indicate the free energy barrier an ion has to overcome for a successful jump between the sites. Among the various factors that influence the ionic conductivity of a crystal the activation energy is of utmost importance since the dependence is exponential. It can be measured quiet conveniently by experiments. The activation energies are most commonly deduced using the Arrhenius expression:

$$s = (A/T)\, e\, (-Ea/KBT)$$

where s is the conductivity at temperature T in K, kB is the Boltzmann's constant, Ea is the activation energy and A is called the pre-exponential factor. The pre-exponential factor, A, contains all the remaining factors, i.e., other than the activation energy, that influences the ionic conductivity. The activation energy, Ea, may be deduced easily from the slope of the $\ln_e(sT)$ versus $T^{-1}$ plot. The random walk theory supports the above functional form of s and also de scribes A in terms of other factors that influence the ionic conduction.

The Nernst–Einstein expression relates the ionic conductivity to the diffusion coefficient of ions and is particularly useful in molecular dynamics study. The Nernst–Einstein expression suggest that the conductivity,

$$s = nq^2 D/k_\beta T$$

where n is the number of ions per unit volume, q is its charge and D the self-diffusion coefficient of ions,

$$D = zNc(1-c)a_l^2\, v/k_\beta T$$

where z is the number of nearest neighbor sites of density N, c is the concentration of ions, $\alpha_l$ the distance between the sites and n is the jump frequency given by,

$$v = v_0 \exp(-\frac{E_a}{k_\beta T})$$

where $E_a$ is the free energy barrier associated with the ion hop between two sites and $v_0$ is the cage frequency (site frequency) of the ion. The expression suggest that for high diffusivity in solids,

1.  high density of mobile ions (c),
2.  the availability of vacant sites (that can be accessed by the mobile ions) $(1-c)$,
3.  good connectivity among the sites (requiring conduction channels with low free energy (Ea) barriers between the sites).[86]

26

### 2.2.4    Defects Structure

Defects in a crystalline structure can have a tremendous effect on the behavior of a material. Point defects are primarily responsible for electrical conduction in solid electrolytes. Ionic solids contain these defects at all temperatures above 0°K. Aliovalent impurities also introduce an excessed defect whose concentration is fixed mainly by composition and is often independent of temperature. Presence of ionic defects give rise to ionic conductivity, while that of electronic conductivity, which is undesirable in a solid electrolyte. In practice, for a solid electrolyte to be useful, the ratio ionic/electronic conductivity should be 100 or greater. The total electrical conductivity ($\sigma_t$) in an electrolyte is given by the equation:

$$\sigma_t = \sum_i n_i(z_i e)\mu_i$$

Where $n_i$, $z_i$, $\mu_i$ are the concentration, valency, and mobility respectively, of the $i$ th charge carrying species and e is the electronic charge. The relationship between the structure-including defects- of solid electrolytes and their transport proprieties are examined here. The emphasis is a massively defective ionic solid (with defect concentration up to several percent) rather than those with defects at the ppm level.

The different kinds of ionic and electronic defects which may be present in an ionic solid are conveniently present using Kröger-Vink notation, which specifies the nature, location, and effective charge of a defect. The nature of point defect and their concentration in any solid are determined by the consideration of chemical equilibrium between the various species. Clustering of defect and lattice disorder take place at relatively higher defect concentration.

### 2.2.4.1    Types of Defects

The various kinds of point imperfections possible in a ionic crystal MX (M and X are monovalents) taking into account the requirement of charge neutrality, are shown below:

#### 2.2.4.1.1    Point Defects: Vacancies

Vacancies happen when an ion $M^+$ in a pure binary compound MX leaves from its normal site. A perfect crystal with regular arrangement of atoms cannot exist. There are always defects, and the most common defects are point defects. This is especially true at high temperatures when atoms are frequently and randomly changing their positions leaving behind empty lattice sites, called vacancies. In most cases, diffusion (mass transport by atomic motion), can only occur because of vacancies.
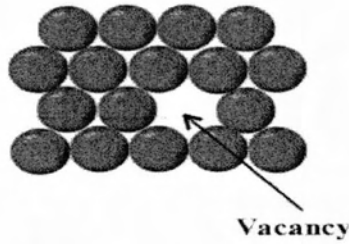
Vacancy

**Figure 2-9 Schematic illustration of a simple point vacancy defect in a monatomic solid.**

### 2.2.4.1.2    Number of Vacancies

The higher is the temperature, more often atoms are jumping from one equilibrium position to another and larger number of vacancies can be found in a crystal. Actually, the number of vacancies, Nv, increases exponentially with the absolute temperature, T, and can be estimated using the equation (Boltzmann Distribution):

$$N_v = N_s e^{-Ev/k_B T}$$

Where $N_s$ is the number of regular lattice sites, k is the Boltzmann constant, and Ev is the energy needed to form a vacant lattice site in a perfect crystal. Using this simple equation we can estimate that at room temperature in copper there is one vacancy per 1015 lattice atoms, whereas at high temperature, just below the melting point there is one vacancy for every 10,000 atoms. These are the lower end estimations, a large numbers of additional vacancies can be introduced in a growth process or as a result of further treatment (plastic deformation, quenching from high temperature to the ambient one, etc.).

### 2.2.4.1.3    Frequency of vacancies jumps

In order for an atom to jump into a vacancy site, it needs to possess enough energy (for example, thermal energy) to squeeze through its neighbors. The energy needed for this jump (Em) is called activation energy for vacancy motion. The average thermal energy of an atom is usually much smaller than the activation energy Em and a large fluctuation in energy (when the energy is "pooled together" in a small volume) is needed for a jump.



28
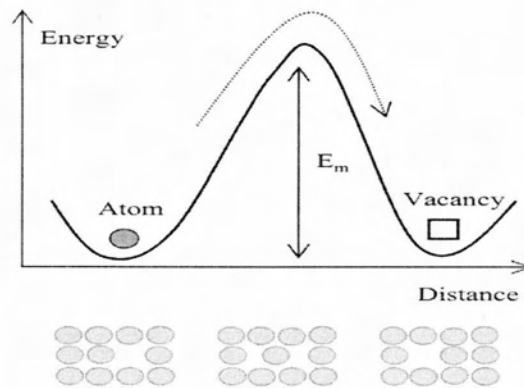
**Figure 2-10 Schematic representation of the diffusion of an atom from its original position into a vacant lattice site. Activation energy Em has to be applied to the atom so that it could break inter-atomic bonds in order to move into the new position.**

The probability of such fluctuation or frequency of jumps, Rj, depends exponentially from temperature and can be described by equation that is attributed to Swedish chemist Arrhenius:

$$R_j = R_0 e^{-Ev/k_B T}$$

Where $R_0$ is an attempt frequency proportional to the frequency of atomic oscillations.

### 2.2.4.1.4    Interstitial Defect

Interstitials are formed when an ion $M^+$ (or $X^-$) occur in an interstitial site, then the defect is $M^+$ (OR $X^-$). In other words an interstitial impurity occurs when an extra atom is positioned in a lattice site that should be vacant in an ideal structure. Since all the adjacent lattice sites are filled the additional atom will have to squeeze itself into the interstitial site, resulting in distortion of the lattice and alteration in the local electronic behaviour of the structure. Small atoms, such as carbon, will prefer to occupy these interstitial sites. Interstitial impurities readily diffuse through the lattice via interstitial diffusion, which can result in a change of the properties of a material as a function of time. Oxygen impurities in silicon generally are located as interstitials[87].



**Interstitial Atoms**
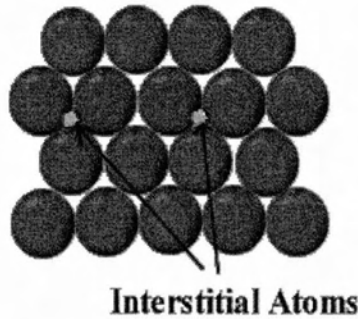
**Figure 2-11 Interstitial impurity in a crystal lattice.**

### 2.2.4.1.5    Schottky Defects

These imperfections are similar to vacancies. This defect is caused, whenever a pair of positive and negative ions is missing from a crystal. If in an ionic crystal of type $M^+X^-$ an equal number of cations and anions are missing from their lattice sites the electrical neutrality as well as stoichiometry is nevertheless maintained. It is a vacancy defect (due to missing ions) and also a stoichiometric defect, as the ratio of the number of cations and anions remains the same. It occurs only when there is small difference in size between cations and anions. This is produced as the result of the thermal incorporation of unoccupied lattice sites from the exterior of the crystal. The lattice undergoes thermal vibration and thermal expansion when the temperature is raised above $0°K$.

When it happens the pair of vacancies is incorporated in the crystal. The Schottky defect is the predominant defect in alkali halides. [88].



(a) Schottky defect      (b) Frenkel defect
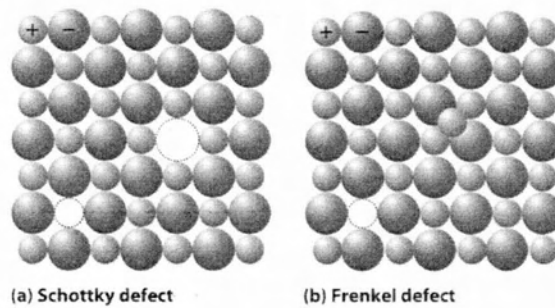
**Figure 2-12 Schottky Defects: whenever a pair of positive and negative ions is missing from a crystal, Frenkel Defects: whenever an atom or ion leaves its own lattice site vacant and instead occupies a normally vacant site.**

### 2.2.4.1.6  Frenkel Defects

The Frenkel Defect explains a defect in the molecule where an atom or ion (normally the cation) leaves its own lattice site vacant and instead occupies a normally vacant site. As depicted in the picture, the cation leaves its own lattice site open and places itself between the area of all the other cations and anions. This defect is only possible if the cations are smaller in size when compared to the anions. Silver halides generally have Frenkel defects. The number of Frenkel Defects can be calculated using the equation:

$$n = \sqrt{NN^*}e^{\Delta H/2RT}$$

where N is the number of normally occupied positions, N* is the number of available positions for the moving ion, the $\Delta H$ of formation is the enthalpy formation of one Frenkel defect, and R is the gas constant. Frenkel defects are intrinsic defects because the existence causes the Gibbs energy of a crystal to decrease, which means it's favorable to occur.[89]

### 2.2.5  Conduction mechanisms

Two types of defects important in the context of ion mobility in crystals are 'Schottky' and 'Frenkel' defect. These belong to the class of 'point defects' in crystals. Schottky defect refers to the crystal imperfection in which a pair of ions, one cation and the other an anion, disappears leaving their positions vacant. A single ion missing from its regular position, wandering in interstitial sites results in Frenkel defect. Interstitial sites have different environments, in terms of the number or type of their neighbors or its separation from the neighbors, than the regular sites. Interstitial sites, or simply interstitials, are not energetically favorable for ions; their occupancy, though, is driven by entropy enhancement discussed earlier.
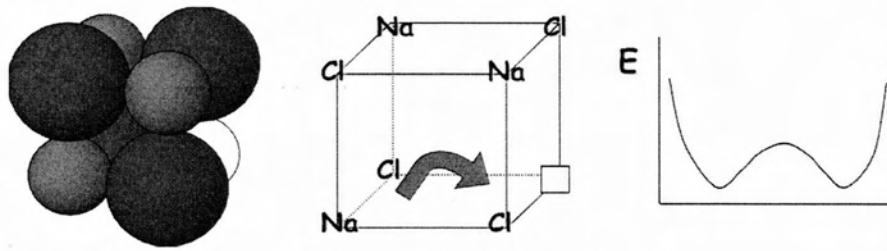
**Figure 2-13 Vacancy Migration: To get across the unit cell into the vacancy the Na+ ion must jump through the center of the cube where it squeezes by 4 Cl- and 2 Na+. The energy of this "transition state" will determine the ease of migration.**

Both Frenkel and Schottky defects result in vacant sites in the crystal and any ion in the immediate vicinity can jump to one of the vacant sites. This leaves the previous site of the ion vacant which could now host another ion. This process can lead to transport of ions across the solid giving rise to conductivity. This mechanism is termed vacancy migration. NaCl is a typical example wherein the ionic conduction is through vacancy migration.
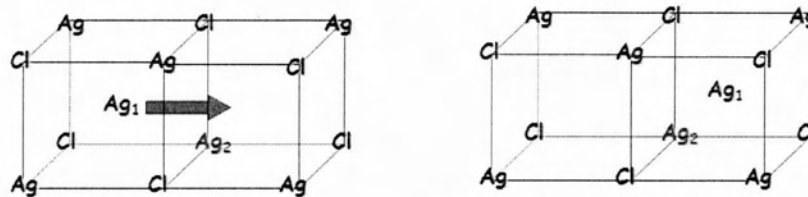


**Figure 2-14 Interstitial Migration: Vacant sites in the crystal and any ion in the immediate vicinity can jump to one of the vacant sites leaving the previous site of the ion vacant.**
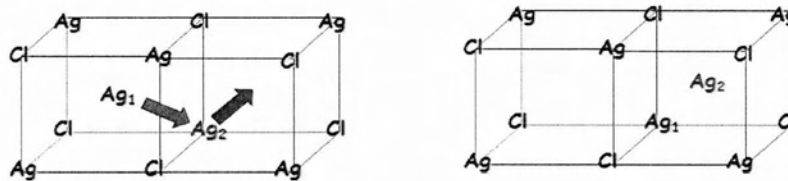


**Figure 2-15 Interstitially Diffusion Mechanism: An ion that moves to the interstitial site can subsequently jump to a neighboring interstitial site and so on.**

The ion that moves to the interstitial site, giving rise to a Frenkel defect, can subsequently jump to a neighboring interstitial site and so on, resulting in long distance motion of the ion. This mechanism is referred to as interstitial migration. Apart from these two mechanisms, there is yet another mechanism called interstitially diffusion mechanism.

This refers to the conduction mechanism through cooperative movement of two or more ions. In crystals where this mechanism is known to operate, the occupancies of the sites as well as the interstitials are such that for an ion to jump to a neighboring site or interstitial requires one or more neighboring ions to be pushed elsewhere. This is believed to be the conduction mechanism in Na-$\beta$-alumina.[86]

### 2.2.6 Types of Solid Electrolytes

All the solid electrolytes can be classified based on the mobile ions and also based on the microstructure/ phase of the solids. So, based on the mobile ions, these are classified into two different types:

1. Anionic conductors
2. Cationic conductors

### 2.2.6.1 Anionic conductors

Ionic conductors with negative ions as charge carriers are called anionic conductors. Anionic conductors do not exhibit good ionic conductivity at ambient temperature. There are two types:

a) Oxide ion conductors and

b) Fluoride ion conductors.

a. Oxide ion conductors

Motion of oxygen ion is responsible for the conduction mechanism. Most of the oxygen ion conductors show significant value of conductivity only at high temperatures (1273 K). Also, their conductivity depends strongly on the doping of aliovalent impurities ($Ca^{2+}$, $Y^{3+}$, $Sr^{2+}$, etc. in $HfO2$, $GeO_2$ etc.), which control the number of point defects and their mobility. Examples: $Bi_2Zn_{0.1} V_{0.99} O_{5.35}$, $Bi_2O_3$-$WO_3$, $ZrO_2$-$Y_2O_3$ etc.

b. Fluoride ion conductors

In general, fluoride ion is more conductive than oxide ion, because, the former is univalent even though the ionic radii of these two ions are almost the same.

Example: $CaF_2$, $SrF_2$, $KBiF_4$, $LaF_3$, Zr-Ba-CCs-F etc.[90, 91]

### 2.2.6.2 Cationic conductors

In such conductors, electrical conductivity is due to the presence of positive ions as charge carriers are called as cationic conductors. Examples are $Li^+$, $Na^+$, and $Ag^+$ etc.[92, 93]

- Lithium ion conductors

Lithium ion is the mobile carrier in the lithium superionic conducting (LISICON) compounds. The ionic radius of lithium ion is small compared to those of $K^+$ and $Rh^+$ ions. Hence, lithium compounds are having ore conductivity than $Na^+$ and $K^+$ ion conductors. Lithium compounds are useful for high energy density batteries due to their high electrochemical potential.[94] Some of the lithium ion conductors are Lil, $Li_3N$. $LiAISiO_4$, LisGaOd, $Li_4AlO_4$.

- Copper ion conductors

In these, the monovalent copper ions are the charge carriers and are responsible for the high ionic conductivity. Examples are $\alpha$-CuI, $Cu_2Cd_4$, $Cu_2HgI_4$, $Cu_2Se$. [95]

- Beta alumina conductors

One of the most extensively studied classes of superionic conductors is the group of materials having the general formula n $A_2O_3B_2O$. ($A^{3+}$ = $Al^{3+}$, $Ca^{3+}$, $Fe^{3+}$, B = $Na^+$, $K^+$, $Rb^+$, etc.). In these compounds, the conductivity is due to the motion of $B^+$ ions in the loosely packed structural planes of the crystal lattices. Such materials have been used mostly in the development of high energy density batteries. The 0 alumina superionic conductors are suitable for high temperature applications[96]. A typical example is sodium sulfur battery.

- Protonic conductors

Proton conducting solids are useful for the fuel cells, sensors, electrochromic devices, etc. Hydrogen uranyl phosphate $H_8UO_2(IO_6)_2*4 H_2O$ has been effectively employed as solid electrolytes in fuel cells. Other examples are polyamides and polysulfinimide, etc.[97]

- Silver ion conductors

In these compounds, silver ions are the mobile carriers. These solids showed high ionic conductivity at ambient temperature compared to all other types. Some examples arc: $Ag_6I_4WO_4$, $RbAg_4I_5$, $KAg_4I_5$, $NH_4Ag_4I_5$, etc.[98]

### 2.2.7 Classification of ionic conductors

Presence of disorder or defects is necessary for ionic transport in a solid. The density of defects, which is the number of defects per unit volume, in a crystal depends considerably on various factors like, the structure, the temperature, the presence of impurity ions, the nature of chemical bonding between constituent ions etc. Thus classification of ionic solids (not necessarily superionic conductors) is proposed based on the type of defect or disorder responsible for ionic conduction. One useful classification of crystalline ionic conductors by Rice and Roth is as follows:

*Type I:* These are ionic solids with low concentration of defects ~1018 $cm^{-3}$ at room temperature. These are generally poor ionic conductors like, NaCl, KCl etc.

*Type II:* Ionic solids with high concentration of defects, typically, ~1020 $cm^{-3}$ at room temperature belong to this category. These are generally good ionic conductors at room temperature and, often,

33

fast ion conductors at high temperatures. Stabilized ZrO2, CaF2 etc. are examples. The conduction mechanism in type I and II conductors is 'vacancy migration'.

*Type III:* Best superionic conductors like Na-*b*- alumina, RbAg4I5 etc. belong to this class of compounds. These solids have a 'molten' sub-lattice or 'liquid like' structure of the mobile ions whose concentration is typically 1022 cm$^{-3}$. In other words at least one type of ions constituting the crystal is highly delocalized over the sites available to them. The free energy associated with the regular sites and interstitial sites, in these solids, are very similar and hence they are almost equally favorable for occupancy of ions. The conduction mechanism in such solids is mostly 'interstitial migration' or 'interstitially diffusion migration' or a mix of both.[86]

### 2.2.8  Applications of solid electrolytes

The main applications of solid electrolytes can be distinguished for their electromotive force (EMF), or for the electrochemical ion transport through the solid electrolyte. A general criterion for classification is the way of connecting the electrochemical cell with the other components of a circuit. Principally there are two different modes of operation:

- Open circuit applications, which involves the use of passive operation of the electrochemical cell (SEP, fuel cells in normal conditions, oxygen sensors, etc.)
- Closed-loop applications, involving the use of active operation of the electrochemical cell (EIP and fuel cells at the laboratory level).
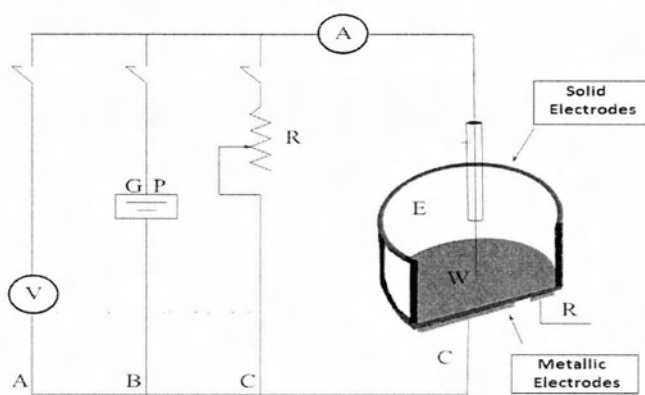


**Figure 2-16 Representation of principal applications of solid electrolytes in heterogeneous catalysis.**

- A. Solid electrolyte potentiometry (SEP)
- B. Electrochemical ion pumping (EIP)
- C. Fuel Cells (S.O.F.C)

In circuit A, a voltmeter is connected between the anode and the cathode of the cell and measures the voltage drop. However because of high resistance (theoretically infinite), the circuit is traversed

34

by a minimum current (basically nothing). The technique that has been developed for this connection is called solid electrolyte potentiometry (SEP) and is used in gas sensors.[83]

In circuit B, a source of electricity and an ammeter are connected at the ends of the cell (galvanostat - potentiostat). The technique for this connection is called electrochemical ion extraction (Electrochemical Ion Pumping - EIP) and is used mainly in the solid electrolyte membrane reactors.

In circuit C, an electricity consumption devise and an ammeter are connected at the ends of the cell (ohmic resistance).The ammeter is used to measure the electrical current flowing through the circuit. This connection is used for laboratory level fuel cells and it is an active operation of the electrochemical cell (Solid Oxide Fuel Cell - SOFC).

Many solid electrolytes, anionic or proton conductors have been studied for various electrochemical applications due to extraordinary ionic conductivity that they manifest at high temperature. Many devices were developed to operate as batteries at high temperatures, such as fuel cells that use stabilized zirconia oxide yttrium as solid electrolyte in oxygen concentration.

The required properties of the solid electrolyte depend on their applications: high ionic conductivity is an indispensable feature for the achievement of high or power-efficient devices that exclusively convert energy such as batteries and fuel cells, and not an essential requirement for sensors that convert chemical information into physical quantities. [83, 99]

### 2.2.8.1 Gas Sensors

The principle operations of an instrument able to provide the measure of a size are based on three stages:

1. Detect the quantity to be measured
2. Change the signal obtained from the detecting so that it can be sent to third stage
3. Represent the results of previous operations in an appropriate manner.

The first stage of the measurement chain is constituted by the element that detects the physical quantity that is measured and in general, defines the sensor as it is sensitive to this magnitude. Generally a sensor is defined as a device able to provide an output signal in response to a specific input signal. The output is always an electrical quantity while the input can be any quantity, physical-chemical property or condition.

The sensors can be classified according to:

- input
- operating principle of the transducer
- materials
- applications
- cost
- accuracy

Usually, they are classified according to the input signal and for this reason they can be distinguished into mechanical, thermal, magnetic, optical, chemical, biochemical, etc. sensors.

### 2.2.8.1.1    Electrochemical sensors

The basic components of an electrochemical sensor are a working electrode (or sensitive), a counter electrode, and usually a reference electrode. These electrodes are in contact with an electrolyte that may be liquid or solid. The gas diffuses into the sensor to the working electrode and an electrochemical reaction takes place (oxidation or reduction depending on the nature of the gas). For example CO can be oxidized to $CO_2$ and $O_2$ can be reduced to $H_2O$.

When oxidation reaction takes place, a flow of electrons from working to counter electrode, through the external circuit, begins. On the other hand, for reduction reaction, electrons flow from counter electrode to working electrode. This flow of electrons is a current that is proportional to the concentration of the gases (Nernst equation).[83]

Many gas sensors based on solid electrolytes have been proposed, both for environmental monitoring that for automotive applications. The proposed devices are either potentiometric (the output of the sensor is an electromotive force) or amperometric (the output of the sensor is a current).Depending on the type of electrochemical relationship between the solid electrolyte and the gas to be detected, the sensors can be classified as:

**Type I** sensors that have an electrolyte which contain mobile ions of the chemical species from the gas that is monitored. The commercial product, YSZ oxygen sensor,[100] is an example of type I.

**Type II** sensors that have an electrolyte with no mobile ions of the chemical species from the monitored gas, but an ion related to the target gas which can be diffused in the solid electrolyte to allow equilibration with the atmosphere. Therefore, type I and type II sensors have the same design with gas electrodes combined with a metal and an electrolyte where oxidized or reduced ions can be electrochemically equilibrated through the electrochemical cell.

In the third type of electrochemical sensors, auxiliary phases are added to the electrodes to enhance the selectivity and stability.

**Type III** sensors make the electrode concept even more confusing. With respect to the design of a solid state sensor, the auxiliary phase seems as part of the electrode. However, it cannot be an electrode because auxiliary phase materials are not generally good electrical conductors. In spite of this confusion, type III design offers more feasibility in terms of designing various sensors with different auxiliary materials and electrolytes.

Oxygen sensors belong to **type I**. They have been important in various applications for determining oxygen contents of gases and liquids. Most of them are fabricated from a tube of an oxide ion

36

conductor such as yttria-stabilised zirconia (YSZ), bismuth oxide (in oxidizing environments) or thoria (in reducing environments).[101]

As it can be seen from Fig. 2-17, one of the compartments contains a reference gas, e.g. air, $O_2$, or a metal-metal oxide mixture such as Ni-NiO.
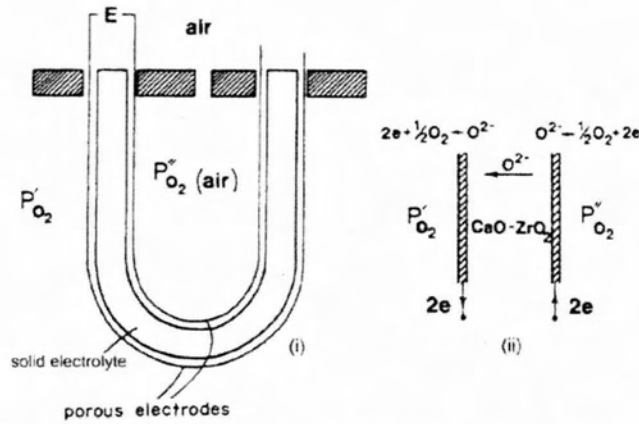


**Figure 2-17. The tube is coated with inner and outer electrodes of porous Pt and the potential difference that develops between the electrodes may be related to the difference in oxygen partial pressure in the two compartments.**

The oxygen sensor works on the principle of a concentration cell in which the conductor of oxygen ions (the stabilized zirconia) acts as a solid electrolyte and separator two compartments with gas mixtures at different partial pressure of oxygen. In the potentiometric sensor is a galvanic cell of the type:

$$O_2, Pt^I \mid YSZ \text{ (conductor } O^{2-}) \mid Pt^{II}, O_2$$
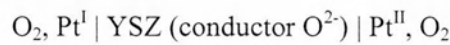
At sensitive and reference electrode takes place electrochemical reaction, promoted by the catalytic effect of Pt:

$$\tfrac{1}{2} O2 + 2 e (Pt) \rightarrow O_2\text{- (YSZ)}$$
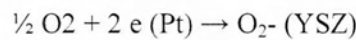
The difference between the partial pressures of oxygen sensitive electrode and reference gives rise to an electromotive force (EMF) given by the Nernst equation:

$$E = \frac{RT}{4F} ln \frac{pO_2^{II}}{pO_2^{I}}$$

where F, R, T are the Faraday constant, the universal constant of gas and the absolute temperature, and $p_{O2}^{II}$ and $p_{O2}^{I}$ are respectively the partial pressures of oxygen at the interface II and I. In this

way, measured EMF, note the $p_{O_2}^{I}$ (the partial pressure of oxygen at the interface reference), it is possible to calculate the $p_{O_2}^{II}$ using the previous formula.

Oxygen sensors are used commercially for monitoring gas compositions in combustion-plant and metallurgical processes and for determining the amount of oxygen dissolved in molten metals. They are also used in car exhaust systems ($\lambda$ probe) to help optimize the fuel: air ratio.[102]

### 2.2.8.2  Fuel cells

Fuel Cells, (FCs) are electrochemical devices that convert the chemical energy of the reaction directly into electrical energy. The basic structure of a fuel cell consists of an electrolyte in contact with a porous anode and a cathode.[103]
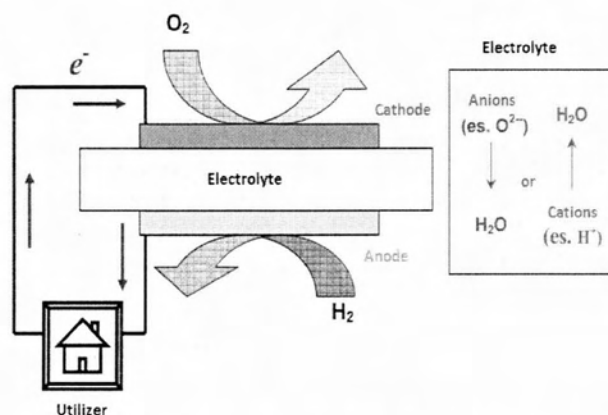


**Figure 2-18 Schematic representation of a Fuel Cell .The fed gases here are H$_2$ and O2. The movement directions of the possible types of charge involved (electrons and ions), the latter potentially cations or anions depending on the characteristics of the considered cell are presented.**

The fuel feeds the anode while the oxidant, usually the oxygen presented in the air, feeds the cathode in a continuous way. The electrochemical reaction produces electricity current at the electrodes. Therefore it is crucial to emphasize that the FCs differ in various aspects from the classical batteries. In fact the fuel cell has the advantage of producing electricity as long as the electrodes are fed with the proper gases.

As for the principles of the operation, the fuel and the oxidant gas, penetrate through the anode and the cathode, which are generally positioned on opposite faces of the electrolyte. The electrical energy is generated by electrochemical oxidation of the fuel and the electrochemical reduction of oxidant. The oxide - reduction reactions are necessary for the operation of the cell and it can only take place at the interphase ternary, where the gas phase (gas power) and solid (electrode, electrolyte) coexist, and these areas are commonly indicated as TPBS (Triple Phase Boundaries). The electrolyte closes the electrical circuit and conducts the ionic charge between the electrodes as shown in Figure 2-18. It also constitutes as a physical barrier that prevents direct contact between

the oxidant and the fuel. Therefore, unlike the electrodes, the electrolyte must have morphological characteristics of absolute density.

The porous electrodes must be able to:

- Have accessible active sites where ionization or deionization reactions can take place
- Transport the electrons to / from the external circuit through the bulk
- Transport ions from TPB to the electrolyte.

Therefore, the electrode material must be catalytically active, conductive and porous in order to optimize the efficiency of the reactions. The FCS can be divided into cells operating at high temperature (High-Temperature Fuel Cells), operating between 500 and 1000°C and cells operating at low temperature (Low-Temperature Fuel Cells), which operate under 500°C. Another subdivision can be made on the basis of the nature of the electrolyte and for this reason we can distinguish principally six different types of cells.
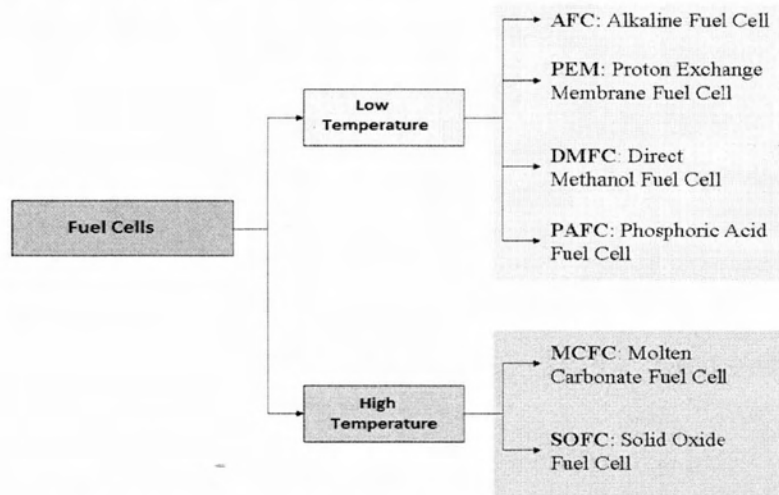


**Figure 2-19 A classification scheme which takes into account the temperature and the nature of the electrolyte.**

### 2.2.8.3    Solid oxide fuel cells

The solid oxide fuel cells (SOFC) are composed of two porous electrodes separated by a solid electrolyte which is able to transport ions ($O^{2-}$or $H^+$), depending on whether it is an anionic or proton conductor. The porosity of the electrodes is necessary in order to ensure a good diffusion of gases, and also to obtain good energy efficiency. It is necessary that the electrolyte material between the electrodes not to be in contact with the gas, because then the gases would react with each other without producing a current. The two types of used electrolytes (that transport $O^{2-}$or $H^+$), differ for the side in which water is produced. In anionic cells the water is produced on the interface electrolyte-anode, where the fuel is fed, while in protonic cells the water is produced at the interface electrolyte-cathode, where the oxidizer has access. Furthermore, in the last type of cells, gases such as CO cannot be used as fuel, because they quickly poison the material of the anode[83].
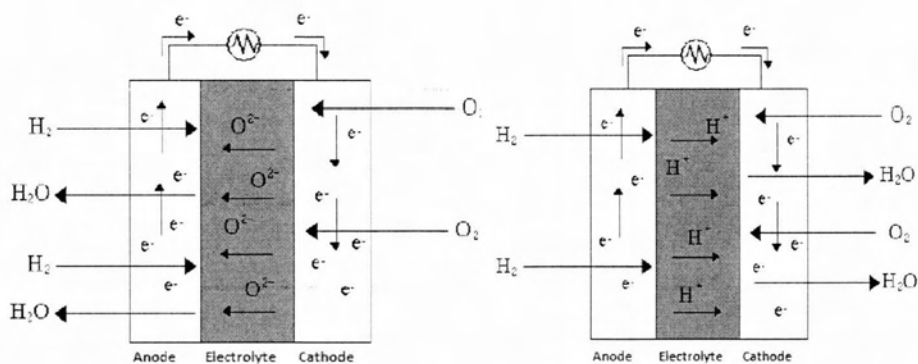
**Figure 2-20 Schematic representation of anionic and cationic fuel cells.**

The most used materials in these systems are:

- zirconia stabilized with yttrium (YSZ) as electrolyte

- mixed oxides based on LaMnO3 as cathode

- metallic nickel as anode

SOFCs have several technical advantages compared to other types of FCs. In fact they use non-precious metals and stable solid electrolytes, which eliminate the problems of corrosion and evaporation, reducing this way the costs of management of the entire system. Particularly advantageous is also the versatility of the system to operate with different fuel. Theoretically any gas which has the capacity to reduce or oxidize, can possible be used as fuel or oxidant in a SOFC. The $O_2$ is the most common oxidant, because it is cheap and available in the air. The $H_2$ is currently the most used fuel, because it has high reactivity and high calorific value, and also it can be easily produced by common fuels such as hydrocarbons and alcohols.

### 2.2.8.4 Electrochemical Ion Pumping

Another important application of solid electrolytes is Electrochemical Ion Pumping (EIP). Unlike the SEP in which the solid electrolyte is used in a passive way to measure the voltage, the EIP technique requires a voltage or an external current that allows the passage of ions through the solid electrolyte. In general ion pumping devices are used to separate a compound from a gaseous mixture and to make oxidation, hydrogenation and dehydrogenation reactions. The main techniques of EIP are[83]:

- Electrochemical Oxygen Pumping, EOP
- Electrochemical Hydrogen Pumping, EHP

The first is the most diffused, while the second is more recent because the protonic conductors at high temperature were discovered only in 1980. The ion pumping device consists of three electrodes:

1. working electrode, usually the catalyst,

2. measuring or counter electrode

3. reference electrode

The reactors used for this technique can be classified according to the arrangement of the electrodes, in fact we have:

- Single chamber reactor: in which all three electrodes are in contact with the same gas mixture. This cell does not provide separate feed in two chambers. The solid electrolyte disk is suspended in a flow of the reacting mixture. A big advantage of the single chamber cell is that it is easy to apply to existing catalytic processes since it does not require reactants to be separated. The solid electrolyte can simply replace the conventional catalyst support.
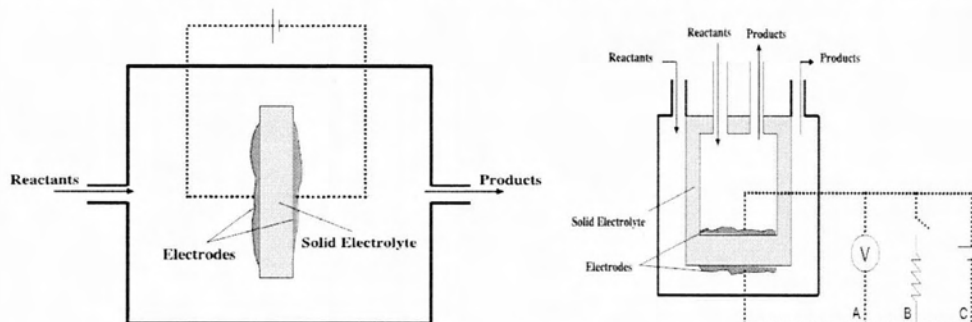


**Figure 2-21 Schematic representation of single and double chamber reactors.**

- Double chamber reactor: a typical configuration of a solid electrolyte cell, in which anode and cathode are separated so that each of them can be exposed to different gaseous mixtures. The cell consists of a dense solid electrolyte membrane and two or three porous electrodes. The working electrode is exposed to the reacting mixture. The cell may operate either in the open-circuit or in the closed-circuit mode. In the open-circuit operation, there is no net current through the electrolyte. The difference in chemical potential is converted into the open-circuit electromotive force of the cell. Catalytic data can be combined with potentiometric open-circuit measurements in order to elucidate the reaction mechanism.

This technique, named solid electrolyte potentiometry (SEP), has been used in the study of several important catalytic systems. In the closed-circuit operation, the conducting ion travels from one electrode to the other where it reacts with the gaseous content of that chamber. One of the advantages of EMRs is that they can operate in a temperature range within which reaction rates attain values of practical interest. If, in an industrial process, useful compounds and electrical energy are cogenerated, such a process would be much more attractive. This concept, named chemical cogeneration (CHECOG), has been demonstrated in a large number of reactions including the conversion of $NH_3$ to $NO$, $H_2S$ to $SO_2$, $C_2H_6$ to $C_2H_4$ and $CH_4$ to synthesis gas[83].

Providing a current, I, or a potential, V, through a current generator, the oxygen will begin to flow in the form of ions from the cathode to the anode. Oxygen flow can be estimated through the Faraday's equation:

$$F_{O_2} = \frac{I}{n \cdot F} = \frac{I}{4 \cdot F} \qquad \text{mol } O_2 \cdot s^{-1}$$

In which, n is the number of electrons involved in the charge transfer (for the case of $O_2$ is equal to 4). This equation is valid assuming that the number of ionic transport is equal to unity. Otherwise the number of ion transport $t_o$ is introduced into the equation:

$$F_{O_2} = \frac{I}{4 \cdot F} \cdot t_o \qquad \text{mol } O_2 \cdot s^{-1}$$

A thin catalyst layer (typical film thickness: 3-30 mm) is connected with a metallic wire in order or to provide/remove electrons. The film should be porous enough so that its surface is catalytically active as long as it's in contact with the gaseous phase. The surface area and the porosity of the catalyst film depend largely on the temperature during sintering process. Another important parameter during the preparation of the catalyst is the thickness of the surface area which must be sufficiently small in order to avoid external or internal mass transfer phenomenon at the desired temperature range.

The reference electrode must be polarized the lowest possible, so that equilibrium is re-established fast enough at the charge transfer reaction. The same should also apply to the counter electrode. High polarization on the counter electrode would have resulted in a large proportion of the applied voltage to be consumed on the counter electrode rather than the working electrode which is what really interests. Therefore the sintering temperature of counter and reference electrodes should be lower than the sintering temperature of the working electrode.

The use of the Electrochemical Ion Pumping technique has shown that irreversible changes can be caused on the electrochemical properties of the electrolyte. This technique can therefore lead to complex phenomena, the occurrence of which depends mainly on the following:

• The nature of the electrode (porosity, grain size, etc..).
• The nature of the electrolyte.
• The composition of the mixture of reactants.
• The ratio of the catalyst surface to the surface area in which the transfer of ions .
• The operating temperature.
• The mechanism of the reaction.

Finally it should be noted that one of the effects that Electrochemical Ion Pumping technique can lead is the NEMCA effect (Non-Faradaic Electrochemical Modification of Catalytic Activity).

## 2.3    Electrochemical Thermodynamics and Kinetics

The spectacular development of the scientific field of solid electrolytes in recent years, has led to great interest in technological applications such as in a fuel cells, SEP and EIP techniques. Both methods use the potential of the solid electrolytes during their application. In fact, most of the electrochemical relations used for aqueous electrolytes are valid for solid electrolytes as well. Therefore, if a metal electrode is in contact with a solid electrolyte, a potential difference will be developed at the metal - electrolyte interface in analogy to what happens in the case of an electrode in contact with a liquid electrolyte. Thus an exchange of electrons and ions occurs between metal and solid electrolyte.

If the circuit is open the system reaches an equilibrium state. At this point, the potential can be calculated using the Nernst equation, while if the circuit is closed, inside the cell, a different potential is established. In the latter case, other parameters have to be considered.[83]

### 2.3.1    Nernst Equation (Thermodynamics)

The Nernst equation describes the electrochemical equilibrium distribution of an ion between two compartments that are separated by a membrane that contains channels selective for that ion. In an ideal case, the membrane separating the two compartments allows only the passage of the ion of interest and no other ion. The distribution of the ion across the membrane is governed by the ion concentration gradient across the membrane and leads to the establishment of a potential difference across the membrane. At equilibrium, this potential difference is described by the Nernst equation, and is referred to as the equilibrium potential ($V_{eq.}$) or Nernst potential for that ion[104].

The Nernst equation can be derived based on simple thermodynamic principles. The maximum useful work which can be accomplished by the reaction is equal to the change in the Gibbs free energy. At constant temperature and pressure the change in Gibbs free energy is given by the chemical potentials. The chemical potential of compound A is given by[105]:

$$\mu_A = \mu_A^o + RT ln[A]$$

where [A] is the concentration (activity) of A and $\mu_A^o$ denotes the standard chemical potential. If a redox reaction is written as:
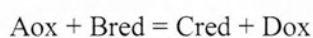
$$Aox + Bred = Cred + Dox$$

The change of free energy is given by the following equation:

$$\Delta G = \mu_{Cred}^o + RT ln[Cred] + \mu_{Dox}^o + RT ln[Dox] - \mu_{Aox}^o - RT ln[Aox] - \mu_{Bred}^o - RT ln[Bred]$$

which can be written as

$$\Delta G = \Delta G^\circ + RTln\frac{[C][D]}{[A][B]} = \Delta G^\circ + RTlnQ$$

In electrochemical processes the work done by the displacement of charged particles equals to the product of voltage and charge. In the ideal case this is equal to the maximum useful work of the reaction.

$$\Delta G = \Delta G^\circ + RTlnQ = zFE$$

where z is the number of moles of participating electrons, F is the Faraday number (charge of 1 mole of electrons, 96500 Coulomb). The standard Gibbs free energy change can also be calculated from the standard electrode potentials:

$$\Delta G^\circ = -zFE^\circ = -zF(\varepsilon_1^O - \varepsilon_2^O)$$

$\varepsilon_1$ and $\varepsilon_2$ are the standard electrode potentials of the half-reactions:

$$Cred = Aox + ze^-$$

$$Bred = Dox + ze^-$$
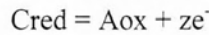
Thus, the general form of the Nernst equation is:

$$-zFE = -zFE^\circ + RTlnQ$$

$$E = E^\circ - \frac{RT}{zF}lnQ$$

That, at room temperature (25 °C) and using demical logarithm, can be written as:

$$E = E^\circ - \frac{0.059}{z}logQ$$

### 2.3.2 Electrochemical Kinetics – Electrode Overpotential.

Thermodynamics defines the maximum equilibrium potential established in a fuel cell according to the Nernst equation. However, kinetic analysis of the processes of charge transfer taking place at the gas/electrode or electrode/electrolyte interfaces reveals potential losses that render Nernst potential unattainable in practice. These potential losses, usually termed as "overpotentials".

44

Overpotential is the potential difference (voltage) between a half-reaction's thermodynamically determined reduction potential and the potential at which the redox event is experimentally observed, and it can be classified as follows:

- **activation overpotential** ($\eta_{act}$) – due to slow charge transfer processes in the interfaces,
- **resistance overpotential** ($\eta_o$) – equal to the product of the current intensity, I, and the overall ohmic resistance, R, of the cell, and
- **concentration overpotential**, ($\eta_{conc}$) – due to the concentration gradient of the reactants and products on the catalytic surfaces[83]

## • Activation overpotential

The activation potential is the potential difference above the equilibrium value required to produce a current that depends on the activation energy of the redox event. While ambiguous, "activation overpotential" often refers exclusively to the activation energy necessary to transfer an electron from an electrode to an analyte. This sort of overpotential can also be called "electron transfer overpotential" and is a component of "polarization overpotential", a phenomenon observed in cyclic voltammetry and partially described by the Cottrell equation.

### • Reaction overpotential

Reaction overpotential is an activation overpotential that specifically relates to chemical reactions that precede electron transfer. Reaction overpotential can be reduced or eliminated with the use of electrocatalysts. The electrochemical reaction rate and related current density is dictated by the kinetics of the electrocatalyst and substrate concentration.

The platinum electrode, common to much of electrochemistry is electrocatalytically involved in many reactions. For example, hydrogen is oxidized and protons are reduced readily at the platinum surface of a standard hydrogen electrode in aqueous solution. Substituting an electrocatalytically inert glassy carbon electrode for the platinum electrode produces irreversible reduction and oxidation peaks with large overpotentials.

## • Resistance overpotential

Resistance overpotentials are those tied to a cell design. These include "junction overpotentials" that occur at electrode surfaces and interfaces like electrolyte membranes. They can also include aspects of electrolyte diffusion, surface polarization (capacitance) and other sources of counter electromotive forces.

45

## • Concentration overpotential

Concentration overpotential spans a variety of phenomena that involve the depletion of charge-carriers at the electrode surface. Bubble overpotential is a specific form of concentration overpotential in which the concentration of charge-carriers is depleted by the formation of a physical bubble. The "diffusion overpotential" can refer to a concentration overpotential created by slow diffusion rates as well as "polarization overpotential", whose overpotential is derived mostly from activation overpotential but whose peak current is limited by diffusion of analyte.

The potential difference is caused by differences in the concentration of charge-carriers between bulk solution and the electrode surface. It occurs when electrochemical reaction is sufficiently rapid to lower the surface concentration of the charge-carriers below that of bulk solution. The rate of reaction is then dependent on the ability of the charge-carriers to reach the electrode surface.

## • Bubble overpotential

Bubble overpotential is a specific form of concentration overpotential and is due to the evolution of gas at either the anode or cathode. This reduces the effective area for current and increases the local current density. An example is the electrolysis of an aqueous sodium chloride solution—although oxygen should be produced at the anode based on its potential, bubble overpotential causes chlorine to be produced instead, which allows the easy industrial production of chlorine and sodium hydroxide by electrolysis.

### 2.3.2.1  Butler Volmer Equation

The Butler-Volmer equation is one of the most fundamental relationships in electrochemistry. It describes how the electrical current on an electrode depends on the electrode potential, considering that both a cathodic and an anodic reaction occur on the same electrode. We consider a model reaction, for the ion transfer at the electrode metal /electrolyte, to demonstrate the Butler-Volmer equation:

$$M_\alpha^+ \leftrightarrow M_b^+$$
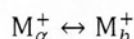
The rate constants of the reactions, which take place at the electrodes, are functions of the change in Gibbs free energy according to:

$$k_{a,c} = Z e^{-\Delta a,c G/RT}$$

According to the Butler-Volmer model the free energy is a function of electrode potential, in fact we can write that:

$$\Delta_c G = \alpha n F E + \Delta_c G_o$$

46

$$\Delta_a G = -(1 - \alpha)nFE + \Delta_c G_o$$

where α is a symmetry factor (transfer coefficient, its value is between 0 and 1, typically 0.5).Taking appropriate considerations on the reaction rates and intensity current ,we can write the defined Butler-Volmer equation:

$$I = Ai_o \left\{ e^{\frac{\alpha_a nF(E-E_{eq})}{RT}} - e^{\frac{-\alpha_c nF(E-E_{eq})}{RT}} \right\}$$

Where: I: measured current, A: electrode surface area ($cm^2$), $i_0$: exchange current density (mA $cm^{-2}$), E: electrode potential (V), Eeq: equilibrium potential, T: absolute temperature (K), n: number of electrons involved in the electrode reaction, F: Faraday constant (96485 C $mol^{-1}$), R: universal gas constant (8.314 J $mol^{-1}$ $K^{-1}$), $\alpha_a$: so-called anodic charge transfer coefficient (dimensionless), $\alpha_c$: so-called cathodic charge transfer coefficient (dimensionless) and $E-E_{eq}$ = η (V): activation overpotential. At values of positive or negative overpotential typically greater than ±10 mV one term from the Butler-Volmer equation is usually more significant than the other and the lower contributing term can be ignored. The resulting forms are known as the cathodic and anodic Tafel equations .
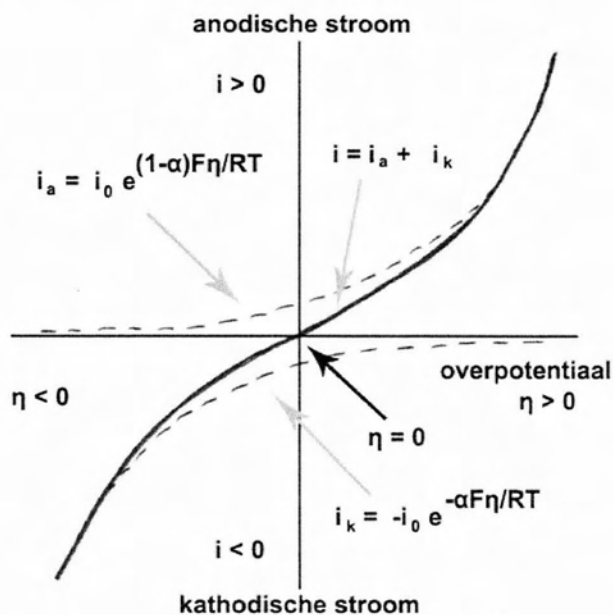


**Figure 2-22 Butler-Volmer dependence of the electrode current on overpotential η=E-Eeq. The anodic and cathodic currents are shown as ia and ik, respectively. The total current i=ia+ik.**
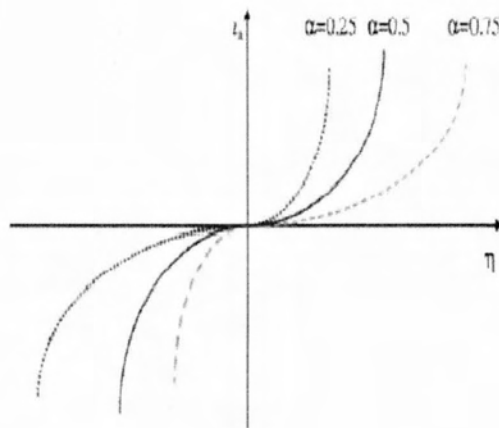
**Figure 2-23 The effect of the value a<sub>c</sub> on the current density. a) ac=0.25: oxidation favored; (b) ac=0.5:symmetric; (ac=0.75: reduction favored.**

### 2.3.2.2 Tafel Equation

The Tafel equation links the overpotential of the electrode to the current, in conditions far from equilibrium state. The equation can be written as:

$$I = I_o \exp[\frac{aF\eta}{RT}]$$

$$lni = lni_0 + \frac{aF\eta}{RT}$$

Rewriting the equation in logarithmic form gives:

$$\log i = \log i_0 + \frac{aF}{2,3RT}\eta$$
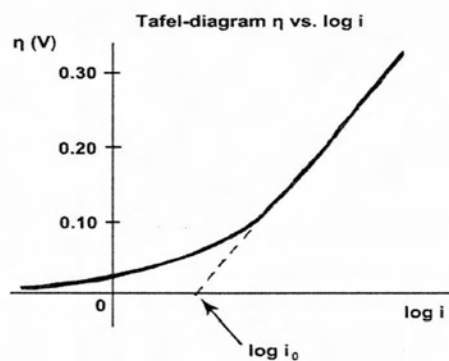


**Figure 2-24 Tafel-diagram n vs logi for an anodic process. The exchange current density is calculated from the intercept at y-axis.**

Alternatively, the Tafel equation can be presented in the following equation:

$$n = a + b\log i$$

48

where 'a' and 'b' are related to a y-axis intercept and the measured slope, respectively of a current density (logarithmic scale) *vs.* overpotential plot. From Tafel plot (log *vs.* η) two significant kinetic parameters can be derived:

- the exchange current density ( $i_0$ )-value that give relative rates of reaction at equilibrium being calculated from the intercept at y-axis and

- charge transfer coefficient ($a_A$ or $a_C$)-that gives valuable information regarding the mechanism of a reaction and indications as to the identity of a rate-determining step of the overall reaction scheme.

In this paper, three different catalysts: i) copper (Cu), ii) a cobalt (Co) and iii) iron (Fe) applied in cationic conductor $BaCe_{0.5}Zr_{0.3}Y_{0.08}Yb_{0.08}Cu_{0.04}O_3-\delta$ will be studied. From the experimental data, electrochemical parameters $I_o$, $a_A$ and $a_C$ will be exported. Then we'll be able to calculate the activation energy E (E=-aFn), the energy barrier that a reaction should overcome in order to proceed. The reactions we are interested in are the electrochemical reduction of $CO_2$ and promotion of $H_2$ .With these values we will be able to find which catalyst of those three is better.

# CHAPTER III

## Carbon dioxide hydrogenation:

## A Thermodynamic analysis

In the first part of this chapter the theoretical background of the thermodynamics applied to the study of carbon dioxide hydrogenation is investigated.

The first method used is based to the reaction equilibrium constant calculation as a function of the temperature, while the second one is based on the free energy Gibbs minimization.

In the second part of the chapter, the obtained results (based on the simple thermodynamic constant calculation and the method of free energy Gibbs minimization) are compared.

# 3 Carbon dioxide hydrogenation

## 3.1 Introduction

It is known that the thermodynamic analysis of a reaction could provide the compositions of the products which can be composed under equilibrium conditions. According to the thermodynamic analysis, the hydrogenation of carbon dioxide could theoretically provide a plurality of products such as:

- hydrocarbons (methane - $CH_4$, ethane - C2H6, etc.)
- alcohols (methanol - $CH_3OH$, C2H5OH ethanol etc.)
- carbon monoxide (CO) , water ($H_2O$) etc.

More precisely by using this analysis at different temperatures and pressures the expected values of compositions of products can be determined

## 3.2 Part One – Theory

### 3.2.1 Reaction Coordinate

The general chemical reaction is:

$$|v_1|A_1 + |v_2|A_2 + \cdots + |v_3|A_3 + |v_4|A_4 + \cdots$$
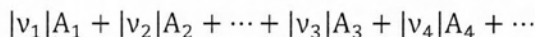
**Equation 3.1**

Where $|v_i|$ is a stoichiometric coefficients and $A_i$ stands for a chemical formula. $v_i$ itself is called a stoichiometric *number* and by the sign convention it is positive (+) for a product and negative (-) for a reactant.

Thus for the reaction, $\quad CH_4 + H_2O \rightarrow CO + 3H_2$

the stoichiometric numbers are :

$$vCH_4 = 1 \quad vH_2O = -1 \quad vCO = 1 \quad vH_2 = 3$$

**Equation 3.2**

The stoichiometric number for an inert species is zero.

As the reaction represented by Equation 3.1 progresses, the *changes* in the numbers of moles of species present are in direct proportion to the stoichiometric numbers. Thus for the preceding reaction if 0.5 mol of $CH_4$ disappears by reaction, 0.5 mol of $H_2O$ also disappears; simultaneously 0.5 mol of CO and 1.5 mol of $H_2$ are formed. Applied to a differential amount of reaction this principle provides the equations:

$$\frac{dn2}{v2} = \frac{dn1}{v1} \qquad \frac{dn3}{v3} = \frac{dn1}{v1} \qquad etc$$

The list continues to include all species. Comparison of these equations yields:

$$\frac{dn_1}{\nu_1} = \frac{dn_2}{\nu_2} = \frac{dn_3}{\nu_3} = \frac{dn_4}{\nu_4} = \cdots = d\varepsilon$$

**Equation 3.3**

The general relation connecting the differential change dni with dε is therefore:

$$dn_i = \nu_i \, d\varepsilon$$

**Equation 3.4**

This new variable $\varepsilon$, called reaction coordinate, characterizes the extent or degree to which a reaction has taken place. The definition of ε itself depends for a specific application on setting it equal to zero for the initial state of the system prior to reaction. Thus, integration of Equation 3.4 from an initial unreacted state where ε=0 and $n_i = n_{io}$ to a state reached after an arbitrary amount of reactions and summation of all species yields gives:

$$n = n_0 + \nu\varepsilon$$

where

$$n \equiv \sum n_i \qquad n_0 \equiv \sum n_{i0} \qquad \nu \equiv \sum \nu_i$$

Thus the mole fraction $y_i$ of moles of the species are related to ε by:

$$y_i = \frac{n_i}{n} = \frac{n_{i0} + \nu_i \varepsilon}{n_0 + \nu\varepsilon}$$

**Equation 3.5**

When two or more independent reactions proceed simultaneously, subscript j serves as the reaction index. A separate reaction coordinate $\varepsilon_j$ a apples to each reaction. The stoichiometric numbers are doubly subscripted to identify their association with both a species and a reaction. Thus $\nu_{i,j}$ designates the stoichiometric number of species i in reaction j. Now the mole fraction becomes:

$$y_i = \frac{n_{i0} + \sum_j \nu_{i,j}\varepsilon_j}{n_0 + \sum_j \nu_j\varepsilon_j}$$

**Equation 3.6**

52

### 3.2.2   Chemical Equilibrium

The total Gibbs energy of a closed system at constant T and P must decrease during an irreversible process. The condition for equilibrium is reached when $G^t$ attains its minimum value. At this equilibrium state:

$$(dG^t)_{T,P} = 0$$

**Equation 3.7**

Thus if a mixture of chemical species is not in chemical equilibrium, any reaction that occurs at constant P and T must lead to decrease in the total Gibbs energy of the system. The significance of this for a single chemical reaction is seen in Figure 3-1 which shows a schematic diagram of $G^t$ vs $\varepsilon$, the reaction coordinate. Because $\varepsilon$ is the single variable that determinates the progress of the reaction, and therefore the composition of the system, the total Gibbs energy at constant P and T are determined by $\varepsilon$. The arrows along the curve in Figure 3-1 indicate the directions of changes in $(dG^t)_{T,P}$ that are possible on account of reaction. The reaction coordinate has its equilibrium value $\varepsilon_e$ at the minimum of the curve. The meaning of Equation 3.7 is that differential displacements of the chemical reaction can occur at the equilibrium state without causing changes in the total Gibbs energy of the system.
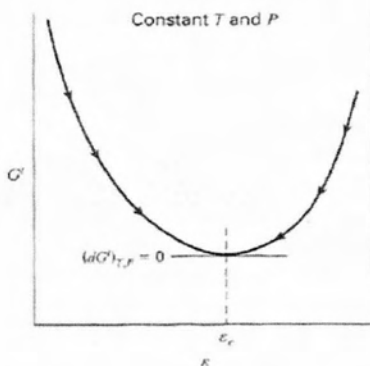


**Figure 3-1 The total Gibbs energy in relation to the reaction coordinate.**

Figure 3-1 indicates the two distinctive features of the equilibrium state for given T and P:

a)   The total Gibbs energy $G^t$ is a minimum

b)   Its differential is zero

Each of these may serve as a criterion of equilibrium. Thus, we may write an expression for $G^t$, as a function of $\varepsilon$ and seek the value of $\varepsilon$ which minimizes $G^t$, or we may differentiate the expression, equate it to zero, and solve for $\varepsilon$. The latter procedure is almost always used for single reactions, and leads to the method of equilibrium constants, as described in the following sections. It may also be extended to multiple reactions, but in this case the direct minimization of $G^t$ is often more convenient.

Although the equilibrium expressions are developed for closed systems at constant T and P, they are not restricted in application to systems that are actually closed and reach equilibrium stated along paths of constant T and P. Once equilibrium state is reached, no further changes occur, and the

53

system continues to exist in this state at fixed T and P. How this state was actually attained does not matter. Once it is known that an equilibrium state exist at given T and P, the criteria apply.

The change in the standard Gibbs energy of a reaction, $DG^\circ$ is associated with the equilibrium constant K in the equation:

$$\Delta G^\circ = \sum v_i \, G_i^\circ = -RT\ln K$$

**Equation 3.8**

Because the standard-state temperature is that of the equilibrium mixture, the standard properties changes of reaction, such as $\Delta G^\circ$ and $\Delta H^\circ$ vary with the equilibrium temperature. The dependence of $\Delta G^\circ$ on T is given by:

$$\frac{d(\Delta G^\circ/RT)}{dT} = \frac{-\Delta H^\circ}{RT^2}$$

**Equation 3.9**

In view of Equation 3.8, this becomes:

$$\frac{d\ln K}{dT} = \frac{\Delta H^\circ}{RT^2}$$

**Equation 3.10**

Equation 3.10 gives the effect of temperature on the equilibrium constant, and hence on the equilibrium conversion. If $\Delta H^\circ$ is negative, i.e. if the reaction is exothermic the equilibrium constant decreases as the temperature increases. Conversely, K increases with T for an endothermic reaction.

If $\Delta H^\circ$ , the standard enthalpy change (heat) of the reaction, is assumed independent of T, integration of Equation 3.10 from a particular temperature $T_1$ to an arbitrary temperature T leads to the simple result:

$$\ln\frac{K}{K_1} = -\frac{\Delta H^\circ}{R}\left(\frac{1}{T} - \frac{1}{T_1}\right)$$

**Equation 3.11**

This approximate equation implies that a plot of lnK vs the reciprocal of absolute temperature is a straight line. Thus Equation 3.11 provides a reasonably accurate relation for the interpolation and extrapolation of equilibrium-constant data.

If the standard heat of reaction is related to the temperature, integration of Equation 3.10 leads to:

$$\ln K = \int \frac{\Delta H^\circ}{RT^2} dT + I$$

**Equation 3.12**

where I is the integration constant. The general expression of $\Delta H^\circ$ is given by:

$$\Delta H^\circ = J + \int \Delta C_p^\circ dT$$

54

**Equation 3.13**

where J is another integration constant. When each $C^o_{(pi)}$ is given by the relation $C_p^{ig} = R(A + BT + CT^2 + DT^{-2})$, then the resulting equation is:

$$\frac{\Delta H^o}{R} = \frac{J}{R} + (\Delta A)T + \frac{\Delta B}{2}T^2 + \frac{\Delta C}{3}T^3 - \frac{\Delta D}{T}$$

**Equation 3.14**

By replacing this in Equation 3.12 and integrating we have:

$$\ln K = \frac{-J}{RT} + \Delta A \ln T + \frac{\Delta B}{2}T + \frac{\Delta C}{6}T^2 + \frac{\Delta D}{2T^2} + I$$

**Equation 3.15**

For the thermodynamic analysis of the following cases there will be used the Equation 3.8, Equation 3.15and Equation 3.14. The tables from which the values for A, B, C, D, $\Delta H$ and $\Delta G$ were taken are the tables 4.1, 4.4 and 15.1 from volumes of "Introduction to Thermodynamics" of JM Smith and HC Van Ness.

### 3.2.3 Thermodynamic Analysis

The K's of each reaction shown below were calculated with two computational tools to compare the accuracy of the results. These tools are the Excel and the programming language FORTRAN. The results are given in PivotTables where the temperature is always at Kelvin. Then the extent of each reaction in each test temperature was calculated and from there the final mole fractions of reactants and products.
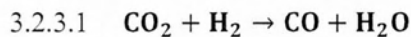
3.2.3.1   $CO_2 + H_2 \rightarrow CO + H_2O$ $\qquad\qquad$ $\Delta H^o_{298} = 41166\ J/mol$

$\Delta = (CO) + (H_2O) - (CO_2) - (H_2)$

$\Delta A = 3.376 + 3.47 - 5.457 - 3.249 = -1.86$

$\Delta B = (0.557 + 1.45 - 1.045 - 0.422) * 10^{-3} = 0.54 * 10^{-3}$

$\Delta C = 0$

$\Delta D = (-0.031 + 0.121 + 1.157 - 0.083) * 10^5 = 1.164 * 10^5$

$\Delta H^o_{298} = -110525 - 241818 + 393509 - 0 = 41166J$

$\Delta G^o_{298} = -137169 - 228572 + 394359 - 0 = 28618J$

According to Equation 3.8 ,Equation 3.14 and Equation 3.15 :

$$\ln K = \frac{-\Delta G^o}{RT} = \frac{-28618}{8.314 \times 298.15} \approx -11.545$$

$$\frac{\Delta H^o}{R} = \frac{J}{R} + (\Delta A)T + \frac{\Delta B}{2}T^2 + \frac{\Delta C}{3}T^3 - \frac{\Delta D}{T} \Rightarrow \frac{41166}{8.314} = \frac{J}{R} = -554.559 + 24 - 390.41 \Rightarrow \frac{J}{R}$$
$$= 5872.369$$

$$\ln K = \frac{-J}{RT} + \Delta A \ln T + \frac{\Delta B}{2}T + \frac{\Delta C}{6}T^2 + \frac{\Delta D}{2T^2} + I \Rightarrow -11.545$$

$$= -\frac{5872.369}{298.15} - 1.86\ln 298.15 + (0.27 \times 10^{-3})298.15 + \frac{58200}{88893.4225} + I \Rightarrow I$$

$$= 17.986$$

The final form of K-T is :

$$\ln K = -\frac{5932.5158}{T} - 1.86\ln T + (0.27 \times 10^{-3})T + \frac{58200}{T^2} + 17.986$$

Table 3-1 Equilibrium constants of reaction $CO_2 + H_2 \rightarrow CO + H_2O$.

| T | Kexcel | Kfortran |
|-----|------------|------------|
| 373 | 2,2175E-04 | 2,6777E-04 |
| 423 | 1,0621E-03 | 1,2583E-03 |
| 473 | 3,6088E-03 | 4,2116E-03 |
| 523 | 9,5992E-03 | 1,1067E-02 |
| 573 | 2,1320E-02 | 2,4336E-02 |
| 623 | 4,1312E-02 | 4,6760E-02 |
| 673 | 7,2030E-02 | 8,0946E-02 |
| 723 | 1,1556E-01 | 1,2906E-01 |
| 773 | 1,7341E-01 | 1,9264E-01 |
| 823 | 2,4651E-01 | 2,7254E-01 |
| 873 | 3,3512E-01 | 3,6897E-01 |
| 923 | 4,3898E-01 | 4,8152E-01 |
| 973 | 5,5740E-01 | 6,0937E-01 |
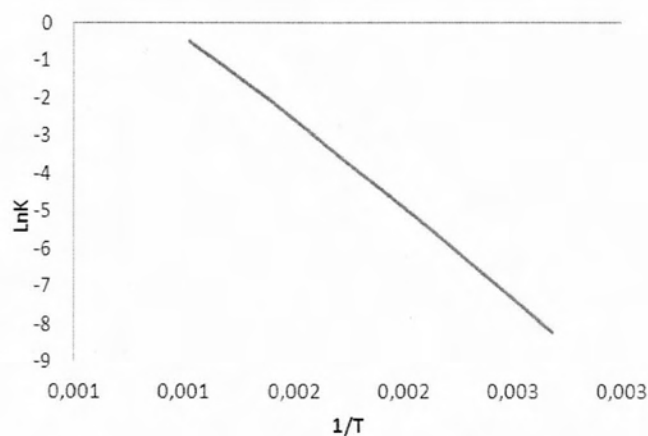


Figure 3-2 Equilibrium constant versus temperature for the reaction $CO_2 + H_2 \rightarrow CO + H_2O$. This reaction is endothermic ($\Delta H^o_{298} > 0$). When temperature increase (T), equilibrium constant K will increase too.

56

For the calculation of y according to the K of the reaction $CO_2 + H_2 \rightarrow CO + H_2O$ follows the procedure:

Initially we consider that we have 1 mol $CO_2$ and 1 mol $H_2$.

$$n_{CO_2} = 1 - \varepsilon = n_{H_2}$$

$$n_{CO} = \varepsilon = n_{H_2O}$$

$$\sum n_i = 2$$

$$y_i = \frac{n_i}{2}$$

$$y_{CO_2} = \frac{1 - \varepsilon}{2} = y_{H_2}$$

$$y_{CO} = \frac{\varepsilon}{2} = y_{H_2O}$$

$$\sum y_i = 1$$

We find the reaction coordinate (expresses the extent or degree to which the reaction takes place):

$$K = \frac{\varepsilon^2}{(1 - \varepsilon)^2} \Rightarrow K(1 - \varepsilon)^2 = \varepsilon^2 \Rightarrow \varepsilon^2(K - 1) - 2K\varepsilon + K = 0$$

$$\varepsilon = \frac{K \pm \sqrt{K}}{K - 1}$$

**Table 3-2 Mole fractions reaction $CO_2 + H_2 \rightarrow CO + H_2O$**

| T | y $CO_2$ = y $H_2$ | y$CO$ = y $H_2O$ | $\varepsilon 1$ | $\varepsilon 2$ |
|---|---|---|---|---|
| 373 | 4,9195E-01 | 8,0500E-03 | -1,6636E-02 | 1,6100E-02 |
| 423 | 4,8287E-01 | 1,7129E-02 | -3,6777E-02 | 3,4258E-02 |
| 473 | 4,6953E-01 | 3,0471E-02 | -6,9401E-02 | 6,0942E-02 |
| 523 | 4,5241E-01 | 4,7594E-02 | -1,1757E-01 | 9,5188E-02 |
| 573 | 4,3253E-01 | 6,7474E-02 | -1,8483E-01 | 1,3495E-01 |
| 623 | 4,1110E-01 | 8,8897E-02 | -2,7590E-01 | 1,7779E-01 |
| 673 | 3,8925E-01 | 1,1075E-01 | -3,9764E-01 | 2,2149E-01 |
| 723 | 3,6785E-01 | 1,3215E-01 | -5,6066E-01 | 2,6430E-01 |
| 773 | 3,4749E-01 | 1,5251E-01 | -7,8224E-01 | 3,0503E-01 |
| 823 | 3,2850E-01 | 1,7150E-01 | -1,0923E+00 | 3,4299E-01 |
| 873 | 3,1106E-01 | 1,8894E-01 | -1,5473E+00 | 3,7789E-01 |
| 923 | 2,9517E-01 | 2,0483E-01 | -2,2671E+00 | 4,0965E-01 |
| 973 | 2,8080E-01 | 2,1920E-01 | -3,5584E+00 | 4,3840E-01 |
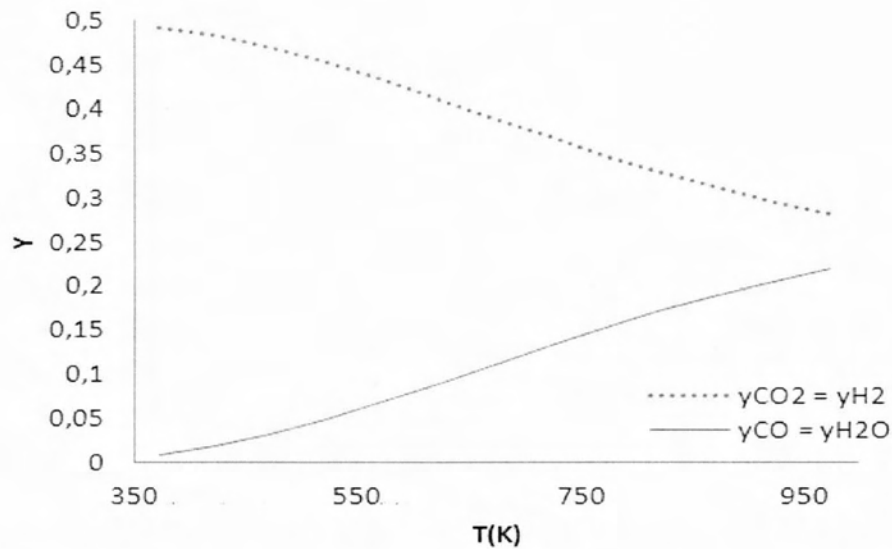
**Figure 3-3 Mole fraction versus temperature for the reaction $CO_2 + H_2 \rightarrow CO + H_2O$. This reaction is endothermic ($\Delta H^o_{298} > 0$). When temperature increase (T), equilibrium constant K will increase and the products formed will increase too ($H_2O + CO$).**

### 3.2.3.2   $CO_2 + 4H_2 \rightarrow CH_4 + 2\,H_2O$ $\qquad\qquad \Delta H^o_{298} = -164647\,J/mol$

The reaction of methane production by hydrogenation of carbon dioxide is an exothermic reaction ($\Delta H^o_{298} < 0$). So unlike the previous case we examined, the K must be reduced, which is confirmed by the following results.

$\Delta A = -9.811$

$\Delta B = 9.248 \times 10^{-3}$

$\Delta C = -2.164 \times 10^{-6}$

$\Delta D = 1.067 \times 10^5$

$\Delta H^o_{298} = -164647\,J/mol$

$\Delta G^o_{298} = -113245\,J/mol$

According to Equation 3.8 ,Equation 3.14 and Equation 3.15:

$$\ln K = +\frac{16912.48277}{T} - 9.811\ln T + (4.624 \times 10^{-3})T - (0.361 \times 10^{-6})T^2 + \frac{53350}{T^2} + 42.914$$

58

**Table 3-3 Equilibrium constants of reaction $CO_2 + 4\,H_2 \rightarrow CH_4 + 2\,H_2O$.**

| T | Kexcel | Kfortran |
|---|--------|----------|
| 373 | 9.87E+17 | 1,03E+14 |
| 423 | 1.54E+16 | 1,63E+11 |
| 473 | 8.79E+08 | 9,45E+08 |
| 523 | 1.27E+07 | 1,39E+07 |
| 573 | 3.70E+09 | 4.13E+05 |
| 623 | 1.83E+09 | 2.09E+04 |
| 673 | 1.38E+09 | 1.61E+06 |
| 723 | 1.45E+09 | 1.74E+06 |
| 773 | 2.01E+09 | 2.48E+05 |
| 823 | 3.49E+09 | 4.42E+06 |
| 873 | 7.30E-01 | 9.54E-01 |
| 923 | 1.79E-01 | 2.42E-01 |
| 973 | 5.04E-02 | 7,04E-02 |
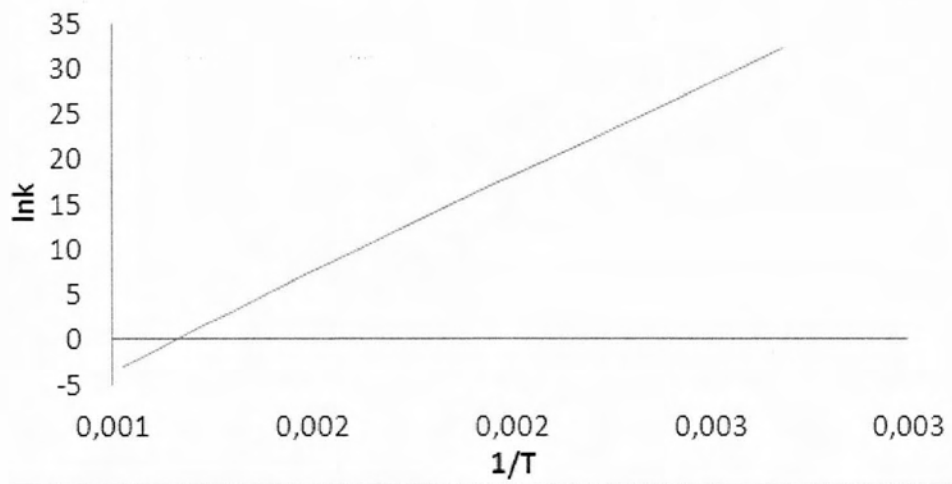


Figure 3-4 Equilibrium constant versus temperature for the reaction $CO_2 + 4\,H_2 \rightarrow CH_4 + 2\,H_2O$. This reaction is exothermic ($\Delta H^o_{298} = -164647\ \text{J/mol} < 0$). When temperature (T) increase, equilibrium constant K will decrease

**Table 3-4 Mole fractions of reaction $CO_2 + 4 H_2 \rightarrow CH_4 + 2 H_2 O$**

| T | ε | Kfortran | y $CO_2$ | y $H_2$ | y $CH_4$ | y $H_2O$ |
|---|---|---|---|---|---|---|
| 523 | 9,7507E-01 | 1,3900E+07 | 8,1730E-03 | 3,2693E-02 | 3,1971E-01 | 6,3942E-01 |
| 573 | 9,5003E-01 | 4,1327E+05 | 1,6119E-02 | 6,4477E-02 | 3,0647E-01 | 6,1294E-01 |
| 623 | 9,1064E-01 | 2,0919E+04 | 2,8113E-02 | 1,1245E-01 | 2,8648E-01 | 5,7296E-01 |
| 673 | 8,5439E-01 | 1,6127E+03 | 4,4242E-02 | 1,7697E-01 | 2,5960E-01 | 5,1919E-01 |
| 723 | 7,8090E-01 | 1,7419E+02 | 6,3726E-02 | 2,5490E-01 | 2,2712E-01 | 4,5425E-01 |
| 773 | 6,9271E-01 | 2,4766E+01 | 8,5014E-02 | 3,4006E-01 | 1,9164E-01 | 3,8329E-01 |
| 823 | 5,9548E-01 | 4,4193E+00 | 1,0620E-01 | 4,2480E-01 | 1,5633E-01 | 3,1267E-01 |
| 873 | 4,9685E-01 | 9,5391E-01 | 1,2559E-01 | 5,0236E-01 | 1,2402E-01 | 2,4804E-01 |
| 923 | 4,0433E-01 | 2,4190E-01 | 1,4212E-01 | 5,6848E-01 | 9,6467E-02 | 1,9293E-01 |
| 973 | 3,2248E-01 | 7,0400E-02 | 1,5557E-01 | 6,2228E-01 | 7,4049E-02 | 1,4810E-01 |
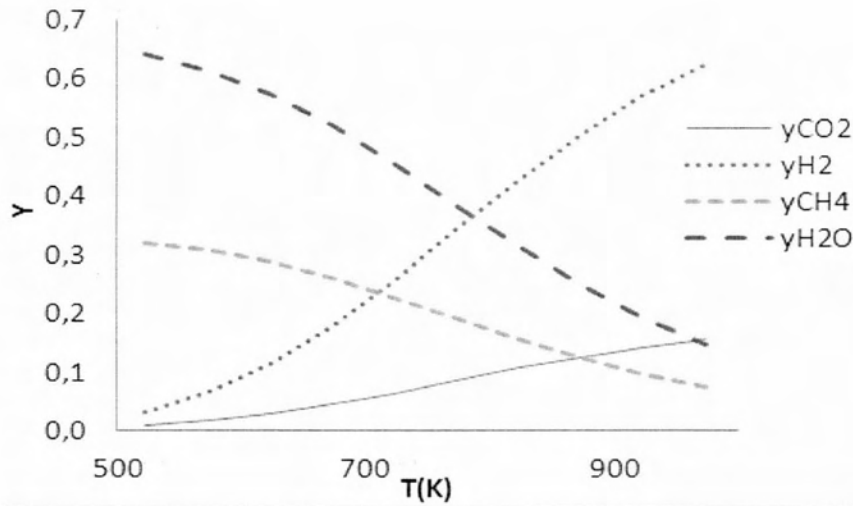
**Figure 3-5 Mole fraction versus temperature for the reaction $CO_2 + 4 H_2 \rightarrow CH_4 + 2 H_2 O$. This reaction is exothermic ($\Delta H^o_{298} < 0$). When temperature (T) increase, equilibrium constant K will decrease and the products formed will decrease too ($H_2O + CO$).**

### 3.2.3.3 $\quad 2CO_2 + 5H_2 \rightarrow CH_4 + CO + 3H_2O \quad \Delta H^o_{298} = -123481 \text{ J/mol}$
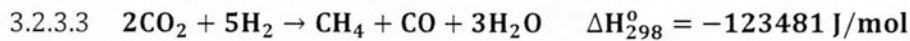
The reaction in which we produce methane and carbon monoxide from the hydrogenation of carbon has ($\Delta H^o_{298} < 0$), thus it is exothermic reaction. This can be seen in Table 4.5 which shows that the equilibrium constant decreases.

$\Delta A = -11.671$

$\Delta B = 9.788 \times 10^{-3}$

$\Delta C = -2.164 \times 10^{-6}$

$\Delta D = 2.231 \times 10^5$

$\Delta H^o_{298} = -123481 \text{ J/mol}$

$\Delta G^o_{298} = -84627 \text{ J/mol}$

60

According to Equation 3.8 ,Equation 3.14 and Equation 3.15 :

$$\ln K = -\frac{11040.1104}{T} - 11.671\ln T + (4.894 \times 10^{-3})T - (0.361 \times 10^{-6})T^2 + \frac{111550}{T^2} + 60.9263$$

**Table 3-5 Equilibrium constants of reaction 2 $CO_2$ +5 $H_2$ → $CH_4$ + CO +3 $H_2$ O**

| T | Kexcel | Kfortran |
|-----|-----------|-----------|
| 373 | 2,6244E+10 | 2,7589E+10 |
| 423 | 1,9257E+08 | 2,0536E+08 |
| 473 | 3,6740E+06 | 3,9820E+06 |
| 523 | 1,3988E+05 | 1,5436E+05 |
| 573 | 8,9357E+03 | 1,0057E+04 |
| 623 | 8,5052E+02 | 9,7816E+02 |
| 673 | 1,1088E+02 | 1,3054E+02 |
| 723 | 1,8620E+01 | 2,2481E+01 |
| 773 | 3,8462E+00 | 4,7708E+00 |
| 823 | 9,4346E-01 | 1,2045E+00 |
| 873 | 2,6738E-01 | 3,5196E-01 |
| 923 | 8,5670E-02 | 1,1648E-01 |
| 973 | 3,0490E-02 | 4,2900E-02 |
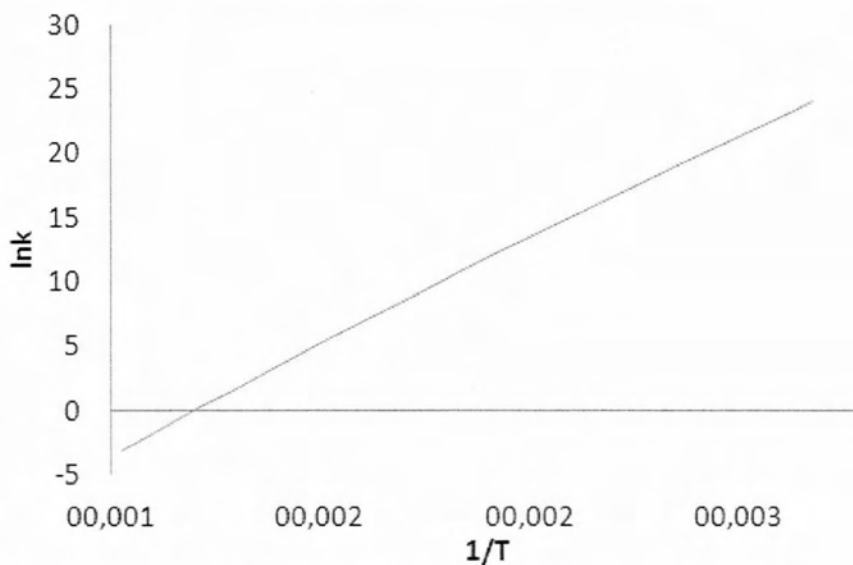


**Figure 3-6 Equilibrium constants versus temperature for the reaction 2 $CO_2$ +5 $H_2$ → $CH_4$ + CO +3 $H_2$O.This reaction is exothermic ($\Delta H_{298}^o = -123481J/mol$<0). When temperature (T) increase, equilibrium constant K decrease.**

According to Hess's law, the above reaction can be split into two separate reactions:

1.  $CO_2 + H_2 \rightarrow CO + H_2O$

2.  $CO_2 + 4H_2 \rightarrow CH_4 + 2H_2O$

61

This is also proven by the energy balance because:

$$\Delta H^o_{298} = -164647 + 41166 = -123481 J/mol$$

Since the two individual reactions have been studied, we choose to use them to study the overall reaction

| j | $CO_2$ | $H_2$ | CO | $CH_4$ | $H_2O$ | $v_j$ |
|---|--------|-------|----|--------|--------|-------|
| 1 | -1 | -1 | 1 | 0 | 1 | 0 |
| 2 | -1 | -4 | 0 | 1 | 2 | -2 |

Initially for 2 mol $CO_2$ and 5 mol $H_2$

$$y_i = \frac{n_i}{7 - 2\varepsilon_2}$$

$$y_{CO_2} = \frac{2 - \varepsilon_1 - \varepsilon_2}{7 - 2\varepsilon_2}$$

$$y_{H_2} = \frac{5 - \varepsilon_1 - 4\varepsilon_2}{7 - 2\varepsilon_2}$$

$$y_{CO} = \frac{\varepsilon_1}{7 - 2\varepsilon_2}$$

$$y_{CH_4} = \frac{\varepsilon_2}{7 - 2\varepsilon_2}$$

$$y_{H_2O} = \frac{\varepsilon_1 + 2\varepsilon_2}{7 - 2\varepsilon_2}$$

$$\sum y_i = 1$$

Therefore:

$$K_1 = \frac{y_{CO} \times y_{H_2O}}{y_{CO_2} \times y_{H_2}} = \frac{\varepsilon_1(\varepsilon_1 + 2\varepsilon_2)}{(2 - \varepsilon_1 - \varepsilon_2)(5 - \varepsilon_1 - 4\varepsilon_2)}$$

$$K_2 = \frac{y_{CH_4} \times y_{H_2O}^2}{y_{CO_2} \times y_{H_2}^4} = \frac{\varepsilon_2(\varepsilon_1 + 2\varepsilon_2)^2(7 - 2\varepsilon_2)^2}{(2 - \varepsilon_1 - \varepsilon_2)(5 - \varepsilon_1 - 4\varepsilon_2)^4}$$

This is a system 2x2. K1 and K2 are known, found earlier, for each temperature.

We find the reaction coordinate (expresses the extent or degree to which the reaction takes place):

**Table 3-6 Solving the 2x2 system**

| T | k1 | k2 | $\varepsilon 1$ | $\varepsilon 2$ |
|---|---|---|---|---|
| 373 | 2,6777E-04 | 1,0300E+14 | 1,0000E-07 | 1,2497E+00 |
| 423 | 1,2583E-03 | 1,6300E+11 | 2,3000E-06 | 1,2485E+00 |
| 473 | 4,2116E-03 | 9,4500E+08 | 2,7700E-05 | 1,2446E+00 |
| 523 | 1,1067E-02 | 1,3900E+07 | 2,1160E-04 | 1,2345E+00 |
| 573 | 2,4336E-02 | 4,1327E+05 | 1,1540E-03 | 1,2131E+00 |
| 623 | 4,6760E-02 | 2,0919E+04 | 4,9114E-03 | 1,1736E+00 |
| 673 | 8,0946E-02 | 1,6127E+03 | 1,7326E-02 | 1,1088E+00 |
| 723 | 1,2906E-01 | 1,7419E+02 | 5,2506E-02 | 1,0114E+00 |
| 773 | 1,9264E-01 | 2,4766E+01 | 1,3814E-01 | 8,7353E-01 |
| 823 | 2,7254E-01 | 4,4193E+00 | 3,1237E-01 | 6,8797E-01 |
| 873 | 3,6897E-01 | 9,5391E-01 | 5,9180E-01 | 4,6108E-01 |
| 923 | 4,8152E-01 | 2,4190E-01 | 9,1583E-01 | 2,3831E-01 |
| 973 | 6,0937E-01 | 7,0406E-02 | 1,1670E+00 | 9,0111E-02 |

**Table 3-7 Mole fractions reaction $2\ CO_2 + 5\ H_2 \rightarrow CH_4 + CO + 3\ H_2O$**

| T | y $CO_2$ | y $H_2$ | yCO | y $CH_4$ | y $H_2O$ |
|---|---|---|---|---|---|
| 373 | 1,6671E-01 | 2,6661E-04 | 2,0000E-08 | 2,7767E-01 | 5,5535E-01 |
| 423 | 1,6689E-01 | 1,3319E-03 | 5,0000E-07 | 2,7726E-01 | 5,5452E-01 |
| 473 | 1,6746E-01 | 4,8001E-03 | 6,1300E-06 | 2,7591E-01 | 5,5182E-01 |
| 523 | 1,6890E-01 | 1,3611E-02 | 4,6700E-05 | 2,7247E-01 | 5,4498E-01 |
| 573 | 1,7179E-01 | 3,2027E-02 | 2,5230E-04 | 2,6522E-01 | 5,3070E-01 |
| 623 | 1,7656E-01 | 6,4634E-02 | 1,0556E-03 | 2,5223E-01 | 5,0552E-01 |
| 673 | 1,8273E-01 | 1,1448E-01 | 3,6229E-03 | 2,3185E-01 | 4,6732E-01 |
| 723 | 1,8808E-01 | 1,8121E-01 | 1,0549E-02 | 2,0320E-01 | 4,1696E-01 |
| 773 | 1,8815E-01 | 2,6038E-01 | 2,6297E-02 | 1,6629E-01 | 3,5888E-01 |
| 823 | 1,7775E-01 | 3,4419E-01 | 5,5543E-02 | 1,2233E-01 | 3,0020E-01 |
| 873 | 1,5583E-01 | 4,2184E-01 | 9,7370E-02 | 7,5862E-02 | 2,4909E-01 |
| 923 | 1,2967E-01 | 4,7996E-01 | 1,4039E-01 | 3,6531E-02 | 2,1345E-01 |
| 973 | 1,0894E-01 | 5,0919E-01 | 1,7111E-01 | 1,3213E-02 | 1,9754E-01 |
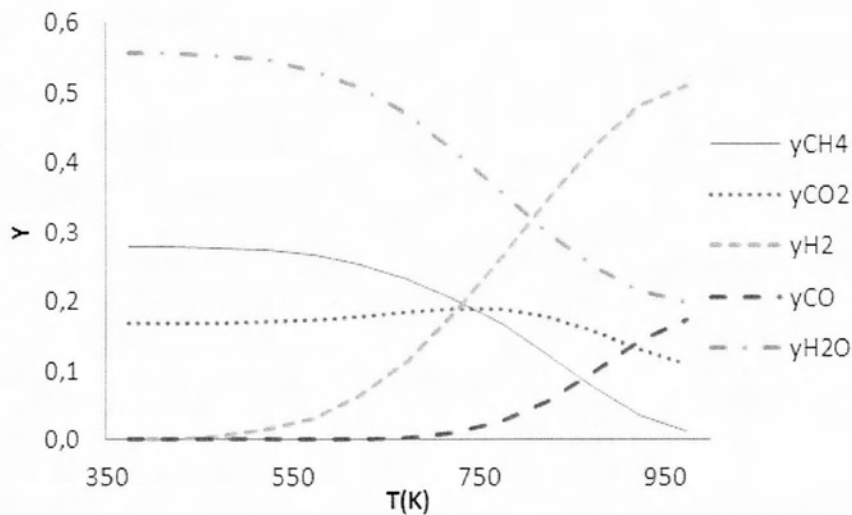
**Figure 3-7 Mole fraction versus temperature for the reaction 2 $CO_2$+5 $H_2 \rightarrow$ $CH_4$+CO+3 $H_2O$. Production of CO increase while production of $CH_4$ decrease as temperature increase.**

3.2.3.4 **CO2 + 3H2 → CH3OH + H2O** $\quad$ **$\Delta H^o{}_{298} = -48969 J/mol$**
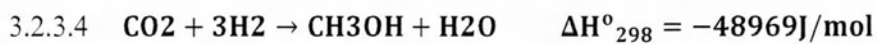
$\Delta = (CH_3OH) + (H_2O) - (CO_2) - 3(H_2)$

$\Delta A = 2.211 + 3.47 - 5.457 - 3 \times 3.249 = -9.523$

$\Delta B = (12.216 + 1.45 - 1.045 - 3 \times 0.422) \times 10^{-3} = 11.355 \times 10^{-3}$

$\Delta C = -3.45 \times 10^{-6}$

$\Delta D = (0 + 0.121 + 1.157 - 3 \times 0.083) \times 10^5 = 1.029 \times 10^5$

$\Delta H^o_{298} = -200660 - 241818 + 393509 - 0 = -48969 \ J/mol$

$\Delta G^o_{298} = -161960 - 228572 + 394359 - 0 = 3827 \ J/mol$


According to Equation 3.8 ,Equation 3.14 and Equation 3.15 :

$$\ln K = \frac{3179.74978}{T} - 9.523 \ln T + (5.6775 \times 10^{-3})T - (0.575 \times 10^{-6})T^2 + \frac{51450}{T^2} + 39.828705$$

**Table 3-8 Equilibrium constants of reaction $CO_2$ +3 $H_2 \rightarrow CH_3OH + H_2O$**

| T | K Fortran | K Excel |
|---|---|---|
| 273 | 1,2899E+05 | 1,2933E+09 |
| 323 | 4,5940E-02 | 4,6044E-02 |
| 373 | 3,5900E-03 | 3,6495E-03 |
| 423 | 4,7271E+01 | 0.00049371 |
| 473 | 9,0057E+00 | 9,7535E+00 |
| 523 | 2,2515E+00 | 2,5506E-01 |
| 573 | 6,9251E-01 | 8,2707E-01 |
| 623 | 2,5054E-01 | 3,1779E-01 |
| 673 | 1,0322E-01 | 1,4004E-01 |
| 723 | 4,7288E-02 | 6,9084E-02 |

Due to very small K we choose to work in the region from 273 to 573 K.
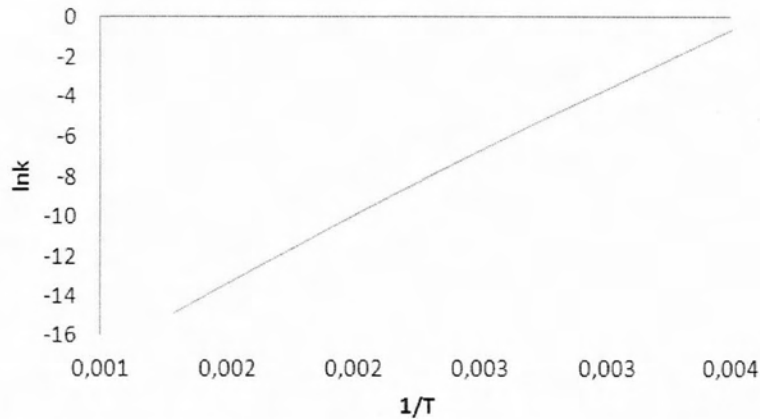


Figure 3-8 Equilibrium constants versus temperature for the reaction $CO_2 + 3\,H_2 \rightarrow CH3\,OH + H_2O$. This reaction is exothermic ($\Delta H^o_{298} = -48969\,J/mol < 0$). When temperature (T) increase, equilibrium constant K will decrease.

Table 3-9 Mole fractions of the reaction $CO_2 + 3\,H_2 \rightarrow CH_3OH + H_2O$.

| T | y $CO_2$ | y $H_2$ | y $CH_3OH$ = y $H_2O$ |
|---|---|---|---|
| 273 | 1,6731E-01 | 5,0193E-01 | 1,6538E-01 |
| 323 | 2,2242E-01 | 6,6727E-01 | 5,5155E-02 |
| 373 | 2,4089E-01 | 7,2268E-01 | 1,8215E-02 |
| 423 | 2,4649E-01 | 7,3948E-01 | 7,0145E-03 |
| 473 | 2,4842E-01 | 7,4525E-01 | 3,1674E-03 |
| 523 | 2,4919E-01 | 7,4756E-01 | 1,6295E-03 |
| 573 | 2,4953E-01 | 7,4860E-01 | 9,3048E-04 |
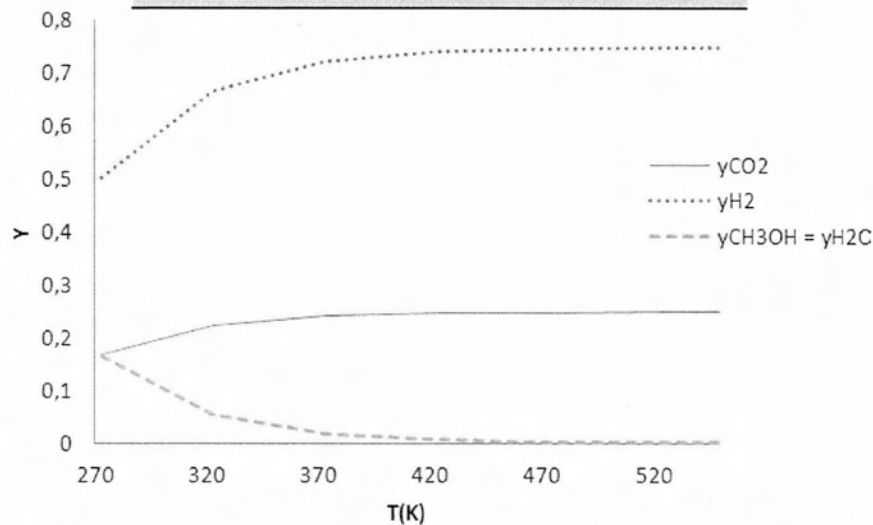


Figure 3-9 Mole fraction versus temperature for the reaction $CO_2 + 3\,H_2 \rightarrow CH_3OH + H_2O$. This reaction is exothermic ($\Delta H^o_{298} < 0$). When temperature (T) increase, equilibrium constant K and the products formed will decrease ($H_2O + CH_3OH$).

65

### 3.2.3.5 $2CO_2 + 4H_2 \rightarrow CH_3OH + CO + 2H_2O$   $\Delta H^o_{298} = -7803 \, J/mol$
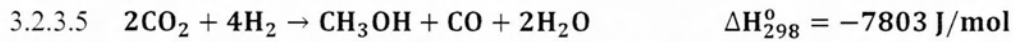
Finally, we examine the hydrogenation reaction of carbon dioxide from which are produced methanol and carbon monoxide. It is likewise an exothermic reaction($\Delta H^o_{298} < 0$).

$\Delta A = -11.383$

$\Delta B = 11.895 \times 10^{-3}$

$\Delta C = -3.45 \times 10^{-6}$

$\Delta D = 2.193 \times 10^5$

$\Delta H^o_{298} = -7803 \, J/mol$

$\Delta G^o_{298} = 32445 \, J/mol$

According to Equation 3.8 ,Equation 3.14 and Equation 3.15 :

$$\ln K = \frac{-2692.62533}{T} - 11.383\ln T + (5.9475 \times 10^{-3})T - (0.575 \times 10^{-6})T^2 + \frac{109650}{T^2} + 58.02$$

**Table 3-10 Equilibrium constants of the reaction $2 \, CO_2 + 4 \, H_2 \rightarrow CH_3OH + CO + 2 \, H_2O$.**

| T | KFortran | KExcel |
|---|---|---|
| 273 | 2,8208E-06 | 3,2280E-06 |
| 323 | 1,6931E-06 | 1,9046E-06 |
| 373 | 1,0410E-06 | 1,1478E-06 |
| 423 | 6,5946E-07 | 7,1067E-07 |
| 473 | 4,3148E-07 | 4,5316E-07 |
| 523 | 2,9171E-07 | 2,9772E-07 |
| 573 | 2,0360E-07 | 2,0135E-07 |
| 623 | 1,4648E-07 | 1,3997E-07 |
| 673 | 1,0844E-07 | 9,9830E-08 |
| 723 | 8,2452E-08 | 7,2917E-08 |
| 773 | 6,4267E-08 | 5,4442E-08 |
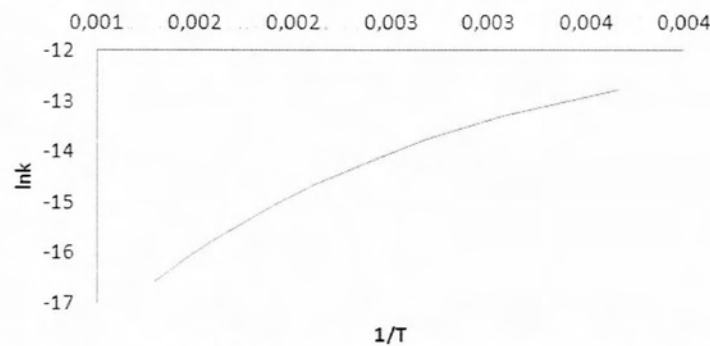


**Figure 3-10 Equilibrium constants versus temperature for the reaction $2 \, CO_2 + 4 \, H_2 \rightarrow CH_3OH + CO + 2H_2O$. This reaction is exothermic ($\Delta H^o_{298} = -7803 J/mol < 0$). When temperature (T) increase, equilibrium constant K decrease.**

As in the previous case, according to Hess's law, the above reaction can be split into two separate reactions:

1.  $CO_2 + 3H_2 \rightarrow CH_3OH + H_2O$
2.  $CO_2 + H_2 \rightarrow CO + H_2O$

This is also proven by the energy balance:

$$\Delta H^o_{298} = -48969 + 41166 = -7803 J/mol$$

Since the two individual reactions have been studied, we choose to use them to study the overall reaction.

**Table 3-11 Mole fractions of the reaction $2\ CO_2 + 4\ H_2 \rightarrow CH_3OH + CO + 2\ H_2O$**

| T | y $CO_2$ | y $H_2$ | yCO | yCH3OH | y $H_2O$ |
|-----|-----------|-----------|-----------|-----------|-----------|
| 273 | 2,8127E-01 | 4,0634E-01 | 1,5300E-06 | 1,5620E-01 | 1,5620E-01 |
| 323 | 3,1556E-01 | 5,7829E-01 | 1,1900E-04 | 5,2955E-02 | 5,3074E-02 |
| 373 | 3,2486E-01 | 6,3671E-01 | 3,1040E-03 | 1,6109E-02 | 1,9213E-02 |
| 423 | 3,1761E-01 | 6,4767E-01 | 1,4908E-02 | 2,4540E-03 | 1,7361E-02 |
| 473 | 3,0476E-01 | 6,3774E-01 | 2,8482E-02 | 2,6800E-04 | 2,8750E-02 |
| 523 | 2,8875E-01 | 6,2203E-01 | 4,4570E-02 | 3,9700E-05 | 4,4610E-02 |
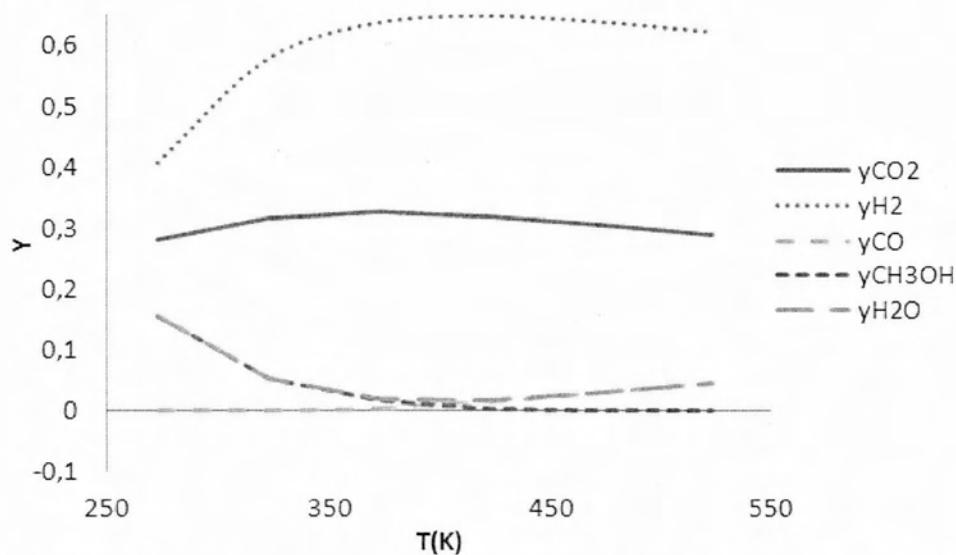


**Figure 3-11 Mole fraction versus temperature for the reaction $2\ CO_2 + 4\ H_2 \rightarrow CH_3OH + CO + 2\ H_2O$. Production of CO increase while production of $CH_3OH$ decrease as temperature increase.**

### 3.3 Part Two- Comparison of the Results with the ones of Gibbs Energy Minimization Process

When the composition of an equilibrium mixture is determined by a number of simultaneous reactions, calculations that are based on equilibrium constants are complex and difficult. An alternative approach ,more direct and general is the one based on the minimization of total Gibbs energy according to the Equation 3.7. In this case, however, we are limited in the gas phase and the problem is to find the equilibrium composition for a given T and P for given initial feed. The detailed methodology of Gibbs energy minimization is:

1. The first step is to formulate the constraining equations, i.e., the material balances. Although reacting molecular species are not conserved in a closed system, the total number of atoms of each element is constant. Let subscript k identify a particular atom. Then define $A_k$ as the total number of the atomic masses of the $kth$ element in the system as determined by the initial constitution of the system. Further, let $a_{ik}$ be the number of atoms of the $kth$ element presents in each molecule of chemical species $i$. The material balance on each element $k$ may be written:

2.

$$\sum_i n_i \alpha_{ik} = A_k \qquad (k = 1, 2, \dots, w)$$

**Equation 3.16**

Or

$$\sum_i n_i \alpha_{ik} - A_k = 0 \qquad (k = 1, 2, \dots, w)$$

3. Next, we introduce the Lagrange multipliers $\lambda_k$, one for each element, by multiplying each element balance by its $\lambda_k$:

4.

$$\lambda_k \left( \sum_i n_i \alpha_{ik} - A_k \right) = 0 \qquad (k = 1, 2, \dots, w)$$

The equations are summed over k, giving:

$$\sum_k \lambda_k \left( \sum_i n_i \alpha_{ik} - A_k \right) = 0$$

5. Then a new function F is formed by addition of this last sum to $G^t$. Thus,

6.

68

$$F = G^t + \sum_k \lambda_k \left( \sum_i n_i \alpha_{ik} - A_k \right)$$

This new function is identical with $G^t$, because the summation term is zero. However, the partial derivatives of F and $G^t$ with respect to $n_i$ are different, because the function F incorporates the constraints of the material balances.

7. The minimum value F (and $G^t$) occurs when all of the partial derivatives $\left( \frac{\partial F}{\partial n_i} \right)_{T,P,n_j}$ are zero. We therefore differentiate the preceding equation and set the resulting derivative equal to zero:

$$= \left( \frac{\partial F}{\partial n_i} \right)_{T,P,n_j} = \left( \frac{\partial G^t}{\partial n_i} \right)_{T,P,n_j} + \sum_k \lambda_k \, \alpha_{ik} = 0$$

Because the first term on the right is the definition of the chemical potential this equation can be written:

$$\mu_i + \sum_k \lambda_k \, \alpha_{ik} = 0 \qquad (i = 1, 2, ..., N)$$

**Equation 3.17**

However the chemical potential is given by:

$$\mu_i = G_i^o + RT \ln \hat{f}_i / f_i^{\,o}$$

For the gas phase reactions and standard states as the pure ideal gases at 1 bar [or 1 atm]:

$$\mu_i = G_i^o + RT \ln \frac{\hat{f}_i}{P^o}$$

If $G_i^o$ is arbitrarily set equal to zero for all elements in their standard states, then for compounds $G_i^o = \Delta G_{f_i}^o$, the standard Gibbs energy change of formation for species i. In addition, the fugacity is eliminated in favor of the fugacity coefficient by $\hat{f}_i = y_i \hat{\varphi}_i P$. With these substitutions, the equation for $\mu_i$ becomes:

$$\mu_i = \Delta G_{f_i}^o + RT \ln \frac{y_i \hat{\varphi}_i P}{P^o}$$

Combination with Equation 3.17 gives:

$$\Delta G_{f_i}^o + RT \ln \frac{y_i \hat{\varphi}_i P}{P^o} + \sum_k \lambda_k \, \alpha_{ik} = 0 \qquad (i = 1, 2, ..., N)$$

**Equation 3.18**

Note that $P^o$ is 1 bar, expressed in the units used for pressure. If species i is an element, $\Delta G_{f_i}^o$ is zero. Equation 3.18 represents N equilibrium equations, one for each chemical species, and Equation 3.16 represents w material-balance equations, one for each element- a total of N+w

69

equations. The unknowns are the $n_i$ (note that $y_i = n_i / \sum_i n_i$), of which there are N, and $\lambda_k$'s, of which there are w – a total of N+w unknowns. Thus the number of equations is sufficient for the determination of all unknowns.

The forgoing discussion has presumed that each $\widehat{\varphi}_i$ is known. If the phase is an ideal gas, then for each species $\widehat{\varphi}_i = 1$. If the phase is an ideal solution, $\widehat{\varphi}_i = \varphi_i$, and values can at least be estimated. For real gases $\widehat{\varphi}_i$ is a function of the set $\{y_i\}$, which is being calculated. Thus an iterative procedure is indicated. The calculations are initiated with $\widehat{\varphi}_i = 1$ for all i. Solution of the equations then provides a preliminary set of $\{y_i\}$.

For low pressures or high temperatures this result is usually adequate. Where it is not satisfactory, an equation of state is used together with the calculated $\{y_i\}$ to give a new and more nearly correct set $\{\widehat{\varphi}_i\}$ for use in Equation 3.18. Then a new set $\{y_i\}$ determined. The process is repeated until successive iterations produce no significant change in $\{y_i\}$. All calculations are well suited to computer solution.

In the procedure just described, the question of what chemical reactions are involved never enters directly into any of the equations. However, the choice of a set of species is entirely equivalent to the choice of a set independent reactions among species.

In any event, a set of species or an equivalent set of independent reactions must always be assumed, and different assumptions produce different results. For the comparison of the two methods, minimization of free energy Gibbs and equilibrium constants, we chose to study the reaction $2CO_2 + 5H_2 \rightarrow CH_4 + CO + 3H_2O$. The method of equilibrium constants were presented in the first subsection of the chapter.

We consider 2 mol of $CO_2$ and 5 mol of $H_2$ at 673 K and atmospheric pressure. When equilibrium is reached:

$$n_1 CO_2 + n_2 H_2 \rightarrow n_3 CH_4 + n_4 CO + n_5 H_2O$$
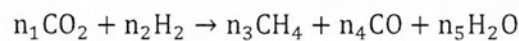
where $n_1, n_2, n_3, n_4, n_5$ is the number of mol of each compound in the balance. According to the equations above the values of $A_k$ are determined by the number of mol of reactants and the values of $\alpha_{ik}$ from the species in each chemical compound. These are given in the following table.

**Table 3-12 Values for Ak (the number of atomic masses of element k (C, O, H) in the whole system) and αik (Number of atoms of element k of molecule i.)**

|  | Carbon | Oxygen | Hydrogen |
|---|---|---|---|
|  | $A_C = 2$ | $A_O = 4$ | $A_H = 10$ |
| $CO_2$ | $\alpha\,CO_2,C=1$ | $\alpha\,CO_2=2$ | $\alpha\,CO_2,H=0$ |
| $H_2$ | $\alpha H2,C=0$ | $\alpha\,H_2,O=0$ | $\alpha H2,H=2$ |
| $CH_4$ | $\alpha\,CH_4,C=1$ | $\alpha\,CH_4,O=0$ | $\alpha\,CH_4,H=4$ |
| $CO$ | $\alpha CO,C=1$ | $\alpha CO,O=1$ | $\alpha CO,H=0$ |
| $H_2O$ | $\alpha\,H_2O,C=0$ | $\alpha\,H_2O,O=1$ | $\alpha\,H_2O,H=2$ |

Assuming that the reaction is performed under atmospheric pressure, at 800 Kelvin and that the gases are ideal, then the Equation 3.18 becomes:

$$\frac{\Delta G_{fi}^0}{RT} + \ln \frac{n_i}{\sum_i n_i} + \sum_k \frac{\lambda_\kappa}{RT} a_{ik} = 0$$

So the five equations of the five resulting compound are:

1. $CO_2$

$$\frac{\Delta G_{f1}^0}{RT} + \ln \frac{n_1}{\sum_1 n_1} + \frac{\lambda_C}{RT} + 2\frac{\lambda_O}{RT} = 0$$

2. $H_2$

$$\ln \frac{n_2}{\sum_i n_i} + 2\frac{\lambda_H}{RT} = 0$$

3. $CH_4$

$$\frac{\Delta G_{f3}^0}{RT} + \ln \frac{n_3}{\sum_i n_i} + \frac{\lambda_C}{RT} + \frac{4\lambda_H}{RT} = 0$$

4. $CO$

$$\frac{\Delta G_{f4}^0}{RT} + \ln \frac{n_4}{\sum_i n_i} + \frac{\lambda_C}{RT} + \frac{\lambda_O}{RT} = 0$$

5. $H_2O$

$$\frac{\Delta G_{f5}^0}{RT} + \ln \frac{n_5}{\sum_i n_i} + 2\frac{\lambda_H}{RT} + \frac{\lambda_O}{RT} = 0$$

The balance for the three elements (C, O, H ) is:

$$C: \quad n_{CH_4} + n_{CO_2} + n_{CO} = 2$$

$$O: \quad n_{CO_2} + n_{CO} + n_{H_2O} = 4$$

$$H: \quad n_{CH_4} + n_{H_2} + n_{H_2O} = 10$$

We obtain the Gibbs free energies of formation for each element in the given temperatures as data from literature. ($\Delta G_{fi}^0$).

Assuming that

$$y_i = \frac{n_i}{\sum_i n_i}$$

we obtain a 8 × 8 system, whose solution gives the required recommendations of chemical compounds in the balance:

$$y_{H_2} = 0.1183, y_{CO} = 0.00376, y_{CO_2} = 0.1833, y_{H_2O} = 0.4644, y_{CH_4} = 0.2303$$

and the values of the Lagrange multipliers λ are:

$$\lambda_C = 24786, \lambda_H = 180868, \lambda_O = 869415$$

The total mole fraction table of the Gibbs method and the results which had been found earlier by the method of equilibrium constants are:

**Table 3-13 Mole fractions of reaction 2 CO$_2$ +4 H$_2$ → CH$_3$OH + CO +2 H$_2$O for both Gibbs energy minimization and equilibrium constants K methods.**

| T | y CO$_2$ | y CO$_2$ | y H$_2$ | y H$_2$ | yCO | yCO |
|---|---|---|---|---|---|---|
| (Kelvin) | K | Gibbs | K | Gibbs | K | Gibbs |
| 673 | 1,563E-01 | 1,833E-01 | 1,220E-01 | 1,183E-01 | 3,670E-02 | 3,760E-02 |
| 773 | 1,858E-01 | 1,885E-01 | 2,704E-01 | 2,700E-01 | 3,100E-02 | 2,785E-02 |
| 873 | 1,466E-01 | 1,535E-01 | 4,352E-01 | 4,348E-01 | 1,110E-01 | 1,028E-01 |
| 973 | 1,007E-01 | 1,072E-01 | 5,107E-01 | 5,145E-01 | 1,812E-01 | 1,743E-01 |

| T | y CH$_4$ | y CH$_4$ | y H$_2$O | y H$_2$O |
|---|---|---|---|---|
| (Kelvin) | K | Gibbs | K | Gibbs |
| 673 | 2,16E-01 | 2,30E-01 | 4,69E-01 | 4,64E-01 |
| 773 | 1,61E-01 | 1,62E-01 | 3,52E-01 | 3,52E-01 |
| 873 | 6,53E-02 | 6,87E-02 | 2,42E-01 | 2,40E-01 |
| 973 | 8,60E-03 | 9,92E-03 | 1,99E-01 | 1,94E-01 |
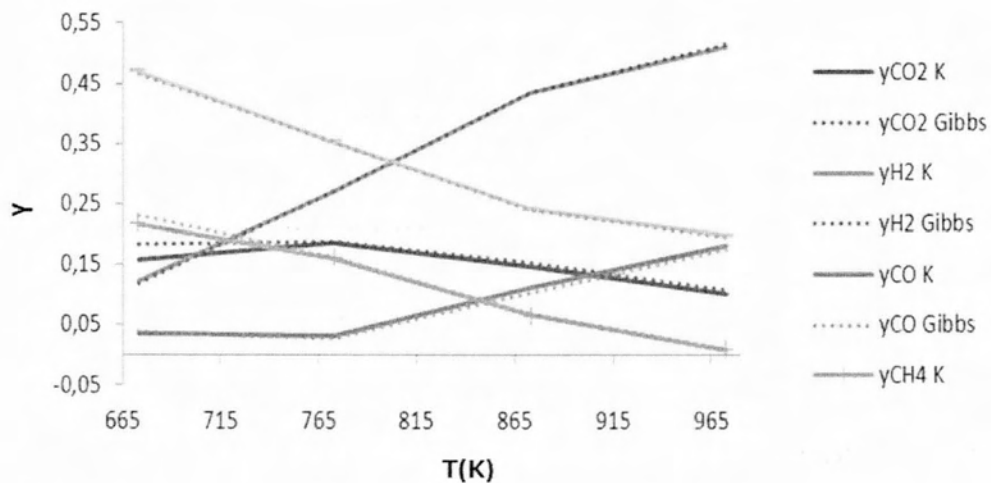


**Figure 3-12 Mole fraction versus temperature for the reaction 2 CO$_2$ +5 H$_2$ → CH$_4$ + CO +3 H$_2$ O by both methods.**

72

# CHAPTER IV

## Experimental setup

In this section, the experimental system is presented, including the three-electrode chamber reactor, the proton conductor and the preparation of the electrodes used in the experiments.

## 4    Experimental setup
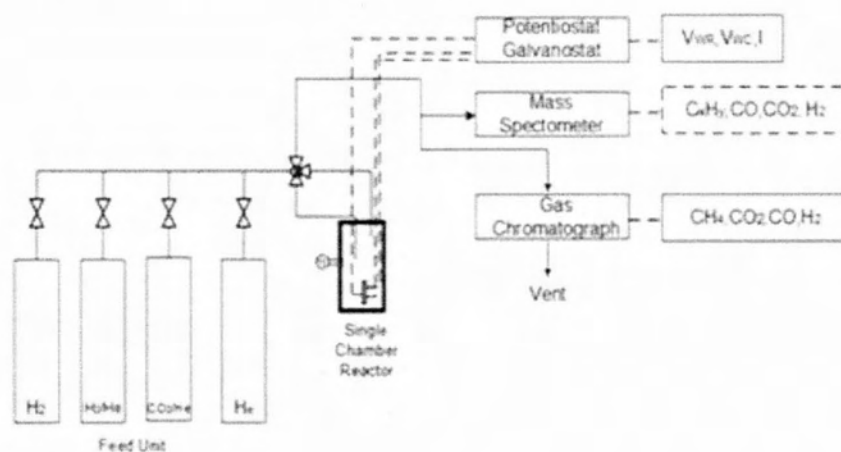


**Figure 4-1 Experimental setup**

According to the flowchart (Figure 4-1), the gas mixture flows from the tanks, through a system of stainless steel tubes (diameter, 1/8 inch) and a piping system (Mass Flow Controller, MFC) followed by a four-way valve, in the mass spectrometer. As shown in Figure 4-1, the reactor is the main part of the experimental system. The output mixture of the reactor could be sent to the Gas Chromatographer ( Shimadzu, GC 14B) or Mass Spectrometer( Omnistar Balzers) for quantitative and qualitative analysis and ends to a vent. A bubble flow meter was used for the verification    of the MFCs correct operation. A potentiostat-galvanostat (AMEL2053) was used, allowing the continuous recording of the potential vs current.
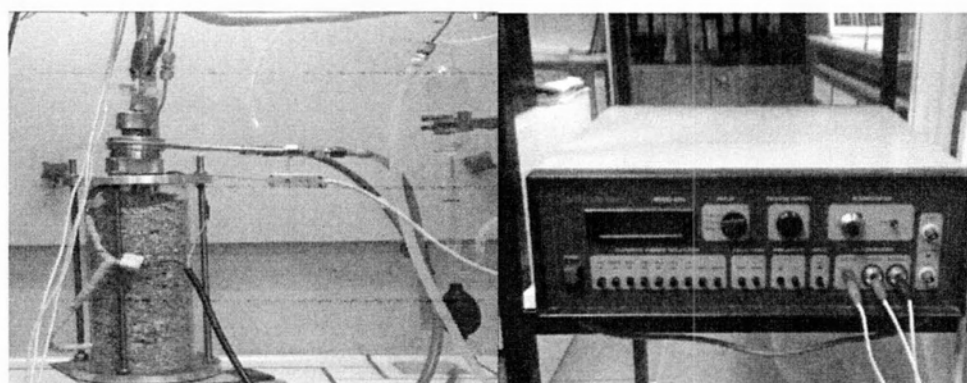


**Figure 4-2 The reactor enclosed in the furnace (height 25cm, diameter 14cm, heating capacity 700°C) next to the bubble flow meter (left) and the potentiostat – galvanostat AMEL 2053 (right).**

### 4.1    Three-electrode single chamber reactor

The single-chamber three electrode system is schematically shown in Figure 4-3. As it can be seen, the protonic disk is suspended in a quartz tube (length 10 cm, 2.9 cm inside diameter and 3.4 cm

74

outside diameter). The tube is closed at the bottom-end, while at the upper-end is placed a metallic head equipped with: i) an inlet and outlet gas system ii) cooling system and iii) gold wires which connect the electrodes with the electrochemical station.
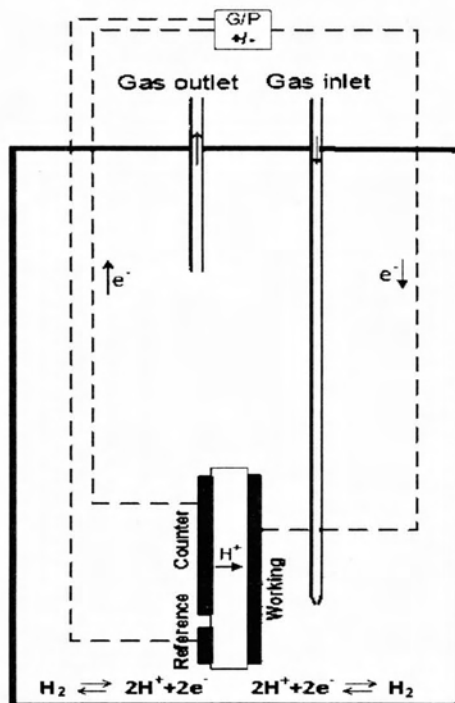


**Figure 4-3 Single chamber CSTR electrochemical reactor and the three electrode system**
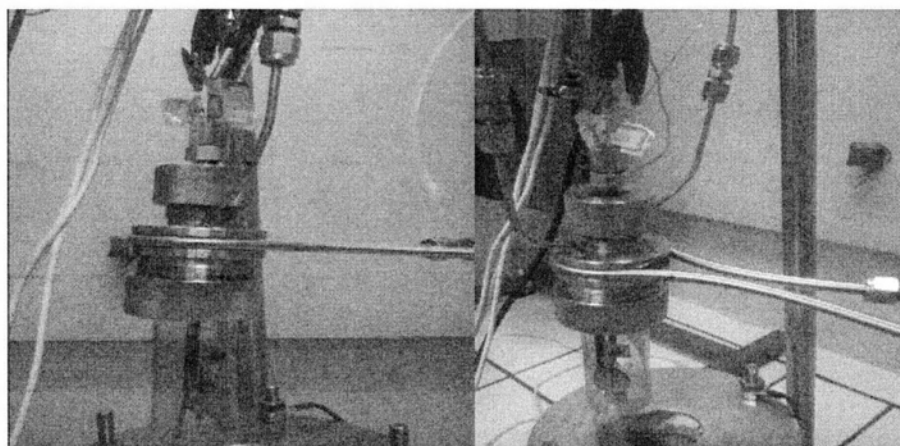


**Figure 4-4 Metallic headed (70 cm$^{3)}$, single chamber quartz reactor for use under atmospheric pressure.**

The temperature (K) is measured with thermocouple connected to a PD temperature controller that is powered by a Variac transformer.

## 4.2    Proton Electrolyte Conductor

High temperature protonic conductors attracted considerable attention of researchers because of phenomena of proton transport in oxide materials. Since 1980, proton conduction was discovered in perovskites based on cerates and zirconates of rare earth elements. Currently systems based on $BaCeO_3$ and $BaCeZrO_3$ are widely investigated as the most popular materials[106].

It is well known that the highest values of proton conductivity reported in literature where achieved for $BaCeO_3$-based oxides[107, 108]. However in presence of atmospheres containing $CO_2$ (as reaction product) this system is not stable due to the chemical interaction with following decomposition of perovskite phase to a mixture of $BaCO_3$ and $CeO_2$-like components[108, 109]. On the other hand, the $BaZrO_3$- based materials are characterized by higher thermodynamic stability in wide temperature range and different atmosphere conditions, but lower ionic (oxygen-ionic and protonic) conductivity.

On the best way to optimize and stabilize the electrical properties is the creation of materials based on $BaCeO_3$- $BaZrO_3$ solid solution. Many of these systems, such as Nd-doped[110], Sm-doped[111], Gd-doped[112], Y-doped $BaCeO_3$- $BaZrO_3$ [113]were investigated for the better electrolytes research. Up to date, among the above mentioned oxides, the $BaCe_{0.7}Zr_{0.1}Y_{0.2-y}Yb_yO_{3-\delta}$ system is considered the most promising, due to the improved electrical and electrochemical properties and thermodynamic and kinetic stability [114]. However, as recently shown (table 13 in [108]) the introduction of 10% Zr ( at B-position of ABO3 perovskite) it is not sufficient to ensure an acceptable stability for the material in corrosive atmospheres. Correspondingly a large degree replacement of Ce by Zr substitution is required. However in this case much attention must be paid to the simple methods of obtaining gas-tight ceramics because with increasing Zr-concentrations the material 's sintering becomes inconvenient [108].

In the present study a novel proton conducting solid oxide electrolyte with $BaCe_{0.5}Zr_{0.3}Y_{0.08}Yb_{0.08}Cu_{0.04}O_3-\delta$ composition has been prepared at relatively low sintering temperature by solid state method combined with addition of small amount of sintering aid (CuO). Phase structure and electrical properties were investigated by the aid of X-ray diffraction (XRD), scanning electron microscopy ( SEM) and conductivity measurements.

The $BaCe_{0.5}Zr_{0.3}Y_{0.08}Yb_{0.08}Cu_{0.04}O_{3-\delta}$ sample was supplied and synthesized according to the conventional solid state reaction method, using $BaCO_3$, $CeO_2$, $ZrO_2$, $Y_2O_3$, $Yb_2O_3$ and CuO of high purity (not less than 99.5%) as initial compounds. The calcination of the sample was carried out at 1100°C for 3 h in air. The calcined powders were milled at a planetary mill (Fritsch Pulverisette 6) for 1 h with a rotation rate of 350 $min^{-1}$, then pressed at 4 ton $cm^{-2}$ and fired at 1400°C for 3 h.

XRD analysis was performed on the milled powders of specimens after sintering by using a DMAX-2500, Rigaku Co. Ltd, diffractometer with Ni-filtered CuKa radiation in the range of

$15° < 2\theta < 85°$ with a scanning rate of $0.5°$ min$^{-1}$. The identification of the phase composition of the crystal structure of the materials were performed according to Joint Committee on Powder Diffraction Standards, Database (JCPDS). The surface morphology of the ceramic samples was measured by employing Archimedes principle and compared to the theoretical one.

The conductivity of the ceramic bar samples 0.1x0.5x2.5 cm was investigated by the standard four probe dc-method utilizing the microprocessor system ZIRCONIA-318 in a wide range of temperatures (500-900°C) in air and wet hydrogen atmospheres as well as in a wide range of oxygen partial pressures ($1x10^{-19}$-0.21 atm)at 600°C,700°C and 800°C.

XRD data of sintered $BaCe_{0.5}Zr_{0.3}Y_{0.08}Yb_{0.08}Cu_{0.04}O_3–\delta$ ceramic are reported in Figure 4-5. According to the presented data, material is characterized by the cubic perovskite structure (space group Pm3m) with unit cell parameter equal to 4.331Å.
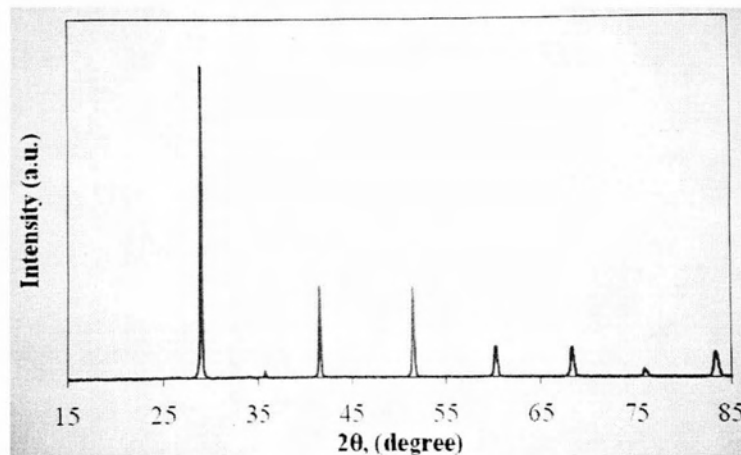


**Figure 4-5 Room temperature XRD patterns of $BaCe_{0.5}Zr_{0.3}Y_{0.08}Yb_{0.08}Cu_{0.04}O_3–\delta$ ceramic sintered at 1400°C for 3h**

It should be noted that symmetry of the perovskite structure has strong dependence on preparation conditions, concentration of dopants ($Y^{3+}$, $Yb^{3+}$ and $Zr^{4+}$) in $BaCeO_3$. The XRD patterns show that no additional reflection related to impurity phases were observed.

The surface of the as-prepared ceramic is homogenous with an average size of grain of about 2 μm. The density of the sample was equal to 90.8% of the density calculated from the XRD data. The obtained high density of $BaCe_{0.5}Zr_{0.3}Y_{0.08}Yb_{0.08}Cu_{0.04}O_3–\delta$ at extremely low sintering temperature(1400°C) is associated with the introduction of sintering agent (CuO) [108].
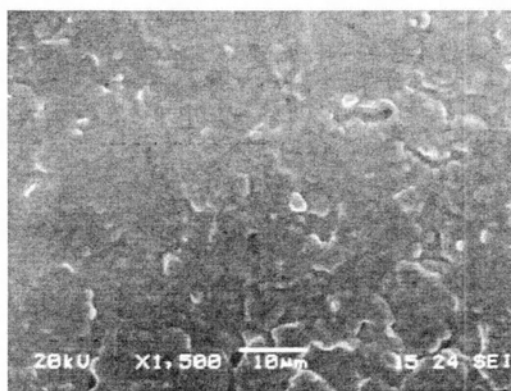
**Figure 4-6 SEM microphotography of BaCe$_{0.5}$Zr$_{0.3}$Y$_{0.08}$Yb$_{0.08}$Cu$_{0.04}$O$_3$–δ ceramic sintered at 1400 °C for 3h.**

The transport properties of cerate –zirconate barium were evaluated by measurements of electrical conductivity in wide range of temperature values ( Figure 4-7). The disk (0,5 mm thickness and 20mm diameter) had a total conductivity of 1.4 mS cm$^{-1}$ at 500°C and 23.9 mS cm$^{-1}$ at 900°C in ambient atmosphere. In 3 H$_2$O% vol + H$_2$ atmosphere it had 1.5 mS cm$^{-1}$ at 500°C and 6.9 mS cm$^{-1}$ total conductivity at 900°C.
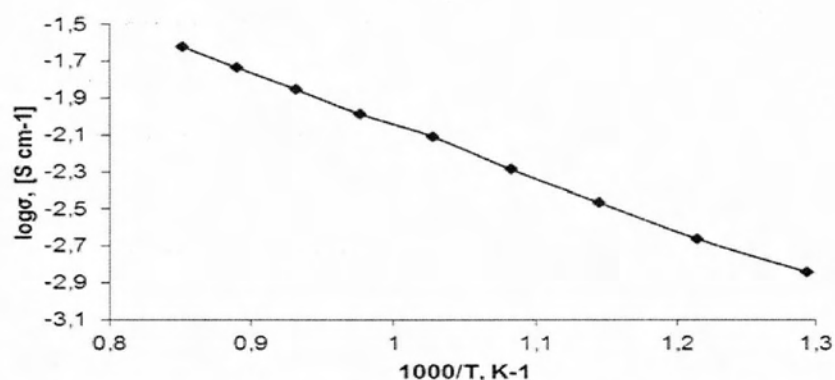


**Figure 4-7 Conductivity versus temperature for BaCe$_{0.5}$Zr$_{0.3}$Y$_{0.08}$Yb$_{0.08}$Cu$_{0.04}$O$_3$–δ.**

The apparent activation energy of conductivity in the temperature intervals of 500-700°C and 700-900°C was calculated equal to 0.63 and 0.65 eV for the oxidizing condition and 0.3 and 0.47 eV for reducing condition.The apparent activarion energy value at low temperature range is lower than for high temperature range.

## 4.3 Preparation of the electrodes

The three electrode –electrolyte system (working-counter-reference) was prepared as follows: the material was in form of powder, dissolved in an oily non-soluble resin. The metal-electrode was deposited on the electrolyte by the aid of a brush.
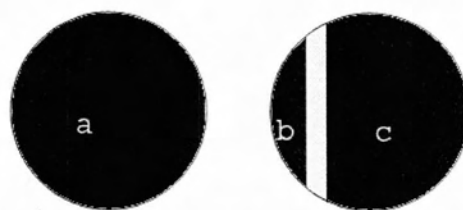
**Figure 4-8 The two surfaces of the pellet after the dyeing with the paste. a) working electrode b) reference electrode, c) counter electrode.**
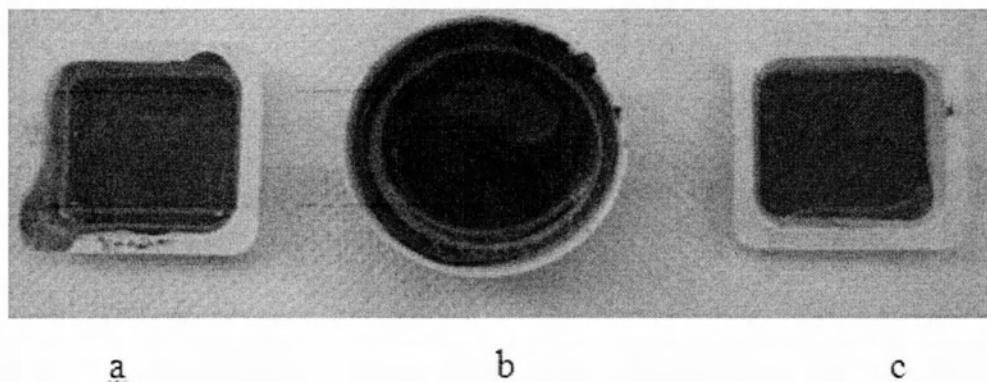


**Figure 4-9 Organometallic paste of a) Copper - Cu, b) Cobalt - Cu, c) iron - Fe**

The analytic preparation method for copper, iron and cobalt is shown below:

## 1. Cu

The paste was prepared by mixing Cu metal powder purity ($\geq$ 99.9) with particle size 40-60 nm (Sigma Aldrich) in mineral oil.

A thin brush was used to deposit a film of the catalyst on the three surfaces of the pellet. The geometrical surface area of the working, counter and reference films were determined to be approximately $2cm^2$, $1.6cm^2$ and $0.2cm^2$ respectively. SEM micrographs showed that the thickness of the electrodes was about 10μm.

The thin films of polycrystalline Cu was initially dried at ambient conditions and then calcined in air till 400°C for 30 min, in order to achieve good adhesion of iron in the proton conductor and finally reduced under $H_2$/He flow till 510°C for 2h (heating rate: 10°C/min in all cases).

## 2. Fe

The three iron-electrode films (working, counter, reference) were prepared as follows: iron-nanosized powder (Sigma-Aldrich), 99.5% purity, particle size <100 nm) was activated in mineral oil, forming a dense paste, which by the aid of a brush was deposited in thin films on both sides of the disk.

The as prepared three electrode system with Fe thin films was calcined in oxidizing atmosphere up to 400°C for 30 minutes (heating rate ~3°C min⁻¹) and then heated in reducing atmosphere up to 725°C (heating rate 5°Cmin⁻¹).

The geometrical surface area of the working, counter and reference films were determined to be approximately 2 cm², 1.6 cm² and 0.2 cm² respectively. SEM micrographs of the Fe electrodes 'films showed that they were relatively well adhered on both sides of the protonic disk and the average thickness of each film was approximately 50μm (Figure 5-20)

### 3. Co

Cobalt powder (Sigma-Aldrich) of ≥99.8% purity, particle size <2μm was mixed in mineral oil, forming a dense paste, which by the aid of a brush was deposited in thin films on both sides of the disk. The as prepared three electrode system with cobalt thin films was calcined in oxidizing atmosphere up to 400°C for 30 minutes (heating rate ~3°C min⁻¹) and then heated in reducing atmosphere up to 725°C (heating rate 5°Cmin⁻¹). The geometrical surface area of the working, counter and reference films were determined to be approximately 2 cm², 1.6 cm² and 0.2 cm² respectively.
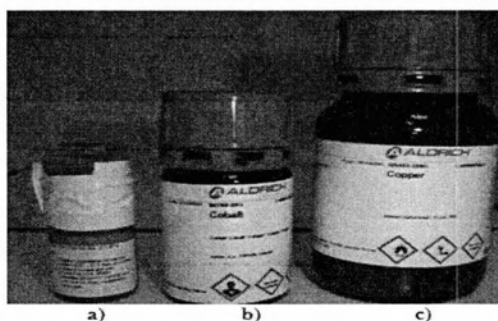


**Figure 4-10 Commercial powders of the catalysts used: a) Fe, b) Co, c) Cu**

### 4.4 Triphase Catalytic Activity

The effect of the overpotential η takes place on the electric current over the catalytic Triphase ( gas phase-electron conductor-electrolyte). The value of the overvpotential is given by $\eta = V^o_{WC} - V^o_{WR}$ where $V^o_{WR}$ represents the open circuit voltage (I=0). We consider that positive overpotentials (η>0) lead to exponential increase of current (I>0) while negative overpotentials (η<0) lead to exponential decrease of current (I<0). In both cases the exponential (Tafel) dependence is in agreement with the high field approach of Butler-Volmer equation (η<200mV) according to:

$$\ln\left(\frac{I}{I_o}\right) = \frac{\alpha_\alpha F\eta}{RT}, \qquad \text{for } \eta>0$$

$$\ln\left(\frac{I}{I_o}\right) = \frac{\alpha_c F\eta}{RT}, \qquad \text{for } \eta<0$$

Where $I_o$ represents exchange current density, the Triphase (gas phase-electron conductor-electrolyte) standard and $\alpha_a$, $\alpha_c$ represent positive and negative charge flow coefficients respectively. The linear part of Tafel diagram means that the coverage area of the main electromotive particle (hydrogen) remains stable. Similar $\alpha_a$, $\alpha_c$ values mean that electrocatalytic charge transfer reaction for the anodic and cathodic part remain stable.

# CHAPTER V

## Experimental data and result analysis

The electrochemical promotions of thin-film catalytic systems of Cu, Fe, Co electrodes deposited on ceramic proton conductor $BaCe_{0.5}Zr_{0.3}Y_{0.08}Yb_{0.08}Cu_{0.04}O_3-\delta$ were studied.

## 5    Experimental data

The catalyst-electrodes were deposited on ceramic materials with cationic conductivity. Three different catalysts: i) copper (Cu), ii) a cobalt (Co) and iii) iron (Fe) applied in the cationic conductor $BaCe_{0.5}Zr_{0.3}Y_{0.08}Yb_{0.08}Cu_{0.04}O_3-\delta$.

The objective of the experiment was to determine the parameters of the electrochemical systems $(I_o, \alpha_\alpha, \alpha_c, E_A)$ as explained in chapter II. The results are studied in the linear part between 0.030V-0.20V of Tafel equation:

$$ln\,i = ln\,i_0 + \frac{aF\eta}{RT}$$

$$\log i = \log i_0 + \frac{aF}{2,3RT}\eta$$

Where I is the applied current, $I_o$ is the exchange current density, $\alpha$ is the charge transfer coefficient which for the anodic and the cathodic operation are denoted $\alpha_a$ and $\alpha_c$, are respectively), $\eta$ is the IR-free overpotential, F is the Faraday's constant, R is the ideal gas constant and T is the temperature in K.

An example of Tafel approximation (of Figure 5-19 ) is presented in Figure 5-1. After the applied apparent fit, slope is used in order to calculate $\alpha$ ($\alpha$=2,3slopeRT/F) while intercept is used to calculate $I_o$ ($I_o$=10^intercept).
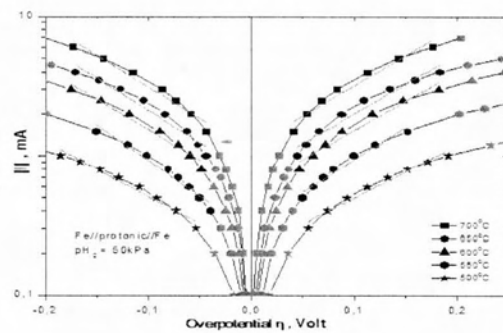


**Figure 5-1 Calculation of $I_o$, $\alpha$ for Fe│BaCe0.5Zr0.3Y0.08Yb0.08Cu0.04O3–δ│Fe cell on Tafel region.**

Activation energy $E_a$ is calculated using the slope of $|I_o|$ vs1/T diagram ($E_a$=$\alpha$F$\eta$=slope*R). An example is presented in

Figure 5-4. $E_a$ is calculated in J mol$^{-1}$ and then it is transformed in eV.

Measurements were taken with a limit at 2000mV whereas the proton electrolyte is a mixture of metals that we do not know when it is likely to be reduced. So it is difficult to arrive at conclusions on the $I_L$ values from these measurements[115]

83

### 5.1.1    Cu | $BaCe_{0.5}Zr_{0.3}Y_{0.08}Yb_{0.08}Cu_{0.04}O_3-\delta$ | Au in $H_2$/He atmospheres

When a three electrode cell is used to perform electroanalytical chemistry, the auxiliary electrode, along with the working electrode, provides circuit over which current is either applied or measured. The potential of the auxiliary electrode is usually not measured and is adjusted so as to balance the reaction occurring at the working electrode.

This configuration allows the potential of the working electrode to be measured against a known reference electrode without compromising the stability of that reference electrode by passing current over it[116]. In this experiment working electrode was made by copper (Cu), Reference and counter were made by Au using the spatter deposition.

Figure 5-2 schematically illustrates the results obtained from the polarization study of the Cu | $BaCe_{0.5}Zr_{0.3}Y_{0.08}Yb_{0.08}Cu_{0.04}O_3-\delta$ | Au system at different temperatures (i.e., 300°C, 350°C, 400°C, 450°C and 500°C) and hydrogen atmospheres (p $H_2$: 101 kPa, 50 kPa and 20 kPa). The dependence of the exchange current on the (IR-free) overpotential, $\eta$ (mV), for anodic and cathodic mode of operation at a total gas flow of 100 ml min$^{-1}$ was determined.

Temperature significantly affected the behavior of the cell, as conductivity increased with increased temperature at which I-V measurements were made. The maximum current value obtained was approximately 150mA at 1.15V and 1.7V at 500°C for positive and negative current respectively for a partial pressure of hydrogen $pH_2$=50kPa.

The electrochemical parameters $\alpha_a$, $\alpha_c$ and $I_o$ were exported, and activation energy was calculated. All the results are presented in Table 5-1. I-$\eta$ curves are symmetrical due to exposition both of the electrodes at the same gas mixture in the reactor suggesting that in both the working and the counter electrode the following reaction occurs:

$$2H^+ + 2e^- \leftrightharpoons H_2$$
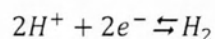
The dependence between current, temperature and hydrogen partial pressure can be observed in Figure 5-3. For temperatures above 400°C, it is observed that current significantly increases (voltages: ±100, ±200mV). Hydrogen partial pressures ($pH_2$ = 20, 50, 101 kPa) is not as important as temperature for the increase of current values.
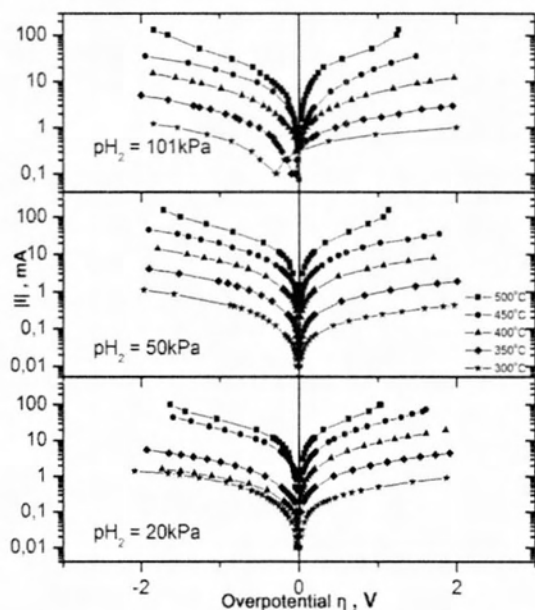
**Figure 5-2 Exchange current density as a function of the anodic and cathodic overpotentials (Tafel plots) of $Cu \mid BaCe_{0.5}Zr_{0.3}Y_{0.08}Yb_{0.08}Cu_{0.04}O_3{-}\delta \mid Au$ system, in the temperature range between 300-500°C and $pH_2$: 20 kPa, 50 kPa and 101kPa**
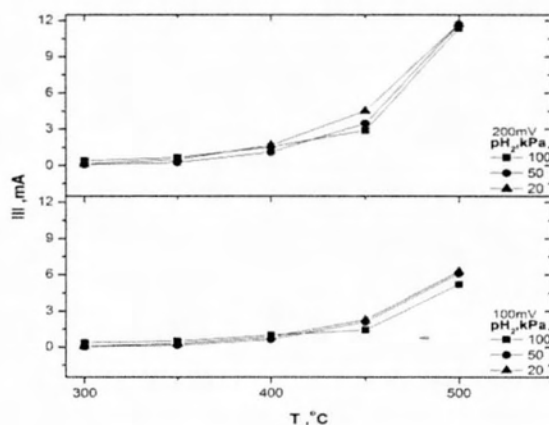


A)
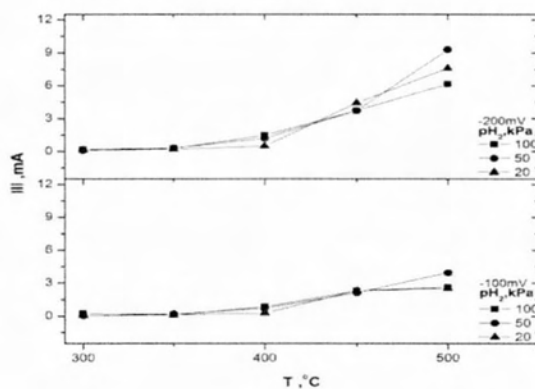


B)

**Figure 5-3 Effect of temperature on current density, for standard overpotential values ±100 and ±200 mV and hydrogen partial pressure: 20kPa, 50 kPa, 101 kPa.**

85

Figure 5-4 shows the graphs of the exchange current density absolute values over the inverse temperature. The activation energy values for hydrogen partial pressure of $pH_2$ (20, 50 and 101kPa) are $0.89 \pm 0.05$ eV, $0.85 \pm 0.05$ eV, $0.5 \pm 0.1$ eV, respectively, whereas the values of the anodic and cathodic charge transfer coefficient at each temperature for hydrogen partial pressure of 20, 50 and 101kPa are 0.3, 0.3 and 0.6 respectively.



A)

B)



C)
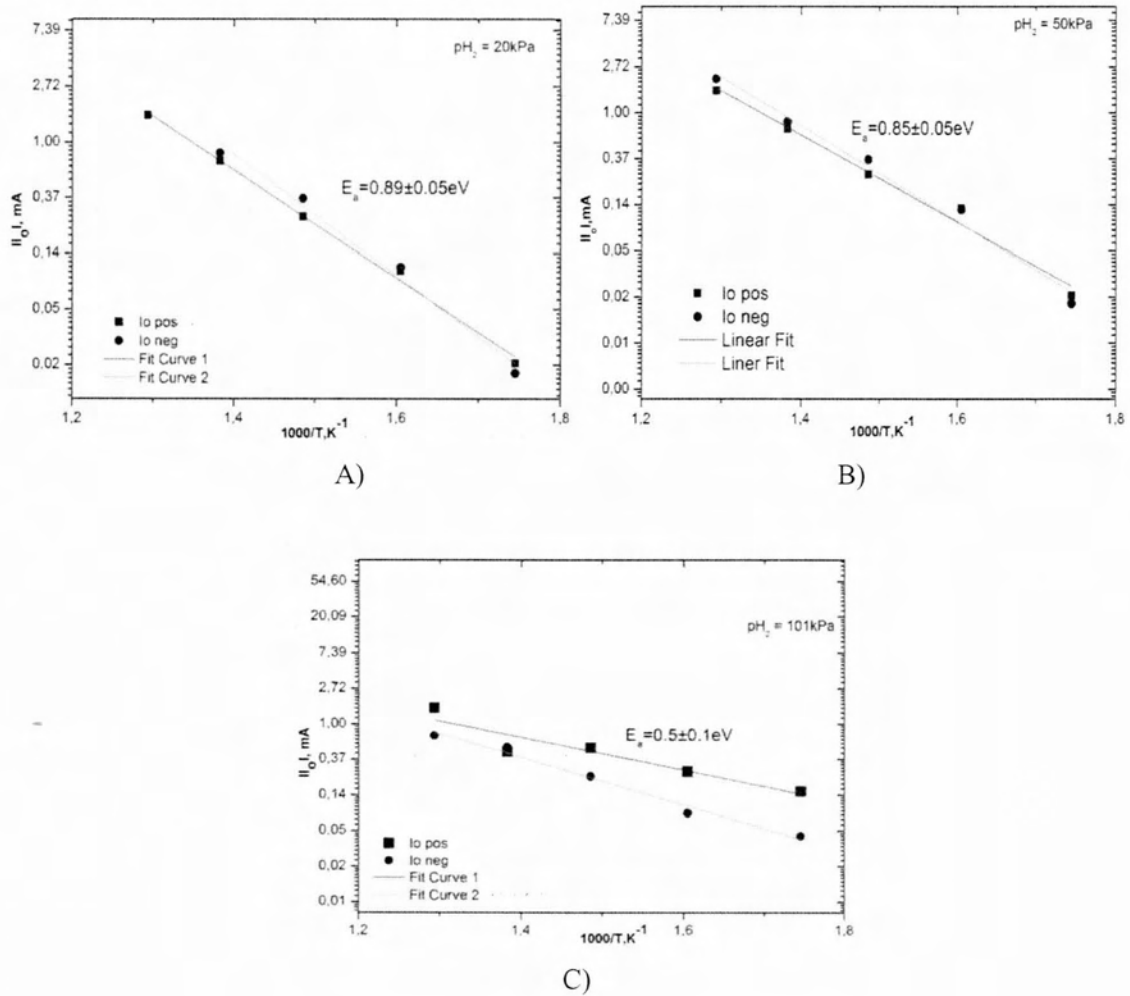
**Figure 5-4 Graphical representation of the anodic and cathodic $I_o$ versus the reverse temperature for the calculation of the activation energy for hydrogen partial pressure of A) 20, B) 50 and C) 101kPa.**

**Table 5-1** Values of exchange current density ($I_o$) and anodic and cathodic charge transfer coefficients ($\alpha_a$, $\alpha_c$) as well as the corresponding energies of activation, for electrochemical system $Cu\,|\,BaCe_{0.5}Zr_{0.3}Y_{0.08}Yb_{0.08}Cu_{0.04}O_3{-}\delta\,|\,Au$ in $H_2$/He at the experimental conditions employed.

| T, °C | pH2=101 kPa | | | | pH2=50 kPa | | | | pH2=20 kPa | | | |
|---|---|---|---|---|---|---|---|---|---|---|---|---|
| | $I_{o,a}$(mA) | $I_{o,c}$(mA) | $\alpha_a$ | $\alpha_c$ | $I_{o,a}$(mA) | $I_{o,c}$(mA) | $\alpha_a$ | $\alpha_c$ | $I_{o,a}$(mA) | $I_{o,c}$(mA) | $\alpha_a$ | $\alpha_c$ |
| 500 | 1.58 | 0.93 | 0.3 | -0,3 | 1.62 | 0.08 | 1.62 | -0.8 | 0.34 | 0,02 | 0.6 | -0.5 |
| 450 | 0.45 | 0.52 | 0,3 | -0,4 | 0.72 | 0.82 | 0.71 | -0.3 | 0.39 | 0.11 | 0.5 | -0.4 |
| 400 | 0.50 | 0.31 | 0.2 | -0,2 | 0.26 | 0.36 | 0.26 | -0.2 | 0.65 | 0.36 | 0.6 | -0.5 |
| 350 | 0.40 | 0.05 | 0,1 | -0,2 | 0.12 | 0.92 | 0.1 | -0.2 | 0.85 | 0.82 | 0.7 | -0.6 |
| 300 | 0.40 | 0,04 | 0,1 | -0,1 | 0.02 | 0.02 | 0.2 | -0.2 | 1.6 | 0.07 | 0.8 | -1.9 |
| E (eV) | 0.39 | 0.57 | | | 0.82 | 0.90 | | | 0.84 | 0.94 | | |

### 5.1.2 $Cu\,|\,BaCe_{0.5}Zr_{0.3}Y_{0.08}Yb_{0.08}Cu_{0.04}O_3{-}\delta\,|\,Cu$ in $H_2$/He atmospheres

Figure 5-5 schematically illustrates the results obtained from the polarization study of the $Cu\,|\,BaCe_{0.5}Zr_{0.3}Y_{0.08}Yb_{0.08}Cu_{0.04}O_3{-}\delta\,|\,Cu$ system at different temperatures (i.e., 250°C, 300°C 350°C, 400°C, 450°C and 510°C) in $H_2$/He atmosphere (p $H_2$: 100 kPa , Ft=100ccm).

The dependence of the exchange current on the (IR-free) overpotential, $\eta$ (mV), for anodic and cathodic mode of operation was determined.

The maximum current value obtained was about 5.3 mA at 1.99V and 11mA at 1.96V at 500°C for positive and negative current, respectively.

The electrochemical parameters $\alpha_a$, $\alpha_c$, and $I_o$ were exported, and the activation energy was calculated. I-$\eta$ curves are symmetrical due to exposition of both electrodes at the same gas mixture in the reactor. All the results are presented in Table 5-2.

Figure 5-6 shows the graphs of the exchange current density absolute values over the inverse temperature. The activation energy value is $0.75 \pm 0.05$eV, while the values of the anodic and cathodic charge transfer coefficients are both 0.5.
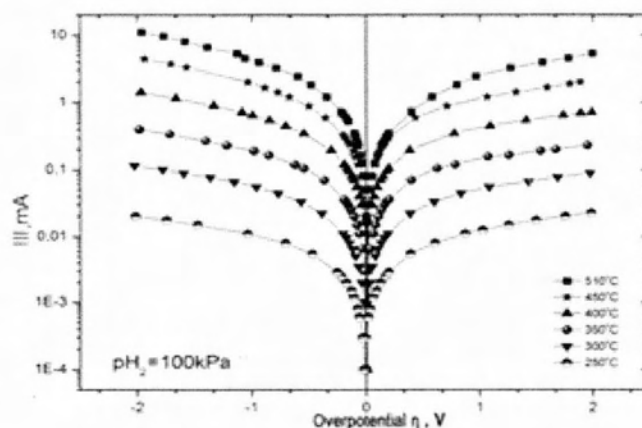
Figure 5-5 Exchange current density as a function of the anodic and cathodic overpotentials (Tafel plots) of Cu│BaCe$_{0.5}$Zr$_{0.3}$Y$_{0.08}$Yb$_{0.08}$Cu$_{0.04}$O$_3$–δ│Cu system, in the temperature range between 250-510°C in H$_2$/He atmosphere (p H$_2$: 100 kPa, Ft=100ccm).
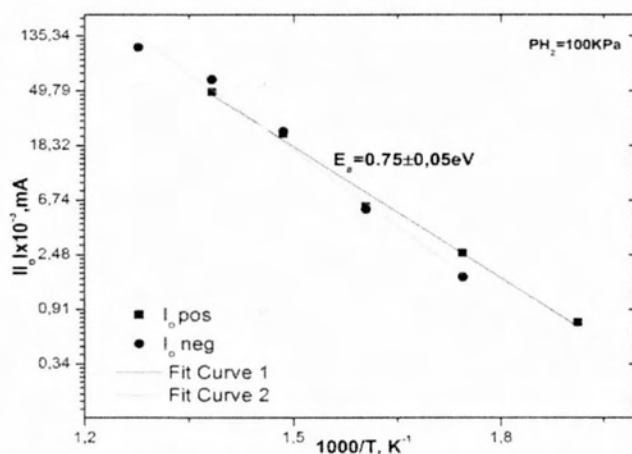


Figure 5-6 Graphical representation of the anodic and cathodic values I$_o$ versus the reverse temperature for the calculation of the activation energy of the reaction system Cu│BaCe$_{0.5}$Zr$_{0.3}$Y$_{0.08}$Yb$_{0.08}$Cu$_{0.04}$O$_3$–δ│Cu galvanostatically under H$_2$ flow for temperatures 250-510°C.

Table 5-2 Values of exchange current density (I$_o$) and anodic and cathodic charge transfer coefficients (α$_a$, α$_c$) as well as the corresponding energies of activation, for electrochemical system Cu│BaCe$_{0.5}$Zr$_{0.3}$Y$_{0.08}$Yb$_{0.08}$Cu$_{0.04}$O$_3$–δ│Cu in H$_2$/He at the experimental conditions employed.

| T, °C | pH$_2$=101kPa | | | |
|---|---|---|---|---|
| | I$_{o,a}$(mA) | I$_{o,c}$(mA) | α$_a$ | α$_c$ |
| 510 | 0.050 | 0.110 | 0.8 | -0.7 |
| 450 | 0.050 | 0.060 | 0.6 | -0.6 |
| 400 | 0.022 | 0.024 | 0.5 | -0.5 |
| 350 | 0.004 | 0.006 | 0.5 | -0.5 |
| 300 | 0.006 | 0.002 | 0.4 | -0.5 |
| 250 | 0.0007 | 0.0004 | 0.3 | -0.5 |
| E (eV) | 0.69 | 0.80 | | |

88

### 5.1.3  Cu | BaCe$_{0.5}$Zr$_{0.3}$Y$_{0.08}$Yb$_{0.08}$Cu$_{0.04}$O$_3$–δ | Cu in H$_2$/ CO$_2$=1/8 mixture

Figure 5-7 schematically illustrates the results obtained from the polarization study of the Cu | BaCe$_{0.5}$Zr$_{0.3}$Y$_{0.08}$Yb$_{0.08}$Cu$_{0.04}$O$_3$–δ | Cu system at different temperatures (i.e., 300°C, 350°C, 400°C and 450°C) in H$_2$/CO$_2$=1/8 mixture with He as carrier gas and total flow 60ccm. The dependence of the exchange current on the (IR-free) overpotential, η (mV), for anodic and cathodic mode of operation was determined.

The maximum voltage was 2.081V at 1.1mA and -1.801V at 11 mA at 450°C.
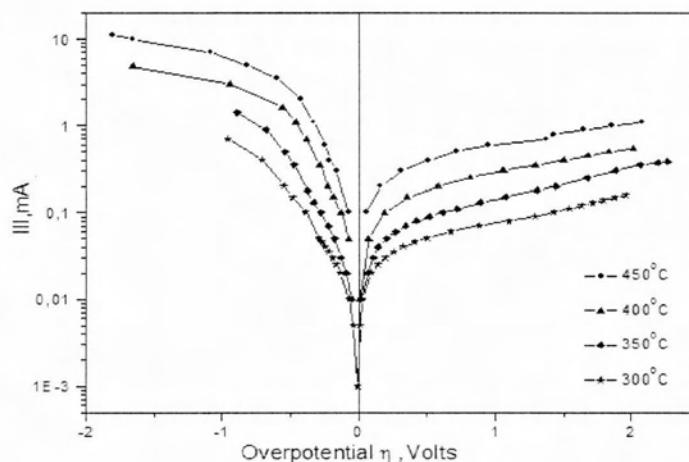


**Figure 5-7 Exchange current density as a function of the anodic and cathodic overpotentials (Tafel plots) of Cu | BaCe$_{0.5}$Zr$_{0.3}$Y$_{0.08}$Yb$_{0.08}$Cu$_{0.04}$O$_3$–δ | Cu system, in the temperature range between 300-450°C in H$_2$ / CO$_2$ mixture (H$_2$/ CO$_2$=1/8, Ft=60ccm).**
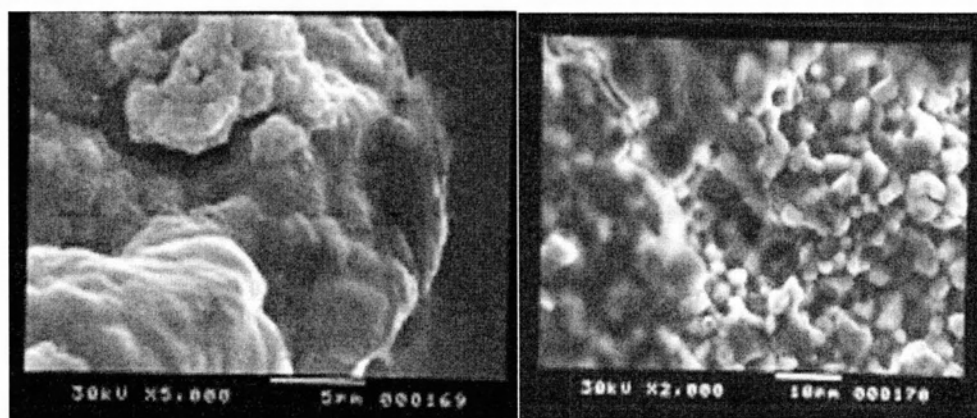


**Figure 5-8 (Left) SEM micrograph of the Cu catalyst particles after the experiments showed that the catalytic surface had a film of CO on the top (faded area). (Right) SEM micrograph of the electrolyte area that probably had CO on top, (faded areas)**

The curves are not symmetrical, probably due to poor adhesion of the catalyst especially after 350°C. Another reason for this asymmetry could be the creation of a CO film on the top of the catalytic area (on one electrode), which reduced its active areas.

The electrochemical parameters $\alpha_a$, $\alpha_c$, and $I_o$ were exported, and the activation energy was calculated. All the results are presented in Table 5-3. Figure 5-9 shows the graphs of the exchange current density absolute values over the inverse temperature. The activation energy value is 0.23eV± 0.02eV, whereas the values of the anodic and cathodic charge transfer coefficient are 0.3, 0.6.
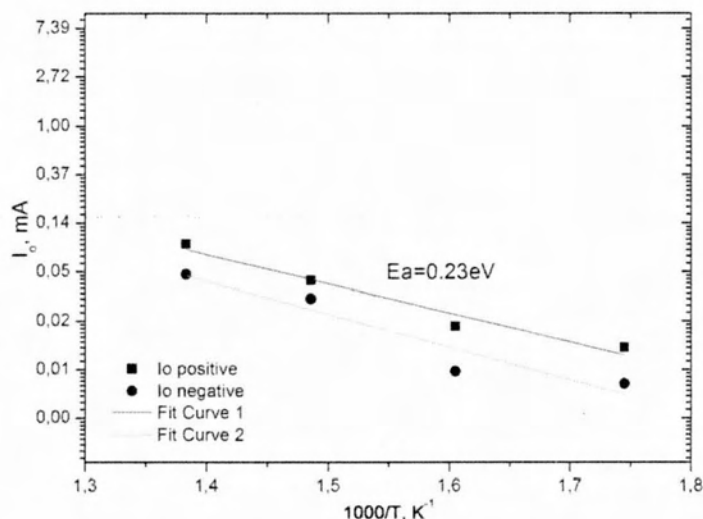


**Figure 5-9 Graphical representation of the anodic and cathodic values $I_o$ over the reverse temperature in order to calculate the activation energy of the reaction system Cu│ BaCe$_{0.5}$Zr$_{0.3}$Y$_{0.08}$Yb$_{0.08}$Cu$_{0.04}$O$_3$–δ │Cu galvanostatically under flow H$_2$/ CO$_2$ with carrier gas He for different temperatures.**

**Table 5-3 Values of exchange current density ($I_o$) and anodic and cathodic charge transfer coefficients ($\alpha_a$, $\alpha_c$) as well as the corresponding energies of activation, for electrochemical system Cu│ BaCe$_{0.5}$Zr$_{0.3}$Y$_{0.08}$Yb$_{0.08}$Cu$_{0.04}$O$_3$–δ │Cu in H$_2$/ CO$_2$ =1/8 at the experimental conditions employed.**

| T, °C | $H_2/CO_2=1/8$ | | | |
|---|---|---|---|---|
| | $I_{o,a}$(mA) | $I_{o,c}$(mA) | $\alpha_a$ | $\alpha_c$ |
| **450** | 0.088 | 0.047 | 0.3 | -0.7 |
| **400** | 0.042 | 0.029 | 0.2 | -0.5 |
| **350** | 0.016 | 0.007 | 0.3 | -0.6 |
| **300** | 0.011 | 0.005 | 0.3 | -0.4 |
| E (eV) | 0.22 | 0.25 | | |

### 5.1.4  Cu | BaCe$_{0.5}$Zr$_{0.3}$Y$_{0.08}$Yb$_{0.08}$Cu$_{0.04}$O$_3$–$\delta$ | Cu in H$_2$/ CO$_2$=1/5 mixture

Figure 5-10 schematically illustrates the results obtained from the polarization study of the Cu | BaCe$_{0.5}$Zr$_{0.3}$Y$_{0.08}$Yb$_{0.08}$Cu$_{0.04}$O$_3$–$\delta$ | Cu system at different temperatures (i.e., 300°C 350°C, 400°C, 450°C and 500°C) in H$_2$/CO$_2$ mixture (H$_2$/ CO$_2$=1/5, Ft=60ccm). The dependence of the exchange current on the (IR-free) overpotential, $\eta$ (mV), for anodic and cathodic mode of operation was determined. The maximum current value obtained was about 2.8 mA at 1.9V and 7.4mA at -1.9V at 500°C. Curves are almost symmetrical.
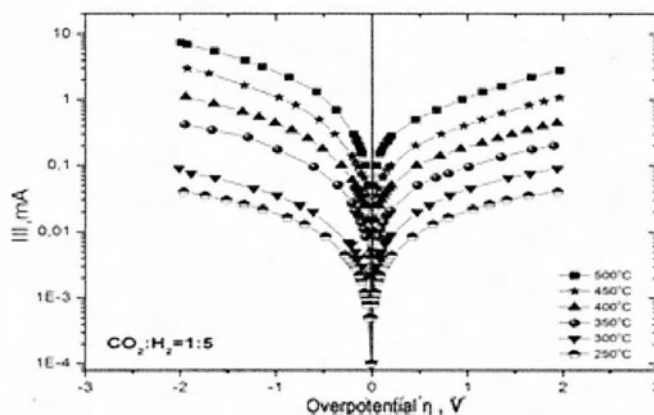


**Figure 5-10 Exchange current density as a function of the anodic and cathodic overpotentials (Tafel plots) of Cu | BaCe$_{0.5}$Zr$_{0.3}$Y$_{0.08}$Yb$_{0.08}$Cu$_{0.04}$O$_3$–$\delta$ | Cu system, in the temperature range between 250-500°C in H$_2$/CO$_2$ mixture (H$_2$/ CO$_2$=1/5, Ft=60ccm).**

The electrochemical parameters $\alpha_a$, $\alpha_c$, and I$_o$ were exported, and the activation energy was calculated. All the results are presented in Table 5-4. Figure 5-11 shows the graphs of the exchange current density absolute values over the inverse temperature. The activation energy value is 0.64eV± 0.015eV, whereas the values of the anodic and cathodic charge transfer coefficient are 0.5, 0.6.
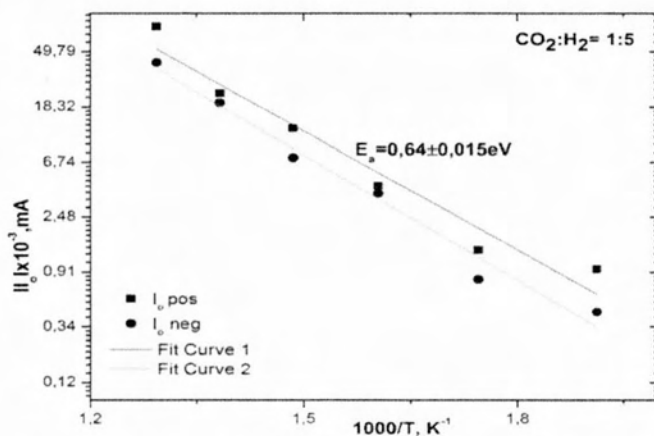


**Figure 5-11 Graphical representation of the anodic and cathodic values I$_o$ vs the reverse temperature in order to calculate the activation energy of the reaction system Cu |**

$BaCe_{0.5}Zr_{0.3}Y_{0.08}Yb_{0.08}Cu_{0.04}O_3–\delta$ │Cu galvanostatically under a flow of $H_2$/ $CO_2$ with He as a carrier gas for different temperatures

Table 5-4 Values of exchange current density ($I_o$) and anodic and cathodic charge transfer coefficients ($\alpha_a$, $\alpha_c$) as well as the corresponding energies of activation, for electrochemical system Cu│ $BaCe_{0.5}Zr_{0.3}Y_{0.08}Yb_{0.08}Cu_{0.04}O_3–\delta$ │Cu in $H_2$/ $CO_2$ =1/5 at the experimental conditions employed.

| T, °C | $H_2/CO_2=1/5$ | | | |
|---|---|---|---|---|
| | $I_{o,a}$(mA) | $I_{o,c}$(mA) | $\alpha_a$ | $\alpha_c$ |
| 500 | 0.079 | 0.040 | 0.5 | -0.8 |
| 450 | 0.023 | 0.02 | 0.5 | -0.7 |
| 400 | 0.012 | 0.007 | 0.5 | -0.7 |
| 350 | 0.004 | 0.004 | 0.5 | -0.6 |
| 300 | 0.001 | 0.001 | 0.7 | -0.6 |
| 250 | 0.001 | 0.0004 | 0.4 | -0.5 |
| E (eV) | 0.62 | 0.65 | | |

### 5.1.5   Co | BaCe$_{0.5}$Zr$_{0.3}$Y$_{0.08}$Yb$_{0.08}$Cu$_{0.04}$O$_3$–δ | Co in H$_2$/He atmospheres

Figure 5-12 schematically illustrates the results obtained from the polarization study of the Co|BaCe0.5Zr0.3Y0.08Yb0.08Cu0.04O3-δ|Co system at different temperatures (i.e., 450°C 500°C, 550°C, 600°C, 650°C and 700°C) and hydrogen atmospheres (pH$_2$: 101 kPa, 50 kPa and 20 kPa).

Maximum current value obtained was 10mA for 200mV at 700°C. I-η curves are almost symmetrical.
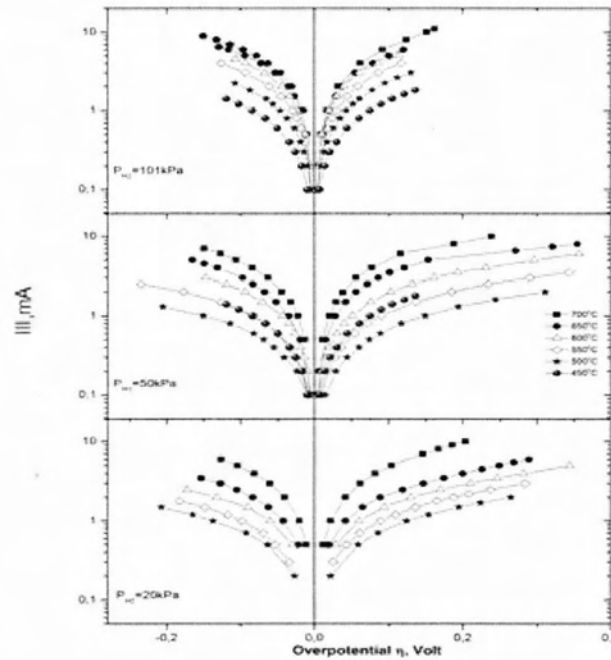


**Figure 5-12 Exchange current density as a function of the anodic and cathodic overpotentials (Tafel plots), in the temperature range between 450 -700°C and pH$_2$: 20 kPa, 50 kPa, 101kPa.**

The increase of hydrogen partial pressure affects positively the conductivity of the cell. This effect is even clearer for hydrogen partial pressure pH$_2$=101kPa. Temperature is also of major importance (Figure 5-13 and Figure 5-14).
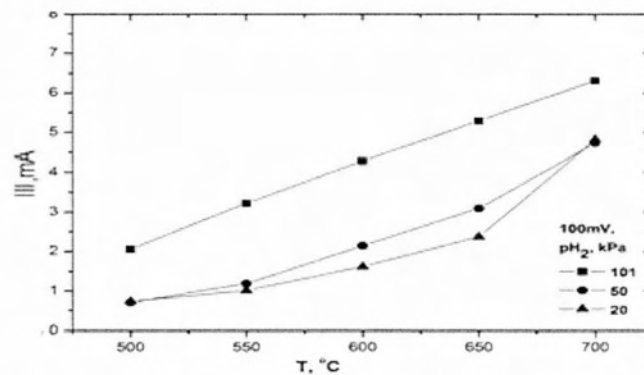


**Figure 5-13 Effect of temperature on current density, for standard overpotential value of 100 mV and hydrogen partial pressure: 20kPa, 50 kPa, 101 kPa.**

93
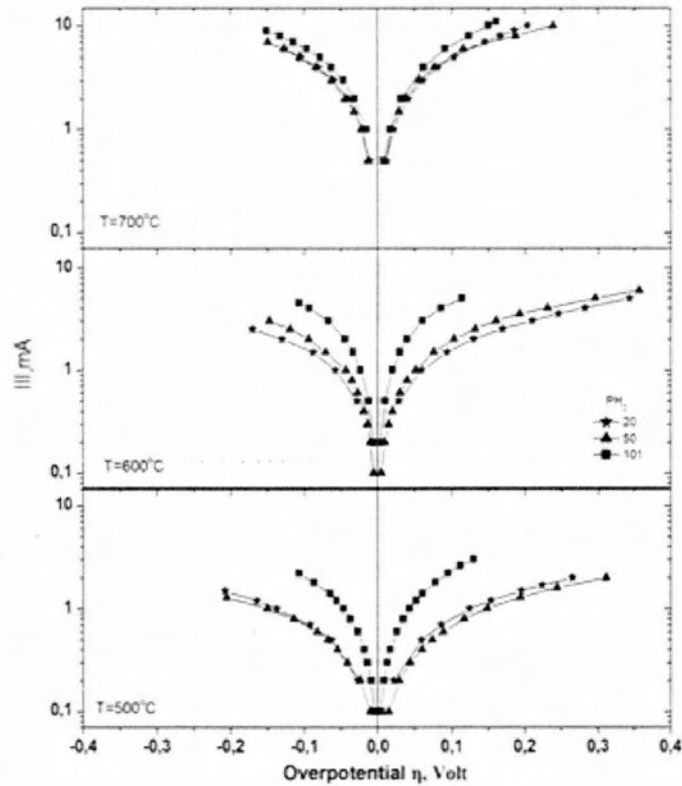
**Figure 5-14 Calculation of $I_o$ for $Co \mid BaCe_{0.5}Zr_{0.3}Y_{0.08}Yb_{0.08}Cu_{0.04}O_3-\delta \mid Co$ cell on Tafel region at partial pressure: 20kPa, 50kPa, 100kPa**

The electrochemical parameters $\alpha_a$, $\alpha_c$, and $I_o$ were exported, and the activation energy was calculated. All the results are presented in Table 5-5. Figure 5-15 shows the graph of the exchange current density absolute value over the inverse temperature, including all hydrogen partial pressures. The activation energy value is $0.45eV \pm 0.005eV$.
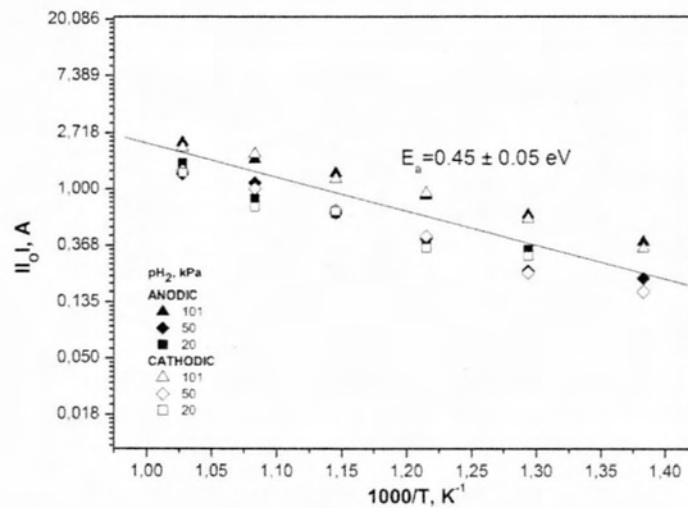


**Figure 5-15 Exchange current densities, $I_o$ versus $1/T$ for p $H_2$: 20 kPa, 50 kPa and 101 kPa.**

94

Table 5-5 Values of exchange current density ($I_o$) and anodic and cathodic charge transfer coefficients ($\alpha_a$, $\alpha_c$) as well as the corresponding energies of activation, for electrochemical system Co | BaCe$_{0.5}$Zr$_{0.3}$Y$_{0.08}$Yb$_{0.08}$Cu$_{0.04}$O$_3$–$\delta$ | Co in H$_2$/He at the experimental conditions employed.

| T, °C | $pH_2$=101kPa | | | | $pH_2$=50 kPa | | | | $pH_2$=20 kPa | | | |
|---|---|---|---|---|---|---|---|---|---|---|---|---|
| | $I_o$(mA) anode | $I_o$(mA) cathode | $\alpha_a$ | $\alpha_c$ | $I_o$(mA) anode | $I_o$(mA) cathode | $\alpha_a$ | $\alpha_c$ | $I_o$(mA) anode | $I_o$(mA) cathode | $\alpha_a$ | $\alpha_c$ |
| 500 | 0,63 | 0,59 | 0,8 | 0,8 | 0,23 | 0,22 | 0,6 | 0,7 | 0,34 | 0,30 | 0,5 | 0,6 |
| 550 | 0,89 | 0,93 | 0,9 | 0,8 | 0,41 | 0,43 | 0,6 | 0,6 | 0,39 | 0,35 | 0,7 | 0,7 |
| 600 | 1,33 | 1,19 | 0,9 | 0,8 | 0,65 | 0,68 | 0,7 | 0,8 | 0,65 | 0,67 | 0,6 | 0,6 |
| 650 | 1,69 | 1,86 | 0,9 | 0,9 | 1,11 | 1,00 | 0,8 | 0,8 | 0,85 | 0,73 | 0,7 | 0,9 |
| 700 | 2,28 | 2,08 | 0,8 | 0,8 | 1,31 | 1,38 | 1,1 | 0,9 | 1,59 | 1,34 | 0,8 | 1,0 |
| E (eV) | 0.43 | 0.39 | | | 0.52 | 0.50 | | | 0.49 | 0.47 | | |

### 5.1.6  Co | BaCe$_{0.5}$Zr$_{0.3}$Y$_{0.08}$Yb$_{0.08}$Cu$_{0.04}$O$_3$–$\delta$ | Co in CO$_2$/ H$_2$ mixture

Figure 5-16 schematically illustrates the results obtained from the polarization study of the Co|BaCe0.5Zr0.3Y0.08Yb0.08Cu0.04O3-δ|Co system at different temperatures (i.e., 500°C, 550°C, 600°C, 650°C and 700°C) in H$_2$/CO$_2$ mixture (H$_2$/CO$_2$=7/1, Ft=102ccm).

Maximum current value was 6.2 mA for 400mV at 700 °C. Exchange current density significantly increases when temperature increases (Figure 5-17). The electrochemical parameters $\alpha_a$, $\alpha_c$, and $I_o$ were exported, and the activation energy was calculated. All the results are presented in Table 5-6 . Figure 5-18 shows the graph of the exchange current density absolute value over the inverse temperature, including all hydrogen partial pressures. The activation energy value is 0.72eV± 0.5eV.
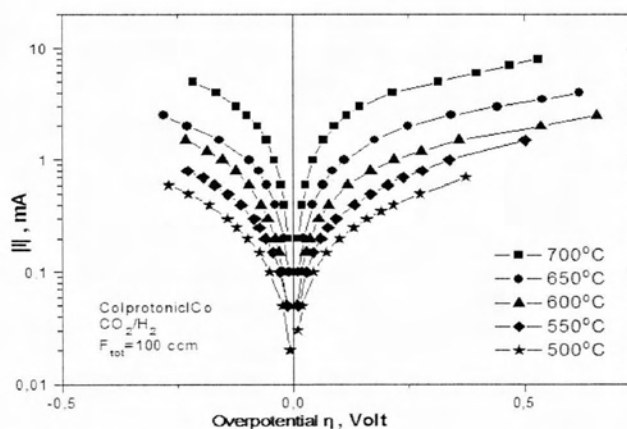


Figure 5-16 Exchange current density as a function of the anodic and cathodic overpotentials (Tafel plots) of Co | BaCe$_{0.5}$Zr$_{0.3}$Y$_{0.08}$Yb$_{0.08}$Cu$_{0.04}$O$_3$–$\delta$ | Co system, in the temperature range between 500-700°C in H$_2$ / CO$_2$ mixture (H$_2$/ CO$_2$=7/1, Ft=102ccm)
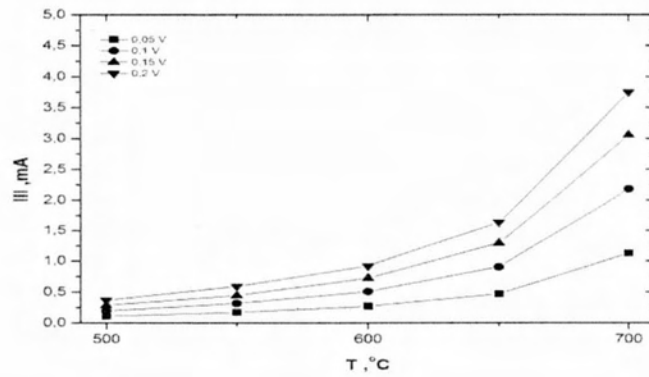
A)
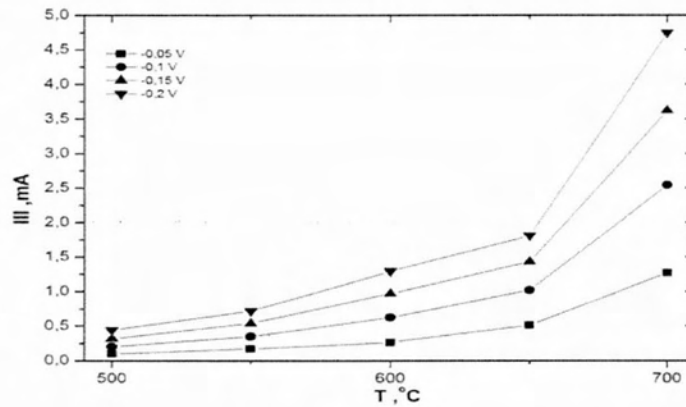


B)

Figure 5-17 Absolute current values vs. temperature at A) 50, 100, 150, 200mV and B)-50,-100,-150,-200mV for the electrochemical system Co│BaCe0.5Zr0.3Y0.08Yb0.08Cu0. 04O3-d│Co under a flow of $H_2$/ $CO_2$ with He as carrier gas.
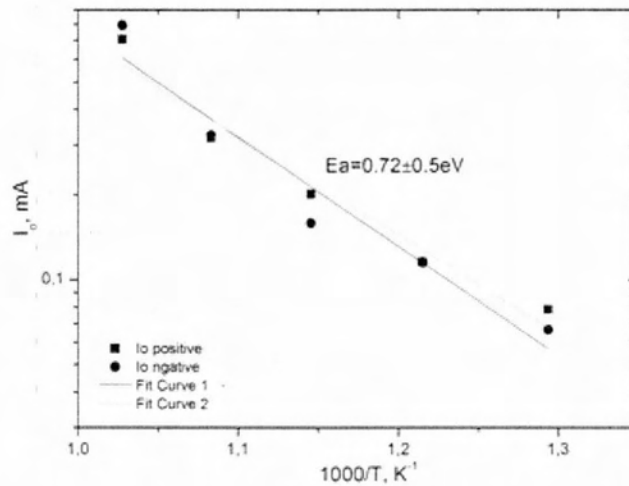


Figure 5-18 Graphical representation of the anodic and cathodic values $I_o$ as a function of the reverse temperature in order to calculate the activation energy of the reaction system Co│BaCe$_{0.5}$Zr$_{0.3}$Y$_{0.08}$Yb$_{0.08}$Cu$_{0.04}$O$_3$–δ │Co in $H_2$/ $CO_2$ mixture with He as carrier gas

Table 5-6 Values of exchange current density ($I_o$) and anodic and cathodic charge transfer coefficients ($\alpha_a$, $\alpha_c$) as well as the corresponding energies of activation, at the experimental conditions employed.

| T, °C | $H_2/CO_2=7/1$ | | | |
|---|---|---|---|---|
| | $I_{o,a}$(mA) | $I_{o,c}$(mA) | $\alpha_a$ | $\alpha_c$ |
| 500 | 0,08 | 0,07 | 0,6 | -0,7 |
| 550 | 0,12 | 0,12 | 0,7 | -0,7 |
| 600 | 0,20 | 0,16 | 0,6 | -0,9 |
| 650 | 0,32 | 0,33 | 0,7 | -0,8 |
| 700 | 0,71 | 0,80 | 0,9 | -0,9 |
| E (ev) | 0.70 | 0.76 | | |

CO was found with a maximum of 50 ppm at 700°C.

### 5.1.7 Fe | BaCe$_{0.5}$Zr$_{0.3}$Y$_{0.08}$Yb$_{0.08}$Cu$_{0.04}$O$_3$–$\delta$ | Fe in H$_2$/He atmospheres

Figure 5-19 schematically illustrates the results obtained from the polarization study of the Fe|BaCe0.5Zr0.3Y0.08Yb0.08Cu0.04O3-δ|Fe system at different temperatures (i.e., 500°C, 550°C, 600°C, 650°C and 700°C) and hydrogen atmospheres (p H$_2$: 101 kPa, 50 kPa and 20 kPa). The dependence of the exchange current on the (IR-free) overpotential, η (mV), for anodic and cathodic mode of operation at a total gas flow of 100 ml min$^{-1}$ was determined.

**As it can be seen, the obtained I-η curves are quasi symmetrical,(this can be also justified by the good adhesion of the catalyst on both sides of the protonic disk**

Figure 5-20).

The electrochemical parameters $\alpha_a$, $\alpha_c$, and I$_o$ were exported, and the activation energy was calculated. All the results are presented in Table 5-7. Figure 5-21 shows the graph of the exchange current density absolute value over the inverse temperature, including all hydrogen partial pressures.

The activation energy values for hydrogen partial pressure of pH$_2$ (20, 50 and 101kPa) are 0.55 ± 0.05 eV, 0.54 ± 0.05 eV, 0.63 ± 0.05 eV, respectively, whereas the value of the anodic and cathodic charge transfer coefficient at each temperature for hydrogen partial pressure of 20, 50 and 101kPa is 0.8. Overall activation energy value is 0.55+0.05 eV Figure 5-22
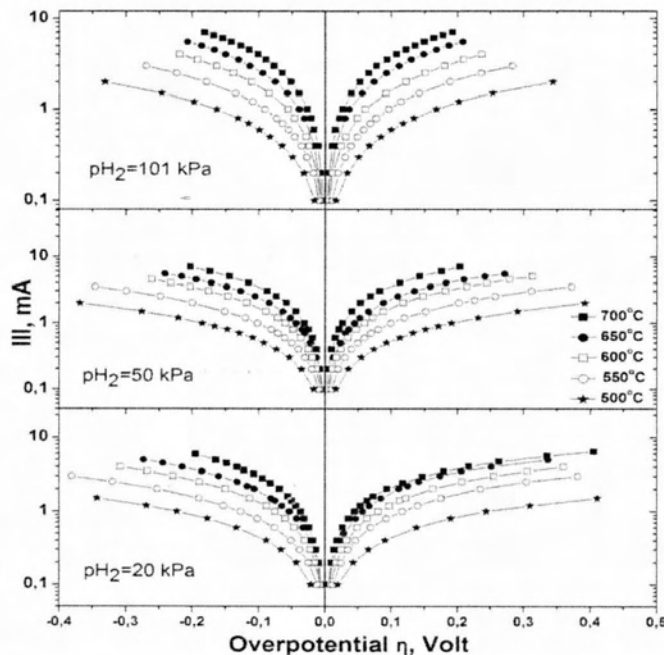


**Figure 5-19 Exchange current density as a function of the anodic and cathodic overpotentials (Tafel plots), in the temperature range between 500-700°C and pH$_2$: 20 kPa, 50 kPa, 101kPa**
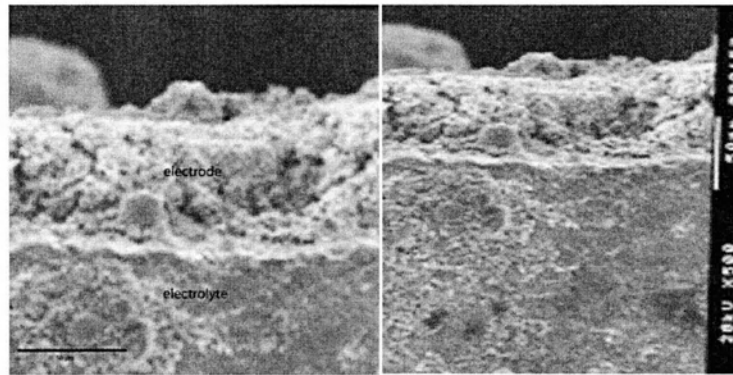
**Figure 5-20 SEM** micrographs of the Fe electrodes' films (after the experiments) showed that they were relatively well adhered on both sides of the protonic disk and the average thickness of each film was approximately 50μm.
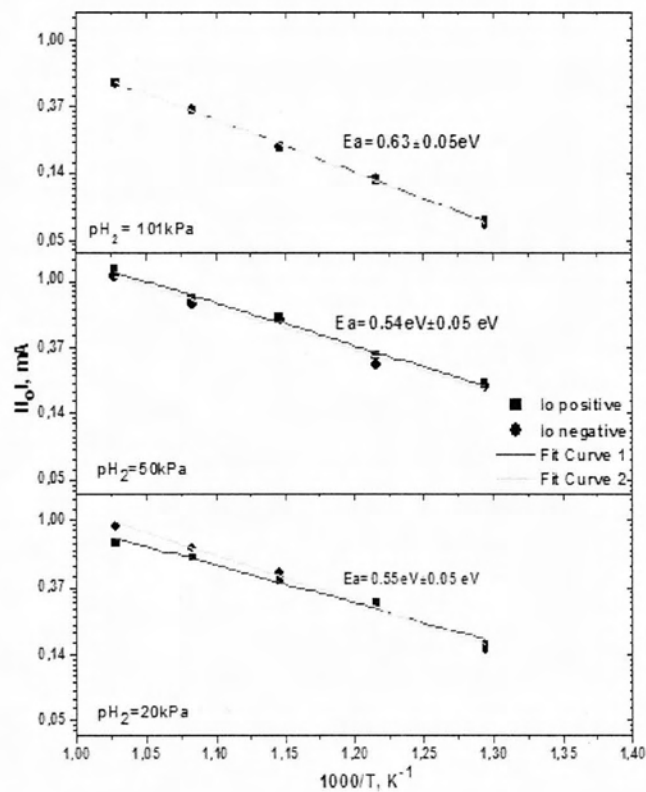


**Figure 5-21 Graphical representation of the anodic and cathodic values $I_o$ as a function of the reverse temperature in order to calculate the activation energy of the reaction system Fe | BaCe$_{0.5}$Zr$_{0.3}$Y$_{0.08}$Yb$_{0.08}$Cu$_{0.04}$O$_3$–δ | Fe in H$_2$/He atmosphere for different hydrogen partial pressures (pH$_2$:20, 50, 100 kPa).**
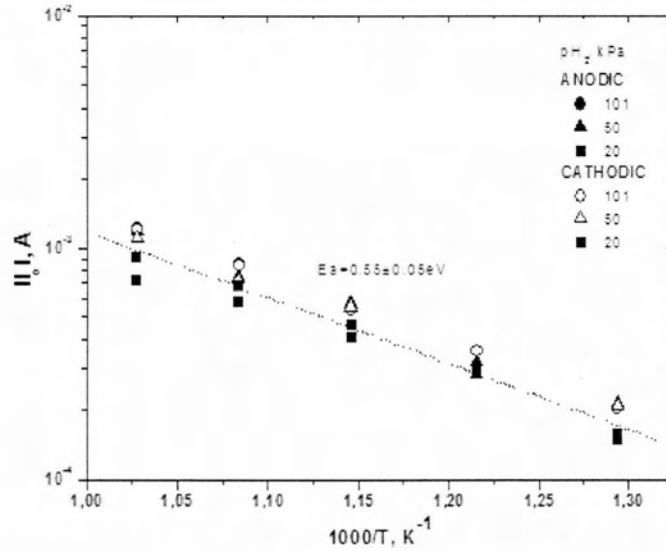
**Figure 5-22 Temperature dependence of conductivity and exchange current density for electrochemical cell Fe | $BaCe_{0.5}Zr_{0.3}Y_{0.08}Yb_{0.08}Cu_{0.04}O_3$–δ | Fe**

**Table 5-7 Values of exchange current density ($I_o$) and anodic and cathodic charge transfer coefficients ($\alpha_a$, $\alpha_c$) as well as the corresponding energies of activation, at the experimental conditions employed.**

| T, °C | $pH_2$=20 kPa | | | | $pH_2$=50 kPa | | | | $pH_2$=101 kPa | | | |
|---|---|---|---|---|---|---|---|---|---|---|---|---|
| | $I_o(\mu A)$ anode | $I_o(\mu A)$ cathode | $\alpha_a$ | $\alpha_c$ | $I_o(\mu A)$ anode | $I_o(\mu A)$ cathode | $\alpha_a$ | $\alpha_c$ | $I_o(\mu A)$ anode | $I_o(\mu A)$ cathode | $\alpha_a$ | $\alpha_c$ |
| **500** | 0,16 | 0,15 | 0,6 | 0,7 | 0,18 | 0,17 | 0,7 | 0,7 | 0,17 | 0,19 | 0,8 | 0,7 |
| **550** | 0,20 | 0,20 | 0,9 | 0,8 | 0,26 | 0,25 | 0,9 | 0,8 | 0,28 | 0,29 | 0,8 | 0,9 |
| **600** | 0,34 | 0,38 | 0,9 | 0,8 | 0,51 | 0,49 | 0,8 | 0,8 | 0,45 | 0,48 | 0,9 | 0,9 |
| **650** | 0,58 | 0,54 | 0,8 | 0,9 | 0,62 | 0,64 | 0,9 | 0,9 | 0,86 | 0,72 | 0,8 | 0,9 |
| **700** | 0,72 | 0,76 | 0,8 | 1,0 | 1,18 | 1,10 | 0,8 | 0,9 | 0.94 | 0.92 | 0,9 | 0,9 |
| E (eV) | 0.51 | 0.55 | | | 0.60 | 0.59 | | | 0.59 | 0.53 | | |

Temperature significantly affected the behavior of the cell, as conductivity increased with increased temperature at which I-V measurements were made.

According to Figure 5-23 and Figure 5-24, the increase of temperature and partial hydrogen pressure, increases the absolute current value thus conductivity. Current values increase significantly with the increase of partial hydrogen especially for values over 50kPa.
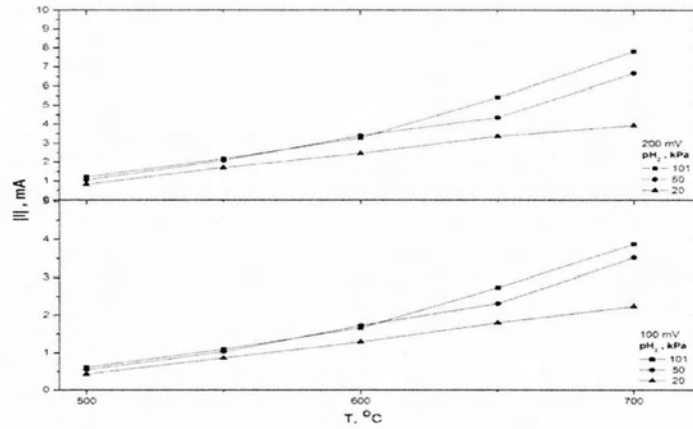
**Figure 5-23 Effect of temperature on current density, for standard overpotential values 100 and 200 mV and hydrogen partial pressure: 20kPa, 50 kPa, 101 kPa.**
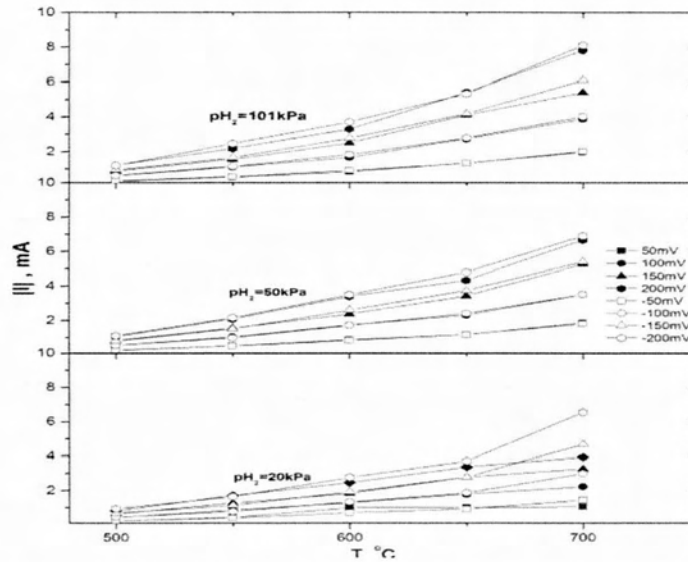


**Figure 5-24 Exchange current density as a function of temperature, for the electrochemical cell Fe | BaCe$_{0.5}$Zr$_{0.3}$Y$_{0.08}$Yb$_{0.08}$Cu$_{0.04}$O$_3$–δ | Fe in H$_2$/He atmosphere pH$_2$: 20 kPa, 50 kPa, 101kPa.**

### 5.1.8    Fe | BaCe$_{0.5}$Zr$_{0.3}$Y$_{0.08}$Yb$_{0.08}$Cu$_{0.04}$O$_3$–δ | Fe in CO$_2$/ H$_2$ mixture

Figure 5-25 schematically illustrates the results obtained from the polarization study of the Fe|BaCe0.5Zr0.3Y0.08Yb0.08Cu0.04O3-δ|Fe system at different temperatures (i.e., 500°C, 550°C, 600°C, 650°C and 700°C) in H$_2$/ CO$_2$ mixture (H$_2$/ CO$_2$=5/1, Ft=102ccm

The maximum voltage is 0.55mV at 5.1mA and -0.7V at 2mA at 600°C.

Exchange current density significantly increases when temperature increases (Figure 5-26).

101
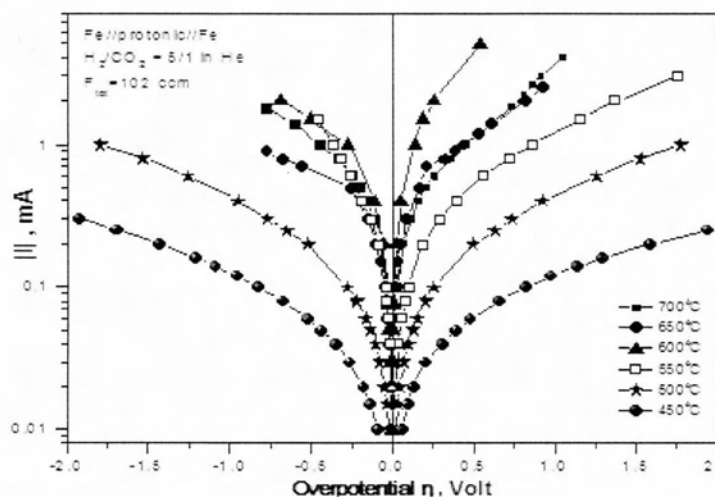
**Figure 5-25 Exchange current density as a function of the anodic and cathodic overpotentials (Tafel plots), in the temperature range between 450-700°C $H_2/CO_2$ mixture ($H_2/CO_2=5/1$, Ft=102ccm).**

As it can be seen, the obtained I-$\eta$ curves are not symmetrical enough, probably due to poor adhesion of the catalyst on the disk especially for temperatures over 600°C.
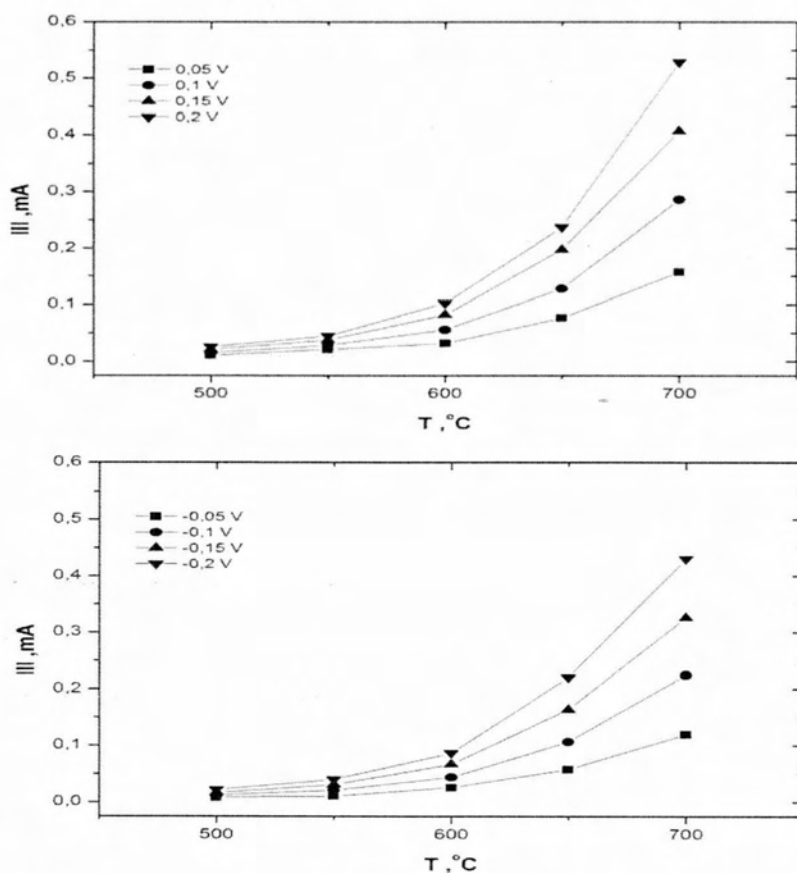




**Figure 5-26 Absolute values of current vs. temperature at ±50,± 100, ± 150, ± 200mV for the electrochemical cell Fe│BaCe0.5Zr0.3Y0.08Yb0.08Cu0. 04O3-d│Fe in $H_2/CO_2$ mixture ($H_2/CO_2=5/1$, Ft=102 ccm).**

The electrochemical parameters $\alpha_a$, $\alpha_c$, and $I_o$ were exported, and the activation energy was calculated. All the results are presented in Table 5-8. Figure 5-27 shows the graph of the exchange current density absolute value over the inverse temperature, including all hydrogen partial pressures. The activation energy value is 0.8eV± 0.05eV.
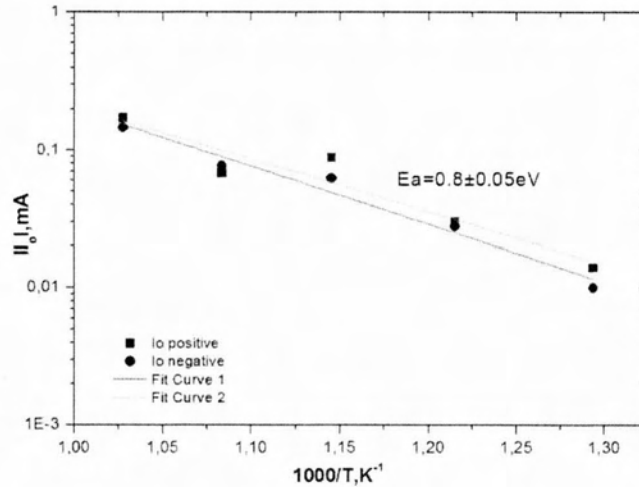


Figure 5-27 Graphical representation of the anodic and cathodic values $I_o$ as a function of the reverse temperature in order to calculate the activation energy of the reaction system Fe | $BaCe_{0.5}Zr_{0.3}Y_{0.08}Yb_{0.08}Cu_{0.04}O_3–\delta$ | Fe in $H_2$/ $CO_2$ mixture with He as carrier gas.

Table 5-8 Values of exchange current density ($I_o$) and anodic and cathodic charge transfer coefficients ($\alpha_a$, $\alpha_c$) as well as the corresponding energies of activation, at the experimental conditions employed.

| T, °C | $H_2/CO_2=5/1$ | | | |
|---|---|---|---|---|
| | $I_{o.a}$(mA) | $I_{o.c}$(mA) | $\alpha_a$ | $\alpha_c$ |
| 500 | 0,014 | 0,010 | 0,9 | -1 |
| 550 | 0,030 | 0,028 | 0,9 | -0,9 |
| 600 | 0,093 | 0,062 | 0,8 | -0,9 |
| 650 | 0,068 | 0,077 | 1,2 | -1,1 |
| 700 | 0,172 | 0,147 | 1,1 | -1,1 |
| E (ev) | 0.76 | 0.84 | | |

# CHAPTER VI

## Comparison and general Conclusions

The results from the previous experimental data are analyzed in this section.

# 6 Results analysis

## 6.1 Study of $Cu|BaCe_{0.5}Zr_{0.3}Y_{0.08}Yb_{0.08}Cu_{0.04}O_{3-\delta}|Au$

High current density values ($\sim$1 mA/cm$^2$ at 300$^\circ$C) were measured at relatively low temperatures and electrical potential values. Maximum current values observed where $\sim$100 mA at 500$^\circ$C. The anodic and cathodic charge transfer coefficients (in the potential range 0.03V–0.20V) were calculated to be close to 0.3 (Table 5-1), for $pH_2$=100. For other partial hydrogen pressures, charge transfer coefficient value was not stable. The activation energy, for the hydrogen de-electronation and proton electronation processes in the three phase boundary, tpb was calculated to be 0.87$\pm$0.05 eV (Figure 5-6) for $pH_2$=50, 20 kPa, and 0.5$\pm$0.1 eV for $pH_2$=100kPa (Figure 5-4).

It is observed that hydrogen partial pressure significantly affects activation energy, as well as the stability of charge transfer coefficient value. Even if the current values are affected significantly only by temperature Figure 5-3, hydrogen partial pressure is still of major importance. Also anodic and cathodic current values are close to each other, meaning that Cu can, under certain circumstances, give as good results as Au.

## 6.2 Study of $Cu|BaCe_{0.5}Zr_{0.3}Y_{0.08}Yb_{0.08}Cu_{0.04}O_{3-\delta}|Cu$

Current density values ($\sim$600 $\mu$A/cm$^2$ at 300$^\circ$C) were measured at relatively low temperatures and electrical potential values. Maximum current values observed where $\sim$10 mA at 510$^\circ$C. The apparent anodic and cathodic charge transfer coefficients (in the potential range 0.03V–0.20V) were calculated to be close to 0.5 (Table 5-2).

The apparent activation energy, for the hydrogen de-electronation and proton electronation processes in the three phase boundary, tpb was calculated to be 0.75 $\pm$ 0.05 eV (Figure 5-6).

Comparing $Cu|BaCe_{0.5}Zr_{0.3}Y_{0.08}Yb_{0.08}Cu_{0.04}O_{3-\delta}|Au$ with the $Cu|BaCe_{0.5}Zr_{0.3}Y_{0.08}Yb_{0.08}Cu_{0.04}O_{3-\delta}|Cu$ cell, for the same hydrogen partial pressure, it is observed that the first system studied, gives higher current values and better activation energy. This result is expected because Au has an overall better behavior than Cu. However results are relatively close to each other. Poor adhesion of Cu electrode can be a possible explanation for this difference.

$Cu|BaCe_{0.5}Zr_{0.3}Y_{0.08}Yb_{0.08}Cu_{0.04}O_{3-\delta}|Cu$ cell in $H2/$ $CO_2$=1/8 mixture gave no symmetrical measurement for both anode and cathode (Figure 5-7). A possible explanation could be CO films deposited on the top of the catalytic surface. That's the reason of using a different mixture of $H_2/CO_2$=1/5 with lower $CO_2$ concentration. This change restored the original graph symmetry (Figure 5-10). However, poor adhesion can still be a possible explanation for the asymmetry of the $H2/$ $CO_2$=1/8 mixture experiment. Activation energy for the $H2/$ $CO_2$=1/5 mixture is 0.64eV$\pm$

0.015eV, maximum current value is~10 mA at 500°C and ~500 μA at 300 °C. Charge transfer coefficients were calculated to be close to 0.6.

Possible products where either not created, or their concentration was low enough that they could not be measured.

### 6.3 Study of $Co|BaCe_{0.5}Zr_{0.3}Y_{0.08}Yb_{0.08}Cu_{0.04}O_{3-\delta}|Co$

High current density values (~2,5 mA/cm$^2$ at 500°C) were measured at relatively low temperatures and electrical potential values. The apparent anodic and cathodic charge transfer coefficients (in the potential range 0.03V–0.20V) were calculated to be close to 0.8 (Table 5-5).

The activation energy, for the hydrogen de-electronation and proton electronation processes in the three phase boundary, tpb were calculated to be is 0.45eV± 0.005eV (Figure 5-15).

Moreover, it was found that the concentration of hydrogen partial pressure affected the current density values, especially for a pH$_2$ change from 50 to 100 kPa. Temperature significantly affected the behavior of the cell as well (Figure 5-13, Figure 5-14).

When $H_2 / CO_2$ =7/1 mixture used for the cell, (rich H$_2$ mixture) the activation energy significantly increased. It s value was 0.72eV± 0.5eV. That means that the energy barrier of the de-electronation and proton electronation process increased. Exchange current density significantly increased, especially for values over 650 °C when temperature increases (Figure 5-17)

The only product measured was CO, found with a maximum of 50 ppm at 700°C.

### 6.4 Study of $Fe|BaCe_{0.5}Zr_{0.3}Y_{0.08}Yb_{0.08}Cu_{0.04}O_{3-\delta}|Fe$

High current density values (~2 mA/cm$^2$ at 500°C) were measured at relatively low temperatures and electrical potential values. The apparent anodic and cathodic charge transfer coefficients (in the potential range 0.03V–0.20V) were calculated to be close to 0.8 (Table 5-7).

The apparent activation energy, for the hydrogen de-electronation and proton electronation processes in the three phase boundary, tpb were calculated to be $0.55 \pm 0.05$ eV (Figure 5-22). Moreover, it was found that the concentration of hydrogen partial pressure and the temperature directly affected the current density values (Figure 5-23,Figure 5-24).

Activation energy value increased to 0.8eV± 0.05eV for the $H_2/ CO_2$=5/1 mixture.

Possible products where either not created, or their concentration was low enough that they could not be measured

106

## 6.5 Comparison

From the experiments performed with the Fe, Co, Cu electrodes for the proton conductor $BaCe_{0.5}Zr_{0.3}Y_{0.08}Yb_{0.08}Cu_{0.04}O_3–\delta$ under a gas mixture $CO_2/ H_2$, and the characterization of the products by the method of gas chromatography, no system gives the reduction of $CO_2$.

However relatively good electrochemical characteristics are obtained from the experimental data.
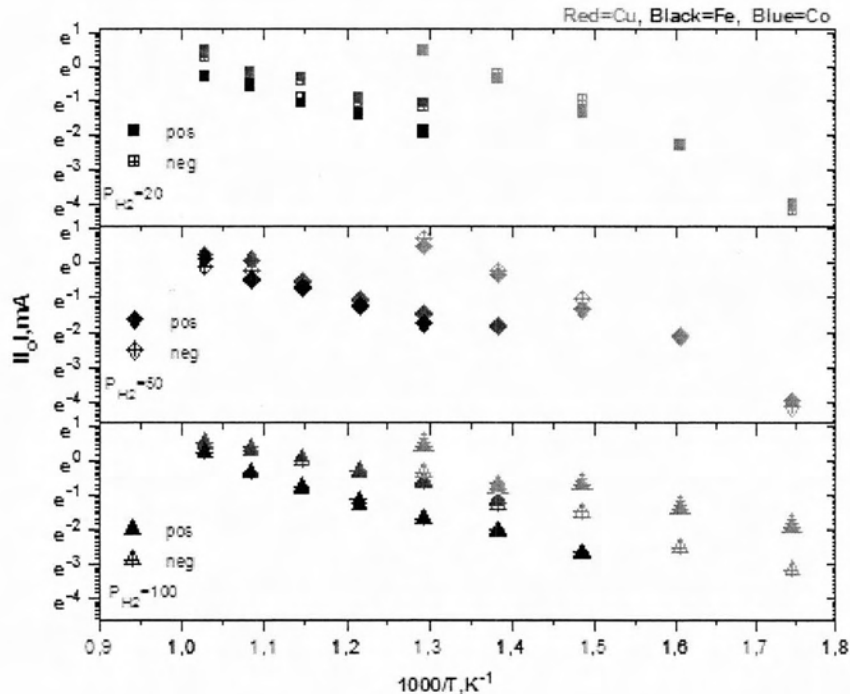


**Figure 6-1 Comparison of the electrochemical characteristics for the three electrodes**

Using the data from Figure 6-1 we can compare the three electrodes for their electrochemical characteristics.

Comparing Fe and Co we can see that Co has bigger $I_o$ in all three partial pressures of $H_2$ (20, 50, 100 kPa). $I_o$ shows the difficulty of the reaction (anode cathode). In that case Co is preferable.

Slope is pretty much the same for those materials except for $pH_2=100kPa$ where slope for Fe is higher, meaning activation energy for that pressure is also higher. Activation energy indicates the energy barrier that a reaction must overcome in order to operate. In this case, Co is also preferable.

**As for Co and Cu, it is obvious that Cu has significantly higher slope for $pH_2=50,20kPa$ energy higher). However Cu can give data for much lower temperatures. For $pH_2=100kPa$, for Co and Cu is pretty much the same (**

Table 6-1).

On the other hand, $I_o$ values of Cu are higher than the values of Co for the temperatures that both can give measurements.

107

In conclusion, Co is better than Fe for temperatures between 700 and 500°C. Cu can give results for lower temperatures, but activation energy is not as low as for Co (except for $pH_2$=100kPa).Cu has better $I_o$ than Co (For T=500, 450).

**Table 6-1 Activation energy of Fe,Co,Cu for different partial pressures of $H_2$**

| $pH_2$,(kPa) | Activation energy, (eV) anodic/cathodic | | |
|:---:|:---:|:---:|:---:|
| | Cu | Co | Fe |
| **20** | 0,83/0,94 | 0,47/0,49 | 0,53/0,50 |
| **50** | 0,82/0,9 | 0,50/0,52 | 0,53/0,58 |
| **100** | 0,39/0,57 | 0,39/0,44 | 0,52/0,53 |

## 6.6 Conclusions

- In all cases, good electron conductivity though the electrocatalytic system electrolyte/electrode was observed according to the polarization study. Electrodes are in the same $H_2$/He gas mixture. That is the reason of the symmetrical graphs. Non-symmetrical graphs are either result of poor adhesion of the catalyst on the electrolyte or due to the presence of carbon on the electrode surface.

- For the case of $H_2$/ $CO_2$ mixture, small amount of products were observed ( CO ~500 ppm)

- Cu presents poor stability, for $H_2$=100kPa partial pressure.

- Co is obviously the best of the catalysts used, due to its low activation energy. Also graphs for Co were all symmetrical. Further study should be made

- Cu is offered for future studies, if the difficulties of poor adhesion on the electrolyte are solved.
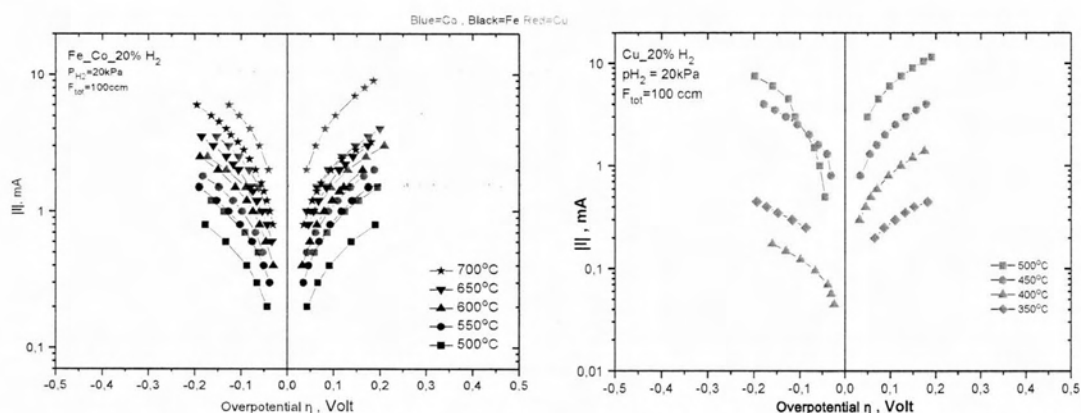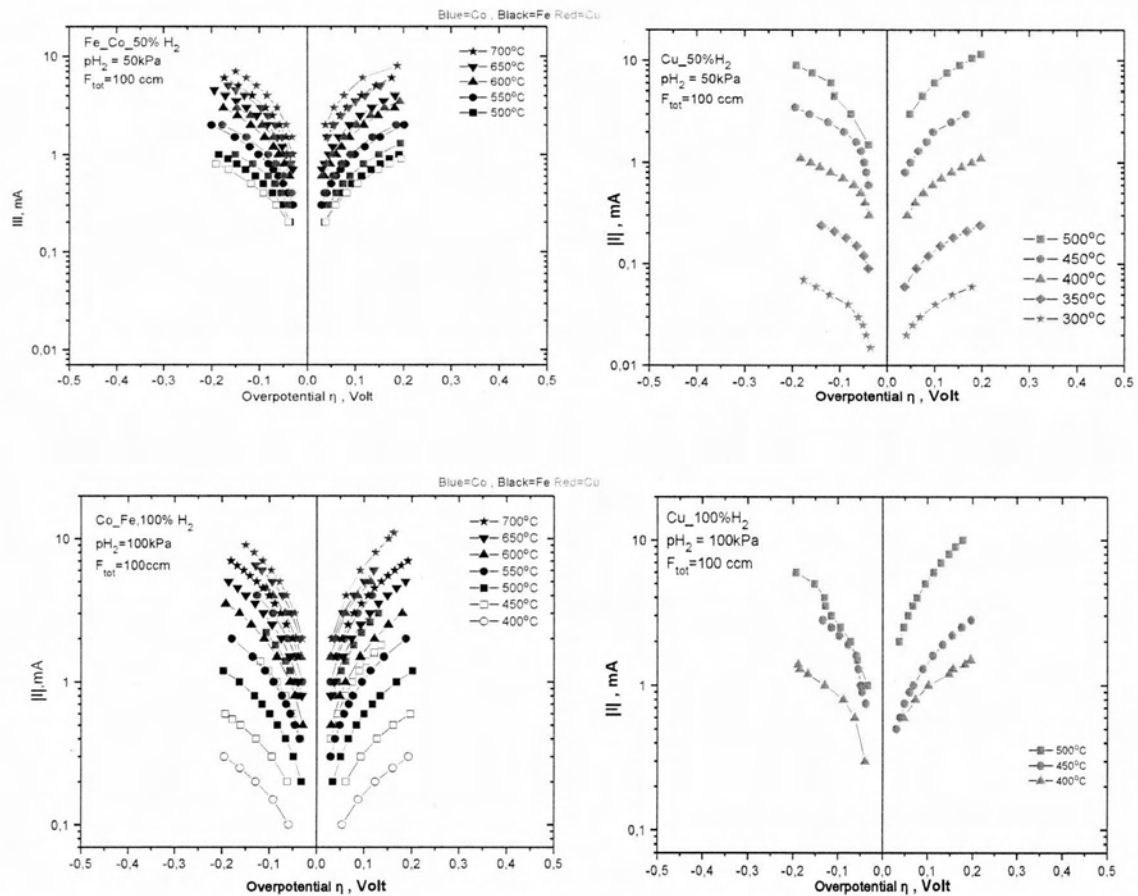
Figure 6-2 Tafel Plots of the three catalytic systems for different hydrogen partial pressures

## 7  Appendix

The program used to compute the values of equilibrium constants K is presented below. The programming language was FORTRAN.

```
        program K
        implicit none
INTEGER :: DH,DG,i
Real :: DA,DB,DC,DD,lnk,J,I0
real :: R=8.314,T0=298.15 ,T


!DA=-1.86
!DB=0.00054
!DC=0
!DD=116400
!DH=41166
!DG=28618


DA=-9.811
DB=0.009248
DC=-0.000002164
DD=106700
DH=-164647
DG=-113245


!DA=-11.671
!DB=0.009788
!DC=-0.000002164
!DD=223100
!DH=-123481
!DG=-84627


!DA=-9.523
!DB=0.011355
!DC=-0.00000345
!DD=102900
!DH=-48969
!DG=3827
```

```
!DA=-11.383
!DB=0.011895
!DC=-0.00000345
!DD=219300
!DH=-7803
!DG=32445


open(100,File='C:\Documents and Settings\data.txt')
        lnk=-DG/(R*T0)
        print*, lnk
        J=(DH/R)-(DA*T0)-((DB/2)*(T0)**2)-((DC/3)*(T0)**3)+(DD/T0)
        print*, J
        I0=lnk +(J/T0)-(DA*Log(T0))-((DB/2)*T0)-((DC/6)*(T0**2))-(DD/(2*(T0**2)))
        print*, I0
                Do T=373,973,50
                lnk=-(J/T)+(DA*Log(T))+((DB/2)*T)+((DC/6)/(T**2))+(DD/(2*(T**2)))+I0
        Print* , 'Gia T=',T, 'LnK=',lnk,'k=',exp(lnk)
        write (100,*) , 'Gia T=',T ,'LnK=',lnk,'k=',exp(lnk)
end do
        close(100)
        end program K
```

**The experimental data are presented below :**

- Au-Cu:
- $pH_2 = 100 kPa$

500°C

| I | V | V | I | V | V |
|---|---|---|---|---|---|
| mA | Volt_pos | Volt | mA | Volt_neg | Volt |
| 100 pos | | Correct | 100 neg | | Correct |
| 0,07369 | 0,004 | 0,004 | 0,2 | 0,006 | -0,003 |
| 0,5 | 0,009 | 0,009 | 0,5 | 0,018 | -0,015 |
| 1 | 0,018 | 0,018 | 1 | 0,036 | -0,033 |
| 1,5 | 0,027 | 0,027 | 1,5 | 0,059 | -0,056 |
| 2 | 0,037 | 0,037 | 2 | 0,074 | -0,071 |
| 2,5 | 0,047 | 0,047 | 2,5 | 0,097 | -0,094 |
| 3 | 0,057 | 0,057 | 3 | 0,118 | -0,115 |
| 3,5 | 0,067 | 0,067 | 3,5 | 0,131 | -0,128 |
| 4 | 0,076 | 0,076 | 4 | 0,133 | -0,13 |

111

| | | | | | |
|---|---|---|---|---|---|
| 5 | 0,095 | 0,095 | 5 | 0,155 | -0,152 |
| 6 | 0,113 | 0,113 | 6 | 0,196 | -0,193 |
| 7 | 0,13 | 0,13 | 7 | 0,233 | -0,23 |
| 8 | 0,147 | 0,147 | 8 | 0,27 | -0,267 |
| 9 | 0,162 | 0,162 | 9 | 0,303 | -0,3 |
| 10 | 0,178 | 0,178 | 10 | 0,338 | -0,335 |
| 12 | 0,208 | 0,208 | 12 | 0,4 | -0,397 |
| 15 | 0,25 | 0,25 | 15 | 0,49 | -0,487 |
| 20 | 0,319 | 0,319 | 20 | 0,58 | -0,577 |
| 30 | 0,549 | 0,549 | 30 | 0,845 | -0,842 |
| 50 | 0,93 | 0,93 | 50 | 1,255 | -1,252 |
| 100 | 1,238 | 1,238 | 100 | 1,66 | -1,657 |
| 130 | 1,266 | 1,266 | 130 | 1,84 | -1,837 |

## 450°C

| I | V | V | I | V | V |
|---|---|---|---|---|---|
| mA | Volt_pos | Volt | mA | Volt_neg | Volt |
| 100 pos | | Correct | 100 neg | | Correct |
| 0 | 1,00E-03 | 0 | 0 | 0,002 | 0 |
| 0,4 | 0,025 | 0,024 | 0,4 | 0,02 | -0,018 |
| 0,5 | 0,032 | 0,031 | 0,5 | 0,024 | -0,022 |
| 0,6 | 0,04 | 0,039 | 0,6 | 0,029 | -0,027 |
| 0,75 | 0,05 | 0,049 | 0,75 | 0,039 | -0,037 |
| 0,9 | 0,061 | 0,06 | 0,9 | 0,047 | -0,045 |
| 1 | 0,07 | 0,069 | 1 | 0,051 | -0,049 |
| 1,3 | 0,091 | 0,09 | 1,3 | 0,056 | -0,054 |
| 1,6 | 0,113 | 0,112 | 1,6 | 0,06 | -0,058 |
| 1,9 | 0,135 | 0,134 | 1,9 | 0,078 | -0,076 |
| 2,2 | 0,156 | 0,155 | 2,2 | 0,098 | -0,096 |
| 2,5 | 0,177 | 0,176 | 2,5 | 0,117 | -0,115 |
| 2,8 | 0,198 | 0,197 | 2,8 | 0,136 | -0,134 |
| 6 | 0,405 | 0,404 | 6 | 0,323 | -0,321 |
| 9,5 | 0,6 | 0,599 | 9,5 | 0,526 | -0,524 |
| 14 | 0,789 | 0,788 | 14 | 0,83 | -0,828 |
| 18 | 0,952 | 0,951 | 18 | 1,053 | -1,051 |
| 25 | 1,171 | 1,17 | 25 | 1,401 | -1,399 |
| 35 | 1,488 | 1,487 | 35 | 1,95 | -1,948 |

## 400°C

| I | V | V | I | V | V |
|---|---|---|---|---|---|
| mA | Volt_pos | Volt | mA | Volt_neg | Volt |
| 10 pos | | Correct | 10 neg | | Correct |
| 0 | 1,00E-03 | 0 | 0 | 1,00E-03 | 0 |
| 0,1 | -0,015 | -0,016 | 0,1 | 0,017 | -0,016 |
| 0,3 | -0,003 | -0,004 | 0,3 | 0,04 | -0,039 |

| | | | | | |
|---|---|---|---|---|---|
| 0,6 | 0,048 | 0,047 | 0,6 | 0,063 | -0,062 |
| 0,8 | 0,074 | 0,073 | 0,8 | 0,088 | -0,087 |
| 1 | 0,103 | 0,102 | 1 | 0,13 | -0,129 |
| 1,2 | 0,149 | 0,148 | 1,2 | 0,168 | -0,167 |
| 1,3 | 0,158 | 0,157 | 1,3 | 0,186 | -0,185 |
| 1,4 | 0,184 | 0,183 | 1,4 | 0,189 | -0,188 |
| 1,5 | 0,197 | 0,196 | 1,5 | 0,214 | -0,213 |
| 1,6 | 0,212 | 0,211 | 1,6 | 0,232 | -0,231 |
| 2 | 0,285 | 0,284 | 2 | 0,289 | -0,288 |
| 2,5 | 0,384 | 0,383 | 2,5 | 0,373 | -0,372 |
| 3 | 0,485 | 0,484 | 3 | 0,443 | -0,442 |
| 4 | 0,67 | 0,669 | 4 | 0,581 | -0,58 |
| 5 | 0,847 | 0,846 | 5 | 0,718 | -0,717 |
| 7 | 1,194 | 1,193 | 7 | 0,984 | -0,983 |
| 9 | 1,5 | 1,499 | 9 | 1,233 | -1,232 |
| 10 | 1,666 | 1,665 | 10 | 1,346 | -1,345 |
| 12 | 1,969 | 1,968 | 12 | 1,56 | -1,559 |
| | | | 15 | 1,85 | -1,849 |

350°C

| I | V | V | I | V | V |
|---|---|---|---|---|---|
| mA | Volt_pos | Volt | mA | Volt_neg | Volt |
| 10 pos | | Correct | 10 neg | | Correct |
| 0 | 0,003 | 0 | 0 | 0,003 | 0 |
| 0,1 | -0,044 | -0,047 | 0,1 | 0,095 | -0,092 |
| 0,2 | -0,023 | -0,026 | 0,2 | 0,151 | -0,148 |
| 0,3 | -- | -- | 0,3 | 0,214 | -0,211 |
| 0,4 | 0,03 | 0,027 | 0,4 | 0,255 | -0,252 |
| 0,5 | 0,097 | 0,094 | 0,5 | 0,308 | -0,305 |
| 0,6 | 0,17 | 0,167 | 0,6 | 0,322 | -0,319 |
| 0,7 | 0,227 | 0,224 | 0,7 | 0,373 | -0,37 |
| 1 | 0,468 | 0,465 | 1 | 0,504 | -0,501 |
| 1,2 | 0,6 | 0,597 | 1,2 | 0,623 | -0,62 |
| 1,5 | 0,821 | 0,818 | 1,5 | 0,754 | -0,751 |
| 1,7 | 1,047 | 1,044 | 1,7 | 0,805 | -0,802 |
| 2 | 1,268 | 1,265 | 2 | 0,927 | -0,924 |
| 2,5 | 1,559 | 1,556 | 2,5 | 1,12 | -1,117 |
| 2,8 | 1,798 | 1,795 | 2,8 | 1,259 | -1,256 |
| 3 | 1,954 | 1,951 | 3 | 1,337 | -1,334 |
| | | | 4 | 1,66 | -1,657 |
| | | | 5 | 2,003 | -2 |

## 300°C

| I mA<br>1 pos | V Volt_pos | V Volt<br>Correct | I mA<br>1 neg | V Volt_neg | V Volt<br>Correct |
|---|---|---|---|---|---|
| 0 | 0,021 | 0 | 0 | -0,002 | 0 |
| 0,1 | -0,268 | -0,289 | 0,1 | 0,275 | -0,277 |
| 0,2 | -0,159 | -0,18 | 0,2 | 0,487 | -0,489 |
| 0,3 | -0,006 | -0,027 | 0,3 | 0,595 | -0,597 |
| 0,5 | 0,399 | 0,378 | 0,5 | 0,853 | -0,855 |
| 0,7 | 0,992 | 0,971 | 0,7 | 1,157 | -1,159 |
| 1 | 2,016 | 1,995 | 1 | 1,539 | -1,541 |
| | | | 1,2 | 1,842 | -1,844 |

- Au-Cu:
- pH$_2$=50kPa

## 500°C

| I mA<br>10-100 pos | V Volt_pos | V Volt<br>Correct | I mA<br>10-100 neg | V Volt_neg | V Volt<br>Correct |
|---|---|---|---|---|---|
| 0,5 | 0,008 | 0,007 | 0,5 | -0,012 | -0,015 |
| 1 | 0,015 | 0,014 | 1 | -0,024 | -0,027 |
| 1,5 | 0,024 | 0,023 | 1,5 | -0,036 | -0,039 |
| 3 | 0,049 | 0,048 | 3 | -0,073 | -0,076 |
| 4,5 | 0,075 | 0,074 | 4,5 | -0,109 | -0,112 |
| 6 | 0,101 | 0,1 | 6 | -0,116 | -0,119 |
| 7,5 | 0,127 | 0,126 | 7,5 | -0,155 | -0,158 |
| 9 | 0,154 | 0,153 | 9 | -0,189 | -0,192 |
| 10,5 | 0,18 | 0,179 | 10,5 | -0,223 | -0,226 |
| 11,5 | 0,199 | 0,198 | 11,5 | -0,247 | -0,25 |
| 20 | 0,333 | 0,332 | 20 | -0,44 | -0,443 |
| 40 | 0,63 | 0,629 | 40 | -0,83 | -0,833 |
| 65 | 0,875 | 0,874 | 65 | -1,17 | -1,173 |
| 100 | 1,069 | 1,068 | 100 | -1,501 | -1,504 |
| 150 | 1,134 | 1,133 | 150 | -1,712 | -1,715 |

## 450°C

| I mA<br>1-10-100 pos | V Volt_pos | V Volt<br>Correct | I mA<br>1-10-100 neg | V Volt_neg | V Volt<br>Correct |
|---|---|---|---|---|---|
| 0,2 | 0,009 | 0,006 | 0,2 | -0,013 | -0,017 |
| 0,4 | 0,02 | 0,017 | 0,4 | -0,025 | -0,029 |
| 0,6 | 0,03 | 0,027 | 0,6 | -0,035 | -0,039 |

| 0,8 | 0,041 | 0,038 | 0,8 | -0,04 | -0,044 |
|---|---|---|---|---|---|
| 1 | 0,052 | 0,049 | 1 | -0,044 | -0,048 |
| 1,3 | 0,069 | 0,066 | 1,3 | -0,051 | -0,055 |
| 1,6 | 0,086 | 0,083 | 1,6 | -0,061 | -0,065 |
| 2 | 0,1 | 0,097 | 2 | -0,087 | -0,091 |
| 2,5 | 0,138 | 0,135 | 2,5 | -0,121 | -0,125 |
| 3 | 0,169 | 0,166 | 3 | -0,16 | -0,164 |
| 3,5 | 0,204 | 0,201 | 3,5 | -0,19 | -0,194 |
| 4 | 0,235 | 0,232 | 4 | -0,22 | -0,224 |
| 5 | 0,292 | 0,289 | 5 | -0,283 | -0,287 |
| 7 | 0,4 | 0,397 | 7 | -0,4 | -0,404 |
| 9 | 0,502 | 0,499 | 9 | -0,512 | -0,516 |
| 11 | 0,6 | 0,597 | 11 | -0,62 | -0,624 |
| 15 | 0,811 | 0,808 | 15 | -0,838 | -0,842 |
| 20 | 1,03 | 1,027 | 20 | -1,007 | -1,011 |
| 25 | 1,38 | 1,377 | 25 | -1,24 | -1,244 |
| 30 | 1,59 | 1,587 | 30 | -1,395 | -1,399 |
| 35 | 1,783 | 1,78 | 35 | -1,536 | -1,54 |
|  |  |  | 45 | -1,9 | -1,904 |

## 400°C

| I | V | V | I | V | V |
|---|---|---|---|---|---|
| mA | Volt_pos | Volt | mA | Volt_neg | Volt |
| 10-100 pos |  | Correct | 10-100neg |  | Correct |
| 0,03 | -0,002 | 0 | 0,03 | 0,004 | 0 |
| 0,01 | -0,004 | -0,002 | 0,01 | 0,003 | -1,00E-03 |
| 0,2 | 0,023 | 0,025 | 0,2 | -0,024 | -0,028 |
| 0,3 | 0,04 | 0,042 | 0,3 | -0,034 | -0,038 |
| 0,4 | 0,057 | 0,059 | 0,4 | -0,043 | -0,047 |
| 0,5 | 0,074 | 0,076 | 0,5 | -0,052 | -0,056 |
| 0,6 | 0,094 | 0,096 | 0,6 | -0,066 | -0,07 |
| 0,7 | 0,112 | 0,114 | 0,7 | -0,089 | -0,093 |
| 0,8 | 0,133 | 0,135 | 0,8 | -0,116 | -0,12 |
| 0,9 | 0,155 | 0,157 | 0,9 | -0,138 | -0,142 |
| 1 | 0,176 | 0,178 | 1 | -0,158 | -0,162 |
| 1,1 | 0,196 | 0,198 | 1,1 | -0,179 | -0,183 |
| 2,5 | 0,494 | 0,496 | 1,2 | -0,2 | -0,204 |
| 4 | 0,86 | 0,862 | 2,5 | -0,41 | -0,414 |
| 5 | 1,065 | 1,067 | 4 | -0,638 | -0,642 |
| 6,5 | 1,385 | 1,387 | 5 | -0,787 | -0,791 |
| 8 | 1,7 | 1,702 | 6,5 | -0,999 | -1,003 |
|  |  |  | 8 | -1,197 | -1,201 |
|  |  |  | 10 | -1,413 | -1,417 |
|  |  |  | 14 | -1,788 | -1,792 |

350°C

| I mA 1 pos | V Volt_pos | V Volt Correct | I mA 1 neg | V Volt_neg | V Volt Correct |
|---|---|---|---|---|---|
| 0 | -0,004 | 0 | 0 | 0,003 | 0 |
| 0,01 | -1,00E-03 | 0,003 | 0,01 | -0,004 | -0,007 |
| 0,02 | 0,006 | 0,01 | 0,02 | -0,009 | -0,012 |
| 0,04 | 0,019 | 0,023 | 0,04 | -0,018 | -0,021 |
| 0,06 | 0,033 | 0,037 | 0,06 | -0,025 | -0,028 |
| 0,09 | 0,057 | 0,061 | 0,09 | -0,037 | -0,04 |
| 0,12 | 0,082 | 0,086 | 0,12 | -0,047 | -0,05 |
| 0,15 | 0,107 | 0,111 | 0,15 | -0,061 | -0,064 |
| 0,18 | 0,135 | 0,139 | 0,18 | -0,084 | -0,087 |
| 0,21 | 0,163 | 0,167 | 0,21 | -0,109 | -0,112 |
| 0,24 | 0,192 | 0,196 | 0,24 | -0,136 | -0,139 |
| 0,55 | 0,53 | 0,534 | 0,55 | -0,335 | -0,338 |
| 0,8 | 0,824 | 0,828 | 0,8 | -0,472 | -0,475 |
| 1,1 | 1,15 | 1,154 | 1,1 | -0,63 | -0,633 |
| 1,4 | 1,472 | 1,476 | 1,4 | -0,779 | -0,782 |
| 1,65 | 1,745 | 1,749 | 1,65 | -0,898 | -0,901 |
| 1,9 | 1,999 | 2,003 | 1,9 | -1,014 | -1,017 |
| | | | 3 | -1,518 | -1,521 |
| | | | 4 | -1,901 | -1,904 |

300°C

| I mA 1 pos | V Volt_pos | V Volt Correct | I mA 1 neg | V Volt_neg | V Volt Correct |
|---|---|---|---|---|---|
| -0,009 | -0,02 | -0,013 | -0,009 | -0,02 | -0,024 |
| 0 | -0,009 | -0,002 | 0,01 | -0,023 | -0,027 |
| 0,005 | 0 | 0,007 | 0,015 | -0,031 | -0,035 |
| 0,01 | 0,01 | 0,017 | 0,02 | -0,04 | -0,044 |
| 0,015 | 0,02 | 0,027 | 0,025 | -0,047 | -0,051 |
| 0,02 | 0,034 | 0,041 | 0,03 | -0,057 | -0,061 |
| 0,025 | 0,047 | 0,054 | 0,04 | -0,078 | -0,082 |
| 0,03 | 0,062 | 0,069 | 0,05 | -0,118 | -0,122 |
| 0,04 | 0,094 | 0,101 | 0,06 | -0,146 | -0,15 |
| 0,05 | 0,13 | 0,137 | 0,07 | -0,172 | -0,176 |
| 0,06 | 0,171 | 0,178 | 0,12 | -0,287 | -0,291 |
| 0,07 | 0,207 | 0,214 | 0,16 | -0,37 | -0,374 |
| 0,12 | 0,43 | 0,437 | 0,2 | -0,445 | -0,449 |
| 0,16 | 0,624 | 0,631 | 0,24 | -0,523 | -0,527 |

116

| 0,2 | 0,838 | 0,845 | 0,29 | -0,612 | -0,616 |
| 0,24 | 1,048 | 1,055 | 0,35 | -0,72 | -0,724 |
| 0,29 | 1,3 | 1,307 | 0,4 | -0,81 | -0,814 |
| 0,35 | 1,587 | 1,594 | 0,43 | -0,864 | -0,868 |
| 0,4 | 1,823 | 1,83 | 0,85 | -1,579 | -1,583 |
| 0,43 | 1,96 | 1,967 | 1,1 | -1,965 | -1,969 |

- Au-Cu:
- $pH_2$=20kPa

500°C

| I | V | V | I | V | V |
| --- | --- | --- | --- | --- | --- |
| mA | Volt_pos | Volt | mA | Volt_neg | Volt |
| 10-100 pos | | Correct | 10-100 neg | | Correct |
| 0,01 | -0,003 | 0 | 0,01 | -1,00E-03 | -0,031 |
| 0,5 | 0,006 | 0,009 | 0,5 | -0,014 | -0,044 |
| 1 | 0,014 | 0,017 | 1 | -0,026 | -0,056 |
| 1,5 | 0,022 | 0,025 | 1,5 | -0,038 | -0,068 |
| 3 | 0,046 | 0,049 | 3 | -0,08 | -0,11 |
| 4,5 | 0,071 | 0,074 | 4,5 | -0,095 | -0,125 |
| 6 | 0,095 | 0,098 | 6 | -0,129 | -0,159 |
| 7,5 | 0,121 | 0,124 | 7,5 | -0,168 | -0,198 |
| 9 | 0,146 | 0,149 | 9 | -0,208 | -0,238 |
| 10,5 | 0,17 | 0,173 | 10,5 | -0,247 | -0,277 |
| 11,5 | 0,188 | 0,191 | 11,5 | -0,275 | -0,305 |
| 12 | 0,199 | 0,202 | 12 | -0,29 | -0,32 |
| 20 | 0,309 | 0,312 | 20 | -0,501 | -0,531 |
| 40 | 0,623 | 0,626 | 40 | -1,005 | -1,035 |
| 65 | 0,888 | 0,891 | 65 | -1,41 | -1,44 |
| 100 | 1,035 | 1,038 | 100 | -1,6 | -1,63 |
| 97,01837 | 1,018 | 1,021 | | | |

450°C

| I | V | V | I | V | V |
| --- | --- | --- | --- | --- | --- |
| mA | Volt_pos | Volt | mA | Volt_neg | Volt |
| 10-100 pos | | Correct | 10-100 neg | | Correct |
| 0,01 | -0,006 | 0 | 0,01 | -0,004 | 0,002 |
| 0,2 | 0,003 | 0,009 | 0,2 | -0,013 | -0,007 |
| 0,4 | 0,011 | 0,017 | 0,4 | -0,022 | -0,016 |
| 0,8 | 0,028 | 0,034 | 0,8 | -0,037 | -0,031 |
| 1,3 | 0,049 | 0,055 | 1,3 | -0,045 | -0,039 |
| 1,6 | 0,064 | 0,07 | 1,6 | -0,064 | -0,058 |

| | | | | | |
|---|---|---|---|---|---|
| 2 | 0,082 | 0,088 | 2 | -0,085 | -0,079 |
| 2,5 | 0,105 | 0,111 | 2,5 | -0,111 | -0,105 |
| 3 | 0,128 | 0,134 | 3 | -0,136 | -0,13 |
| 3,5 | 0,151 | 0,157 | 3,5 | -0,16 | -0,154 |
| 4 | 0,173 | 0,179 | 4 | -0,184 | -0,178 |
| 4,5 | 0,196 | 0,202 | 4,5 | -0,209 | -0,203 |
| 5 | 0,217 | 0,223 | 5 | -0,233 | -0,227 |
| 9 | 0,368 | 0,374 | 9 | -0,437 | -0,431 |
| 11 | 0,44 | 0,446 | 11 | -0,545 | -0,539 |
| 15 | 0,577 | 0,583 | 15 | -0,746 | -0,74 |
| 20 | 0,714 | 0,72 | 20 | -0,94 | -0,934 |
| 25 | 0,857 | 0,863 | 25 | -1,137 | -1,131 |
| 35 | 1,09 | 1,096 | 35 | -1,37 | -1,364 |
| 45 | 1,29 | 1,296 | 45 | -1,6 | -1,594 |
| 55 | 1,432 | 1,438 | | | |
| 65 | 1,561 | 1,567 | | | |
| 75 | 1,61 | 1,616 | | | |

400°C

| I | V | V | I | V | V |
|---|---|---|---|---|---|
| mA | Volt_pos | Volt | mA | Volt_neg | Volt |
| 10-100 pos | | Correct | 10-100 neg | | Correct |
| 0,01 | -0,006 | -1,00E-03 | 0,01 | -0,006 | 0 |
| 0,2 | 0,015 | 0,02 | 0,2 | -0,021 | -0,015 |
| 0,3 | 0,027 | 0,032 | 0,3 | -0,026 | -0,02 |
| 0,4 | 0,04 | 0,045 | 0,4 | -0,03 | -0,024 |
| 0,5 | 0,052 | 0,057 | 0,5 | -0,036 | -0,03 |
| 0,6 | 0,065 | 0,07 | 0,6 | -0,044 | -0,038 |
| 0,8 | 0,091 | 0,096 | 0,8 | -0,072 | -0,066 |
| 1 | 0,118 | 0,123 | 1 | -0,104 | -0,098 |
| 1,2 | 0,144 | 0,149 | 1,2 | -0,136 | -0,13 |
| 1,4 | 0,17 | 0,175 | 1,4 | -0,166 | -0,16 |
| 1,6 | 0,196 | 0,201 | 1,6 | -0,194 | -0,188 |
| 3,2 | 0,401 | 0,406 | 3,2 | -0,403 | -0,397 |
| 5 | 0,607 | 0,612 | 5 | -0,633 | -0,627 |
| 7 | 0,819 | 0,824 | 7 | -0,878 | -0,872 |
| 9 | 1,017 | 1,022 | 9 | -1,106 | -1,1 |
| 11 | 1,204 | 1,209 | 11 | -1,33 | -1,324 |
| 13 | 1,378 | 1,383 | 13 | -1,505 | -1,499 |
| 16 | 1,61 | 1,615 | 16 | -1,741 | -1,735 |
| 19,5 | 1,856 | 1,861 | 19 | -1,932 | -1,926 |

## 350°C

| I | V | V | I | V | V |
|---|---|---|---|---|---|
| mA | Volt_pos | Volt | mA | Volt_neg | Volt |
| 10 pos | | Correct | 10 neg | | Correct |
| 0 | -0,006 | 0 | 0 | -0,003 | 0 |
| 0,01 | -0,01 | -0,004 | 0,01 | -0,008 | -0,005 |
| 0,1 | 0,019 | 0,025 | 0,1 | -0,032 | -0,029 |
| 0,2 | 0,059 | 0,065 | 0,2 | -0,062 | -0,059 |
| 0,25 | 0,08 | 0,086 | 0,25 | -0,089 | -0,086 |
| 0,3 | 0,104 | 0,11 | 0,3 | -0,119 | -0,116 |
| 0,35 | 0,126 | 0,132 | 0,35 | -0,151 | -0,148 |
| 0,4 | 0,146 | 0,152 | 0,4 | -0,175 | -0,172 |
| 0,45 | 0,176 | 0,182 | 0,45 | -0,196 | -0,193 |
| 0,5 | 0,197 | 0,203 | 0,5 | -0,216 | -0,213 |
| 1 | 0,435 | 0,441 | 1 | -0,423 | -0,42 |
| 1,5 | 0,672 | 0,678 | 1,5 | -0,62 | -0,617 |
| 2 | 0,896 | 0,902 | 2 | -0,808 | -0,805 |
| 2,5 | 1,111 | 1,117 | 2,5 | -0,993 | -0,99 |
| 3 | 1,326 | 1,332 | 3 | -1,164 | -1,161 |
| 3,5 | 1,533 | 1,539 | 3,5 | -1,34 | -1,337 |
| 4 | 1,724 | 1,73 | 4 | -1,499 | -1,496 |
| 4,5 | 1,908 | 1,914 | 4,5 | -1,651 | -1,648 |
| | | | 5,5 | -1,931 | -1,928 |

## 300°C

| I | V | V | I | V | V |
|---|---|---|---|---|---|
| mA | Volt_pos | Volt | mA | Volt_neg | Volt |
| 1 pos | | Correct | 1 neg | | Correct |
| 0,1 | 0,135 | 0,147 | 0,1 | -0,175 | -0,177 |
| 0,12 | 0,17 | 0,182 | 0,12 | -0,206 | -0,208 |
| 0,15 | 0,225 | 0,237 | 0,15 | -0,252 | -0,254 |
| 0,18 | 0,289 | 0,301 | 0,18 | -0,295 | -0,297 |
| 0,2 | 0,334 | 0,346 | 0,2 | -0,322 | -0,324 |
| 0,22 | 0,375 | 0,387 | 0,22 | -0,352 | -0,354 |
| 0,25 | 0,447 | 0,459 | 0,25 | -0,391 | -0,393 |
| 0,3 | 0,553 | 0,565 | 0,3 | -0,463 | -0,465 |
| 0,35 | 0,66 | 0,672 | 0,35 | -0,528 | -0,53 |
| 0,4 | 0,773 | 0,785 | 0,4 | -0,597 | -0,599 |
| 0,5 | 0,996 | 1,008 | 0,5 | -0,735 | -0,737 |
| 0,7 | 1,431 | 1,443 | 0,67 | -1 | -0,91781 |
| 0,9 | 1,86 | 1,872 | 0,9 | -1,26 | -1,262 |
| | | | 1,1 | -1,511 | -1,513 |
| | | | 1,2 | -1,656 | -1,658 |
| | | | 1,4 | -2,08 | -2,082 |

- Cu-Cu in $H_2$/He

  - pH2=100kPa

510°C

| I | V | V | I | V | V |
|---|---|---|---|---|---|
| mA | Volt_pos | Volt | mA | Volt_neg | Volt |
| 10 pos | | Correct | 10 neg | | Correct |
| 1,00E-04 | -0,002 | 0 | 1,00E-04 | 1,00E-03 | 0 |
| 1,00E-03 | -1,00E-03 | 1,00E-03 | 1,00E-03 | 0 | -1,00E-03 |
| 0,03 | 0,018 | 0,02 | 0,03 | -0,009 | -0,01 |
| 0,05 | 0,029 | 0,031 | 0,05 | -0,014 | -0,015 |
| 0,08 | 0,047 | 0,049 | 0,08 | -0,022 | -0,023 |
| 0,125 | 0,075 | 0,077 | 0,125 | -0,036 | -0,037 |
| 0,165 | 0,099 | 0,101 | 0,165 | -0,049 | -0,05 |
| 0,23 | 0,129 | 0,131 | 0,23 | -0,068 | -0,069 |
| 0,26 | 0,152 | 0,154 | 0,26 | -0,077 | -0,078 |
| 0,31 | 0,173 | 0,175 | 0,31 | -0,09 | -0,091 |
| 0,35 | 0,196 | 0,198 | 0,35 | -0,102 | -0,103 |
| 0,73 | 0,396 | 0,398 | 0,53 | -0,155 | -0,156 |
| 1,2 | 0,575 | 0,577 | 0,6 | -0,175 | -0,176 |
| 1,8 | 0,795 | 0,797 | 0,68 | -0,199 | -0,2 |
| 2,4 | 0,965 | 0,967 | 0,73 | -0,215 | -0,216 |
| 3,2 | 1,27 | 1,272 | 1,2 | -0,34 | -0,341 |
| 3,9 | 1,55 | 1,552 | 1,8 | -0,48 | -0,481 |
| 4,5 | 1,78 | 1,782 | 2,4 | -0,595 | -0,596 |
| 5,3 | 1,995 | 1,997 | 3,2 | -0,786 | -0,787 |
| | | | 3,9 | -0,934 | -0,935 |
| | | | 4,5 | -1,058 | -1,059 |
| | | | 5,3 | -1,125 | -1,126 |
| | | | 6,6 | -1,386 | -1,387 |
| | | | 8 | -1,58 | -1,581 |
| | | | 9,5 | -1,77 | -1,771 |
| | | | 11 | -1,96 | -1,961 |

450°C

| I | V | V | I | V | V |
|---|---|---|---|---|---|
| mA | Volt_pos | Volt | mA | Volt_neg | Volt |
| 10 pos | | Correct | 10 neg | | Correct |
| 1,00E-04 | 0,003 | 0 | 1,00E-04 | 0,004 | 0 |
| 0,02 | 0,015 | 0,012 | 0,02 | -0,01 | -0,014 |
| 0,05 | 0,034 | 0,031 | 0,08 | -0,043 | -0,047 |

120

| | | | | | |
|---|---|---|---|---|---|
| 0,08 | 0,053 | 0,05 | 0,12 | -0,069 | -0,073 |
| 0,12 | 0,078 | 0,075 | 0,155 | -0,091 | -0,095 |
| 0,155 | 0,102 | 0,099 | 0,19 | -0,112 | -0,116 |
| 0,19 | 0,126 | 0,123 | 0,24 | -0,137 | -0,141 |
| 0,24 | 0,159 | 0,156 | 0,26 | -0,155 | -0,159 |
| 0,26 | 0,176 | 0,173 | 0,3 | -0,177 | -0,181 |
| 0,3 | 0,203 | 0,2 | 0,33 | -0,196 | -0,2 |
| 0,6 | 0,433 | 0,43 | 0,6 | -0,35 | -0,354 |
| 0,88 | 0,708 | 0,705 | 0,88 | -0,498 | -0,502 |
| 1,2 | 1,066 | 1,063 | 1,2 | -0,667 | -0,671 |
| 1,4 | 1,322 | 1,319 | 1,4 | -0,769 | -0,773 |
| 1,65 | 1,596 | 1,593 | 1,65 | -0,884 | -0,888 |
| 1,85 | 1,795 | 1,792 | 1,99 | -1,03 | -1,034 |
| 1,99 | 1,888 | 1,885 | 3,3 | -1,565 | -1,569 |
| | | | 3,7 | -1,704 | -1,708 |
| | | | 4,4 | -1,933 | -1,937 |

400°C

| I | V | V | I | V | V |
|---|---|---|---|---|---|
| mA | Volt_pos | Volt | mA | Volt_neg | Volt |
| 1 pos | | Correct | 1 neg | | Correct |
| 1,00E-04 | 0,01 | 0 | 1,00E-04 | 0,01 | 0,01 |
| 0,003 | 0,015 | 0,005 | 0,003 | 0,005 | 0,005 |
| 0,016 | 0,037 | 0,027 | 0,016 | -0,019 | -0,019 |
| 0,03 | 0,059 | 0,049 | 0,03 | -0,042 | -0,042 |
| 0,04 | 0,078 | 0,068 | 0,04 | -0,059 | -0,059 |
| 0,055 | 0,108 | 0,098 | 0,055 | -0,083 | -0,083 |
| 0,07 | 0,137 | 0,127 | 0,07 | -0,108 | -0,108 |
| 0,08 | 0,157 | 0,147 | 0,08 | -0,125 | -0,125 |
| 0,095 | 0,188 | 0,178 | 0,095 | -0,15 | -0,15 |
| 0,105 | 0,208 | 0,198 | 0,105 | -0,165 | -0,165 |
| 0,195 | 0,392 | 0,382 | 0,12 | -0,191 | -0,191 |
| 0,35 | 0,782 | 0,772 | 0,195 | -0,306 | -0,306 |
| 0,45 | 1,099 | 1,089 | 0,35 | -0,545 | -0,545 |
| 0,55 | 1,415 | 1,405 | 0,45 | -0,705 | -0,705 |
| 0,65 | 1,745 | 1,735 | 0,55 | -0,846 | -0,846 |
| 0,7 | 1,898 | 1,888 | 0,65 | -0,996 | -0,996 |
| 0,72 | 1,998 | 1,988 | 0,72 | -1,088 | -1,088 |
| | | | 0,9 | -1,331 | -1,331 |
| | | | 1,15 | -1,665 | -1,665 |
| | | | 1,4 | -1,969 | -1,969 |

350°C

| I | V | V | I | V | V |
|---|---|---|---|---|---|
| mA | Volt_pos | Volt | mA | Volt_neg | Volt |

| 1 pos | | Correct | 1 neg | | Correct |
|---|---|---|---|---|---|
| 1,00E-04 | 0,018 | 0 | 1,00E-04 | 0,023 | 0 |
| 0,003 | 0,033 | 0,015 | 0,003 | 0,007 | -0,016 |
| 0,0065 | 0,052 | 0,034 | 0,0065 | -0,014 | -0,037 |
| 0,011 | 0,076 | 0,058 | 0,011 | -0,037 | -0,06 |
| 0,015 | 0,099 | 0,081 | 0,015 | -0,06 | -0,083 |
| 0,02 | 0,125 | 0,107 | 0,02 | -0,085 | -0,108 |
| 0,025 | 0,151 | 0,133 | 0,025 | -0,112 | -0,135 |
| 0,03 | 0,178 | 0,16 | 0,03 | -0,138 | -0,161 |
| 0,034 | 0,2 | 0,182 | 0,034 | -0,159 | -0,182 |
| 0,036 | 0,218 | 0,2 | 0,036 | -0,171 | -0,194 |
| 0,07 | 0,415 | 0,397 | 0,07 | -0,341 | -0,364 |
| 0,105 | 0,639 | 0,621 | 0,105 | -0,522 | -0,545 |
| 0,12 | 0,799 | 0,781 | 0,12 | -0,602 | -0,625 |
| 0,1555 | 1,088 | 1,07 | 0,165 | -0,829 | -0,852 |
| 0,165 | 1,273 | 1,255 | 0,19 | -0,959 | -0,982 |
| 0,19 | 1,55 | 1,532 | 0,23 | -1,193 | -1,216 |
| 0,2 | 1,685 | 1,667 | 0,27 | -1,378 | -1,401 |
| 0,23 | 1,969 | 1,951 | 0,34 | -1,695 | -1,718 |
| | | | 0,4 | -1,96 | -1,983 |

## 300°C

| I | V | V | I | V | V |
|---|---|---|---|---|---|
| mA | Volt_pos | Volt | mA | Volt_neg | Volt |
| 1 pos | | Correct | 1 neg | | Correct |
| 1,00E-04 | 0,019 | -0,003 | 1,00E-04 | 0,033 | -0,003 |
| 1,00E-03 | 0,033 | 0,011 | 1,00E-03 | 0,017 | -0,019 |
| 0,002 | 0,05 | 0,028 | 0,002 | -0,004 | -0,04 |
| 0,0035 | 0,075 | 0,053 | 0,0035 | -0,032 | -0,068 |
| 0,005 | 0,1 | 0,078 | 0,005 | -0,059 | -0,095 |
| 0,0065 | 0,125 | 0,103 | 0,0065 | -0,086 | -0,122 |
| 0,008 | 0,153 | 0,131 | 0,008 | -0,111 | -0,147 |
| 0,0095 | 0,179 | 0,157 | 0,0095 | -0,139 | -0,175 |
| 0,011 | 0,212 | 0,19 | 0,011 | -0,164 | -0,2 |
| 0,022 | 0,405 | 0,383 | 0,022 | -0,35 | -0,386 |
| 0,033 | 0,615 | 0,593 | 0,033 | -0,535 | -0,571 |
| 0,044 | 0,853 | 0,831 | 0,044 | -0,735 | -0,771 |
| 0,055 | 1,102 | 1,08 | 0,055 | -0,925 | -0,961 |
| 0,066 | 1,449 | 1,427 | 0,066 | -1,118 | -1,154 |
| 0,077 | 1,705 | 1,683 | 0,077 | -1,326 | -1,362 |
| 0,088 | 1,995 | 1,973 | 0,088 | -1,559 | -1,595 |
| | | | 0,1 | -1,745 | -1,781 |
| | | | 0,115 | -1,989 | -2,025 |

250°C

| I | V | V | I | V | V |
|---|---|---|---|---|---|
| mA | Volt_pos | Volt | mA | Volt_neg | Volt |
| 1 pos | | Correct | 1 neg | | Correct |
| 1,00E-04 | 0,006 | -0,011 | 1,00E-04 | 0,007 | -0,021 |
| 3,00E-04 | 0,014 | -0,003 | 3,00E-04 | -0,007 | -0,035 |
| 6,00E-04 | 0,034 | 0,017 | 6,00E-04 | -0,032 | -0,06 |
| 8,00E-04 | 0,052 | 0,035 | 8,00E-04 | -0,048 | -0,076 |
| 0,0012 | 0,076 | 0,059 | 0,0012 | -0,081 | -0,109 |
| 0,0015 | 0,105 | 0,088 | 0,0015 | -0,102 | -0,13 |
| 0,002 | 0,142 | 0,125 | 0,002 | -0,149 | -0,177 |
| 0,0025 | 0,184 | 0,167 | 0,0025 | -0,19 | -0,218 |
| 0,0029 | 0,214 | 0,197 | 0,0029 | -0,226 | -0,254 |
| 0,0055 | 0,405 | 0,388 | 0,0055 | -0,444 | -0,472 |
| 0,008 | 0,615 | 0,598 | 0,008 | -0,679 | -0,707 |
| 0,011 | 0,887 | 0,87 | 0,011 | -1,01 | -1,038 |
| 0,0125 | 1,039 | 1,022 | 0,015 | -1,446 | -1,474 |
| 0,015 | 1,271 | 1,254 | 0,0175 | -1,72 | -1,748 |
| 0,0175 | 1,509 | 1,492 | 0,02 | -1,989 | -2,017 |
| 0,02 | 1,768 | 1,751 | | | |
| 0,0225 | 1,999 | 1,982 | | | |

- Cu-Cu in $H_2/CO_2=1/5$

500°C

| I | V | V | I | V | V |
|---|---|---|---|---|---|
| mA | Volt_pos | Volt | mA | Volt_neg | Volt |
| 10 pos | | Correct | 10 neg | | Correct |
| 0,01 | -0,012 | -0,012 | 0,01 | -0,014 | -0,02 |
| 0,05 | 0,009 | 0,009 | 0,05 | -0,032 | -0,038 |
| 0,1 | 0,048 | 0,048 | 0,1 | -0,065 | -0,071 |
| 0,15 | 0,085 | 0,085 | 0,15 | -0,096 | -0,102 |
| 0,17 | 0,105 | 0,105 | 0,17 | -0,107 | -0,113 |
| 0,2 | 0,127 | 0,127 | 0,2 | -0,123 | -0,129 |
| 0,23 | 0,161 | 0,161 | 0,23 | -0,145 | -0,151 |
| 0,25 | 0,176 | 0,176 | 0,25 | -0,154 | -0,16 |
| 0,28 | 0,204 | 0,204 | 0,3 | -0,183 | -0,189 |
| 0,5 | 0,455 | 0,455 | 0,7 | -0,362 | -0,368 |
| 0,7 | 0,677 | 0,677 | 1,3 | -0,572 | -0,578 |
| 1 | 0,946 | 0,946 | 2,2 | -0,855 | -0,861 |
| 1,3 | 1,159 | 1,159 | 3,2 | -1,136 | -1,142 |

| 1,6 | 1,355 | 1,355 | 4 | -1,314 | -1,32 |
|---|---|---|---|---|---|
| 2,2 | 1,668 | 1,668 | 5,5 | -1,635 | -1,641 |
| 2,8 | 1,965 | 1,965 | 7 | -1,922 | -1,928 |
| | | | 7,4 | -1,986 | -1,992 |

## 450°C

| I | V | V | I | V | V |
|---|---|---|---|---|---|
| mA | Volt_pos | Volt | mA | Volt_neg | Volt |
| 10 pos | | Correct | 10 neg | | Correct |
| 0,01 | 1,00E-03 | -0,003 | 0,01 | 0,005 | -0,004 |
| 0,015 | 0,021 | 0,017 | 0,015 | -0,015 | -0,024 |
| 0,025 | 0,038 | 0,034 | 0,025 | -0,033 | -0,042 |
| 0,035 | 0,055 | 0,051 | 0,035 | -0,046 | -0,055 |
| 0,045 | 0,075 | 0,071 | 0,045 | -0,061 | -0,07 |
| 0,065 | 0,114 | 0,11 | 0,065 | -0,075 | -0,084 |
| 0,07 | 0,126 | 0,122 | 0,075 | -0,104 | -0,113 |
| 0,085 | 0,16 | 0,156 | 0,095 | -0,133 | -0,142 |
| 0,095 | 0,186 | 0,182 | 0,115 | -0,164 | -0,173 |
| 0,1 | 0,203 | 0,199 | 0,14 | -0,196 | -0,205 |
| 0,2 | 0,46 | 0,456 | 0,3 | -0,377 | -0,386 |
| 0,3 | 0,728 | 0,724 | 0,5 | -0,54 | -0,549 |
| 0,4 | 0,966 | 0,962 | 0,83 | -0,783 | -0,792 |
| 0,5 | 1,155 | 1,151 | 1,08 | -0,96 | -0,969 |
| 0,63 | 1,363 | 1,359 | 1,65 | -1,32 | -1,329 |
| 0,83 | 1,645 | 1,641 | 2,5 | -1,69 | -1,699 |
| 0,95 | 1,803 | 1,799 | 3 | -1,918 | -1,927 |
| 1,08 | 1,965 | 1,961 | | | |

## 400°C

| I | V | V | I | V | V |
|---|---|---|---|---|---|
| mA | Volt_pos | Volt | mA | Volt_neg | Volt |
| 1 pos | | Correct | 1 neg | | Correct |
| 1,00E-03 | 0,005 | -0,005 | 1,00E-03 | 0,011 | -0,006 |
| 0,005 | 0,015 | 0,005 | 0,005 | -0,006 | -0,023 |
| 0,01 | 0,031 | 0,021 | 0,01 | -0,021 | -0,038 |
| 0,015 | 0,052 | 0,042 | 0,015 | -0,037 | -0,054 |
| 0,025 | 0,088 | 0,078 | 0,025 | -0,07 | -0,087 |
| 0,03 | 0,112 | 0,102 | 0,03 | -0,087 | -0,104 |
| 0,035 | 0,134 | 0,124 | 0,035 | -0,103 | -0,12 |
| 0,04 | 0,159 | 0,149 | 0,04 | -0,12 | -0,137 |
| 0,045 | 0,187 | 0,177 | 0,045 | -0,138 | -0,155 |
| 0,05 | 0,214 | 0,204 | 0,05 | -0,155 | -0,172 |
| 0,1 | 0,479 | 0,469 | 0,06 | -0,186 | -0,203 |

| I mA | V Volt_pos | V Volt Correct | I mA | V Volt_neg | V Volt Correct |
|---|---|---|---|---|---|
| 0,14 | 0,72 | 0,71 | 0,1 | -0,3 | -0,317 |
| 0,18 | 0,94 | 0,93 | 0,18 | -0,496 | -0,513 |
| 0,22 | 1,161 | 1,151 | 0,26 | -0,652 | -0,669 |
| 0,26 | 1,325 | 1,315 | 0,35 | -0,819 | -0,836 |
| 0,3 | 1,473 | 1,463 | 0,45 | -0,995 | -1,012 |
| 0,35 | 1,635 | 1,625 | 0,55 | -1,159 | -1,176 |
| 0,4 | 1,794 | 1,784 | 0,66 | -1,333 | -1,35 |
| 0,45 | 1,947 | 1,937 | 0,875 | -1,634 | -1,651 |
| | | | 1,1 | -1,927 | -1,944 |

## 350°C

| I mA 1 pos | V Volt_pos | V Volt Correct | I mA 1 neg | V Volt_neg | V Volt Correct |
|---|---|---|---|---|---|
| 1,00E-04 | 0,015 | -1,00E-03 | 1,00E-04 | 0,032 | -1,00E-03 |
| 0,0025 | 0,032 | 0,016 | 0,0025 | 0,014 | -0,019 |
| 0,0045 | 0,048 | 0,032 | 0,0045 | -0,003 | -0,036 |
| 0,0085 | 0,08 | 0,064 | 0,0085 | -0,032 | -0,065 |
| 0,011 | 0,104 | 0,088 | 0,011 | -0,051 | -0,084 |
| 0,014 | 0,136 | 0,12 | 0,014 | -0,078 | -0,111 |
| 0,0175 | 0,167 | 0,151 | 0,0175 | -0,103 | -0,136 |
| 0,019 | 0,188 | 0,172 | 0,019 | -0,115 | -0,148 |
| 0,021 | 0,211 | 0,195 | 0,021 | -0,139 | -0,172 |
| 0,05 | 0,495 | 0,479 | 0,027 | -0,171 | -0,204 |
| 0,065 | 0,685 | 0,669 | 0,05 | -0,32 | -0,353 |
| 0,075 | 0,815 | 0,799 | 0,095 | -0,571 | -0,604 |
| 0,095 | 1,027 | 1,011 | 0,175 | -0,95 | -0,983 |
| 0,135 | 1,365 | 1,349 | 0,27 | -1,259 | -1,292 |
| 0,175 | 1,689 | 1,673 | 0,35 | -1,635 | -1,668 |
| 0,2 | 1,919 | 1,903 | 0,42 | -1,92 | -1,953 |

## 300°C

| I mA 1 pos | V Volt_pos | V Volt Correct | I mA 1 neg | V Volt_neg | V Volt Correct |
|---|---|---|---|---|---|
| 1,00E-04 | 0,005 | 0,005 | 1,00E-04 | 0,032 | -0,006 |
| 1,00E-03 | 0,013 | 0,013 | 1,00E-03 | 0,003 | -0,035 |
| 0,002 | 0,033 | 0,033 | 0,002 | -0,032 | -0,07 |
| 0,003 | 0,056 | 0,056 | 0,003 | -0,065 | -0,103 |
| 0,004 | 0,079 | 0,079 | 0,004 | -0,1 | -0,138 |
| 0,005 | 0,102 | 0,102 | 0,005 | -0,134 | -0,172 |

| 0,0065 | 0,136 | 0,136 | 0,0065 | -0,17 | -0,208 |
|---|---|---|---|---|---|
| 0,007 | 0,152 | 0,152 | 0,007 | -0,205 | -0,243 |
| 0,008 | 0,176 | 0,176 | 0,02 | -0,574 | -0,612 |
| 0,009 | 0,202 | 0,202 | 0,025 | -0,712 | -0,75 |
| 0,02 | 0,473 | 0,473 | 0,035 | -0,946 | -0,984 |
| 0,025 | 0,6 | 0,6 | 0,045 | -1,194 | -1,232 |
| 0,035 | 0,812 | 0,812 | 0,065 | -1,598 | -1,636 |
| 0,045 | 1,03 | 1,03 | 0,075 | -1,849 | -1,887 |
| 0,065 | 1,425 | 1,425 | 0,09 | -1,975 | -2,013 |
| 0,075 | 1,65 | 1,65 | | | |
| 0,09 | 1,94 | 1,94 | | | |

250°C

| I | V | V | I | V | V |
|---|---|---|---|---|---|
| mA | Volt_pos | Volt | mA | Volt_neg | Volt |
| 1 pos | | Correct | 1 neg | | Correct |
| 1,00E-04 | 0,009 | -0,007 | 1,00E-04 | 0,018 | -0,007 |
| 5,00E-04 | 0,023 | 0,007 | 5,00E-04 | -0,009 | -0,034 |
| 8,00E-04 | 0,036 | 0,02 | 8,00E-04 | -0,023 | -0,048 |
| 1,00E-03 | 0,045 | 0,029 | 1,00E-03 | -0,038 | -0,063 |
| 0,0012 | 0,058 | 0,042 | 0,0012 | -0,053 | -0,078 |
| 0,0018 | 0,084 | 0,068 | 0,0018 | -0,083 | -0,108 |
| 0,0022 | 0,106 | 0,09 | 0,0022 | -0,106 | -0,131 |
| 0,003 | 0,146 | 0,13 | 0,003 | -0,155 | -0,18 |
| 0,0035 | 0,173 | 0,157 | 0,0035 | -0,185 | -0,21 |
| 0,004 | 0,197 | 0,181 | 0,004 | -0,219 | -0,244 |
| 0,0045 | 0,228 | 0,212 | 0,0045 | -0,253 | -0,278 |
| 0,0085 | 0,438 | 0,422 | 0,0085 | -0,454 | -0,479 |
| 0,013 | 0,652 | 0,636 | 0,013 | -0,678 | -0,703 |
| 0,0165 | 0,815 | 0,799 | 0,0165 | -0,855 | -0,88 |
| 0,022 | 1,073 | 1,057 | 0,022 | -1,111 | -1,136 |
| 0,026 | 1,246 | 1,23 | 0,026 | -1,308 | -1,333 |
| 0,03 | 1,424 | 1,408 | 0,03 | -1,494 | -1,519 |
| 0,035 | 1,655 | 1,639 | 0,035 | -1,715 | -1,74 |
| 0,04 | 1,96 | 1,944 | 0,04 | -1,94 | -1,965 |

- Cu-Cu in $H_2/CO_2 = 1/8$

126

## 500°C

| I | V | V | I | V | V |
|---:|---:|---:|---:|---:|---:|
| mA | Volt_pos | Volt | mA | Volt_neg | Volt |
| 10 pos | | Correct | 10-100 neg | | Correct |
| 0,1 | -0,152 | 0,048 | 0,1 | -0,089 | -0,039 |
| 0,2 | -0,091 | 0,109 | 0,2 | -0,122 | -0,072 |
| 0,4 | 0,05 | 0,25 | 0,4 | -0,175 | -0,125 |
| 0,6 | 0,204 | 0,404 | 0,6 | -0,215 | -0,165 |
| 0,8 | 0,369 | 0,569 | 0,8 | -0,25 | -0,2 |
| 1 | 0,533 | 0,733 | 1 | -0,28 | -0,23 |
| 1,2 | 0,705 | 0,905 | 1,2 | -0,302 | -0,252 |
| 1,4 | 0,895 | 1,095 | 1,4 | -0,32 | -0,27 |
| 1,6 | 1,086 | 1,286 | 1,6 | -0,337 | -0,287 |
| 1,8 | 1,273 | 1,473 | 1,8 | -0,35 | -0,3 |
| 2 | 1,455 | 1,655 | 2 | -0,361 | -0,311 |
| 2,25 | 1,668 | 1,868 | 2,25 | -0,374 | -0,324 |
| 2,5 | 1,903 | 2,103 | 2,5 | -0,386 | -0,336 |
| | | | 3 | -0,413 | -0,363 |
| | | | 4 | -0,465 | -0,415 |
| | | | 6 | -0,578 | -0,528 |
| | | | 8 | -0,72 | -0,67 |
| | | | 10 | -0,85 | -0,8 |
| | | | 12,5 | -1,011 | -0,961 |
| | | | 15 | -1,192 | -1,142 |
| | | | 17,5 | -1,23 | -1,18 |
| | | | 20 | -1,241 | -1,191 |
| | | | 40 | -1,54 | -1,49 |
| | | | 60 | -2 | -1,95 |

## 450°C

| I | V | V | I | V | V |
|---:|---:|---:|---:|---:|---:|
| mA | Volt_pos | Volt | mA | Volt_neg | Volt |
| 1 pos | | Correct | 10 neg | | Correct |
| 0,1 | -0,115 | 0,054 | 0,1 | -0,15 | -0,076 |
| 0,2 | -0,008 | 0,161 | 0,3 | -0,239 | -0,165 |
| 0,3 | 0,145 | 0,314 | 0,4 | -0,284 | -0,21 |
| 0,4 | 0,337 | 0,506 | 0,6 | -0,318 | -0,244 |
| 0,5 | 0,547 | 0,716 | 1,1 | -0,404 | -0,33 |
| 0,6 | 0,775 | 0,944 | 2 | -0,501 | -0,427 |
| 0,7 | 1,205 | 1,374 | 3,5 | -0,675 | -0,601 |
| 0,8 | 1,26 | 1,429 | 5 | -0,893 | -0,819 |
| 0,9 | 1,477 | 1,646 | 7 | -1,16 | -1,086 |
| 1 | 1,683 | 1,852 | 10 | -1,73 | -1,656 |
| 1,1 | 1,912 | 2,081 | 11 | -1,875 | -1,801 |

## 400°C

| I | V | V | I | V | V |
|---|---|---|---|---|---|
| mA | Volt_pos | Volt | mA | Volt_neg | Volt |
| 1 pos | | Correct | 10 neg | | Correct |
| 0,01 | -0,165 | 0,01 | 0,05 | -0,152 | -0,07 |
| 0,05 | -0,101 | 0,074 | 0,1 | -0,213 | -0,131 |
| 0,1 | 0,013 | 0,188 | 0,15 | -0,267 | -0,185 |
| 0,15 | 0,182 | 0,357 | 0,2 | -0,309 | -0,227 |
| 0,2 | 0,404 | 0,579 | 0,35 | -0,367 | -0,285 |
| 0,25 | 0,641 | 0,816 | 0,7 | -0,463 | -0,381 |
| 0,3 | 0,884 | 1,059 | 1,1 | -0,542 | -0,46 |
| 0,35 | 1,117 | 1,292 | 1,6 | -0,64 | -0,558 |
| 0,4 | 1,325 | 1,5 | 3 | -1,025 | -0,943 |
| 0,45 | 1,5 | 1,675 | 4,8 | -1,737 | -1,655 |
| 0,5 | 1,659 | 1,834 | | | |
| 0,55 | 1,847 | 2,022 | | | |

## 350°C

| I | V | V | I | V | V |
|---|---|---|---|---|---|
| mA | Volt_pos | Volt | mA | Volt_neg | Volt |
| 1 pos | | Correct | 1 neg | | Correct |
| 0,01 | -0,283 | 0,018 | 0,01 | -0,115 | -0,053 |
| 0,02 | -0,235 | 0,066 | 0,02 | -0,156 | -0,094 |
| 0,03 | -0,198 | 0,103 | 0,03 | -0,191 | -0,129 |
| 0,04 | -0,155 | 0,146 | 0,05 | -0,244 | -0,182 |
| 0,05 | -0,1 | 0,201 | 0,07 | -0,289 | -0,227 |
| 0,06 | -0,034 | 0,267 | 0,1 | -0,341 | -0,279 |
| 0,07 | 0,041 | 0,342 | 0,13 | -0,389 | -0,327 |
| 0,08 | 0,122 | 0,423 | 0,18 | -0,441 | -0,379 |
| 0,09 | 0,215 | 0,516 | 0,35 | -0,536 | -0,474 |
| 0,1 | 0,312 | 0,613 | 0,5 | -0,606 | -0,544 |
| 0,11 | 0,415 | 0,716 | 0,9 | -0,739 | -0,677 |
| 0,13 | 0,588 | 0,889 | 1,4 | -0,955 | -0,893 |
| 0,15 | 0,771 | 1,072 | | | |
| 0,18 | 1,001 | 1,302 | | | |
| 0,2 | 1,142 | 1,443 | | | |
| 0,25 | 1,377 | 1,678 | | | |
| 0,3 | 1,581 | 1,882 | | | |
| 0,35 | 1,772 | 2,073 | | | |
| 0,37 | 1,9 | 2,201 | | | |
| 0,38 | 1,973 | 2,274 | | | |

300°C

| I | V | V | I | V | V |
|---|---|---|---|---|---|
| mA | Volt_pos | Volt | mA | Volt_neg | Volt |
| 1 pos | | Correct | 1 neg | | Correct |
| 1,00E-03 | -0,063 | -0,003 | 1,00E-03 | 0,047 | -0,004 |
| 0,005 | -0,051 | 0,009 | 0,005 | 0,01 | -0,041 |
| 0,01 | -0,034 | 0,026 | 0,01 | -0,022 | -0,073 |
| 0,02 | 0,031 | 0,091 | 0,02 | -0,084 | -0,135 |
| 0,025 | 0,081 | 0,141 | 0,025 | -0,113 | -0,164 |
| 0,03 | 0,136 | 0,196 | 0,03 | -0,143 | -0,194 |
| 0,035 | 0,198 | 0,258 | 0,035 | -0,169 | -0,22 |
| 0,04 | 0,265 | 0,325 | 0,04 | -0,195 | -0,246 |
| 0,045 | 0,346 | 0,406 | 0,045 | -0,22 | -0,271 |
| 0,05 | 0,44 | 0,5 | 0,05 | -0,24 | -0,291 |
| 0,06 | 0,613 | 0,673 | 0,1 | -0,337 | -0,388 |
| 0,07 | 0,82 | 0,88 | 0,15 | -0,432 | -0,483 |
| 0,08 | 1,038 | 1,098 | 0,2 | -0,497 | -0,548 |
| 0,09 | 1,23 | 1,29 | 0,4 | -0,655 | -0,706 |
| 0,1 | 1,365 | 1,425 | 0,7 | -0,907 | -0,958 |
| 0,11 | 1,48 | 1,54 | | | |
| 0,12 | 1,572 | 1,632 | | | |
| 0,13 | 1,652 | 1,712 | | | |
| 0,14 | 1,733 | 1,793 | | | |
| 0,15 | 1,814 | 1,874 | | | |
| 0,16 | 1,9 | 1,96 | | | |

- Co-Co:
- $pH_2=20kPa$

500°C

| I | V | V | I | V | V |
|---|---|---|---|---|---|
| mA | Volt_pos | Volt | mA | Volt_neg | Volt |
| 10 pos | | Correct | 10 neg | | Correct |
| 0,2 | 0,022 | 0,022 | 0,2 | -0,025 | -0,027 |
| 0,5 | 0,059 | 0,059 | 0,5 | -0,061 | -0,063 |
| 0,7 | 0,086 | 0,086 | 0,7 | -0,09 | -0,092 |
| 1 | 0,124 | 0,124 | 1 | -0,135 | -0,137 |
| 1,2 | 0,154 | 0,154 | 1,2 | -0,162 | -0,164 |
| 1,5 | 0,195 | 0,195 | 1,5 | -0,205 | -0,207 |
| 1,7 | 0,224 | 0,224 | | | |
| 2 | 0,265 | 0,265 | | | |

## 550°C

| I | V | V | I | V | V |
|---|---|---|---|---|---|
| mA | Volt_pos | Volt | mA | Volt_neg | Volt |
| 10 pos | | Correct | 10 neg | | Correct |
| 0,3 | 0,024 | 0,025 | 0,3 | -0,024 | -0,034 |
| 0,5 | 0,042 | 0,043 | 0,5 | -0,043 | -0,053 |
| 0,7 | 0,06 | 0,061 | 0,7 | -0,059 | -0,069 |
| 1 | 0,088 | 0,089 | 1 | -0,088 | -0,098 |
| 1,2 | 0,108 | 0,109 | 1,2 | -0,107 | -0,117 |
| 1,5 | 0,135 | 0,136 | 1,5 | -0,138 | -0,148 |
| 1,8 | 0,164 | 0,165 | 1,8 | -0,172 | -0,182 |
| 2 | 0,187 | 0,188 | | | |
| 2,2 | 0,207 | 0,208 | | | |
| 2,5 | 0,236 | 0,237 | | | |
| 3 | 0,283 | 0,284 | | | |

## 600°C

| I | V | V | I | V | V |
|---|---|---|---|---|---|
| mA | Volt_pos | Volt | mA | Volt_neg | Volt |
| 10 pos | | Correct | 10 neg | | Correct |
| 0,5 | 0,029 | 0,029 | 0,5 | -0,028 | -0,03 |
| 1 | 0,06 | 0,06 | 1 | -0,058 | -0,06 |
| 1,5 | 0,094 | 0,094 | 1,5 | -0,088 | -0,09 |
| 2 | 0,13 | 0,13 | 2 | -0,13 | -0,132 |
| 2,5 | 0,17 | 0,17 | 2,5 | -0,17 | -0,172 |
| 3 | 0,21 | 0,21 | | | |
| 3,5 | 0,246 | 0,246 | | | |
| 4 | 0,282 | 0,282 | | | |
| 5 | 0,344 | 0,344 | | | |

## 650°C

| I | V | V | I | V | V |
|---|---|---|---|---|---|
| mA | Volt_pos | Volt | mA | Volt_neg | Volt |
| 10 pos | | Correct | 10 neg | | Correct |
| 0,5 | 0,021 | 0,02 | 0,5 | -0,019 | -0,022 |
| 1 | 0,043 | 0,042 | 1 | -0,039 | -0,042 |
| 1,5 | 0,066 | 0,065 | 1,5 | -0,059 | -0,062 |
| 2 | 0,09 | 0,089 | 2 | -0,08 | -0,083 |
| 2,5 | 0,12 | 0,119 | 2,5 | -0,102 | -0,105 |
| 3 | 0,148 | 0,147 | 3 | -0,124 | -0,127 |
| 3,5 | 0,176 | 0,175 | 3,5 | -0,15 | -0,153 |
| 4 | 0,201 | 0,2 | | | |
| 4,5 | 0,227 | 0,226 | | | |
| 5 | 0,25 | 0,249 | | | |

| I | V | V | I | V | V |
|---|---|---|---|---|---|
| | | | | | |
| 5,5 | 0,27 | 0,269 | | | |
| 6 | 0,29 | 0,289 | | | |

## 700°C

| I | V | V | I | V | V |
|---|---|---|---|---|---|
| mA | Volt_pos | Volt | mA | Volt_neg | Volt |
| 10 pos | | Correct | 10 neg | | Correct |
| 0,5 | 0,01 | 0,012 | 0,5 | -0,011 | -0,011 |
| 1 | 0,02 | 0,022 | 1 | -0,02 | -0,02 |
| 2 | 0,04 | 0,042 | 2 | -0,04 | -0,04 |
| 3 | 0,06 | 0,062 | 3 | -0,06 | -0,06 |
| 4 | 0,08 | 0,082 | 4 | -0,081 | -0,081 |
| 5 | 0,102 | 0,104 | 5 | -0,104 | -0,104 |
| 7 | 0,144 | 0,146 | 6 | -0,126 | -0,126 |
| 8 | 0,165 | 0,167 | | | |
| 9 | 0,184 | 0,186 | | | |
| 10 | 0,202 | 0,204 | | | |

- Co-Co:
- $pH_2 = 50kPa$

## 450°C

| I | V | V | I | V | V |
|---|---|---|---|---|---|
| mA | Volt_pos | Volt | mA | Volt_neg | Volt |
| 10 pos | | Correct | 10 neg | | Correct |
| 0,1 | 0,015 | 0,018 | 0,1 | -0,022 | -0,019 |
| 0,2 | 0,035 | 0,038 | 0,2 | -0,043 | -0,04 |
| 0,3 | 0,056 | 0,059 | 0,3 | -0,068 | -0,065 |
| 0,4 | 0,079 | 0,082 | 0,4 | -0,095 | -0,092 |
| 0,5 | 0,102 | 0,105 | 0,5 | -0,121 | -0,118 |
| 0,7 | 0,145 | 0,148 | 0,7 | -0,168 | -0,165 |
| 0,8 | 0,168 | 0,171 | 0,8 | -0,194 | -0,191 |
| 0,9 | 0,192 | 0,195 | 0,9 | -0,223 | -0,22 |
| 1 | 0,217 | 0,22 | | | |
| 1,25 | 0,276 | 0,279 | | | |
| 1,4 | 0,312 | 0,315 | | | |

## 500°C

| I | V | V | I | V | V |
|---|---|---|---|---|---|
| mA | Volt_pos | Volt | mA | Volt_neg | Volt |
| 10 pos | | Correct | 10 neg | | Correct |

| I mA 10 pos | V Volt_pos | V Volt Correct | I mA 10 neg | V Volt_neg | V Volt Correct |
|---|---|---|---|---|---|
| 0,1 | 0,012 | 0,015 | 0,1 | -0,013 | -0,01 |
| 0,2 | 0,026 | 0,029 | 0,2 | -0,027 | -0,024 |
| 0,3 | 0,041 | 0,044 | 0,3 | -0,044 | -0,041 |
| 0,4 | 0,057 | 0,06 | 0,4 | -0,058 | -0,055 |
| 0,5 | 0,071 | 0,074 | 0,5 | -0,071 | -0,068 |
| 0,6 | 0,086 | 0,089 | 0,6 | -0,085 | -0,082 |
| 0,8 | 0,114 | 0,117 | 0,8 | -0,117 | -0,114 |
| 1 | 0,146 | 0,149 | 1 | -0,153 | -0,15 |
| 1,3 | 0,191 | 0,194 | 1,3 | -0,208 | -0,205 |
| 1,6 | 0,241 | 0,244 | | | |
| 2 | 0,308 | 0,311 | | | |

## 550°C

| I mA 10 pos | V Volt_pos | V Volt Correct | I mA 10 neg | V Volt_neg | V Volt Correct |
|---|---|---|---|---|---|
| 0,1 | 0,008 | 0,01 | 0,1 | -0,009 | -0,008 |
| 0,2 | 0,016 | 0,018 | 0,2 | -0,017 | -0,016 |
| 0,3 | 0,025 | 0,027 | 0,3 | -0,026 | -0,025 |
| 0,4 | 0,034 | 0,036 | 0,4 | -0,034 | -0,033 |
| 0,6 | 0,052 | 0,054 | 0,6 | -0,05 | -0,049 |
| 0,8 | 0,07 | 0,072 | 0,8 | -0,067 | -0,066 |
| 1 | 0,088 | 0,09 | 1 | -0,083 | -0,082 |
| 1,5 | 0,134 | 0,136 | 1,5 | -0,128 | -0,127 |
| 2 | 0,183 | 0,185 | 2 | -0,178 | -0,177 |
| 2,5 | 0,232 | 0,234 | 2,5 | -0,236 | -0,235 |
| 3 | 0,288 | 0,29 | | | |
| 3,5 | 0,341 | 0,343 | | | |

## 600°C

| I mA 10 pos | V Volt_pos | V Volt Correct | I mA 10 neg | V Volt_neg | V Volt Correct |
|---|---|---|---|---|---|
| 0,1 | 0,005 | 0,005 | 0,1 | -0,004 | -0,006 |
| 0,2 | 0,01 | 0,01 | 0,2 | -0,008 | -0,01 |
| 0,3 | 0,015 | 0,015 | 0,3 | -0,012 | -0,014 |
| 0,4 | 0,02 | 0,02 | 0,4 | -0,017 | -0,019 |
| 0,6 | 0,03 | 0,03 | 0,6 | -0,025 | -0,027 |
| 0,8 | 0,04 | 0,04 | 0,8 | -0,033 | -0,035 |
| 1 | 0,051 | 0,051 | 1 | -0,041 | -0,043 |
| 1,5 | 0,076 | 0,076 | 1,5 | -0,069 | -0,071 |
| 2 | 0,103 | 0,103 | 2 | -0,092 | -0,094 |
| 2,5 | 0,132 | 0,132 | 2,5 | -0,117 | -0,119 |
| 3 | 0,161 | 0,161 | 3 | -0,145 | -0,147 |

| | | | |
|---:|---|---|---|
| 3,5 | 0,193 | 0,193 | |
| 4 | 0,231 | 0,231 | |
| 5 | 0,296 | 0,296 | |
| 6 | 0,357 | 0,357 | |

## 650°C

| I mA 10 pos | V Volt_pos | V Volt Correct | I mA 10 neg | V Volt_neg | V Volt Correct |
|---:|---|---|---:|---|---|
| 0,1 | 0,003 | 0,004 | 0,1 | -0,002 | -0,005 |
| 0,2 | 0,006 | 0,007 | 0,5 | -0,016 | -0,019 |
| 0,5 | 0,014 | 0,015 | 1 | -0,032 | -0,035 |
| 1 | 0,027 | 0,028 | 1,5 | -0,049 | -0,052 |
| 1,5 | 0,041 | 0,042 | 2 | -0,064 | -0,067 |
| 2 | 0,055 | 0,056 | 2,5 | -0,08 | -0,083 |
| 2,5 | 0,07 | 0,071 | 3 | -0,094 | -0,097 |
| 3 | 0,085 | 0,086 | 4 | -0,128 | -0,131 |
| 3,5 | 0,1 | 0,101 | 4,5 | -0,146 | -0,149 |
| 4 | 0,12 | 0,121 | 5 | -0,162 | -0,165 |
| 5 | 0,152 | 0,153 | | | |
| 6 | 0,27 | 0,271 | | | |
| 7 | 0,32 | 0,321 | | | |
| 8 | 0,354 | 0,355 | | | |

## 700°C

| I mA 10 pos | V Volt_pos | V Volt Correct | I mA 10 neg | V Volt_neg | V Volt Correct |
|---:|---|---|---:|---|---|
| 0,5 | 0,009 | 0,011 | 0,5 | -0,012 | -0,013 |
| 1 | 0,018 | 0,02 | 1 | -0,021 | -0,022 |
| 1,5 | 0,027 | 0,029 | 1,5 | -0,031 | -0,032 |
| 2 | 0,036 | 0,038 | 2 | -0,043 | -0,044 |
| 3 | 0,054 | 0,056 | 3 | -0,062 | -0,063 |
| 4 | 0,075 | 0,077 | 4 | -0,083 | -0,084 |
| 6 | 0,114 | 0,116 | 5 | -0,105 | -0,106 |
| 8 | 0,186 | 0,188 | 6 | -0,126 | -0,127 |
| 10 | 0,237 | 0,239 | 7 | -0,148 | -0,149 |

- Co-Co:
- $pH_2 = 100 kPa$

133

## 450°C

| I | V | V | I | V | V |
|---|---|---|---|---|---|
| mA | Volt_pos | Volt | mA | Volt_neg | Volt |
| 10 pos | | Correct | 10 neg | | Correct |
| 0,1 | 0,008 | 0,007 | 0,1 | -0,008 | -0,009 |
| 0,2 | 0,015 | 0,014 | 0,2 | -0,016 | -0,017 |
| 0,3 | 0,022 | 0,021 | 0,3 | -0,025 | -0,026 |
| 0,4 | 0,031 | 0,03 | 0,4 | -0,033 | -0,034 |
| 0,6 | 0,045 | 0,044 | 0,6 | -0,049 | -0,05 |
| 0,8 | 0,061 | 0,06 | 0,8 | -0,065 | -0,066 |
| 1 | 0,076 | 0,075 | 1 | -0,083 | -0,084 |
| 1,2 | 0,091 | 0,09 | 1,2 | -0,101 | -0,102 |
| 1,4 | 0,106 | 0,105 | 1,4 | -0,118 | -0,119 |
| 1,6 | 0,122 | 0,121 | | | |
| 1,8 | 0,137 | 0,136 | | | |

## 500°C

| I | V | V | I | V | V |
|---|---|---|---|---|---|
| mA | Volt_pos | Volt | mA | Volt_neg | Volt |
| 10 pos | | Correct | 10 neg | | Correct |
| 0,1 | 0,006 | 0,004 | 0,1 | -0,004 | -0,005 |
| 0,2 | 0,011 | 0,009 | 0,2 | -0,008 | -0,009 |
| 0,3 | 0,015 | 0,013 | 0,3 | -0,013 | -0,014 |
| 0,4 | 0,019 | 0,017 | 0,4 | -0,017 | -0,018 |
| 0,6 | 0,028 | 0,026 | 0,6 | -0,026 | -0,027 |
| 0,8 | 0,037 | 0,035 | 0,8 | -0,036 | -0,037 |
| 1 | 0,045 | 0,043 | 1 | -0,045 | -0,046 |
| 1,2 | 0,054 | 0,052 | 1,2 | -0,055 | -0,056 |
| 1,4 | 0,063 | 0,061 | 1,4 | -0,064 | -0,065 |
| 1,8 | 0,08 | 0,078 | 1,8 | -0,086 | -0,087 |
| 2,2 | 0,097 | 0,095 | 2,2 | -0,106 | -0,107 |
| 2,6 | 0,114 | 0,112 | | | |
| 3 | 0,132 | 0,13 | | | |

## 550°C

| I | V | V | I | V | V |
|---|---|---|---|---|---|
| mA | Volt_pos | Volt | mA | Volt_neg | Volt |
| 10 pos | | Correct | 10 neg | | Correct |
| 0,1 | 0,005 | | 0,1 | -0,002 | -0,004 |
| 0,2 | 0,008 | 0,007 | 0,2 | -0,005 | -0,007 |
| 0,4 | 0,014 | 0,013 | 0,4 | -0,011 | -0,013 |
| 0,6 | 0,02 | 0,019 | 0,6 | -0,016 | -0,018 |

| I | V | V | I | V | V |
|---|---|---|---|---|---|
| mA | Volt_pos | Volt | mA | Volt_neg | Volt |
| 10 pos | | Correct | 10 neg | | Correct |
| 0,8 | 0,025 | 0,024 | 0,8 | -0,022 | -0,024 |
| 1 | 0,031 | 0,03 | 1 | -0,028 | -0,03 |
| 1,5 | 0,045 | 0,044 | 1,5 | -0,043 | -0,045 |
| 2 | 0,059 | 0,058 | 2 | -0,059 | -0,061 |
| 3 | 0,087 | 0,086 | 3 | -0,091 | -0,093 |
| 4 | 0,118 | 0,117 | 4 | -0,124 | -0,126 |

## 600°C

| I | V | V | I | V | V |
|---|---|---|---|---|---|
| mA | Volt_pos | Volt | mA | Volt_neg | Volt |
| 10 pos | | Correct | 10 neg | | Correct |
| 0,2 | 0,006 | 0,004 | 0,2 | -0,003 | -0,006 |
| 0,5 | 0,012 | 0,01 | 0,5 | -0,009 | -0,012 |
| 1 | 0,022 | 0,02 | 1 | -0,02 | -0,023 |
| 1,5 | 0,032 | 0,03 | 1,5 | -0,03 | -0,033 |
| 2 | 0,042 | 0,04 | 2 | -0,041 | -0,044 |
| 3 | 0,063 | 0,061 | 3 | -0,064 | -0,067 |
| 4 | 0,088 | 0,086 | 4 | -0,09 | -0,093 |
| 5 | 0,116 | 0,114 | 4,5 | -0,104 | -0,107 |

## 650°C

| I | V | V | I | V | V |
|---|---|---|---|---|---|
| mA | Volt_pos | Volt | mA | Volt_neg | Volt |
| 10 pos | | Correct | 10 neg | | Correct |
| 0,5 | 0,009 | 0,011 | 0,5 | -0,007 | -0,01 |
| 1 | 0,018 | 0,02 | 1 | -0,015 | -0,018 |
| 1,5 | 0,027 | 0,029 | 1,5 | -0,024 | -0,027 |
| 2 | 0,035 | 0,037 | 2 | -0,032 | -0,035 |
| 3 | 0,053 | 0,055 | 3 | -0,05 | -0,053 |
| 4 | 0,077 | 0,079 | 4 | -0,069 | -0,072 |
| 5 | 0,098 | 0,1 | 5 | -0,091 | -0,094 |
| 6 | 0,118 | 0,12 | 6 | -0,113 | -0,116 |
| | | | 6,5 | -0,126 | -0,129 |

## 700°C

| I | V | V | I | V | V |
|---|---|---|---|---|---|
| mA | Volt_pos | Volt | mA | Volt_neg | Volt |
| 10 pos | | Correct | 10 neg | | Correct |
| 0,5 | 0,008 | 0,009 | 1 | -0,015 | -0,015 |
| 1 | 0,016 | 0,017 | 2 | -0,031 | -0,031 |
| 2 | 0,031 | 0,032 | 3 | -0,046 | -0,046 |
| 4 | 0,061 | 0,062 | 4 | -0,063 | -0,063 |

135

| | | | | | |
|---|---|---|---|---|---|
| 6 | 0,091 | 0,092 | 5 | -0,078 | -0,078 |
| 8 | 0,123 | 0,124 | 6 | -0,096 | -0,096 |
| 10 | 0,15 | 0,151 | 7 | -0,114 | -0,114 |
| 11 | 0,161 | 0,162 | 8 | -0,132 | -0,132 |
| | | | 9 | -0,15 | -0,15 |

- Co-Co:
- $H_2/CO_2 = 7/1$

400°C

| I | V | V | I | V | V |
|---|---|---|---|---|---|
| mA | Volt_pos | Volt | mA | Volt_neg | Volt |
| 10 pos | | Correct | 10 neg | | Correct |
| 0,02 | -0,051 | 0,019 | 0,02 | -0,036 | -0,022 |
| 0,03 | 0,009 | 0,079 | 0,03 | -0,043 | -0,029 |
| 0,05 | 0,028 | 0,098 | 0,05 | -0,071 | -0,057 |
| 0,07 | 0,049 | 0,119 | 0,07 | -0,096 | -0,082 |
| 0,1 | 0,095 | 0,165 | 0,1 | -0,135 | -0,121 |
| 0,12 | 0,119 | 0,189 | 0,12 | -0,15 | -0,136 |
| 0,14 | 0,14 | 0,21 | 0,14 | 0,183 | 0,197 |
| 0,16 | 0,17 | 0,24 | 0,16 | 0,206 | 0,22 |
| 0,18 | 0,19 | 0,26 | 0,18 | 0,232 | 0,246 |
| 0,2 | 0,22 | 0,29 | 0,2 | 0,253 | 0,267 |
| 0,25 | 0,297 | 0,367 | 0,25 | 0,315 | 0,329 |
| 0,35 | 0,413 | 0,483 | | | |

500°C

| I | V | V | I | V | V |
|---|---|---|---|---|---|
| mA | Volt_pos | Volt | mA | Volt_neg | Volt |
| 10 pos | | Correct | 10 neg | | Correct |
| 0,03 | 0 | 0,009 | 0,02 | -0,017 | -0,008 |
| 0,05 | 0,01 | 0,019 | 0,05 | -0,033 | -0,024 |
| 0,1 | 0,035 | 0,044 | 0,1 | -0,06 | -0,051 |
| 0,15 | 0,063 | 0,072 | 0,15 | -0,082 | -0,073 |
| 0,2 | 0,092 | 0,101 | 0,2 | -0,108 | -0,099 |
| 0,25 | 0,122 | 0,131 | 0,25 | -0,131 | -0,122 |
| 0,3 | 0,15 | 0,159 | 0,3 | -0,151 | -0,142 |
| 0,35 | 0,181 | 0,19 | 0,4 | -0,19 | -0,181 |
| 0,4 | 0,208 | 0,217 | 0,5 | -0,235 | -0,226 |
| 0,5 | 0,265 | 0,274 | 0,6 | -0,278 | -0,269 |
| 0,7 | 0,365 | 0,374 | | | |

## 550°C

| I | V | V | I | V | V |
|---|---|---|---|---|---|
| mA | Volt_pos | Volt | mA | Volt_neg | Volt |
| 10 pos | | Correct | 10 neg | | Correct |
| 0,05 | 0,005 | 0,011 | 0,05 | -0,017 | -0,014 |
| 0,1 | 0,021 | 0,027 | 0,1 | -0,031 | -0,028 |
| 0,15 | 0,036 | 0,042 | 0,15 | -0,047 | -0,044 |
| 0,2 | 0,054 | 0,06 | 0,2 | -0,063 | -0,06 |
| 0,25 | 0,069 | 0,075 | 0,25 | -0,076 | -0,073 |
| 0,3 | 0,087 | 0,093 | 0,3 | -0,088 | -0,085 |
| 0,4 | 0,127 | 0,133 | 0,4 | -0,116 | -0,113 |
| 0,5 | 0,162 | 0,168 | 0,5 | -0,144 | -0,141 |
| 0,6 | 0,198 | 0,204 | 0,6 | -0,172 | -0,169 |
| 0,7 | 0,232 | 0,238 | 0,7 | -0,197 | -0,194 |
| 0,8 | 0,273 | 0,279 | 0,8 | -0,231 | -0,228 |
| 1 | 0,332 | 0,338 | | | |

## 600°C

| I | V | V | I | V | V |
|---|---|---|---|---|---|
| mA | Volt_pos | Volt | mA | Volt_neg | Volt |
| 10 pos | | Correct | 10 neg | | Correct |
| 0,05 | 0,003 | 0,008 | 0,05 | -0,012 | -0,015 |
| 0,1 | 0,012 | 0,017 | 0,1 | -0,021 | -0,024 |
| 0,15 | 0,022 | 0,027 | 0,15 | -0,028 | -0,031 |
| 0,2 | 0,031 | 0,036 | 0,2 | -0,037 | -0,04 |
| 0,3 | 0,05 | 0,055 | 0,3 | -0,052 | -0,055 |
| 0,4 | 0,071 | 0,076 | 0,4 | -0,066 | -0,069 |
| 0,6 | 0,113 | 0,118 | 0,6 | -0,093 | -0,096 |
| 0,8 | 0,163 | 0,168 | 0,8 | -0,12 | -0,123 |
| 1 | 0,214 | 0,219 | 1 | -0,15 | -0,153 |
| 1,2 | 0,272 | 0,277 | 1,2 | -0,182 | -0,185 |
| 1,5 | 0,355 | 0,36 | 1,5 | -0,228 | -0,231 |

## 650°C

| I | V | V | I | V | V |
|---|---|---|---|---|---|
| mA | Volt_pos | Volt | mA | Volt_neg | Volt |
| 10 pos | | Correct | 10 neg | | Correct |
| 0,1 | 0,005 | 0,01 | 0,1 | -0,013 | -0,01 |
| 0,2 | 0,016 | 0,021 | 0,2 | -0,023 | -0,02 |
| 0,4 | 0,037 | 0,042 | 0,4 | -0,042 | -0,039 |
| 0,6 | 0,059 | 0,064 | 0,6 | -0,06 | -0,057 |
| 0,8 | 0,081 | 0,086 | 0,8 | -0,077 | -0,074 |
| 1 | 0,107 | 0,112 | 1 | -0,098 | -0,095 |
| 1,5 | 0,172 | 0,177 | 1,5 | -0,162 | -0,159 |

| | | | | | |
|---|---|---|---|---|---|
| 2 | 0,244 | 0,249 | 2 | -0,231 | -0,228 |
| 2,5 | 0,338 | 0,343 | 2,5 | -0,283 | -0,28 |

## 700°C

| I | V | V | I | V | V |
|---|---|---|---|---|---|
| mA | Volt_pos | Volt | mA | Volt_neg | Volt |
| 10 pos | | Correct | 10 neg | | Correct |
| 0,2 | 0,005 | 0,01 | 0,2 | -0,009 | -0,012 |
| 0,4 | 0,014 | 0,019 | 0,4 | -0,016 | -0,019 |
| 0,6 | 0,022 | 0,027 | 0,6 | -0,023 | -0,026 |
| 1 | 0,038 | 0,043 | 1 | -0,037 | -0,04 |
| 1,5 | 0,061 | 0,066 | 1,5 | -0,054 | -0,057 |
| 2 | 0,085 | 0,09 | 2 | -0,073 | -0,076 |
| 2,5 | 0,112 | 0,117 | 2,5 | -0,097 | -0,1 |
| 3 | 0,14 | 0,145 | 3 | -0,12 | -0,123 |
| 4 | 0,211 | 0,216 | 4 | -0,162 | -0,165 |
| 5 | 0,31 | 0,315 | 5 | -0,212 | -0,215 |
| 6 | 0,394 | 0,399 | | | |

- Fe-Fe:
- pH$_2$=20kPa

## 500°C

| I | V | V | I | V | V |
|---|---|---|---|---|---|
| mA | Volt_pos | Volt | mA | Volt_neg | Volt |
| 1 pos | | Correct | 1 neg | | Correct |
| 0,1 | | 0,02 | 0,1 | | -0,021 |
| 0,2 | | 0,043 | 0,2 | | -0,043 |
| 0,3 | | 0,066 | 0,3 | | -0,066 |
| 0,4 | | 0,091 | 0,4 | | -0,088 |
| 0,6 | | 0,138 | 0,6 | | -0,133 |
| 0,8 | | 0,19 | 0,8 | | -0,177 |
| 1 | | 0,244 | 1 | | -0,223 |
| 1,2 | | 0,31 | 1,2 | | -0,269 |
| 1,5 | | 0,411 | 1,5 | | -0,343 |

## 550°C

| I | V | V | I | V | V |
|---|---|---|---|---|---|
| mA | Volt_pos | Volt | mA | Volt_neg | Volt |
| 10 pos | | Correct | 10 neg | | Correct |
| 0,1 | | 0,012 | 0,1 | | -0,012 |

| I mA 10 pos | V Volt_pos | V Volt Correct | I mA 10 neg | V Volt_neg | V Volt Correct |
|---|---|---|---|---|---|
| 0,2 | | 0,024 | 0,2 | | -0,025 |
| 0,3 | | 0,035 | 0,3 | | -0,038 |
| 0,4 | | 0,046 | 0,4 | | -0,051 |
| 0,6 | | 0,069 | 0,6 | | -0,076 |
| 0,8 | | 0,093 | 0,8 | | -0,102 |
| 1 | | 0,117 | 1 | | -0,127 |
| 1,2 | | 0,14 | 1,2 | | -0,153 |
| 1,5 | | 0,175 | 1,5 | | -0,19 |
| 2 | | 0,235 | 2 | | -0,253 |
| 2,5 | | 0,304 | 2,5 | | -0,32 |
| 3 | | 0,381 | 3 | | -0,381 |

## 600°C

| I mA 10 pos | V Volt_pos | V Volt Correct | I mA 10 neg | V Volt_neg | V Volt Correct |
|---|---|---|---|---|---|
| 0,1 | | 0,009 | 0,1 | | -0,007 |
| 0,2 | | 0,017 | 0,2 | | -0,015 |
| 0,3 | | 0,025 | 0,3 | | -0,022 |
| 0,4 | | 0,033 | 0,4 | | -0,03 |
| 0,6 | | 0,049 | 0,6 | | -0,046 |
| 0,8 | | 0,064 | 0,8 | | -0,06 |
| 1 | | 0,08 | 1 | | -0,075 |
| 1,2 | | 0,097 | 1,2 | | -0,088 |
| 1,4 | | 0,113 | 1,5 | | -0,113 |
| 1,5 | | 0,122 | 2 | | -0,15 |
| 2 | | 0,163 | 2,5 | | -0,189 |
| 2,5 | | 0,207 | 3 | | -0,229 |
| 3 | | 0,255 | 3,5 | | -0,268 |
| 3,5 | | 0,306 | 4 | | -0,308 |
| 4 | | 0,36 | | | |

## 650°C

| I mA 10 pos | V Volt_pos | V Volt Correct | I mA 10 neg | V Volt_neg | V Volt Correct |
|---|---|---|---|---|---|
| 0,1 | | 0,007 | 0,1 | | -0,006 |
| 0,2 | | 0,012 | 0,2 | | -0,012 |
| 0,3 | | 0,018 | 0,3 | | -0,017 |
| 0,4 | | 0,023 | 0,4 | | -0,022 |
| 0,5 | | 0,029 | 0,6 | | -0,033 |
| 0,8 | | 0,046 | 0,8 | | -0,043 |
| 1 | | 0,057 | 1 | | -0,054 |
| 1,2 | | 0,067 | 1,2 | | -0,065 |

| | | | | | |
|---|---|---|---|---|---|
| 1,5 | 0,085 | 1,4 | -0,075 |
| 2 | 0,112 | 1,5 | -0,081 |
| 2,2 | 0,125 | 2 | -0,106 |
| 2,5 | 0,142 | 2,2 | -0,117 |
| 3 | 0,174 | 2,5 | -0,132 |
| 3,5 | 0,206 | 3 | -0,16 |
| 4 | 0,252 | 3,5 | -0,185 |
| 5 | 0,337 | 4 | -0,215 |
| | | 4,5 | -0,244 |
| | | 5 | -0,273 |

## 700°C

| I | V | V | I | V | V |
|---|---|---|---|---|---|
| mA | Volt_pos | Volt | mA | Volt_neg | Volt |
| 10 pos | | Correct | 10 neg | | Correct |
| 0,1 | | 0,005 | 0,1 | | -0,006 |
| 0,2 | | 0,01 | 0,2 | | -0,01 |
| 0,3 | | 0,014 | 0,3 | | -0,014 |
| 0,4 | | 0,019 | 0,4 | | -0,018 |
| 0,6 | | 0,027 | 0,6 | | -0,024 |
| 0,8 | | 0,036 | 0,8 | | -0,031 |
| 1 | | 0,045 | 1 | | -0,037 |
| 1,2 | | 0,054 | 1,2 | | -0,044 |
| 1,4 | | 0,064 | 1,4 | | -0,05 |
| 1,6 | | 0,073 | 1,6 | | -0,056 |
| 2 | | 0,094 | 2 | | -0,069 |
| 2,4 | | 0,118 | 2,4 | | -0,082 |
| 2,8 | | 0,148 | 2,8 | | -0,094 |
| 3,2 | | 0,181 | 3,2 | | -0,107 |
| 3,6 | | 0,218 | 3,6 | | -0,122 |
| 4 | | 0,263 | 4 | | -0,132 |
| 4,5 | | 0,335 | 4,5 | | -0,148 |
| 5 | | 0,407 | 5 | | -0,164 |
| 5,5 | | 0,458 | 6 | | -0,195 |

- Fe-Fe:
- $pH_2 = 50kPa$

## 500°C

| I | V | V | I | V | V |
|---|---|---|---|---|---|
| mA | Volt_pos | Volt | mA | Volt_neg | Volt |
| 10 pos | | Correct | 10 neg | | Correct |

| | | | |
|---:|---:|---:|---:|
| 0,1 | 0,017 | 0,1 | -0,017 |
| 0,2 | 0,036 | 0,2 | -0,036 |
| 0,3 | 0,055 | 0,3 | -0,054 |
| 0,4 | 0,074 | 0,4 | -0,073 |
| 0,5 | 0,093 | 0,5 | -0,092 |
| 0,6 | 0,113 | 0,6 | -0,109 |
| 0,7 | 0,133 | 0,7 | -0,129 |
| 0,8 | 0,152 | 0,8 | -0,147 |
| 0,9 | 0,171 | 0,9 | -0,166 |
| 1 | 0,191 | 1 | -0,185 |
| 1,2 | 0,232 | 1,2 | -0,221 |
| 1,5 | 0,291 | 1,5 | -0,276 |
| 2 | 0,392 | 2 | -0,369 |
| 2,5 | 0,446 | 2,5 | -0,405 |

## 550°C

| I | V | V | I | V | V |
|---|---|---|---|---|---|
| mA | Volt_pos | Volt | mA | Volt_neg | Volt |
| 10 pos | | Correct | 10 neg | | Correct |
| 0,1 | | 0,01 | 0,1 | | -0,01 |
| 0,2 | | 0,02 | 0,2 | | -0,02 |
| 0,3 | | 0,03 | 0,3 | | -0,03 |
| 0,4 | | 0,04 | 0,4 | | -0,04 |
| 0,5 | | 0,05 | 0,5 | | -0,05 |
| 0,6 | | 0,06 | 0,6 | | -0,061 |
| 0,7 | | 0,07 | 0,7 | | -0,071 |
| 0,8 | | 0,08 | 0,8 | | -0,081 |
| 1 | | 0,099 | 1 | | -0,102 |
| 1,2 | | 0,12 | 1,2 | | -0,12 |
| 1,5 | | 0,152 | 1,5 | | -0,151 |
| 2 | | 0,202 | 2 | | -0,2 |
| 2,2 | | 0,226 | 2,5 | | -0,248 |
| 2,5 | | 0,257 | 3 | | -0,299 |
| 3 | | 0,312 | 3,5 | | -0,346 |
| 3,5 | | 0,372 | | | |

## 600°C

| I | V | V | I | V | V |
|---|---|---|---|---|---|
| mA | Volt_pos | Volt | mA | Volt_neg | Volt |
| 10 pos | | Correct | 10 neg | | Correct |
| 0,1 | | 0,006 | 0,1 | | -0,007 |
| 0,2 | | 0,012 | 0,2 | | -0,013 |
| 0,3 | | 0,018 | 0,3 | | -0,019 |
| 0,4 | | 0,024 | 0,4 | | -0,025 |

| | | | | | |
|---|---|---|---|---|---|
| 0,6 | | 0,035 | 0,6 | | -0,037 |
| 0,8 | | 0,047 | 0,8 | | -0,048 |
| 1 | | 0,06 | 1 | | -0,06 |
| 1,2 | | 0,072 | 1,2 | | -0,071 |
| 1,5 | | 0,088 | 1,5 | | -0,089 |
| 2 | | 0,118 | 2 | | -0,118 |
| 2,5 | | 0,148 | 2,5 | | -0,146 |
| 3 | | 0,182 | 3 | | -0,175 |
| 3,5 | | 0,214 | 3,5 | | -0,203 |
| 4 | | 0,245 | 4 | | -0,232 |
| 4,5 | | 0,279 | 4,5 | | -0,261 |
| 5 | | 0,313 | | | |

## 650°C

| I | V | V | I | V | V |
|---|---|---|---|---|---|
| mA | Volt_pos | Volt | mA | Volt_neg | Volt |
| 10 pos | | Correct | 10 neg | | Correct |
| 0,1 | | 0,004 | 0,1 | | -0,005 |
| 0,2 | | 0,009 | 0,2 | | -0,009 |
| 0,3 | | 0,013 | 0,3 | | -0,013 |
| 0,5 | | 0,023 | 0,5 | | -0,022 |
| 0,7 | | 0,031 | 0,7 | | -0,03 |
| 0,8 | | 0,036 | 0,8 | | -0,035 |
| 1 | | 0,045 | 1 | | -0,044 |
| 1,2 | | 0,053 | 1,2 | | -0,052 |
| 1,5 | | 0,066 | 1,5 | | -0,063 |
| 2 | | 0,088 | 2 | | -0,084 |
| 2,5 | | 0,11 | 2,5 | | -0,105 |
| 3 | | 0,135 | 3 | | -0,127 |
| 3,5 | | 0,159 | 3,5 | | -0,148 |
| 4 | | 0,183 | 4 | | -0,171 |
| 4,5 | | 0,21 | 4,5 | | -0,194 |
| 5 | | 0,242 | 5 | | -0,216 |
| 5,5 | | 0,271 | 5,5 | | -0,241 |

## 700°C

| I | V | V | I | V | V |
|---|---|---|---|---|---|
| mA | Volt_pos | Volt | mA | Volt_neg | Volt |
| 10 pos | | Correct | 10 neg | | Correct |
| 0,1 | | 0,002 | 0,1 | | -0,005 |
| 0,2 | | 0,005 | 0,2 | | -0,008 |
| 0,4 | | 0,01 | 0,4 | | -0,013 |
| 0,6 | | 0,016 | 0,6 | | -0,019 |
| 0,8 | | 0,021 | 0,8 | | -0,025 |

| | | | | |
|---|---|---|---|---|
| 1 | 0,027 | 1 | | -0,031 |
| 1,5 | 0,041 | 1,5 | | -0,044 |
| 2 | 0,054 | 2 | | -0,058 |
| 2,5 | 0,069 | 2,5 | | -0,073 |
| 3 | 0,083 | 3 | | -0,087 |
| 4 | 0,113 | 4 | | -0,115 |
| 5 | 0,143 | 5 | | -0,144 |
| 6 | 0,176 | 6 | | -0,173 |
| 7 | 0,204 | 7 | | -0,203 |

- Fe-Fe:
- pH$_2$=100kPa

### 400°C

| I | V | V | I | V | V |
|---|---|---|---|---|---|
| mA | Volt_pos | Volt | mA | Volt_neg | Volt |
| 10 pos | | Correct | 10 neg | | Correct |
| 0,05 | | 0,025 | 0,05 | | -0,028 |
| 0,1 | | 0,054 | 0,1 | | -0,059 |
| 0,15 | | 0,088 | 0,15 | | -0,092 |
| 0,2 | | 0,123 | 0,2 | | -0,129 |
| 0,25 | | 0,16 | 0,25 | | -0,162 |
| 0,3 | | 0,193 | 0,3 | | -0,195 |
| 0,35 | | 0,233 | 0,35 | | -0,228 |
| 0,4 | | 0,274 | 0,4 | | -0,267 |
| 0,5 | | 0,355 | 0,5 | | -0,352 |
| 0,6 | | 0,463 | 0,6 | | -0,431 |
| 0,7 | | 0,578 | 0,7 | | -0,511 |

### 450°C

| I | V | V | I | V | V |
|---|---|---|---|---|---|
| mA | Volt_pos | Volt | mA | Volt_neg | Volt |
| 10 pos | | Correct | 10 neg | | Correct |
| 0,1 | | 0,028 | 0,1 | | -0,029 |
| 0,2 | | 0,061 | 0,2 | | -0,062 |
| 0,3 | | 0,093 | 0,3 | | -0,095 |
| 0,4 | | 0,127 | 0,4 | | -0,128 |
| 0,5 | | 0,161 | 0,5 | | -0,161 |
| 0,6 | | 0,197 | 0,55 | | -0,178 |
| 0,7 | | 0,232 | 0,6 | | -0,193 |
| 0,8 | | 0,27 | 0,7 | | -0,229 |
| 0,9 | | 0,31 | 0,8 | | -0,262 |

| I | V | V | I | V | V |
|---|---|---|---|---|---|
| | | | 1 | 0,352 | 0,9 | -0,295 |

| I | V | V | I | V | V |
|---|---|---|---|---|---|
| 1 | | 0,352 | 0,9 | | -0,295 |
| 1,2 | | 0,435 | 1 | | -0,333 |
| | | | 1,2 | | -0,409 |

## 500°C

| I | V | V | I | V | V |
|---|---|---|---|---|---|
| mA | Volt_pos | Volt | mA | Volt_neg | Volt |
| 10 pos | | Correct | 10 neg | | Correct |
| 0,1 | | 0,017 | 0,1 | | -0,016 |
| 0,2 | | 0,034 | 0,2 | | -0,032 |
| 0,3 | | 0,051 | 0,3 | | -0,049 |
| 0,4 | | 0,067 | 0,4 | | -0,065 |
| 0,5 | | 0,084 | 0,5 | | -0,083 |
| 0,6 | | 0,1 | 0,6 | | -0,099 |
| 0,7 | | 0,118 | 0,7 | | -0,115 |
| 0,8 | | 0,134 | 0,8 | | -0,131 |
| 1 | | 0,168 | 1 | | -0,163 |
| 1,2 | | 0,202 | 1,2 | | -0,197 |
| 1,5 | | 0,254 | 1,5 | | -0,246 |
| 2 | | 0,344 | 2 | | -0,331 |

## 550°C

| I | V | V | I | V | V |
|---|---|---|---|---|---|
| mA | Volt_pos | Volt | mA | Volt_neg | Volt |
| 10 pos | | Correct | 10 neg | | Correct |
| 0,1 | | 0,011 | 0,1 | | -0,01 |
| 0,2 | | 0,02 | 0,2 | | -0,018 |
| 0,3 | | 0,03 | 0,3 | | -0,028 |
| 0,4 | | 0,039 | 0,4 | | -0,036 |
| 0,5 | | 0,049 | 0,5 | | -0,046 |
| 0,6 | | 0,058 | 0,6 | | -0,055 |
| 0,7 | | 0,068 | 0,7 | | -0,064 |
| 0,8 | | 0,077 | 0,8 | | -0,073 |
| 1 | | 0,096 | 1 | | -0,091 |
| 1,2 | | 0,114 | 1,2 | | -0,109 |
| 1,5 | | 0,142 | 1,5 | | -0,135 |
| 2 | | 0,188 | 2 | | -0,179 |
| 2,5 | | 0,236 | 2,5 | | -0,224 |
| 3 | | 0,283 | 3 | | -0,27 |

## 600°C

| I | V | V | I | V | V |
|---|---|---|---|---|---|
| mA | Volt_pos | Volt | mA | Volt_neg | Volt |

144

| 10 pos | Correct | 10 neg | Correct |
|---|---|---|---|
| 0,1 | 0,006 | 0,1 | -0,007 |
| 0,2 | 0,012 | 0,2 | -0,013 |
| 0,4 | 0,024 | 0,4 | -0,024 |
| 0,5 | 0,031 | 0,5 | -0,029 |
| 0,8 | 0,049 | 0,8 | -0,046 |
| 1 | 0,061 | 1 | -0,056 |
| 1,5 | 0,092 | 1,5 | -0,084 |
| 2 | 0,122 | 2 | -0,111 |
| 2,5 | 0,151 | 2,5 | -0,138 |
| 3 | 0,18 | 3 | -0,163 |
| 3,5 | 0,209 | 3,5 | -0,192 |
| 4 | 0,237 | 4 | -0,219 |

650°C

| I | V | V | I | V | V |
|---|---|---|---|---|---|
| mA | Volt_pos | Volt | mA | Volt_neg | Volt |
| 10 pos | | Correct | 10 neg | | Correct |
| 0,1 | | 0,004 | 0,1 | | -0,005 |
| 0,4 | | 0,015 | 0,4 | | -0,017 |
| 0,8 | | 0,03 | 0,8 | | -0,031 |
| 1 | | 0,037 | 1 | | -0,039 |
| 1,5 | | 0,056 | 1,5 | | -0,057 |
| 2 | | 0,074 | 2 | | -0,075 |
| 2,5 | | 0,093 | 2,5 | | -0,094 |
| 3 | | 0,112 | 3 | | -0,113 |
| 3,5 | | 0,13 | 3,5 | | -0,13 |
| 4 | | 0,149 | 4 | | -0,15 |
| 4,5 | | 0,168 | 4,5 | | -0,167 |
| 5 | | 0,187 | 5 | | -0,186 |
| 5,5 | | 0,208 | 5,5 | | -0,207 |

700°C

| I | V | V | I | V | V |
|---|---|---|---|---|---|
| mA | Volt_pos | Volt | mA | Volt_neg | Volt |
| 10 pos | | Correct | 10 neg | | Correct |
| 0,1 | | 0,003 | 0,1 | | -0,004 |
| 0,2 | | 0,006 | 0,2 | | -0,007 |
| 0,4 | | 0,011 | 0,4 | | -0,011 |
| 0,6 | | 0,016 | 0,6 | | -0,017 |
| 0,8 | | 0,022 | 0,8 | | -0,021 |
| 1 | | 0,027 | 1 | | -0,027 |
| 1,5 | | 0,04 | 1,5 | | -0,039 |
| 2 | | 0,053 | 2 | | -0,051 |

| | | | |
|---|---|---|---|
| 2,5 | 0,066 | 2,5 | -0,064 |
| 3 | 0,078 | 3 | -0,077 |
| 3,5 | 0,094 | 3,5 | -0,089 |
| 4 | 0,108 | 4 | -0,101 |
| 4,5 | 0,122 | 4,5 | -0,114 |
| 5 | 0,136 | 5 | -0,127 |
| 5,5 | 0,15 | 5,5 | -0,141 |
| 6 | 0,164 | 6 | -0,154 |
| 6,5 | 0,178 | 6,5 | -0,168 |
| 7 | 0,192 | 7 | -0,181 |

- Fe-Fe:
- $H_2/CO_2 = 5/1$

450°C

| I | V | V | I | V | V |
|---|---|---|---|---|---|
| mA | Volt_pos | Volt | mA | Volt_neg | Volt |
| 10 pos | | Correct | 10 neg | | Correct |
| 0,01 | 0,043 | 0,058 | 0,01 | -0,067 | -0,087 |
| 0,015 | 0,076 | 0,091 | 0,015 | -0,116 | -0,136 |
| 0,02 | 0,115 | 0,13 | 0,02 | -0,162 | -0,182 |
| 0,03 | 0,184 | 0,199 | 0,03 | -0,244 | -0,264 |
| 0,04 | 0,286 | 0,301 | 0,04 | -0,33 | -0,35 |
| 0,05 | 0,378 | 0,393 | 0,05 | -0,419 | -0,439 |
| 0,06 | 0,466 | 0,481 | 0,06 | -0,501 | -0,521 |
| 0,08 | 0,641 | 0,656 | 0,08 | -0,656 | -0,676 |
| 0,1 | 0,802 | 0,817 | 0,1 | -0,804 | -0,824 |
| 0,12 | 0,963 | 0,978 | 0,12 | -0,941 | -0,961 |
| 0,14 | 1,118 | 1,133 | 0,14 | -1,072 | -1,092 |
| 0,16 | 1,273 | 1,288 | 0,16 | -1,188 | -1,208 |
| 0,2 | 1,567 | 1,582 | 0,2 | -1,411 | -1,431 |
| 0,25 | 1,915 | 1,93 | 0,25 | -1,676 | -1,696 |
| | | | 0,3 | -1,903 | -1,923 |

500°C

| I | V | V | I | V | V |
|---|---|---|---|---|---|
| mA | Volt_pos | Volt | mA | Volt_neg | Volt |
| 10 pos | | Correct | 10 neg | | Correct |
| 0,01 | 0,008 | 0,021 | 0,01 | 0,003 | -0,018 |
| 0,015 | 0,02 | 0,033 | 0,015 | -0,013 | -0,034 |
| 0,02 | 0,031 | 0,044 | 0,02 | -0,03 | -0,051 |
| 0,03 | 0,056 | 0,069 | 0,03 | -0,057 | -0,078 |

| 0,04 | 0,081 | 0,094 | 0,04 | -0,084 | -0,105 |
|---|---|---|---|---|---|
| 0,05 | 0,113 | 0,126 | 0,05 | -0,115 | -0,136 |
| 0,06 | 0,138 | 0,151 | 0,06 | -0,145 | -0,166 |
| 0,08 | 0,187 | 0,2 | 0,08 | -0,201 | -0,222 |
| 0,1 | 0,238 | 0,251 | 0,1 | -0,258 | -0,279 |
| 0,2 | 0,48 | 0,493 | 0,2 | -0,497 | -0,518 |
| 0,25 | 0,62 | 0,633 | 0,25 | -0,627 | -0,648 |
| 0,3 | 0,724 | 0,737 | 0,3 | -0,747 | -0,768 |
| 0,4 | 0,91 | 0,923 | 0,4 | -0,93 | -0,951 |
| 0,6 | 1,242 | 1,255 | 0,6 | -1,236 | -1,257 |
| 0,8 | 1,511 | 1,524 | 0,8 | -1,512 | -1,533 |
| 1 | 1,754 | 1,767 | 1 | -1,775 | -1,796 |

## 550°C

| I | V | V | I | V | V |
|---|---|---|---|---|---|
| mA | Volt_pos | Volt | mA | Volt_neg | Volt |
| 10 pos | | Correct | 10 neg | | Correct |
| 0,04 | 0,026 | 0,037 | 0,04 | -0,004 | -0,013 |
| 0,06 | 0,045 | 0,056 | 0,06 | -0,013 | -0,022 |
| 0,08 | 0,066 | 0,077 | 0,08 | -0,025 | -0,034 |
| 0,1 | 0,087 | 0,098 | 0,1 | -0,034 | -0,043 |
| 0,2 | 0,176 | 0,187 | 0,2 | -0,074 | -0,083 |
| 0,3 | 0,275 | 0,286 | 0,3 | -0,124 | -0,133 |
| 0,4 | 0,381 | 0,392 | 0,4 | -0,181 | -0,19 |
| 0,6 | 0,546 | 0,557 | 0,6 | -0,249 | -0,258 |
| 0,8 | 0,707 | 0,718 | 0,8 | -0,304 | -0,313 |
| 1 | 0,848 | 0,859 | 1 | -0,354 | -0,363 |
| 1,5 | 1,144 | 1,155 | 1,5 | -0,457 | -0,466 |
| 2 | 1,352 | 1,363 | | | |
| 3 | 1,744 | 1,755 | | | |

## 600°C

| I | V | V | I | V | V |
|---|---|---|---|---|---|
| mA | Volt_pos | Volt | mA | Volt_neg | Volt |
| 10 pos | | Correct | 10 neg | | Correct |
| 0,01 | -0,005 | 1,00E-03 | 0,01 | 0,005 | -0,003 |
| 0,02 | -0,004 | 0,002 | 0,02 | -0,002 | -0,01 |
| 0,03 | -0,003 | 0,003 | 0,03 | -0,006 | -0,014 |
| 0,05 | 1,00E-03 | 0,007 | 0,05 | -0,013 | -0,021 |
| 0,075 | 0,004 | 0,01 | 0,075 | -0,02 | -0,028 |
| 0,1 | 0,007 | 0,013 | 0,1 | -0,026 | -0,034 |
| 0,2 | 0,019 | 0,025 | 0,2 | -0,048 | -0,056 |
| 0,4 | 0,044 | 0,05 | 0,4 | -0,103 | -0,111 |

| 0,6 | 0,69 | 0,696 | 0,6 | -0,148 | -0,156 |
| 1 | 0,126 | 0,132 | 1 | -0,264 | -0,272 |
| 1,5 | 0,179 | 0,185 | 1,5 | -0,498 | -0,506 |
| 2 | 0,249 | 0,255 | 2 | -0,681 | -0,689 |
| 5 | 0,536 | 0,542 | | | |

650°C

| I | V | V | I | V | V |
| mA | Volt_pos | Volt | mA | Volt_neg | Volt |
| 10 pos | | Correct | 10 neg | | Correct |
| 0,02 | -0,004 | 0,002 | 0,02 | -0,021 | -0,008 |
| 0,04 | 0 | 0,006 | 0,04 | -0,03 | -0,017 |
| 0,06 | 0,005 | 0,011 | 0,06 | -0,042 | -0,029 |
| 0,1 | 0,014 | 0,02 | 0,1 | -0,062 | -0,049 |
| 0,15 | 0,028 | 0,034 | 0,15 | -0,088 | -0,075 |
| 0,2 | 0,046 | 0,052 | 0,2 | -0,119 | -0,106 |
| 0,3 | 0,08 | 0,086 | 0,3 | -0,168 | -0,155 |
| 0,5 | 0,158 | 0,164 | 0,5 | -0,268 | -0,255 |
| 0,7 | 0,198 | 0,204 | 0,7 | -0,568 | -0,555 |
| 0,8 | 0,319 | 0,325 | 0,8 | -0,688 | -0,675 |
| 0,9 | 0,376 | 0,382 | 0,9 | -0,789 | -0,776 |
| 1 | 0,43 | 0,436 | | | |
| 1,2 | 0,52 | 0,526 | | | |
| 1,4 | 0,602 | 0,608 | | | |
| 2 | 0,818 | 0,824 | | | |
| 2,5 | 0,919 | 0,925 | | | |

700°C

| I | V | V | I | V | V |
| mA | Volt_pos | Volt | mA | Volt_neg | Volt |
| 10 pos | | Correct | 10 neg | | Correct |
| 0,1 | 0,006 | 0,024 | 0,1 | -0,018 | -0,028 |
| 0,2 | 0,045 | 0,063 | 0,2 | -0,054 | -0,064 |
| 0,3 | 0,095 | 0,113 | 0,3 | -0,096 | -0,106 |
| 0,4 | 0,139 | 0,157 | 0,4 | -0,145 | -0,155 |
| 0,5 | 0,186 | 0,204 | 0,5 | -0,194 | -0,204 |
| 0,6 | 0,238 | 0,256 | 0,6 | -0,238 | -0,248 |
| 0,8 | 0,336 | 0,354 | 0,8 | -0,321 | -0,331 |
| 1 | 0,429 | 0,447 | 1 | -0,438 | -0,448 |
| 1,4 | 0,587 | 0,605 | 1,4 | -0,594 | -0,604 |
| 1,8 | 0,712 | 0,73 | 1,8 | -0,763 | -0,773 |
| 2,2 | 0,794 | 0,812 | | | |
| 2,6 | 0,845 | 0,863 | | | |
| 3 | 0,897 | 0,915 | | | |

| 4 | 1,029 | 1,047 |

# 8  References

[1]     W. Wang, S. Wang, X. Ma, J. Gong, Chemical Society Reviews 40 (2011) 3703-3727.

[2]     J.-R. Petit, J. Jouzel, D. Raynaud, N.I. Barkov, J.-M. Barnola, I. Basile, M. Bender, J. Chappellaz, M. Davis, G. Delaygue, Nature 399 (1999) 429-436.

[3]     BP, (2012).

[4]     S. Riduan, Y. Zhang, Dalton transactions (Cambridge, England: 2003) 39 (2010) 3347.

[5]     J. Tollefson, Nature 462 (2009) 966-967.

[6]     H. Yang, Z. Xu, M. Fan, R. Gupta, R.B. Slimane, A.E. Bland, I. Wright, Journal of Environmental Sciences 20 (2008) 14-27.

[7]     M. Mikkelsen, M. Jørgensen, F.C. Krebs, Energy & Environmental Science 3 (2010) 43-81.

[8]     A.J. Hunt, E.H. Sin, R. Marriott, J.H. Clark, ChemSusChem 3 (2010) 306-322.

[9]     G. Férey, C. Serre, T. Devic, G. Maurin, H. Jobic, P.L. Llewellyn, G. De Weireld, A. Vimont, M. Daturi, J.-S. Chang, Chemical Society Reviews 40 (2011) 550-562.

[10]    C. Song, Catalysis Today 115 (2006) 2-32.

[11]    G. Centi, S. Perathoner, Studies in surface science and catalysis 153 (2004) 1-8.

[12]    J. Ma, N. Sun, X. Zhang, N. Zhao, F. Xiao, W. Wei, Y. Sun, Catalysis Today 148 (2009) 221-231.

[13]    A. Baiker, Applied organometallic chemistry 14 (2000) 751-762.

[14]    W.C. Chueh, C. Falter, M. Abbott, D. Scipio, P. Furler, S.M. Haile, A. Steinfeld, Science 330 (2010) 1797-1801.

[15]    G.A. Olah, A. Goeppert, G.S. Prakash, The Journal of organic chemistry 74 (2008) 487-498.

[16]    I. Omae, Catalysis Today 115 (2006) 33-52.

[17]    P. Jessop, Coord. Chem. Rev 248 (2004) 2425-2442.

[18]    G. Centi, S. Perathoner, Catalysis Today 148 (2009) 191-205.

[19]    W.-L. Dai, S.-L. Luo, S.-F. Yin, C.-T. Au, Applied Catalysis A: General 366 (2009) 2-12.

[20]    Y. Liu, D. Liu, International journal of hydrogen energy 24 (1999) 351-354.

[21]    F.S. Stone, D. Waller, Topics in catalysis 22 (2003) 305-318.

[22]    C.-S. Chen, W.-H. Cheng, S.-S. Lin, Applied Catalysis A: General 238 (2003) 55-67.

[23]    C.-S. Chen, W.-H. Cheng, S.-S. Lin, Chem. Commun. (2001) 1770-1771.

[24]    C.-S. Chen, W.-H. Cheng, S.-S. Lin, Applied Catalysis A: General 257 (2004) 97-106.

[25]    C.S. Chen, J.H. Lin, J.H. You, C.R. Chen, Journal of the American Chemical Society 128 (2006) 15950-15951.

[26]    A. Trovarelli, Catal Rev Sci Eng 38 (1996) 439-520.

[27]     L. WANG, S. ZHANG, Y. LIU, Journal of Rare Earths 26 (2008) 66-70.

[28]     A. Goguet, F. Meunier, J. Breen, R. Burch, M. Petch, A. Faur Ghenciu, Journal of Catalysis 226 (2004) 382-392.

[29]     K. Kitamura Bando, K. Soga, K. Kunimori, H. Arakawa, Applied Catalysis A: General 175 (1998) 67-81.

[30]     H. Kusama, K.K. Bando, K. Okabe, H. Arakawa, Applied Catalysis A: General 205 (2001) 285-294.

[31]     S.D. Kim, Y. Kang, Chemical engineering science 52 (1997) 3639-3660.

[32]     J.S. Kim, H.K. Kim, S.B. Lee, M.J. Choi, K.W. Lee, Y. Kang, Korean Journal of Chemical Engineering 18 (2001) 463-467.

[33]     G. Karagiannakis, S. Zisekas, M. Stoukides, Solid State Ionics 162 (2003) 313-318.

[34]     G. Pekridis, K. Kalimeri, N. Kaklidis, E. Vakouftsi, E. Iliopoulou, C. Athanasiou, G. Marnellos, Catalysis Today 127 (2007) 337-346.

[35]     S. Bebelis, H. Karasali, C. Vayenas, Solid State Ionics 179 (2008) 1391-1395.

[36]     K.-H. Ernst, C.T. Campbell, G. Moretti, Journal of Catalysis 134 (1992) 66-74.

[37]     C.S. Chen, J.H. Wu, T.W. Lai, The Journal of Physical Chemistry C 114 (2010) 15021-15028.

[38]     F. Boccuzzi, A. Chiorino, G. Martra, M. Gargano, N. Ravasio, B. Carrozzini, Journal of Catalysis 165 (1997) 129-139.

[39]     V. Arunajatesan, B. Subramaniam, K. Hutchenson, F. Herkes, Chemical engineering science 62 (2007) 5062-5069.

[40]     A. Goguet, F.C. Meunier, D. Tibiletti, J.P. Breen, R. Burch, The Journal of Physical Chemistry B 108 (2004) 20240-20246.

[41]     S. Qin, C. Hu, H. Yang, Z. Su, The Journal of Physical Chemistry A 109 (2005) 6498-6502.

[42]     A.C. Society, ( 2004 ).

[43]     C. Liu, L. Munjanja, T.R. Cundari, A.K. Wilson, The Journal of Physical Chemistry A 114 (2010) 6207-6216.

[44]     A.C. Society, (2010).

[45]     K. Fujimoto, T. Shikada, Applied catalysis 31 (1987) 13-23.

[46]     P.S. Prasad, J.W. Bae, K.-W. Jun, K.-W. Lee, Catalysis surveys from Asia 12 (2008) 170-183.

[47]     M. Fujiwara, R. Kieffer, H. Ando, Y. Souma, Applied Catalysis A: General 121 (1995) 113-124.

[48]     R.W. Dorner, D.R. Hardy, F.W. Williams, B.H. Davis, H.D. Willauer, Energy & Fuels 23 (2009) 4190-4195.

[49]     F. Tihay, A. Roger, G. Pourroy, A. Kiennemann, Energy & Fuels 16 (2002) 1271-1276.

[50]     A.N. Akin, M. Ataman, A.E. Aksoylu, Z.I. Önsan, Reaction Kinetics and Catalysis Letters 76 (2002) 265-270.

[51]     C.G. Visconti, L. Lietti, E. Tronconi, P. Forzatti, R. Zennaro, E. Finocchio, Applied Catalysis A: General 355 (2009) 61-68.

[52]     S. Fujita, H. Terunuma, H. Kobayashi, N. Takezawa, Reaction Kinetics and Catalysis Letters 33 (1987) 179-184.

[53]    M.E. Dry, Applied Catalysis A: General 138 (1996) 319-344.

[54]    R.W. Dorner, D.R. Hardy, F.W. Williams, H.D. Willauer, Applied Catalysis A: General 373 (2010) 112-121.

[55]    P.J. Lunde, F.L. Kester, Industrial & Engineering Chemistry Process Design and Development 13 (1974) 27-33.

[56]    G. Du, S. Lim, Y. Yang, C. Wang, L. Pfefferle, G.L. Haller, Journal of Catalysis 249 (2007) 370-379.

[57]    J.-N. Park, E.W. McFarland, Journal of Catalysis 266 (2009) 92-97.

[58]    F.-W. Chang, M.-S. Kuo, M.-T. Tsay, M.-C. Hsieh, Applied Catalysis A: General 247 (2003) 309-320.

[59]    S. Sane, J. Bonnier, J. Damon, J. Masson, Applied catalysis 9 (1984) 69-83.

[60]    G.D. Lee, M.J. Moon, J.H. Park, S.S. Park, S.S. Hong, Korean Journal of Chemical Engineering 22 (2005) 541-546.

[61]    J. Sehested, K.E. Larsen, A.L. Kustov, A.M. Frey, T. Johannessen, T. Bligaard, M.P. Andersson, J.K. Nørskov, C.H. Christensen, Topics in catalysis 45 (2007) 9-13.

[62]    M. Agnelli, H. Swaan, C. Marquez-Alvarez, G. Martin, C. Mirodatos, Journal of Catalysis 175 (1998) 117-128.

[63]    A. Kustov, A.M. Frey, K.E. Larsen, T. Johannessen, J.K. Nørskov, C.H. Christensen, Applied Catalysis A: General 320 (2007) 98-104.

[64]    Z. Kowalczyk, K. Stołecki, W. Raróg-Pilecka, E. Miśkiewicz, E. Wilczkowska, Z. Karpiński, Applied Catalysis A: General 342 (2008) 35-39.

[65]    T. Abe, M. Tanizawa, K. Watanabe, A. Taguchi, Energy & Environmental Science 2 (2009) 315-321.

[66]    L. Luo, L. Songjun, Y. Zhu, Journal of the Serbian Chemical Society 70 (2005) 1419-1425.

[67]    M. Kuśmierz, Catalysis Today 137 (2008) 429-432.

[68]    Elsevier, (2009).

[69]    K.-P. Yu, W.-Y. Yu, M.-C. Kuo, Y.-C. Liou, S.-H. Chien, Applied Catalysis B: Environmental 84 (2008) 112-118.

[70]    A. Lapidus, N. Gaidai, N. Nekrasov, L. Tishkova, Y.A. Agafonov, T. Myshenkova, Petroleum Chemistry 47 (2007) 75-82.

[71]    M. Marwood, R. Doepper, A. Renken, Applied Catalysis A: General 151 (1997) 223-246.

[72]    Elsevier, (1997).

[73]    S.J. Choe, H.J. Kang, S.J. Kim, S.B. Park, D.H. Park, D.S. Huh, Bulletin of the Korean Chemical Society 26 (2005) 1682-1688.

[74]    T. Inui, T. Takeguchi, Catalysis Today 10 (1991) 95-106.

[75]    B. Liaw, Y. Chen, Applied Catalysis A: General 206 (2001) 245-256.

[76]    X.-M. Liu, G. Lu, Z.-F. Yan, J. Beltramini, Industrial & engineering chemistry research 42 (2003) 6518-6530.

[77]    I.A. Fisher, A.T. Bell, Journal of Catalysis 172 (1997) 222-237.

[78]    R. Koeppel, A. Baiker, A. Wokaun, Applied Catalysis A: General 84 (1992) 77-102.

[79]     W. Jansen, J. Beckers, A. Denier vd Gon, A. Bliek, H. Brongersma, Journal of Catalysis 210 (2002) 229-236.

[80]     Q.-L. Tang, Q.-J. Hong, Z.-P. Liu, Journal of Catalysis 263 (2009) 114-122.

[81]     R.P.C. Chattopadhyay D., D. Chattopadhyay, P.C. Rakshit, Electronics Fundamentals and Applications, New Age International (P) Limited, 2008.

[82]     K. Perzyna, R. Borkowska, J. Syzdek, A. Zalewska, W. Wieczorek, Electrochimica Acta 57 (2011) 58-65.

[83]     P. Tsiakaras, (Patra,1993) 14-52.

[84]     H.-H. Moєbius, Solid State Electrochem 1 (1997).

[85]     R. Turton, (2000).

[86]     P.P.K.a.S. Yashonath, Chem. Sci 118 (2006) 136-138.

[87]     A.R.B.C. Smith, (2010).

[88]     C. Kittel, Introduction to Solid State Physics, Wiley, 2004.

[89]     R.J.D. Tilley, Defects in Solids, 2008.

[90]     D.R. D. Leroy, C. R. Acad. Sci., 286C (1978) 413.

[91]     M.W.S. G. V. Chandrasekhar, Ext. Abs. Electrochem. Soc., Seattle Wash (1978) 260.

[92]     T. Takahashi, (1980).

[93]     T. Minarni, Non-Cryst. Solids 73 (1985) 273.

[94]     C.C.L. C. R. Schlaikjer, (1973).

[95]     J.C. Philips, Electrochem. Soc 123 (1976) 934.

[96]     e.a. T. Qui, 3-4 (1981) 219.

[97]     H.Y. K. Tadanaga, A. Matsuda, T. Minami, and M. Tatsumisago 70(12) (2002) 998-1000.

[98]     G.R.A. B. B. Owens, Science 157 (1967) 308.

[99]     C. Kokkofitis, (2007).

[100]    T.M.P.A. Gur, CA), Huggins, Robert A. (Ulm, DE), (1998).

[101]    A.R. West, MATER. CHEM 1(2) (1991) 158.

[102]    S.A.A. A. M. Azad, * S. G. Mhaisalkar, ~ L. D. Birkefeld,** and K. S. Goto b, Electrochem. Soc. 139 (1992) 3690-3692.

[103]    E.G.&G. Services for the U.S. Department of Energy, National

Technical Information Service: Springfield (2004).

[104]    PhysiologyWeb, (2014 ).

[105]    D.o.I.a.A.C. BUTE.

[106]    T. Norby, M. Widerøe, R. Glöckner, Y. Larring, Dalton transactions (2004) 3012-3018.

[107]    E. Fabbri, L. Bi, D. Pergolesi, E. Traversa, Advanced Materials 24 (2012) 195-208.

[108]    D. Medvedev, A. Murashkina, E. Pikalova, A. Demin, A. Podias, P. Tsiakaras, Progress in Materials Science 60 (2014) 72-129.

[109]    K. Kreuer, Annual Review of Materials Research 33 (2003) 333-359.

[110]   S.J. Zhan, X.F. Zhu, W.P. Wang, W.S. Yang, Advanced Materials Research 554 (2012) 404-407.

[111]   R. Kannan, S. Gill, N. Maffei, V. Thangadurai, Journal of The Electrochemical Society 160 (2013) F18-F26.

[112]   K.H. Ryu, S.M. Haile, Solid State Ionics 125 (1999) 355-367.

[113]   P. Sawant, S. Varma, B. Wani, S. Bharadwaj, International journal of hydrogen energy 37 (2012) 3848-3856.

[114]   L. Yang, S. Wang, K. Blinn, M. Liu, Z. Liu, Z. Cheng, M. Liu, Science 326 (2009) 126-129.

[115]   G. Pekridis, K. Kalimeri, N. Kaklidis, C. Athanasiou, G. Marnellos, Solid State Ionics 178 (2007) 649-656.

[116]   P. Kissinger, W.R. Heineman, Laboratory Techniques in Electroanalytical Chemistry, revised and expanded, CRC press, 1996.